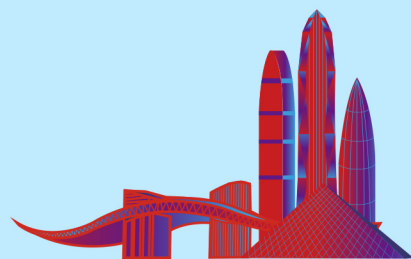


2024 CHPC

CHINA HEAT PUMP CONFERENCE



EXTENDED ABSTRACT COLLECTION



Hisense



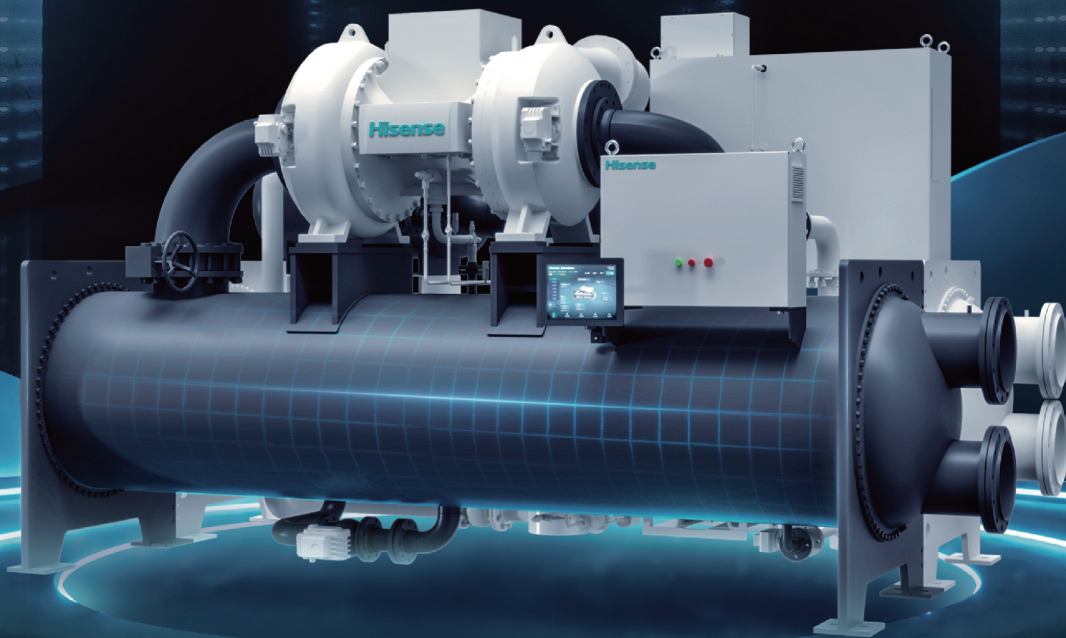
UEFA
EURO2024
GERMANY

2024欧洲杯™官方指定中央空调

海信无油变频离心式冷水机组

正压液浮系列

核心科技 国际领先



超高能效

国标COP 7.23
国标IPLV 10.26



高稳定性

航天级陶瓷轴承
轴承设计寿命20万小时



无油运行

整机无需润滑油
维保更便捷



宽域调节

10%低负荷运行
10℃低冷却水温运行



智慧便捷

性能在线显示
ECO-B智慧运维平台

注：“核心科技 国际领先”为中国制冷学会科技评估专家组2023年8月鉴定结论



青岛海信日立空调系统有限公司

公司地址：中国青岛经济技术开发区前湾港路218号

全国客户服务热线：4006-111-111（转7）



International quality·Trust

国际品质 信成未来



中广 OUTES 欧特斯

热泵空调 选中广



制热快 · 效果好 · 超省钱

高圆圆
品牌代言人



热泵空调 | 热泵采暖 | 热泵热水 | 热泵烘干 | 热泵衣物护理机 | 净水 | 新风

“中国航天事业战略合作伙伴”“热泵行业领军品牌”，中广欧特斯深耕热泵行业十八年，利用空气实现人居环境中冷、暖、风、水的高效调节，构建起居家可享的五星级舒适体验。让爱有温度，中广欧特斯。



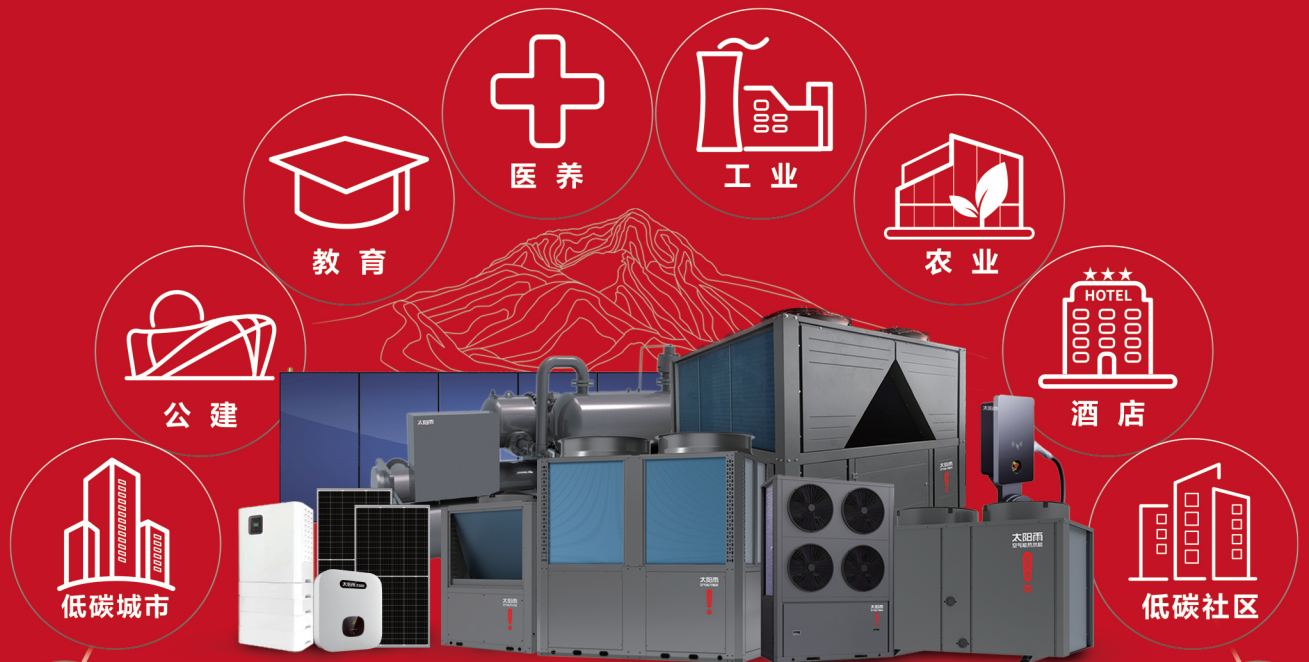
中广欧特斯公众号



中广欧特斯抖音号

太阳雨低碳清洁能源系统解决方案

不同领域/不同场景一站式解决



太阳雨GAIA智能操作系统

盖亚 GAIA OS

让控制更智能 让设计更简单 让运维更高效

15年省出一套清洁能源站

智能联控系统

智能设计系统

智慧运维系统

5min
快速出方案

工程造价
降低30%

误差控制在
5%左右

减少售后人员
60%以上

较传统人控方式节能
20%以上

售后效率提升
70%以上



CONTENTS

HFO refrigerants of GWP less than 150 as sustainable alternatives in air conditioner and heat pump	3
Refrigeration oil development for R-290 heat pump	3
Evaluating the explosion risk of R32 refrigerant leakage with CFD Simulation	3
Study on the Impacts of Refrigerant Leakage on the Performance of Heat Pump System Using R513A as Replacement of R134a	7
Study the influence of oil return hole size on oil mass flow rate in accumulator with multiphase flow model	10
Technical Trends and Risk Management of Heat Pumps Using Flammable Refrigerant	13
A novel two-stage type II absorption thermal battery with low charging temperature for high temperature lift	14
Performance comparison of different refrigerants in the frosting-defrosting cycles for air source heat pumps: R410A and R32 as an example	17
Experimental Performance Analysis of Superhydrophobic Heat Exchanger in Active-passive Combined Frost Suppression Mode	17
Commercializable superhydrophobic coating for air source heat pumps frost suppression	18
Investigation of Thermal Characteristics in Ground Source Heat Pump System with Phase Change Thermal Storage and Radiant Floor Heating	19
Heat pump assisted LiBr-water absorption thermal energy storage under low ambient temperature	19
Optimization of Sorption Thermal Battery for heat pump water heater applications	23

Simulation and Experimental Study on the Structural Optimization of Cabinet Dryers	25
Experimental Study and Numerical Optimization of Heat Flow Characteristics in Dense Tobacco Drying Room	29
Effect of Waste Heat Recovery on the Thermal Performance of Heat Pump Drying Systems	29
Performance study of the Reverse Brayton air cycle drying system for agricultural application	30
Optimization and performance analysis of semiconductor heat pump clothes dryers	33
Efficiency Analysis and Optimization of Heat Pump Systems for Urban Sludge Drying: A Comparative Study of CO ₂ and R134a Circulation.....	33
Performance Analysis of a Semi-Open Heat Pump Drying System in South African Climatic Conditions	34
Experiments on off-design performance of PV driven refrigerated warehouse based on vapor compression refrigeration with ice thermal storage	34
Study on the Optimal Working Conditions of Closed Trans-critical CO ₂ Heat Pump Drying System	35
Simulation and optimization of solar phase change heat storage heat pump integrated system ..	36
Design and Application of a Multi-Objective Optimization Framework for Identifying Optimal Operating Conditions in Hybrid Heat Pump Systems	36
Research on Building Resistance-Capacity Model Identification and Indoor Temperature Prediction Based on Genetic Algorithm	45
A novel power output prediction framework based on an early labelling approach for open absorption heat pump	45
Data-driven models when data is missing for heat pumps	46

Investigation on Multiple Degrees of Freedom Hybrid Modeling Method for High Temperature Heat Pump	46
Physics-Guided Neural Network for Multi-Step Prediction of Heat Pump Heating Capacity	54
Performance investigations on a nonflammable eco-friendly mixture for an air-source heat pump water heater during wintertime	56
Thermodynamic analysis of a large temperature lift heat pump strategy: combining water vapor compressor and exploring performance boundaries	57
Application and analysis of two-stage heat recovery and flash vaporization process in high-temperature heat pump systems for steam production	58
Performance study of a quasi-saturated compression high-temperature heat pump system with water vapour	58
Thermodynamic performance analysis of a novel energy storage power plant based on high-temperature heat pump and molten salt heat storage systems	59
Application Analysis of Complex High-Temperature Heat Pump in Petroleum Process	61
Performance analysis of an air source high temperature heat pump steam system with large temperature rise	61
Innovative internal Cooling Thermodynamic Cycles for High-temperature heat pump Thermal Management	62
Experimental investigation of a multi-energy complementary absorption heat pump applied for combined cooling and heating in distributed regions	65
Potential of applying a novel trans-critical CO ₂ cycle with multi-heat recovery for combined cooling and heating in the ice rank	65
Design and Operational Optimization Low Carbon Integrated Energy System between Data Centers and Buildings based on Heating Pump	66

Study and economic analysis of the form of multi-energy complementary system for airport rooms in severe cold regions	68
Study on the operation mode and control strategy of a multi-heat source heat pump coupled energy storage system for plant factory heating and grid peaking.....	69
Energy consumption, Exergy and techno-economic analysis of an industrial building temperature and humidity control system based on low-grade waste heat recovery	71
Optimising steam generating heat pump integration in industries: performance analysis across different heat sources and heating demands	76
Experimental Research of CO ₂ Two-stage Compression Refrigeration System with Vapor-injection	76
Research and analysis on the usage patterns and typical scenarios of people in public spaces based on machine vision.....	77
Advanced control strategy of ground-source heat pump	78
Finite time thermodynamics optimization of indirect sewage source heat pump system	78
Study on the characteristics and influence of cold and wet island effect from air source heat pump array	80
Research on energy-saving optimization control of air-cooled heat pump combined with floor heating system	80
Investigation of a novel dual-temperature district heating substation for radiant combined with convection systems	81
High-Performance Hydrogen-Powered Heat Pumps	84
An Advanced Cascade Method for Optimal Industrial Heating Performance in Air Source Hybrid Heat Pump	87
Multi-Objective Optimization of a Direct Air Capture System Integrated with Air-Source Heat Pumps.....	87

Preliminary characterization of a three-source passive condenser air conditioning integrating sky radiative cooling and evaporative cooling	88
A novel hybrid-energy heat pump using refrigerant/ionic liquids for solar cooling	89
Experimental investigation on heat transfer characteristics of a reversible reaction-based heat exchanger-reactor for chemical heat pump	89
Cooling load analysis and energy-saving strategies for VAC system in subway station: A case study	90
A Comparative View on Challenges and Opportunities of District Heating's Zero-Carbon Transition in China and Sweden	90
Analysis of energy consumption and energy efficiency of the central air conditioning system of water source heat pump: taking an energy station in Nanjing as an example	91
Study on a micro-cogeneration system coupled with PV/T solar energy and air source heat pump	92
Performance Analysis of a DC inverter Heat Pump System for PV integrated Building in Hot-summer and Cold-winter Region	94
Design and Operating Experiences of a High Temperature Heat Pump for Steam Generation	97
Thermal-structural coupling characteristic analysis of shield energy tunnel under typical condition	97
Transient and steady performance of a microchannel membrane-based absorption refrigeration system	105
Study on the Drainage Performance of Microchannel Heat Exchangers (Louvered Fins) Combining CFD and Image Recognition Technologies	105
High Differential Pressure Expansion Work Recovery in Trans-Critical CO ₂ Heat Pumps using a Rotary Gas Pressure Exchanger	108
Research and optimization of cold water phase change heat exchanger	109

Effect of fin structure variation on performance of finned-tube heat exchangers in air-source heat pumps	111
Steady-state heat pump performance model including irreversibility in the heat exchangers and the compressor for R290 and R32	111
Theoretical Study on the Mismatch of Thermal Quality and Heat Capacity in the Heating Process of Transcritical CO ₂ Heat Pumps.....	112
Thermodynamics analysis of the transcritical CO ₂ heat pump for heating applications.....	113
Enhancing carbon dioxide (CO ₂) refrigeration efficiency in different climates: experimental analysis of four configurations and annual performance prediction in different Cities	122
Study on Performance of Trans-critical CO ₂ Air Source Heat Pump System in Cold Region	123
Performance analysis and research on optimization of CO ₂ heat pump system for hybrid electric vehicles based on Dymola	125
Performance Analysis of an Integrated Thermal Management System for Electric Buses	126
Research on efficient heating method of solar composite heat pump based on evaporative thermal accumulator	126

美的多场景智慧供暖解决方案

美的作为清洁供暖的智慧合伙人，能根据不同客户的需求，提供多种高效、灵活、创新的清洁供热方案。凭借多年积累的清洁供热经验和大量优秀的样板案例，美的助力众多企业实现节能降碳，降本增效的双碳目标。

在软件层，美的iBUILDING能源管理平台

基于数字孪生和云计算的能力，对项目运营精准监控和高效管理，推动清洁供暖的智慧化发展。

在设备层，美的可定制多种形式

(离心热泵、螺杆热泵、涡旋热泵、转子热泵等)不同制热量和能力段的热泵产品，充分利用各种形式的可再生热源，实现多能互补的清洁供暖。





热管理系统核心零部件与集成方案的提供者

北方供热采暖 | 家用户式空调 | 商用空调
数据中心 | 轨道交通 | 工农业应用



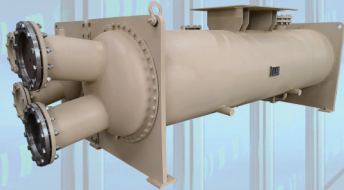
壳管式换热器



板式换热器



套管式换热器



降膜壳管换热器



蒸发式冷凝器



液冷散热器

- ◆ 国家高新技术企业
- ◆ 国家专精特新“小巨人”企业
- ◆ 《制冷与空调用同轴套管式换热器》国家标准负责起草单位
- ◆ 《带分配器的壳管式换热器》行业标准负责起草单位
- ◆ 通过ISO9001、ISO14001、ISO45001、UL认证
- ◆ 压力容器制造许可证(GB、ASME、PED)

浙江英特科技股份有限公司
Zhejiang Extek Technology Co.,Ltd.
地址：中国 浙江 安吉
E-mail:extek@extek.com.cn
www.extek.com.cn

HFO refrigerants of GWP less than 150 as sustainable alternatives in air conditioner and heat pump

Guanxing Zou^(a), Bin Wang^(b)

^(a) Honeywell Integrated Technology (China) Co., Ltd.
Shanghai, 201203, China, guanxing.zou@honeywell.com

^(b) Honeywell Advanced Materials (China) Co., Ltd.
Suzhou, 215699, China, bin.wang7@honeywell.com

ABSTRACT

R410A of high global warming potential (GWP) are widely used in residential and light commercial air conditioner and heat pump. As the implementation of Kigali Amendment and global environmental regulations at recent years, refrigerants of GWP<750 such as R32, R452B, R454B are widely adopted to replace R410A. Additionally to reduce carbon emission further, HFO refrigerants of GWP<150 were developed. In this paper, the detailed performance evaluation of two HFO refrigerants of GWP<150 R454C and R455A was conducted. The thermal properties, the system performance and the safety requirement are compared between the baseline refrigerant (R410A), HFO refrigerants of GWP<150 (R454C & R455A) and natural refrigerant (R290).

Keywords: HFO refrigerant, GWP<150, R454C, R455A, air conditioner, heat pump

Refrigeration oil development for R-290 heat pump

Zhaofei Chen, Peng-hui Jia, Mei-juan Ma, Mike Costello, Xin-zhong Chen

Lubrizol Management (Shanghai) Co., Ltd, Shanghai 201206, China, Feyman.chen@lubrizol.com

ABSTRACT

Heat pump development with Low GWP refrigerants is a hot area in China under the background of the double carbon target and the Kigali amendment. R-290 is a key low GWP refrigerant with excellent performance and the main OEMs in China are working on the compressor development with R-290. This article introduces the development of refrigeration oil suitable for R-290 heat pump. By testing basic physical property, anti-wearing, miscibility test, seal tube stability testing (ASHRAE 97), and PVT testing. Finally, a refrigeration oil suitable for R-290 heat pump has been successfully developed for the R-290 heat pump application.

Keywords: Double carbon target Kigali amendment R-290 heat pump refrigeration oil development

Evaluating the explosion risk of R32 refrigerant leakage with CFD Simulation

Chaochao Wang^(a)

^(a) Johnson Controls - Hitachi Air Conditioning Technology (Wuxi) Co., Ltd.
Wuxi, 214000, China, e-mail chaochao.wang@jci-hitachi.com

ABSTRACT

This research introduces a method to use CFD simulation to estimate the R32 Refrigerant leakage in a closed space filled with air, which is very helpful to the development of new product of R32 heat pump product. Simulation cases in this research uses Fluent's species transport equation, which is used to simulate the transport of different chemical species in a fluid. It solves the transport equations for each species separately and considers various transport mechanisms such as diffusion, convection, and chemical reactions. The Species Transport model in Fluent is a powerful tool for simulating and understanding the transport and interaction of different chemical species in a fluid system. It allows for detailed analysis of species concentrations, fluxes, and reaction rates, enabling engineers and researchers to study a wide range of applications, including combustion, chemical reactions, pollution control, and more.^[1]

In this research, different chemical species are Gas R32 and Air. With the help of Species Transport model, explosion risks and vulnerable positions in different products and scenarios are analyzed. The newly developed refrigerant leakage simulation model not only helps in understanding the distribution pattern of leaked refrigerant for development and marketing purposes but also allows for predicting the specific size and location of the flammable volume after leakage, providing robust assurance for improving product safety.

Keywords: Refrigerant Leakage, explosion, closed space, ANSYS Fluent, environmentally friendly refrigerant, VRF

1. INTRODUCTION

Under the background of carbon neutrality, the application scope of environmentally friendly refrigerant R32 is continuously expanding. However, when the concentration of R32 is between 13.29% and 29.31%, it is prone to explosions, posing a significant threat to the safety of customers' lives and properties. To create a safer and healthier environment, it is necessary to evaluate common environments where air conditioning systems are used. Due to the high-risk nature of R32 gas, conducting experimental evaluations of leakage is highly dangerous. Therefore, a simulation approach is adopted to assess safety and provide detailed analysis.

2. REFRIGERANT LEAKAGE OF R32 IN THE BEDROOM

2.1 Install environment of IDU.

As shown in the figure 1, the study focuses on a bedroom in a villa with VRF units installed. The bedroom is 3.5 meters long, 3 meters wide, and 2.5 meters high. There are many IDU connected to the same ODU, and the entire machine is filled with 88.1kg of R32 refrigerant. One of the IDU has a leak at the connection of the heat exchanger pipeline, and all the refrigerant has leaked from the damaged area, with a leakage rate of 10kg/h.

Refrigerant flows into the bedroom from the outlet of IDU, flows out from the gap under the door (W800mmXH4mm), which set as pressure outlet in CFD simulation.

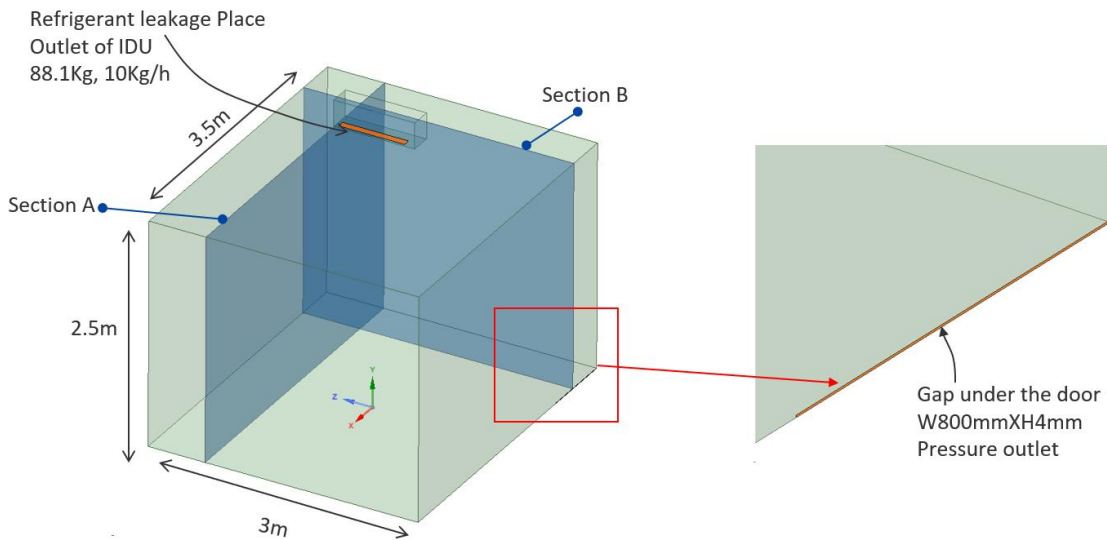


Figure 1: 3D Layout of the room.

2.2 meshing setting

Due to transient simulation needs very long simulation time, mesh number should be small. Cut cell mesh is considered in this simulation to generate high-quality hexahedral meshes.

Mesh setting: max size=128mm, Growth rate=2.0, Proximity min size=2mm. element size at inlet =15mm; total volume mesh number is 44,945.

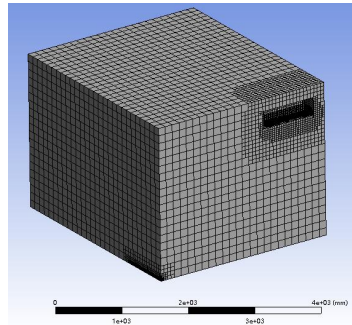


Figure 2: mesh setting.

2.3 material parameters

In this research, 2 species are considered which are Gas R32 and Air, idea gas model is adopted to describe the density. Parameter of the 2 species shows as below, Diffusion coefficient of air and R32 is $1.36987 \times 10^{-5} [m^2/s]$.

	Molecular mass: [Kg/Kmol]	specific heat: [J/Kg · K]	Thermal conductivity: [W/m · K]	viscosity coefficient: [Pa · s]
Air	28.9664	1003.62	0.0260305	1.85508×10^{-5}
R32	52.024	847.46	0.012508	1.2607×10^{-5}

Table 1: material parameters.

2.4 simulation results

Experimental research has found that explosions are prone to occur when the concentration of R32 is between 13.29% and 29.31%^[2]. Use custom functions to monitor the flammable volume over time. The simulation results show that the flammable volume is 0 within 5 hours. After 7.24 hours, the flammable volume rapidly increases, and after 8.2 hours, all rooms are in an explosive range.

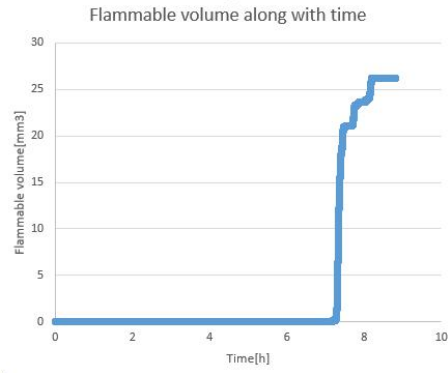


Figure 3: flammable volume along with time.

Following figure shows the R32 mole fraction contour at different time.

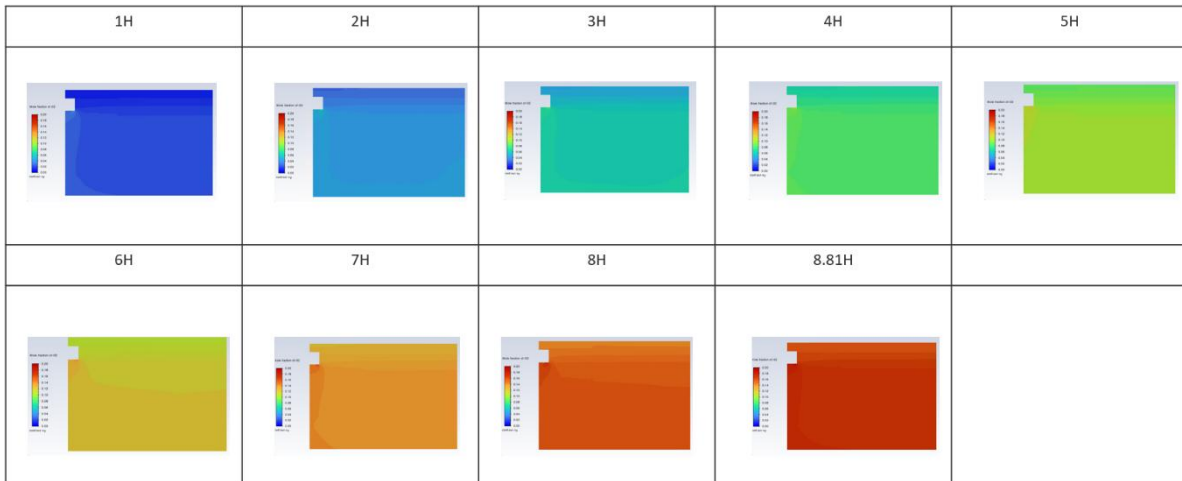


Figure 4: mole fraction of R32 contour on section A.

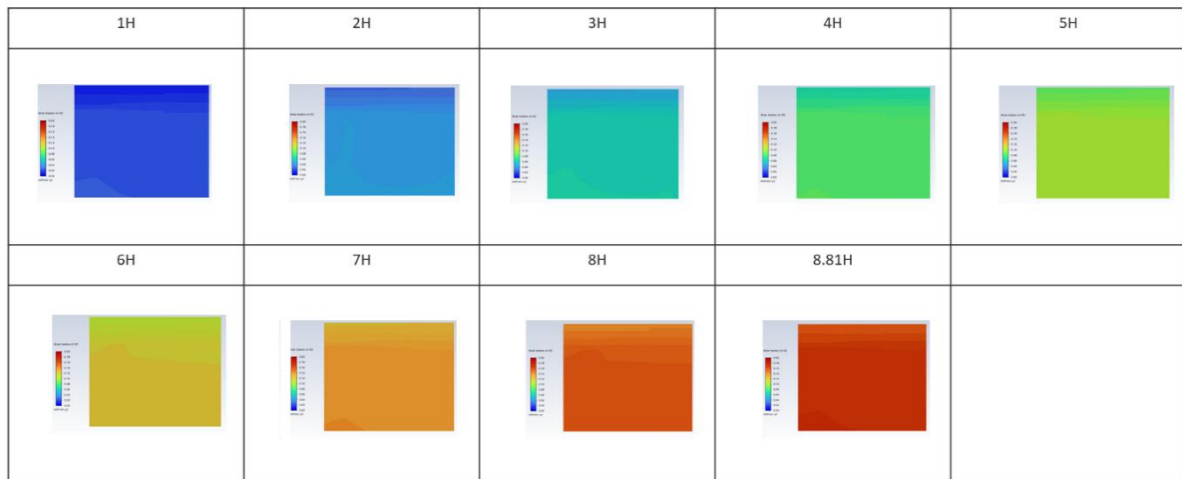


Figure 5: mole fraction of R32 on section B.

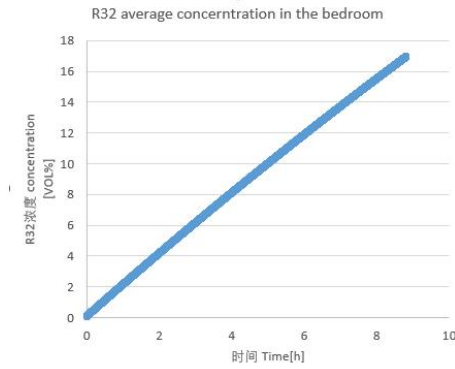


Figure 6: R32 average concentration in the bedroom.

3. CONCLUSIONS

CFD simulation can calculate the R32 concentration and show the R32 dissipation behavior, which can identify the explosion risk and provide strong support to the product development. Simulation results show that the flammable volume is 0 within 5 hours. After 7.24 hours, the flammable volume rapidly increases, and after 8.2 hours, all rooms are in an explosive range.

ACKNOWLEDGEMENT

This work was supported by Johnson Controls - Hitachi Air Conditioning Technology (Wuxi) Co., Ltd.

REFERENCES

- [1] Ansys_Fluent_Theory_Guide.
- [2] Refrigerant supplier's test results.

Study on the Impacts of Refrigerant Leakage on the Performance of Heat Pump System Using R513A as Replacement of R134a

Yansong Hu^(a), Zhao Yang^{(a)*}

^(a)Tianjin University, Tianjin, 300350, China

* zhaoyang@tju.edu.cn

ABSTRACT

The intensification of global warming has underscored the urgency of mitigating the greenhouse effect. R513A represents a pragmatic alternative to R134a, offering reduced global warming potential while maintaining comparable thermodynamic performance. However, refrigerant leakage is one of the common faults in heat pump equipment. The ability of the system to cope with failures when charged with different refrigerants should be considered. When the heat pump reached the optimal COP, the optimal refrigerant charge of R513A is greater than that of R134a. The leakage experiment was carried out under the optimal charge of two refrigerants. The results showed that the increase of pressure ratio and exhaust temperature were reduced when the R513A was used in comparison with the R134a under refrigerant leaking. In addition, the heating capacity of R513A and R134a decreased by 6.35% and 8.91%, respectively. At the same time, COP of R513A system and R134a system also decreased with refrigerant leakage, The COP of R513A system was reduced by 8.35%, The COP of R134a system was reduced by 10.15%. The change in COP in the leakage and charge experiments was also compared, and lacking the same mass of refrigerant, the COP was significantly lower in leakage experiment. This paper presented a comprehensive experimental comparison of the variation of various parameters of a heat pump with the leakage of two refrigerants. The experimental results showed that the

system charged with R513A was more stable than the system charged with R134a when encountering refrigerant leakage fault.

Keywords: Refrigerant replacement, Heat pump, Refrigerant leakage, System performance, R513A

1. INTRODUCTION

To achieve the goal of energy conservation, reduction of emissions, and sustainable development, it is essential to begin with the primary source of energy consumption and implement measures to reduce energy consumption. Drying is one of the most energy-consuming processes in industrial production, with a wide range of applications in agriculture, food, pharmaceutical preparation, construction, and other fields. Currently, the utilization of drying heat pumps in the pharmaceutical and chemical industries is expanding. The drying process for pharmaceuticals and chemicals demands exceptionally high-quality standards, as any deviation may result in significant production issues. Consequently, the utilization of alternative refrigerants in drying heat pumps necessitates that the alternative refrigerant meets the efficiency, reliability, and environmental benefits criteria set forth by the original refrigerant.

The current study primarily examines the impact of alternative refrigerants on the performance of heat pumps during normal operation. However, in the practical application of heat pumps, refrigerant leakage is a common source of failure. For drying heat pumps, refrigerant micro-seam leakage will result in a rapid deterioration of

performance, which will lead to a change in system heat production and the destruction of system stability. This, in turn, will affect the quality of drying products (e.g., pharmaceuticals and chemicals), and problems such as inhomogeneous drying of pharmaceuticals and chemicals may lead to serious consequences. Consequently, it is of paramount importance to investigate the impact of the original refrigerant and alternative refrigerant on system performance and stability in the event of leakage.

2. CHARACTERIZATION OF ALTERNATIVE REFRIGERANTS IN THE FACE OF REFRIGERANT LEAKAGE FAULT

The experiment was set up with a fixed leakage rate of 20 g/min and a continuous leakage from the evaporator outlet line for 45 minutes. The pressure ratio between the compressor inlet and outlet gradually increased with the leakage of refrigerant, and the exhaust temperature of the compressor also increased, and, as the refrigerant leakage proceeds, the pressure ratio and exhaust temperature increased more and more rapidly. Due to the large amount of refrigerant leakage, the evaporating pressure was decreasing, the compressor suction pressure was also decreasing, the refrigerant mass flow at the suction line is decreasing, which led to an increase in the pressure ratio. R513A system operated with a higher refrigerant mass flow rate, and the evaporating pressure was more stable during the leakage process, so the rise in its pressure ratio was lower than that of R134a. And because its pressure ratio rise was small, so its exhaust temperature rise was also smaller than R134a.

With the leakage of refrigerant, the heating capacity and COP of the heat pump system decreased, specifically, the heating capacity of the R513A system decreased by 6.35% and the heating capacity of the R134a system decreased by 8.91%. The COP of the R513A system decreased by 8.35%, and the COP of the R134a system decreased by 10.15%. The decreasing trend of the two parameters was also basically the same. Although the leakage rate was constant, the rate of decrease of the two parameters became faster and faster as the leakage increased. However, the COP of R513A system decreased less; this might be due to its greater heating capacity per unit volume which also resulted in more stable heating capacity in case of leakage.

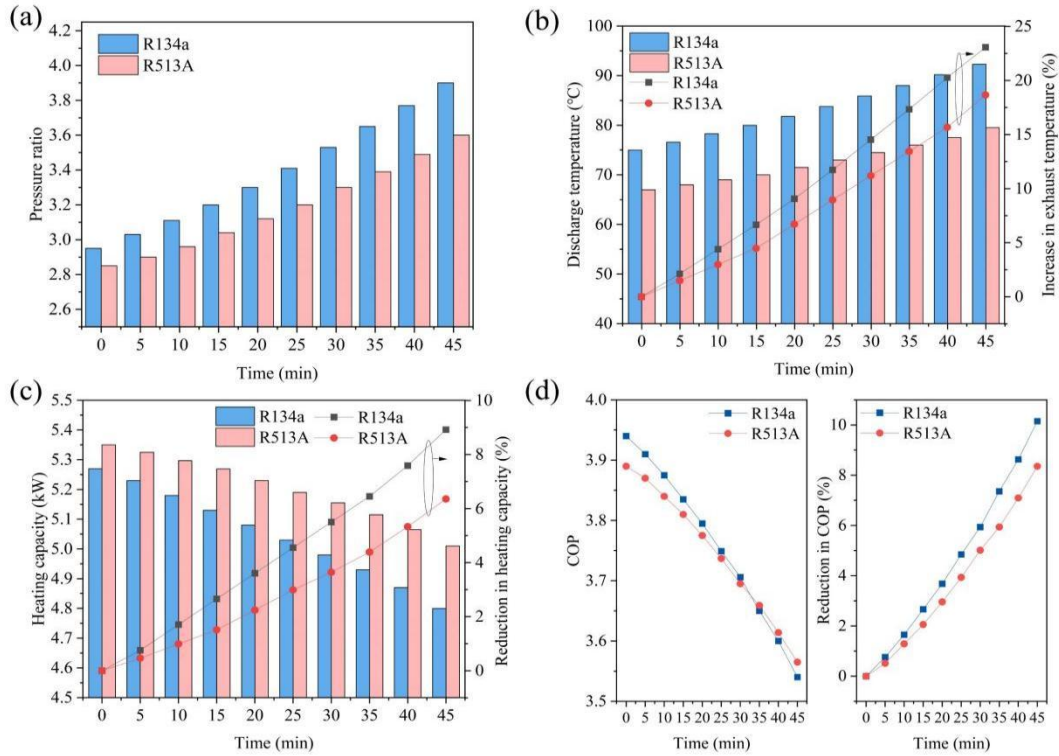


Figure 1: The impact of refrigerant leakage on pressure ratio (a), exhaust temperature (b), heating capacity (c), and COP (d).

In addition, as shown in Fig. 2(a), this paper compared the change of COP during the leakage experiment and the change of COP during the charge experiment, and found that in both experimental processes, when the system had the same amount of refrigerant deficit, the COP in the leakage experiment was lower. This may be due to the drastic change of the system operation state during the leakage process, resulting in low energy utilization efficiency, while during the charge experiment only the refrigerant amount is insufficient, the system still runs stably, just not in the optimal state. Fig. 2(b) comprehensively analyzed some of the parameters of the two refrigerants in the application process. Overall, it seemed that the leakage process had the largest percentage of change in exhaust temperature and pressure ratio. The overall advantage of R513A is more obvious.

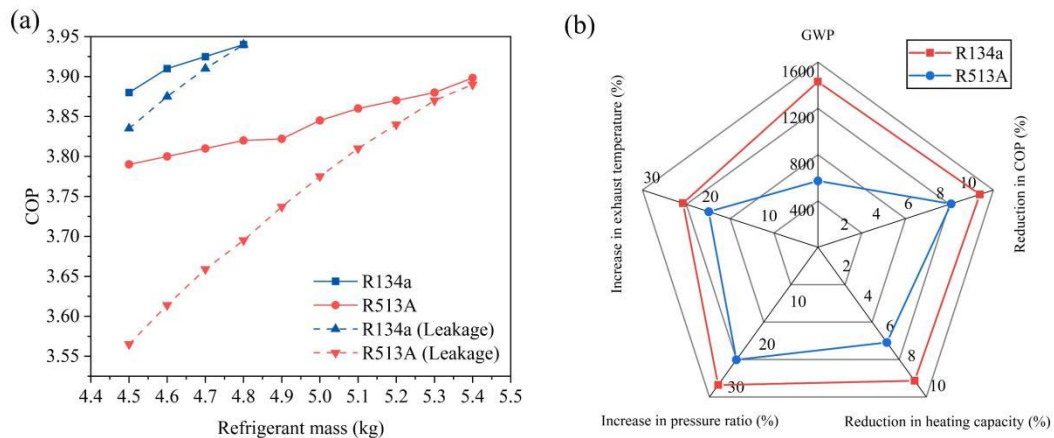


Figure 2: The comparison of leakage tests and charging volume tests (a), R513A and R134a (b).

3. CONCLUSIONS

By charging two kinds of refrigerants into the heat pump system for comparison, it can be found that the difference between the parameters of the R513A system and the R134a system is very small during normal operation, and when encountering refrigerant fault, the changes in the parameters of the R513A system are significantly smaller, indicating that the stability of the R513A system is stronger than that of the R134a system. The stability of alternative refrigerants to cope with various fault is also a key point that should not be ignored when refrigerant replacement is carried out.

ACKNOWLEDGEMENT

This work was supported by Key Program of National Natural Science Foundation of China (Grant no. 51936007).

REFERENCES

- [1] Colak N, Hepbasli A. A review of heat pump drying: Part 1 – Systems, models and studies. *Energy Conversion and Management*. 2009;50(9):2180-6.
- [2] Minea V. Drying heat pumps – Part II: Agro-food, biological and wood products. *International Journal of Refrigeration*. 2013;36(3):659-73.
- [3] Yang Z, Feng B, Ma H, Zhang L, Duan C, Liu B, et al. Analysis of lower GWP and flammable alternative refrigerants. *International Journal of Refrigeration*. 2021;126:12-22.
- [4] Fatouh M, Metwally MN, Helali AB, Shedid MH. Herbs drying using a heat pump dryer. *Energy Conversion and Management*. 2006;47(15):2629-43.
- [5] Pence I, Yıldırım R, Siseci Cismeli M, Güngör A, Akyüz A. Evaluation of machine learning approaches for estimating thermodynamic properties of new generation refrigerant R513A. *Sustainable Energy Technologies and Assessments*. 2023;55:102973.
- [6] Méndez-Méndez D, Pérez-García V, Morales-Fuentes A. Experimental energy evaluation of R516A and R513A as replacement of R134a in refrigeration and air conditioning modes. *International Journal of Refrigeration*. 2023;154:73-83.
- [7] Chen G, Fang J, Li Z, Zhang S. Theoretical analysis of the impacts of refrigerant leakage on the performance of a flash tank vapor injection heat pump. *International Journal of Refrigeration*. 2023;147:10-9.

Study the influence of oil return hole size on oil mass flow rate in accumulator with multiphase flow model

Chaochao Wang^(a)

^(a) Johnson Controls - Hitachi Air Conditioning Technology (Wuxi) Co., Ltd.
Wuxi, 214000, China, e-mail chaochao.wang@jci-hitachi.com

ABSTRACT

This research introduces a method to use CFD simulation to estimate oil flow behavior in the accumulator, which is very helpful to the design of accumulator and the healthy running of the air conditioner. Simulation cases in this research uses Fluent's VOF Model, which is used to simulate and analyze the behavior of multiple immiscible fluids or phases interacting with each other. In the VOF model, a volume fraction is assigned to each phase within a computational cell. The volume fraction represents the ratio of the volume occupied by a specific phase to the total volume of the cell. The interface between the phases is tracked using a sharp interface method.

In this paper, the influence of oil return hole diameter (1.5mm, 2mm, 2.5mm, and 3mm) on oil mass flow rate is studied. Besides, the simulation results have been compared with experimental results, showing good consistency. Furthermore, the flow behavior of oil in the accumulator and the movement of gas refrigerant at the equal pressure hole are investigated. This study is helpful to improve product robust.

Keywords: Compressor oil shortage, multiphase flow of oil and Refrigerant, oil return hole size.

1. INTRODUCTION

Regarding air conditioning design, the control of compressor oil in the refrigerant Cycle is a crucial issue. The circulation of compressor oil with the refrigerant in the circuit can lead to improper functioning of the compressor, affecting the cooling and heating performance. Therefore, it is necessary to use an accumulator to intercept the compressor oil, reduce its entry into the refrigerant system, and return the accumulated compressor oil back to the compressor to ensure proper operation.

The flow behavior of gas refrigerant and liquid oil the fields of multiphase flow, which can use VOF model in Fluent to investigate. The Volume of Fluid (VOF) model is a widely used approach in computational fluid dynamics (CFD) simulations for tracking the interface between two immiscible fluids. This model is particularly useful for simulating multiphase flows, such as the interaction between air and water, oil and water, or any other combination of fluids. The benefit of using the VOF model is its ability to accurately capture the behavior of the interface between the two fluids, including the formation of waves, splashing, and mixing. This makes it a valuable tool for studying a wide range of phenomena, including sloshing in tanks, wave impact on structures, and the behavior of liquid jets.[1]

2. OIL FLOW BEHAVIOR IN THE ACCUMULATOR

2.1 Accumulator introduction

The following image is the 3D model of accumulator, consisting of two pipes and a tank. Gas refrigerant which contains liquid oil enters the accumulator from tube 1, and oil droplets gather at the bottom of the tank under the action of gravity, while gas flows out from tube 2. To prevent oil from being sucked away from the accumulator during startup, a pressure hole is installed in tube 2.

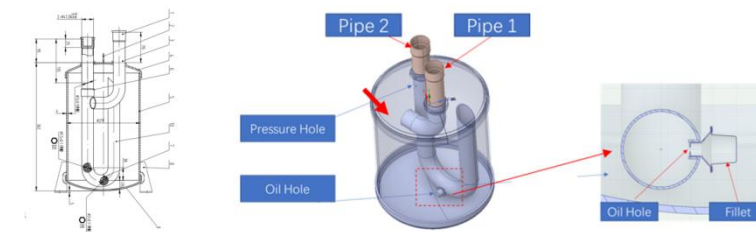


Figure 1: introduction of accumulator

The experimental measurement shows that the outlet pressure of tube 2 is 1MPa and the temperature is 10 °C. According to the Pressure-temperature-solubility-viscosity chart^[2] and the refrigerant property parameter table, the property parameters for oil and R32 are as follows:

- Gas R32: density=27.238kg/m³, viscosity= 11.831e-6Pa.s
- Liquid Oil: density=1000kg/m³, viscosity=6e-3Pa.s

According to experimental measurements, the height of oil in the accumulator accounts for approximately 1/4 of the total height of the accumulator. The mass flow rate of oil and refrigerant at inlet are as follows:

- Mass flow inlet: R32 0.12kg/s, Oil= 0.0072kg/s
- Pressure Outlet: 1Mpa.
- Oil Level height:1/4 of the separator (-253.5~-178.5)

Pressure-Temperature-Solubility-Viscosity Chart
Oil/Ref. FW68H/R32

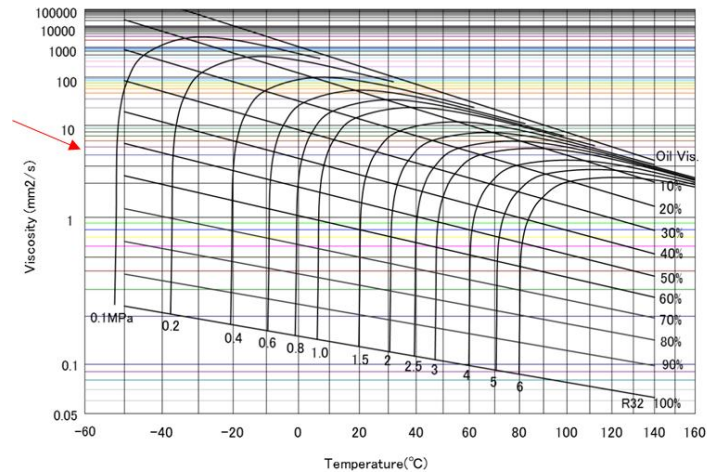


Table 1 : Pressure-temperature-solubility-viscosity chart

2.2 Problem of the accumulator

When using accumulator 1, the compressor experiences a shortage of oil. Attempted to refuel the compressor, but the issue of oil shortage has not improved. Therefore, it is suspected that the oil is stuck inside the oil, and the refrigerant cannot take the oil away.

When changing to accumulator 2, there is an 80% chance that it is good. After changing to accumulator 3, there is 100% no problem.

Evaluate the mass flow rate of the export oil for three accumulators with CFD simulation, determine if there is any oil remaining in the oil fraction from the data of oil mass flow rate.

No	Unit	Volume	Pipe D	Oil Hole	Pressure Hole	Test Result
1	CA	10L	41mm	2.0+1.5mm	3mm	NG
2	CA	10L	41mm	3mm	3mm	80%
3	SA	10L	28.6mm	2.5mm	3mm	100%

Table 2: different accumulator parameters

2.3 Analysis of flow behavior in accumulator

Gas refrigerant which contains liquid oil flows into the accumulator from pipe 1, due to the presence of surface tension, the form of oil is oil droplets, and the droplets are hanging on the pipe wall. Under the impact of high-speed

airflow, oil droplets will flow out of pipe 1 along the pipe wall and impact the oil tank wall. After impacting the oil pipe, oil droplets adhere to the oil tank and converge to the bottom under the action of gravity.

Gas

Gas refrigerant flows out from pipe 2, high velocity in the pipe 2 creates low pressure area around the oil hole. The low-pressure area will absorb oil from the tank.

Due to the presence of surface tension, oil enters tube 2 in the form of oil droplets and adheres to the wall of the tube after impact quickly. Then flow out with high-speed gas refrigerant.

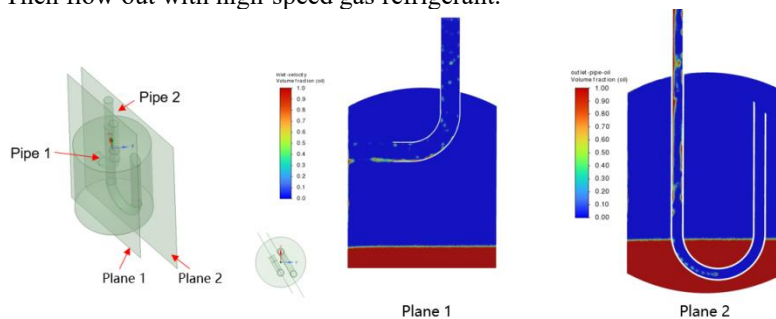


Figure 2: oil flow behavior in the accumulator.

Gas R32 flow into the Pipe 2 from the pressure-Hole, Velocity is around 16m/s.

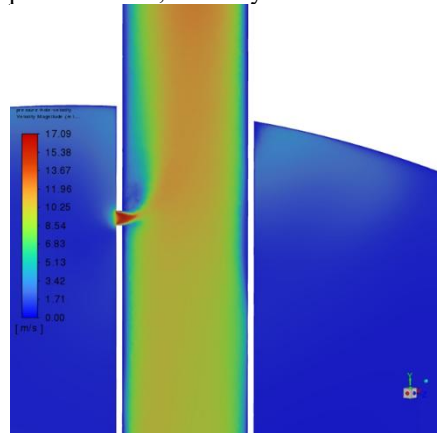


Figure 3: gas refrigerant flow behavior at the pressure hole.

2.4 influence of oil hole diameter to oil mass flow rate

Oil mass flow rate of NO.1 accumulator is 3.59g/s, which is less than the mass flow rate at inlet, so oil stays in the accumulator. Oil shortage problem happens.

Oil mass flow rate of No-2 is larger, but still less than inlet, so risk is still not solved 100%;

Oil mass flow rate of No.3 is larger than inlet, so there is not risk. This is consistent with experimental results.

	No-1	No-2	No-3
Oil Hole Diameter(mm)	2.0+1.5mm	3mm	2.5mm
Pipe Diameter(mm)	41mm	41mm	28.6mm
Pressure Hole Diameter(mm)	3mm	3mm	3mm
mass flow rate of oil(g/s)	3.59	4.85	7.86

Table 3: oil mass flow rate.

3. CONCLUSIONS

The VOF model can calculate the mass flow rate of oil for various accumulator design scenarios, and monitoring the changes in mass flow rate can help identify potential oil shortage risks. The detailed insights from VOF can aid designers in better comprehending the oil's movement within the accumulator, providing strong support for accumulator design.

ACKNOWLEDGEMENT

This work was supported by Johnson Controls - Hitachi Air Conditioning Technology (Wuxi) Co., Ltd.

REFERENCES

- [1] Ansys_Fluent_Theory_Guide
- [2] Oil Manufacturer's operation manual

Technical Trends and Risk Management of Heat Pumps Using Flammable Refrigerant

Minkyu JUNG^(a), Soyeon KIM^(b), Minsung KIM^(c)

^(a) Department of Intelligent Energy and Industry, Chung-Ang University, Seoul, 06974, South Korea, mamba24@cau.ac.kr

^(b) Department of Intelligent Energy and Industry, Chung-Ang University, Seoul, 06974, South Korea, nuri36@cau.ac.kr

^(c) School of Energy Systems Engineering, Chung-Ang University, Seoul, 06974, South Korea, minsungk@cau.ac.kr

ABSTRACT

Heat pump systems are considered key devices for achieving the 2050 carbon neutrality goal. In automotive heat pumps, the refrigerant systems have transitioned to HFO refrigerants (such as R1234yf) to replace traditional HFC refrigerants due to F-gas regulations. However, the risks associated with PFAS (perfluorinated compounds) have recently been highlighted, and regulatory movements in Europe are prompting a shift towards natural refrigerants. Among the candidates for natural refrigerants, R290 is known as an appropriate alternative for heat pumps due to its low GWP (Global Warming Potential) and ODP (Ozone Depletion Potential), along with excellent thermodynamic properties. However, due to R290's high flammability as an A3 refrigerant, considerations regarding operational conditions, installation environments, and explosion risks are needed. This paper aims to introduce various applications of heat pumps using R290 refrigerant and review international technological trends for ensuring safety when using flammable refrigerants.

Keywords: Heat pump, Flammable refrigerant, Propane, R290, Safety measure

A novel two-stage type II absorption thermal battery with low charging temperature for high temperature lift

Zhixiong DING, Wei WU*

School of Energy and Environment, City University of Hong Kong,
Hong Kong, 999077, China, weiwu53@cityu.edu.hk

ABSTRACT

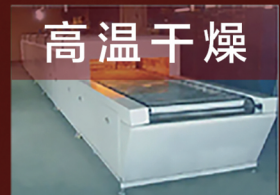
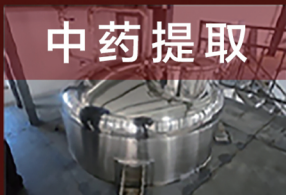
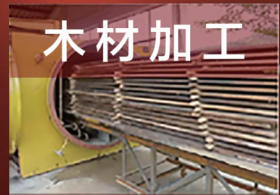
Renewable energy utilization is a critical way to carbon neutrality. Although most renewable energy sources are abundant, they are usually at low grade and unstable or even intermittent, which results in difficulty in direct utilization. Thermal battery, also known as thermal energy storage, plays an important role in eliminating the mismatches between the renewable energy and end users in timing and intensity.

However, the input temperatures of the conventional thermal batteries, including sensible and latent thermal batteries, are always higher than the output temperatures, which means that the heat output is at a lower grade than the heat source. Therefore, the conventional thermal batteries cannot address the low-grade problem. Absorption thermal battery (ATB) demonstrates not only an excellent energy storage performance, but also a unique ability of temperature upgrading, which provides a promising solution for the utilization of low-grade renewable energy.

This study proposed a novel two-stage type II ATB to further lower the charging temperature and improve the temperature lift. Dynamic simulation has been conducted to investigate and compare the performance of the basic and two-stage type II ATBs. Results indicate that the two-stage type II ATB can be charged under extremely low temperatures, e.g., ~ 50 °C. The temperature lift is improved from 30 °C to 60 °C under a charging temperature of 70 °C. Moreover, the energy storage density and efficiency are also significantly enhanced. This study can provide theoretical references and suggestions for the development of ATB technology for low-grade renewable energy utilization.

Keywords: Absorption Thermal Battery, Two Stage, Low Grade, Temperature Lift, Energy Storage Density.

格力大容量高温离心式热泵



好热泵 格力造
格力空气能热泵



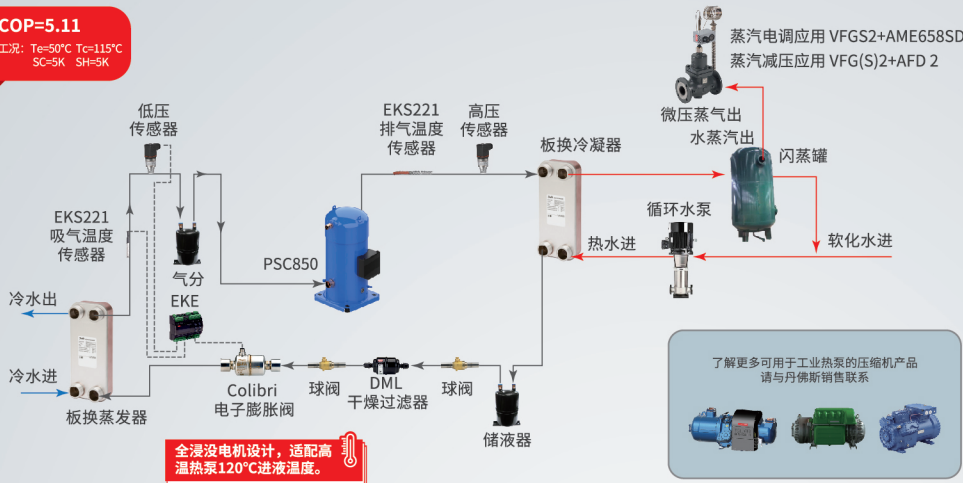
丹佛斯工业热泵整体解决方案



丹佛斯HFC/HFO制冷剂系统工业热泵解决方案

COP=5.11

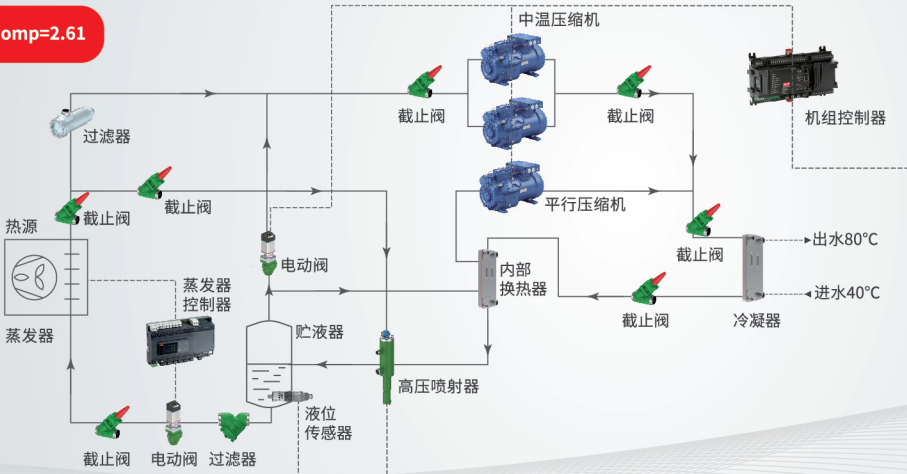
工况: $T_e=50^{\circ}\text{C}$ $T_c=115^{\circ}\text{C}$
SC=5K SH=5K



丹佛斯 HFC/HFO 制冷剂系统工业热泵解决方案, 采用极简设计, 实现高可靠, 高效能, 高经济性的工业热泵系统, 帮助用户取得极好的项目 ROI (投资回报率), 助力企业实现 ESG 目标。

丹佛斯CO₂制冷剂系统工业热泵解决方案

COP_{comp}=2.61



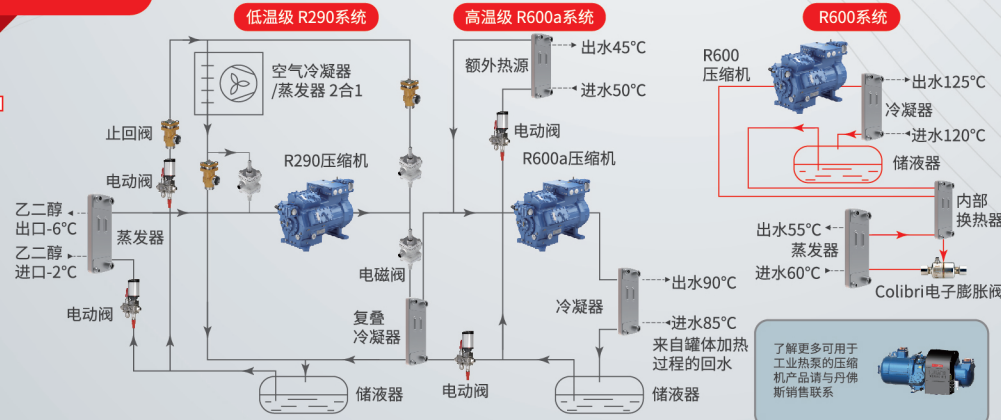
CO₂ 作为天然制冷剂, 符合环保政策要求, 无需担忧未来改造投资。丹佛斯以灵活的 CO₂ 解决方案, 同时满足功能性、成本效益和环保需求。

丹佛斯HC制冷剂系统工业热泵解决方案

COP_{comp}=2.05

制取90°C热水复叠系统

制取125°C热水系统



自然工质 HC 制冷剂, 凭借极低的 GWP 和出色的热力学性能, 即便在超过 100°C 的高温环境下, 仍能保持较高能效。作为您值得信赖的脱碳伙伴, 丹佛斯运用先进技术推动并保障 HC 热泵的环保、高效运行, 降低运营成本。我们深信: “节约下来的能源, 才是最绿色的能源。”

数字化动态平衡电动阀
DN15~250
ABQM
NOVOCON

电动调节阀
高流通能力, 大压差
AME65X, AME20/23
VFM2 DN15-250

动态平衡型电动调节阀
智能型压差控制器
大流量、大压差
DN15~250
AFQM2, AVQM AFP2

静态手动平衡
DN15~250
MSV-F2 MSV-D

可拆式板换



扫码查看丹佛斯工业热泵
应用更多内容

丹佛斯有着全面覆盖压缩机、换热器、阀门、控制器、变频器等产品在内的完善解决方案。从热源、管网分配、和末端控制三个主要环节出发, 构建起的一套能效提升和舒适体验的系统解决方案。

Performance comparison of different refrigerants in the frosting-defrosting cycles for air source heat pumps: R410A and R32 as an example

Shiquan Wang^(a), Wenzhe Wei^(a*), Wei Wang^(a, b*), Yuying Sun^(a), Zhaoyang Li^(a), Chengyang Huang^(a), Shiming Deng^(c, a)

^(a) Beijing Key Laboratory of Green Built Environment and Energy Efficient Technology, Beijing University of Technology
Beijing, 100124, China

^(b) School of Safety Engineering, Beijing Institute of Petrochemical Technology
Beijing, 102627, China

^(c) Department of Mechanical and Industrial Engineering, Qatar University
Doha, 2713, Qatar

*Corresponding author, E-mail address: weiwzhe@126.com (W. Wei); mrwangwei@bjut.edu.cn (W. Wang)

ABSTRACT

With the development of refrigerant substitution technology, existing studies have focused extensively on the environmental impact index, thermodynamic performance, safety, and economics of different refrigerants. However, the effect of different refrigerants on the frosting performance for air source heat pumps (ASHPs) is neglected. To fill the research gap above, this paper investigated the effects of different refrigerants on the frosting performance for ASHPs, including variations of heating capacity reduction, frosting rate, and optimal defrosting initiating time, using R410A and R32. Then based on the experimental data from 21 ASHPs with different configurations and operations, two prediction models for the frosting performance and the optimal defrosting initiating time were established.

The experimental results show: Under the frosting condition of 2/1°C, when the characteristic index for configuration and operation (*CICO*) of R410A ASHPs is 5, 10, 15 and 20, the operation time of 5% reduction of heating capacity is 32.7min, 66.1min, 97.9min and 136.2min respectively, and the optimal defrosting initiating time is 38.3min, 69.0min, 90.3min and 118.6min respectively. Meanwhile, for R32 ASHPs with the same condition, the operation time of 5% reduction of heating capacity is 22.5min, 41.0min, 57.1min and 71.5min respectively, and the optimal defrosting initiating time is 27.1min, 44.4min, 61.3min and 77.5min respectively. It can be seen that compared with R410A refrigerant, the frosting rate of R32 ASHPs is 31%~48% faster, and the defrosting initiating time should be advanced by 29%~35%.

Therefore, different refrigerants have a significant effect on the frosting-defrosting performance of ASHPs. The configurations and operations of ASHPs need to be optimized for different refrigerants to ensure efficient operation in frost conditions.

Keywords: Air source heat pumps, Refrigerants, Frosting performance, Optimal defrosting initiating time, Different configurations and operations

Experimental Performance Analysis of Superhydrophobic Heat Exchanger in Active-passive Combined Frost Suppression Mode

Qingqing XING^(a), Yaqi LI^(a), Fan ZHAO^(a), Yaxiu GU^{(a) (b)}

^(a) School of Civil Engineering, Chang'an University, Xi'an 710061, China

^(b) State Key Laboratory of Green Building in Western China, Xi'an University of Architecture & Technology, Xi'an 710055, China

ABSTRACT

The frost suppression performance of superhydrophobic surfaces decreases significantly in the late frost stage. In this paper, the air source heat pump active-passive joint frost suppression method is adopted, and the experimental investigation of superhydrophobic modification is combined with reverse defrosting and hot gas bypass defrosting respectively, and the control strategy under different defrosting methods is determined based on the temperature difference control method. The experimental results show that regardless of the surface properties, reasonable defrost control can effectively improve the heat absorption performance of the heat exchanger. Different defrosting methods have different optimal defrosting points, and the two defrosting methods also show obvious differences in energy consumption during multiple defrosting cycles. It has been proved that the superhydrophobic heat exchanger shows excellent performance in the active-passive combined defrost suppression mode, while the ordinary heat exchanger has a significant impact on its heat transfer performance due to the retention of defrost water. In this study, the combination of superhydrophobic heat exchanger and two traditional defrosting modes to reduce defrosting energy consumption provides data support for the wide application of superhydrophobic modification technology.

Keywords: Defrost Strategies, Superhydrophobic, Air Source Heat Pumps, Frosting, Active.

Commercializable superhydrophobic coating for air source heat pumps frost suppression

Zhiping Yuan^{*(a)} Yu Mao^(a), Sicheng Fan^(a), Jinbo Li^(b), Rixin Li^(b), Shan Tong^(b)

^(a) Department of Energy and Power Engineering, School of Mechanical Engineering, Beijing Institute of Technology

100081 Beijing, China, nikolatesal@live.com

^(b) Guangdong Midea Refrigeration Equipment Co., Ltd
Foshan, 528311, China

ABSTRACT

Superhydrophobic technology offers a potential solution to the persistent issue of frost formation on heat pump evaporators. However, the practical application of this technology is currently constrained by factors such as cost, environmental impact, frost suppression performance, and durability. In this manuscript, we have developed a superhydrophobic coating that approaches the cost of widely commercialized hydrophilic coatings and is environmentally friendly with no VOCs. This coating can be efficiently applied to the surface of evaporators, benefiting from the self-propelled jumping phenomenon of condensate droplets under supercooling conditions. As a result, the coating significantly extends the defrosting cycle. Under standard frost testing conditions of 2/1°C, the defrosting cycle of a 1.5HP heat pump unit is extended from 50 minutes for hydrophilic coatings to 260 minutes, with a 23% increase in the unit's average heating capacity. In durability tests, the coating exhibits adherence, acid and alkali resistance, salt spray resistance, and UV resistance that meet corresponding standards. Moreover, after undergoing 1500 cycles of frost and defrost, the contact angle of the coating does not significantly decrease, and there is no noticeable change in its frost suppression performance.

Keywords: Anti-frosting Heat Pumps, Superhydrophobic, Evaporators, Energy Efficiency.

Investigation of Thermal Characteristics in Ground Source Heat Pump System with Phase Change Thermal Storage and Radiant Floor Heating

Yuanliang Liu^(a), Di Qi^(a,b,*), Zhimiao Yin^(a), Chuangyao Zhao^(a,b), Angui Li^(a,b)

* Corresponding author: qidiqita@sina.com; qidi@xauat.edu.cn (Di Qi)

(a) School of Building Services Science and Engineering, Xi'an University of Architecture and Technology Xi'an, 710055, China, qidiqita@sina.com; qidi@xauat.edu.cn (Di Qi)

(b) International Joint Laboratory on Low Carbon Built Environment, Ministry of Education of China Xi'an, 710055, China, qidiqita@sina.com; qidi@xauat.edu.cn (Di Qi)

ABSTRACT

Ground source heat pump systems can provide a stable heating source throughout the year, unaffected by outdoor temperature fluctuations. Additionally, phase change materials can balance indoor temperature, avoiding drastic temperature fluctuations, and thereby improving indoor comfort. Consequently, these technologies find extensive use in buildings. This study focuses on an office building in Jinan, Shandong, establishing a simulation model of a radiant floor heating system powered by a ground source heat pump system. Building load simulations were conducted to determine the heating capacity provided by the ground source heat pump. Additionally, phase change materials were integrated at the end of the system to analyze the thermal performance and thermal comfort under different supply water temperatures and flow rates. The results demonstrate that an increase in the water supply temperature and flow rate leads to a decrease in the coefficient of performance (COP) of the heat pump. Specifically, when the water supply flow rate is constant, an increase in the water supply temperature results in an increase in the average performance coefficient COPs of the total system. However, when the water supply temperature is constant, an increase in the water supply flow rate leads to a decrease in COPs. At water supply temperatures between 33-35°C, the indoor temperature of the system does not reach the set temperature. However, with a system water supply temperature of 36°C and a water flow rate of 5000 kg/h, the indoor temperature can reach the set temperature, providing suitable indoor thermal comfort. At this point, the system provides 8460 kWh of heating, with a total energy consumption of 3294 kWh, a system COPs of 2.57, and a heat pump COP of 5.56.

Keywords: Ground source heat pump; phase change thermal storage; thermal characteristics; floor radiant heating system

Heat pump assisted LiBr-water absorption thermal energy storage under low ambient temperature

Jinfang You^(a), Jintong Gao^(a), Ruzhu Wang^(a), Zhenyuan Xu^(a)

^(a) Engineering Research Center of Solar Power and Refrigeration (MOE), Institute of Refrigeration and Cryogenics, Shanghai Jiao Tong University Shanghai, 200240, China, xuzhy@sjtu.edu.cn

ABSTRACT

Absorption thermal energy storage (ATES) using LiBr-water as working pairs can realize high energy storage density and efficiency. However, for domestic hot water demands, the temperature lift ability and operable temperature range of LiBr-water ATES are still limit under low ambient temperature, such as winter in Northern China. In order to extend the application of LiBr-water ATES, this research proposes a heat pump

assisted LiBr-water ATES, which uses heat pump heating or cooling to adjust the ambient temperature into a proper range for ATES. When discharging for heating or domestic hot water supplication at low ambient temperature, the heat pump lifts the evaporation temperature of ATES. When charging and discharging for cooling at high ambient temperature, the heat pump can drop the condensation temperature and absorption temperature of ATES, respectively. By testing the domestic hot water supplication (65 °C output) and refrigeration (7 °C output) working conditions under high or cold ambient, the results shows that the heat pump assisted 3-phase LiBr-water ATES can maintain high energy storage density of 190 kWh/m³ and 210 kWh/m³, respectively. Moreover, a closed cooling tower is added to save the electricity consumption. Then, the electricity-heat conversion efficiency can achieve 2.22, 1.53, and 1.08 at 10 °C, 5 °C, and -9 °C ambient, respectively, while the electricity-cold conversion efficiency can achieve 1.46 at 28 °C ambient. This work is owing to widen the usage of ATES in different scenarios with low ambient temperature and help the cooperation between heat storage and heat pump.

Keywords: Thermal Energy Storage, Absorption, Heat Pump, Conversion Efficiency, Experiment

1. INTRODUCTION

Absorption thermal energy storage (ATES) with advantages of temperature lift/drop ability and high energy storage density (ESD) is considered as a potential widely used energy storage technology in China [1]. However, for ATES in some severe cold or hot ambient, large temperature lift/drop demand conflicts with high ESD performance while common water-based working pairs suffer from freezing risk, which will limit the application of ATES in China's diverse climate.

Air-source heat pump (ASHP) can manage temperature flexibly and efficiently [2]. In this research, an ASHP is used to afford part of large temperature lift/drop demand and adjust the ambient temperature into a proper range for LiBr-water ATES under cold or hot ambient. It believes that the ASHP assisted ATES can maintain the high performance of ATES in cold ambient and thereby broaden the usage of ATES in China.

2. HEAT PUMP ASSISTED ABSORPTION THERMAL ENERGY STORAGE

An ASHP assisted 3-phase LiBr-water ATES has been proposed as shown in Fig. 1, in which the ASHP connects with the heat exchanger in solution tank or water tank of ATES by a switchable water loop. To save the electricity consumption of ASHP, a closed cooling tower is added to connected with ATES and parallel with ASHP. It can provide cooling effect and replace ASHP under some ambient.

The setup was tested in a calorimetric chamber to simulate four typical cold or hot ambient as shown in Table 1. At the cold ambient (conditions 1~3), the heat pump lifts the evaporation temperature of ATES from ambient temperature to 35 °C when discharging for supplying domestic hot water while the condensation heat is released to the ambient by cooling tower when charging. At the hot ambient (condition 4), the heat pump drops the condensation temperature of ATES from ambient temperature to 15 °C when charging while the absorption heat is released to the ambient by ASHP when discharging for refrigeration.

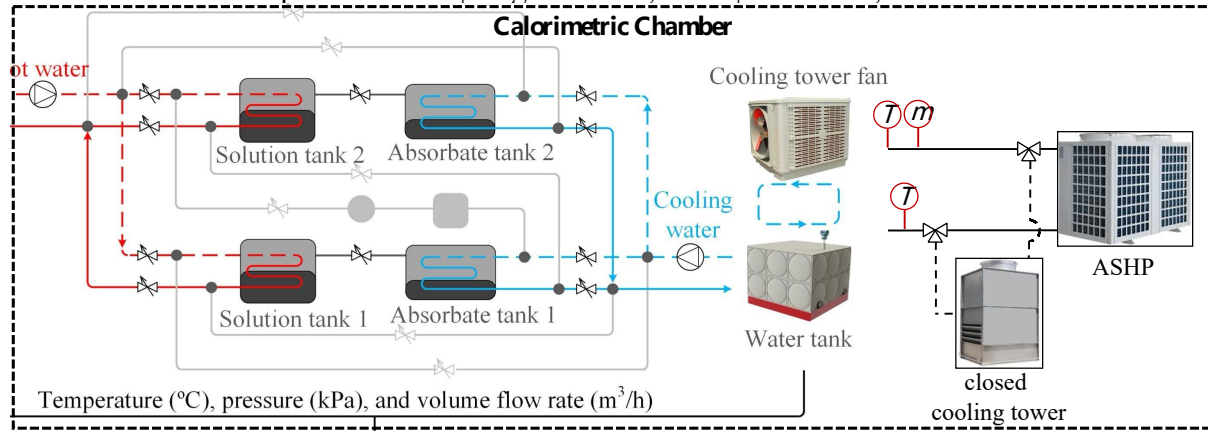


Figure 1: Experiment setup of ASHP assisted ATES.

Table 1: Experimental conditions and results.

Experimental condition	Ambient temperature (°C)	Demand	ESD of ATES (kWh/m ³)	ECOP of system
1-summer in cold region	10	65 °C	210	2.22
2-winter in hot region	5	(domestic hot water)	190	1.53
3-winter in cold region	-9	7 °C	190	1.08
4-summer in hot region	28	(refrigeration)	210	1.46

As can be seen in Table 1, when ambient temperature reduced from 10 °C to -9 °C, the ESD of ATES for domestic hot water does not change much, which is mainly due to the same operating temperature of ATES maintained by ASHP. However, the ECOP of the system decreased significantly because of decreased COP of ASHP and increased heat loss from system to environment with the reduction of ambient temperature.

3. CONCLUSIONS

The heat pump assisted 3-phase LiBr-water ATES can maintain high energy storage density with acceptable electricity-heat conversion efficiency when supplying domestic hot water or refrigerating under low or high ambient temperature, which opens up the possibility of widening the usage of ATES in different scenarios and cooperating between heat storage and heat pump.

ACKNOWLEDGEMENT

This work was supported by the National Natural Science Foundation of China (No. 52293411).

REFERENCES

- [1] Mehari A, Xu Z Y, Wang R Z. Thermal Energy Storage Using Absorption Cycle and System: A Comprehensive Review. *Energy Conversion and Management*, 2020, 206: 112482.
- [2] Fan Y B, Jiang L, Zhang X J, et al. Heat Pump Assisted Open Three-Phase Sorption Thermal Battery for Efficient Heat Storage. *Energy Conversion and Management*, 2023, 277: 116630.

益于地球 始于荏原

Ebara-Always Benefiting The Earth

百年荏原 再献扛鼎力作



高效离心式冷水（热泵）机组

- ◆ 空调 / 热泵 / 蓄冰
- ◆ 制冷量范围：500~5000USRt
- ◆ 两级压缩，一级经济器
- ◆ 环保冷媒R134a/R245fa



吸收式冷水（热泵）机组

- ◆ 非电空调：蒸汽、热水、烟气、燃气等多种驱动热源
- ◆ 两段式蒸发、吸收循环
- ◆ 冷量范围：40USRt~3330USRt / 制热量500kW~8000kW
- ◆ 连续8000小时不停机



消雾节水型冷却塔

- ◆ 单塔能力范围：25~5500m³/h
- ◆ CTI, JCI国际认证
- ◆ 高效可靠
- ◆ 消雾节水



荏原冷热系统（中国）有限公司

EBARA REFRIGERATION EQUIPMENT & SYSTEMS (CHINA) CO.,LTD.

地址：山东省烟台市福山高新技术产业区永达路720号
电话：(0535) 6321588 6988668 传真：(0535) 6325372
邮编：265500

Http://www.ebara-ersc.com
E-mail: market@ebara-ersc.com



www.ebara-ersc.com

Optimization of Sorption Thermal Battery for heat pump water heater applications

Ja Ryong Koo^(a), Hyung Won Choi^(a), Yong Tae Kang^{(b)*}

^(a) School of Mechanical Engineering, Korea University, 145 Anam-ro, Seongbuk-gu, Seoul 02841, Republic of Korea, 2023010990@korea.ac.kr

^(b) School of Mechanical Engineering, Korea University, 145 Anam-ro, Seongbuk-gu, Seoul 02841, Republic of Korea, chw000186@korea.ac.kr

^(c) Research Center for Plus Energy Building Innovative Technology, School of Mechanical Engineering, Korea University, 145 Anam-ro, Seongbuk-gu, Seoul 02841, Republic of Korea, ytkang@korea.ac.kr

ABSTRACT

Decarbonizing the heating and cooling system in buildings is crucial for realizing a plus-energy building with negative carbon emissions. The heat pump is a key strategy for achieving electrified thermal energy management. This study presents a novel system consisting of air source heat pump (ASHP) paired with sorption thermal battery (HPSTB) and compares HPSTB with the conventional water heater, which consists of the heat pump with hot water tank. The time required to reach the required temperature of hot water is reduced by employing thermochemical energy storage compared to sensible heat storage. The required storage volume is drastically reduced under the condition of supplying the same amount of heat. The dynamic characteristics of the sorption thermal battery (STB) are observed using an unsteady dynamic model employing H₂O/LiBr as working fluid. A feasibility study is investigated to compare the performance of the HPSTB with 16 kg of the solution charged and the conventional heat pump water heater with 200 L of H₂O under the conditions of meeting the same amount of heat demand estimated at 2.3 kWh. The time taken to obtain 90 °C of hot water with the HPSTB is estimated at 6000 sec, representing 71.4 % reduction in the required time compared to using a sensible heat storage. The HPSTB achieves 214.8 kWh/m³, while the conventional heat pump water heater shows 11.44 kWh/m³, 18.8 times larger. The HPSTB represents 72.5 % reduction in the required heat input to meet the demand of 2.3 kWh, indicating that HPSTB is more efficient in energy saving than the conventional water heater.

Keywords: COP, ESD, Heat pump water heater, Sorption thermal battery, Thermochemical energy storage

1. INTRODUCTION

Buildings account for 40% of total energy consumption and 25% of greenhouse gas emissions, highlighting the need to implement both existing technologies and innovative solutions to reduce CO₂ emissions efficiently. Heat pump water heaters are more energy-efficient than the conventional boilers but face temporal and spatial disparities between demand and supply, often requiring large hot water tanks that increase system size and heating time.

STB, which store and supply heat via the absorption and generation processes of refrigerants and solutions, presents a viable solution through thermochemical energy storage. This method offers a higher energy storage density (ESD) than sensible or latent energy storage. In the systems of equivalent size, it allows operation with a minimal amount of working fluid, leading to shorter charging/discharging times and reduced heat requirements.

This study proposes a novel combined system of ASHP and STB for building heating and hot water supply. Simulation analysis is conducted to optimize operating points, resulting in increased ESD, shorter heating times, and reduced amount of required heat input.

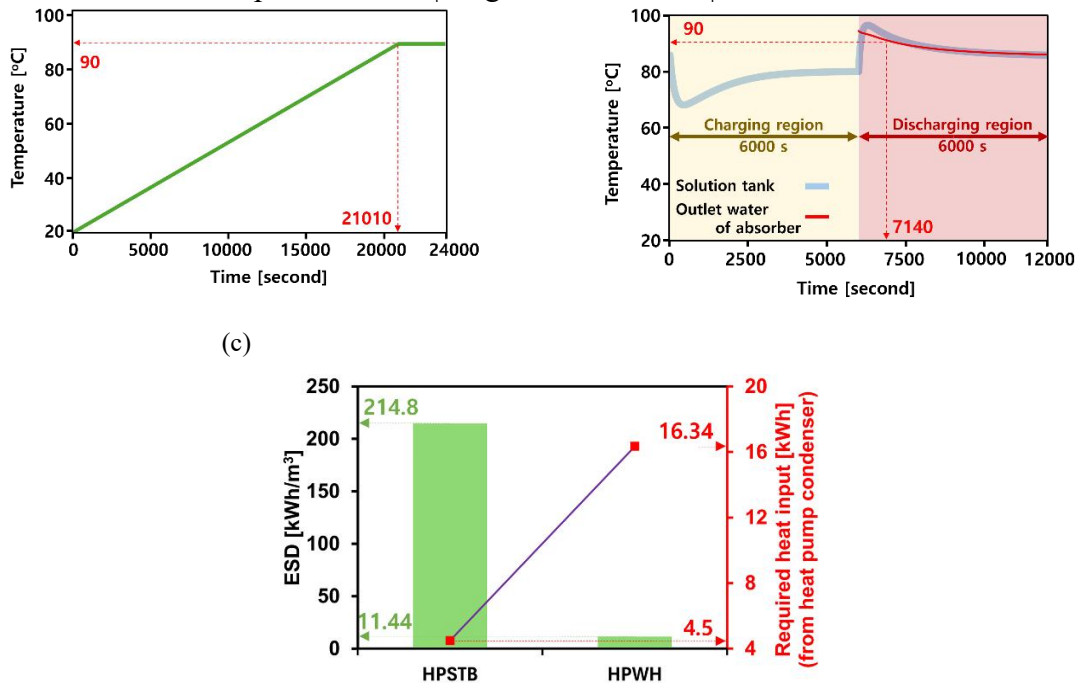


Fig. 2 (a) Temperature of heat pump water heater while heating, (b) Temperature of solution tank and outlet water from absorber of STB, (c) Comparison of ESD and required heat from ASHP

3. CONCLUSIONS

The proposed heat pump integrated sorption thermal battery water heater utilizes a sorption thermal battery with a high ESD. It was found that the proposed HPSTB system required a shorter charging time and a smaller amount of heat input compared to the existing heat pump water heaters of the same output scale.

REFERENCES

- [1] Kim, M., Kim, M. S., Chung, J. D., 2004, Transient thermal behavior of a water heater system driven by a heat pump. *International journal of refrigeration*, 27(4), 415-421.
- [2] Hepbasli, Arif, and Yildiz Kalinci, 2009, A review of heat pump water heating systems., *Renewable and Sustainable Energy Reviews* 13.6-7: 1211-1229.
- [3] Choi, Hyung Won, Jinhee Jeong, Yong Tae Kang, 2024, Optimal discharging of solar driven sorption thermal battery for building cooling applications, *Energy*, 296: 131087.

Simulation and Experimental Study on the Structural Optimization of Cabinet Dryers

Yilin GAI^(a, 1), Enyuan Gao^(b, 1), Zhongbin ZHANG^(a*), Xiaolin WANG^(c)

^(a) School of Energy and Mechanical Engineering, Nanjing Normal University, Nanjing 210046, Jiangsu, China, zhangzhongbin@163.com

^(b) Chinese Association of Refrigeration, Beijing 100142, China

^(c) School of Engineering, The Australian National University, Canberra, ACT, 2601, Australia

ABSTRACT

Energy recovery systems are designed for low-temperature storage of grain to avoid energy waste. The energy recovered can be used for the heat pump dryer in the food industry. However, the non-uniform internal airflow field still remains a problem for heat pump drying. This paper aims to optimize the uniformity of air distribution in a heat pump cabinet dryer, in order to improve performance of the drying equipment and energy recovery efficiency of the energy recovery system by managing the airflow in heat and mass transfer

areas. In this paper, six heat pump cabinet dryer models are designed based on a traditional dryer model, and numerically studied through Computational Fluid Dynamics modelling to determine the configuration that produces the most satisfying airflow uniformity for drying. Experimental validations are performed for both unloaded operations with perforated and non-perforated pallets, respectively, and loaded operations. The effects of air velocity, temperature, humidity and heat and mass transfer are analyzed. According to the simulation results, the configuration with top supply, middle air return, and 4° inclination angle is optimal. It is also found that the air supply velocity of 1.5-2.5 m/s results in the best air uniformity while the air temperature has an insignificant influence. A study on the physico-chemical and sensory properties of dried product using the selected dryer model is conducted. Results show that, with the reformed structure, baffle configuration and perforated pallets, the heat pump dryer manifests satisfying airflow uniformity and good drying performance, which can optimize the utilization efficiency of the energy recovery system.

Keywords: Heat Pump Drying, Structural Reconstruction, Air Distribution Optimization, Computational Fluid Dynamics

1. INTRODUCTION

Combining a heat pump drying system with an energy recovery system can significantly improve energy utilization efficiency during the drying process, reduce operational costs, and ensure the quality and consistency of dried foods. This integrated system is not only applicable to food drying but can also be extended to other drying fields that require high efficiency and energy savings, such as wood, medicinal herbs, and chemical products drying.

The heat pump drying system plays a crucial role in the food drying industry. It is highly efficient and energy-saving, environmentally friendly, and capable of recovering and utilizing the heat discharged during the drying process, thereby improving energy utilization efficiency. Typically, it saves 30-50% more energy compared to traditional drying methods[1], making it the preferred choice for many food processing enterprises. However, ineffective airflow management can increase the energy consumption during the drying process, thereby raising the drying costs of food materials[2].

In a heat pump cabinet drying system, the efficiency of the heat pump and the internal structure of the cabinet dryer have the greatest impact on energy consumption, with structural influence accounting for up to 30% of the total energy savings of the entire system. The uniformity of air distribution within the dryer is critical, as it affects both drying efficiency and the quality of the dried products.

2. HEAT PUMP DRYING AND ITS SIMULATION & EXPERIMENTAL STUDY

In a conventional heat pump drying cabinet, the air inlet and outlet are located at opposite ends of the same cabinet wall, with the heat and mass transfer zone situated between them. In the cabinet dryer, aside from the trays holding the materials to be dried, there are no other structures, resulting in uncontrolled airflow drying the materials. This study aims to numerically design and optimize the heat pump cabinet dryer and conduct experimental validation to draw attention to airflow management in convective dryers for fruits, vegetables, and other agricultural products. Taking an ordinary cabinet dryer for fruits and vegetables as the research object, six CFD models were established. The study investigated the uniformity of airflow distribution in the heat pump cabinet dryer.

Various constructed models were studied to explore the effects of baffle placement, wall inclination angle, and inlet/outlet positions on the uniformity of airflow distribution in the heat and mass transfer zone. By comparing the models, it was found that the model with top air supply, middle air return, and a 4° inclination angle of the side walls (Fig. 1a) achieved the best uniformity in both airflow speed and temperature. The temperature and airflow speed in the drying area were able to meet the drying requirements effectively (Fig. 1b, c).

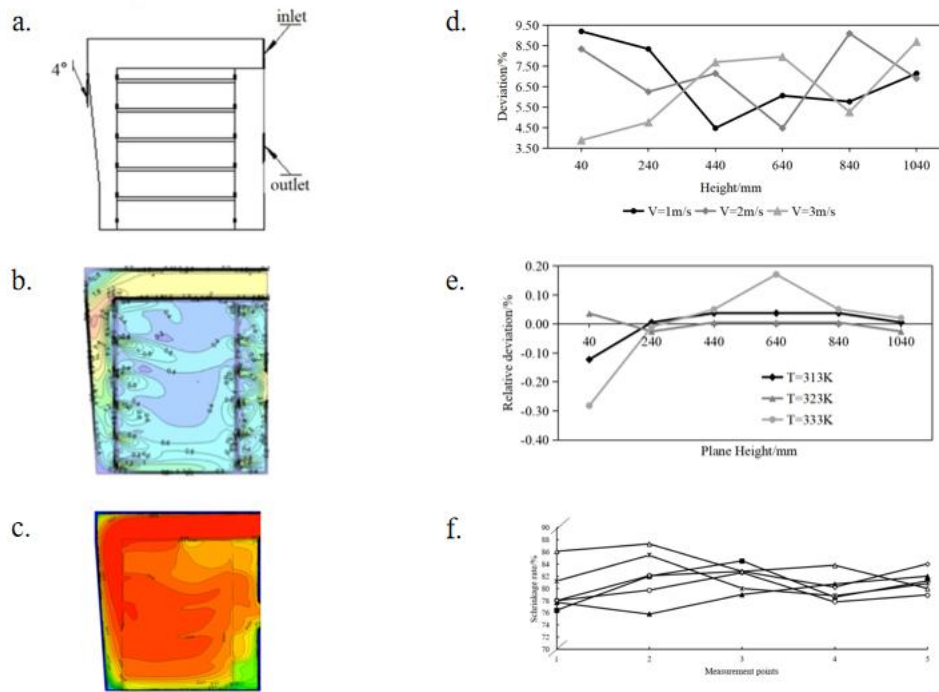


Figure 1: Research on the heat pump drying cabinet: Optimal allocation (a), Simulation of velocity distribution of the optimal structure model at $T=313$ (b), Simulation of temperature distribution of the optimal structure model at $V=2$ (c), Deviations between simulation and experimental results (d), Temperature deviation during no-load experiment (e) and Shrinkage rate of dried material during load experiment (f).

Unloaded and loaded experiments were conducted on the selected optimal structural configuration. Figure 1d shows the deviation between the simulation and experimental results, which remained within 10% under various conditions, indicating a good match between the simulation and experimental results. In the unloaded experiment, with an inlet air speed of $V=2\text{m/s}$, the temperature deviation within the drying area was within $\pm 0.3\%$ (Fig. 1e), demonstrating good uniformity. In the loaded experiment, the dried materials were evaluated for quality and sensory characteristics. The shrinkage rate of the products in different locations remained between 75% and 85% (Fig. 1f), and the smell and taste were good, proving excellent drying uniformity and effectiveness.

3. CONCLUSIONS

The modified structure of the heat pump cabinet dryer ensures good drying uniformity within its interior. Under unloaded conditions, when air velocity was 1.5–2.5 m/s, the internal air distribution was more uniform. The temperature working condition of 313 K yielded the best uniformity. In general, compared to air temperature, air velocity was found to have more effects on uniformity.

ACKNOWLEDGEMENT

This work was supported by the Postgraduate Research & Practice Innovation Program of Jiangsu Province, China (S11330BY1803).

REFERENCES

- [1] K. In'am, F. Jürgen, B. Ruben, B. Derek, 2020, Solar-thermal driven drying technologies for large-scale industrial applications: State of the art, gaps, and opportunities. *International Journal of Energy Research* 44 (13):9864-9888.
- [2] Y. R. Sekhar, A. K. Pandey, I.M. Mahbubul, G. R. S. Avinash, V. Venkat, R. P. Nitin, 2021, Experimental study on drying kinetics for Zingiber Officinale using solar tunnel dryer with thermal energy storage. *Solar Energy* 229:174-186.



智慧申菱 · 数字能环 垂直一体解决方案

满足功能 | 提升性能 | 优化节能

方案
规划



系统
设计



设备
定制



集成
实施



调试
验收



智慧
总控



智能
运维



广东申菱环境系统股份有限公司（证券代码：301018）成立于2000年，公司主营业务围绕专业特种空调为代表的空气环境调节设备开展，集研发设计、生产制造、营销服务、集成实施、运营维护于一体，致力于为数据服务产业环境、工业工艺产研环境、专业特种应用环境、公共建筑及商用环境等应用场景提供专业特种空调设备、数字化的能源及人工环境整体解决方案。

广东申菱环境系统股份有限公司
Guangdong Shenling Environmental Systems Co., Ltd.

📍 地址：广东省佛山市顺德区陈村镇机械装备园兴隆十路8号
☎ 全国客服：4008-330-888 🌐 网址：www.shenling.com



Experimental Study and Numerical Optimization of Heat Flow Characteristics in Dense Tobacco Drying Room

Tang Sheng^(a), Li Ming^{(b)*}

^(a) Solar Energy Research Institute, Yunnan Normal University, Kunming, Yunnan 650500, China, tang000402@163.com

^(b) Solar Energy Research Institute, Yunnan Normal University, Kunming, Yunnan 650500, China, lmllldy@126.com

ABSTRACT

The drying performance of dense tobacco drying room has a significant impact on the drying quality of tobacco leaves, and the drying quality of tobacco leaves is closely related to the index of airflow in the drying room. This article adopts the methods of porous media model and regional rotating fan model to study the velocity and temperature fields inside the drying room, and obtains the distribution pattern of heat flux field inside the drying room. The research results indicate that the uniformity of the internal heat flow in the drying room before optimization is poor, with non-uniform coefficients of temperature and velocity of 0.576 and 0.631. The airflow converges at the air outlet and the back of the drying room, creating vortices. The experimental results and simulation calculation results fit well, with an error within 10%. By optimizing the box structure, the uniformity of heat flow organization inside the dense tobacco curing room was ultimately improved, and the non-uniformity coefficient was increased to 0.701, which was 6% higher than the original structure, thereby improving the drying quality of tobacco leaves in the curing room.

Keywords: Tobacco Drying ,CFD, Numerical Simulation ,Structural Optimization

Effect of Waste Heat Recovery on the Thermal Performance of Heat Pump Drying Systems

Solomzi M. NGALONKULU^(a), Zhongjie HUAN^(b)

1. ^(a) Tshwane University of Technology 1
Pretoria, 0002, South Africa, ngalonkulus@tut.ac.za

^(b) Tshwane University of Technology 2
Pretoria, 0002, South Africa, HuanZ@tut.ac.za

ABSTRACT

The performance of an air source heat pump drying (ASHPD) system varies significantly compared to other heat sources for the heat pump, and its performance is strongly influenced by ambient temperature. This study experimentally evaluated the thermal performance of an air source heat pump drying system with waste heat recovery for operating at 20 °C to -10 °C ambient temperature environments in open, semi-closed and fully closed configurations.

The results show that waste heat recovery enhanced the evaporator temperatures by 1.5 °C and 9.4 °C in the semi-closed and fully closed configurations, respectively, leading to the heating capacity increase of 6.7% and 30.7%. Consequently, the overall coefficient of performance (COP) improved by 4.2% and 16.9%. However, due to higher condenser pressure, the fully closed configuration was limited to operate at 10 °C to -10 °C ambient temperature range. Nonetheless, decreasing ambient temperatures resulted in a pronounced COP degradation of 29.6% and 29.7% in open-loop and semi-closed configurations and 19.9% in the closed-loop configuration.

The results from this study emphasise the importance of waste heat recovery in enhancing HPD system thermal performance, crucially addressing COP degradation in cold ambient conditions. It also stresses the impact of air-loop configuration on HPD system efficiency, suggesting fully closed configurations for colder seasons or climates and open or semi-closed configurations for warmer seasons or regions. These insights facilitate the optimisation of HPD system design and operation across varying environmental conditions, promoting energy efficiency and sustainability in drying processes.

Keywords: Heat pump drying, waste heat recovery, ambient temperature, thermal performance, COP

Performance study of the Reverse Brayton air cycle drying system for agricultural application

Xinyi WEI, Qing CHENG

School of Energy Science and Engineering, Nanjing Tech University, Nanjing, 211816, China,
chengqingny@njtech.edu.cn

ABSTRACT

Drying is a very important part in the field of agriculture, which requires a lot of energy. The air temperature and humidity control is the focus of attention in crop growth, which is also an important dimension to measure the quality of the crops. Current drying methods in the agricultural including electric heating and air source heat pump, while the electric heating can lead to high energy consumption, and the air source heat pump may not reach the ideal temperature when the environment is harsh. In this paper, the reverse Brayton air cycle drying system is proposed to get high temperature and low humidity air quickly by adjusting the pressure ratio. Meanwhile, an improved reverse Brayton air cycle drying system with a water cooler is proposed to improve the system drying efficiency. When the compression ratio is 3.0 and the environmental air temperature is 28 °C, the temperature of air supplied to crops of the system with the water cooler can reach 63.7 °C, and the humidity content of the air supplied to crops is 0.0075 kg/kg_{DA}. Furthermore, the total dehumidification rate of the improved system can reach 9.35 g/s, which is improved by 1.49 g/s compared with the reverse Brayton air cycle drying system. The dehumidification energy efficiency of the improved system can reach 0.82 kg/(kW·h), which is improved by 0.1 kg/(kW·h) compared with the reverse Brayton air cycle drying system. The reverse Brayton air cycle drying system for agricultural application can ensure the stability of the drying process, reduce energy consumption and environmental pollution, and achieve the sustainable agricultural development.

Keywords: Reverse Brayton air cycle, Drying system, Agricultural drying, Dehumidification, Pressure ratio.

1. INTRODUCTION

Drying is considered one of the most effective methods for preserving food in agricultural storage [1]. In developing countries like India, sun drying is the most commonly used method for drying agricultural products. Many scholars have made significant advancements in drying technology, developing a range of highly efficient, energy-saving, and environmentally friendly drying equipment [2]. The integration of the reverse Brayton cycle with drying allows for increased drying efficiency while reducing energy consumption, thereby achieving energy conservation and environmental protection goals. This paper proposes two drying systems based on the reverse Brayton cycle, which use compressor adjustments to achieve high-temperature, low-humidity air, thus regulating the temperature and humidity of agricultural products.

2. REVERSE BRAYTON AIR CYCLE DRYING SYSTEMS

In this paper, a drying system based on the reverse Brayton air cycle is presented in Fig. 1(a), which consists of a compressor, a heat exchanger and expander, and a motor. High temperature and low humidity air is obtained quickly by adjusting the pressure ratio. Meanwhile, an improved reverse Brayton air circulation drying system with the addition of a chiller is proposed. Compared with this system, we proposed an improved drying system with the addition of a chiller, as shown in Fig. 1(b), where we added a chiller behind the heat exchanger so that the system heat dissipation can reach a thermal equilibrium.

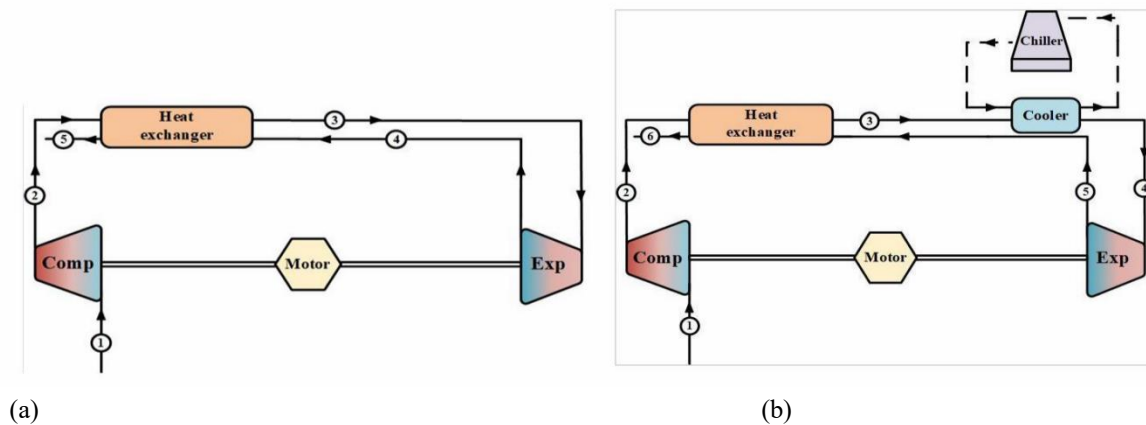


Figure 1: Schematics of reverse Brayton air cycle drying systems: (a), original system (b), an improved system.

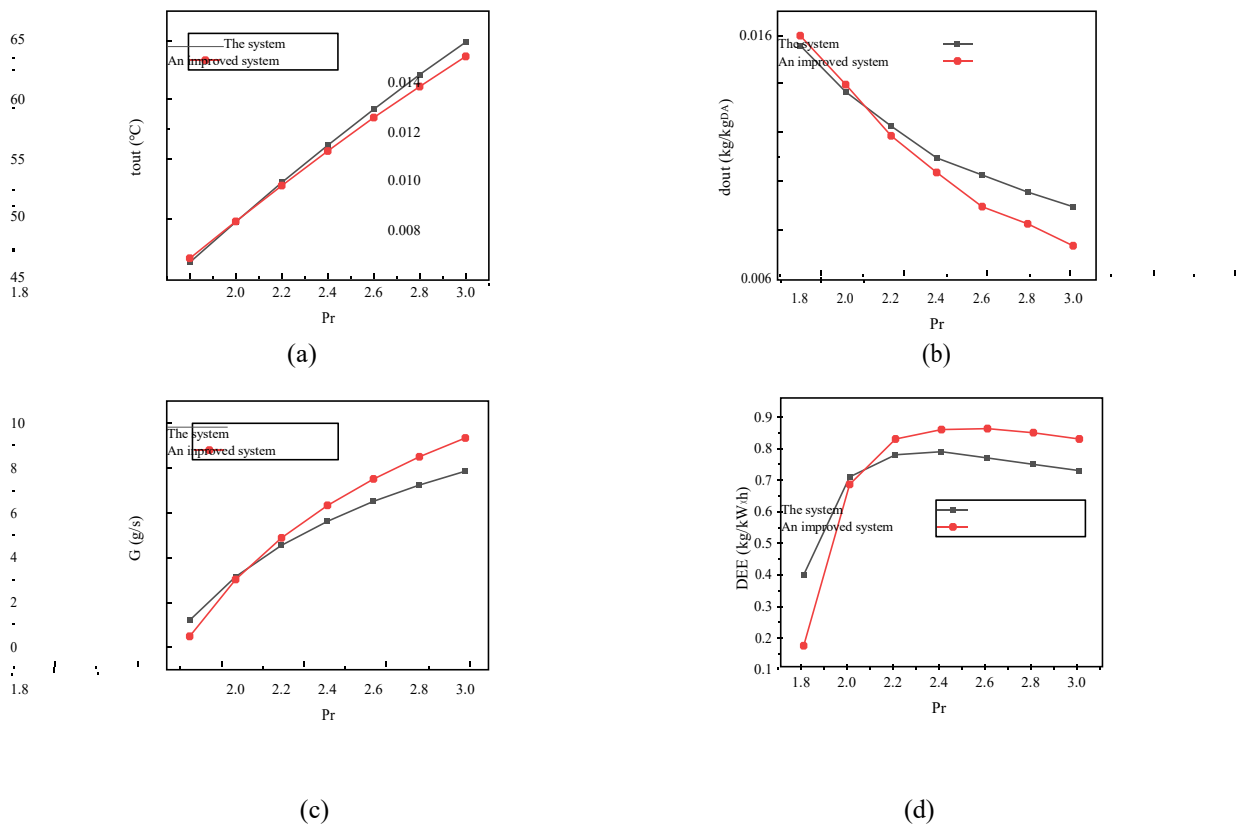


Figure 2: Relationship between pressure ratio and system performance parameters: (a), outlet temperature (b), outlet humidity (c), G (d), DEE .

The relationship between the system pressure ratio and the export air temperature is shown in Fig.2(a), as the pressure ratio increases the export air temperature of the system continues to rise, the pressure ratio of 3.0, the improved system export air temperature of 63.7 °C, the original system export air temperature of 64.8 °C is not much difference, both reach high temperature status. Fig. 2(b) shows the relationship between the pressure ratio and the moisture content of the outlet air, at the air temperature entering the system is 28 °C, the moisture content of the outlet air of the improved system is 0.0075 kg/kgDA at the pressure ratio of 3.0, which is reduced by 0.002 kg/kgDA compared with the original system. as shown in Fig. 2(c), at the entering air temperature of 28° C, the moisture content of the outlet air of the improved system is 0.0075 kg/kgDA. compressor, the dehumidification rate (G) of the two drying systems showed an increasing trend as the pressure ratio increased from 1.8 to 3.0. When the pressure ratio reaches 3.0, the G of the conventional system reaches 7.86 g/s, and the G of the improved system reaches 9.35 g/s, which is an improvement of 1.49 g/s compared with the original system.

The relationship between the pressure ratio and the dehumidification energy efficiency (DEE) of the drying systems is shown in Fig. 2(d), where the DEE of the two drying systems firstly increases and then decreases with the increase of the pressure ratio from 1.8 to 3.0 at an air temperature of 28 °C entering the compressor. At a pressure ratio of 3.0, the DEE of the original system reaches 0.72 kg/kW·h, and that of the improved system reaches 0.82 kg/kW·h, which is an improvement of 0.1 kg/kW·h compared to the original system, indicating that the improved system has higher dehumidification energy efficiency compared to the original system This indicates that the improved system has higher energy efficiency of dehumidification compared with the original system.

3. CONCLUSIONS

For the existing drying technology, two drying systems based on the reverse Brayton cycle are proposed in this paper. The effects of pressure ratio and inlet air temperature, cold source temperature on the system performance are studied, and the system COP , G and DEE are also compared. and for different crops, the drying end working conditions required by different crops are analysed, and the results of the analyses show that:

(1) The two drying systems based on the reverse Brayton air cycle proposed in this paper can quickly get the air supplied to the crops for high temperature drying by adjusting the pressure ratio, comparing with the traditional electric heating and air source heat pump drying methods.

(2) The use of chiller can be utilised to dissipate heat by contacting water with the air, so that the humidity content of the air supplied to the crops can be reduced. When the humidity is 0.0075 kg/kgDA at an inlet air temperature of 28 °C and a pressure ratio of 3.0, the air supplied to the crops for drying has a lower humidity content compared with the original system, which indicates that it has a better drying effect.

(3) Higher G and DEE of the improved system, when the pressure ratio is 3.0, the G of the improved system can reach 9.35 g/s, which elevates the total dehumidification rate G by 1.49 g/s compared with the original system; the DEE of the improved system can reach 0.82 kg/kW·h, which is elevated by

0.1 kg/kW·h, which is more conducive to obtaining high-temperature dry air to supply crops for drying.

ACKNOWLEDGEMENT

This research work in this paper was supported by National Natural Science Foundation of China (No. 52176008).

REFERENCES

- [1] M.A. Kusekwa, A review on the renewable energy resources for rural application in Tanzania, Renewable Energy-Trends and Applications, (2011) 978-979.
- [2] N.S. Rathore, N.L. Panwar, Experimental studies on hemi cylindrical walk-in type solar tunnel dryer for grape drying, Applied Energy, 87 (2010) 2764-2767.

Optimization and performance analysis of semiconductor heat pump clothes dryers

Xinyu ZHANG, Qing CHENG

School of Energy Science and Engineering, Nanjing Tech University
Nanjing, 211816, China, chengqingny@njtech.edu.cn

ABSTRACT

At present, the commonly used clothes dryers are based on electric heating and air source heat pump dehumidification, but small-scale household clothes dryers are still mainly electric heating, which has large energy consumption. The semiconductor heat pump has the advantages of simple structure, low noise, and high heating coefficient under the condition of small temperature difference. In order to improve the energy efficiency and portability of small-scale household clothes dryers, three semiconductor heat pump drying systems (a closed system combining semiconductor and electric heating, a closed system combining two semiconductor heat pumps, and an open system with heat recovery) are developed in this paper. The theoretical models of drying systems are established, and air temperature, humidity, moisture content of the three systems are analyzed under different working conditions. Meanwhile, the energy consumption of the three systems is evaluated based on the semiconductor heating COP and the whole system heating COP. It is found that the COP of the open system with heat recovery is the highest, which can reach 2.184. The semiconductor heating COP of the closed system combining two semiconductor heat pumps is 1.5. The overall heating COP of the closed system combined with semiconductor and electric heating is about 1.082. Among the three semiconductor heat pump drying systems, only the closed system that combines semiconductor and electric heating uses electric heating for auxiliary heating, the closed system that combines two semiconductor heat pumps has the most complex structure, and the open system with heat recovery has the simplest structure. In conclusion, the application of semiconductor heat pumps to the optimization of small-scale household clothes dryers has good environmental benefits and contributes to the energy saving of household appliances.

Keywords: Drying, Semiconductor heat pump, Clothes dryer, COP, Waste heat recovery

Efficiency Analysis and Optimization of Heat Pump Systems for Urban Sludge Drying: A Comparative Study of CO₂ and R134a Circulation

JilinRen^(a)

(A) Xi'an Jiaotong University
Xi'an, 710049, China, renjilin9917@stu.xjtu.edu.cn

ABSTRACT

Urban sludge is a sub-production of sewage water treatment, which has been an inevitable issue for environment management. It is very necessary to heat sludge up to a high temperature before recycling and landfill. In this paper, we presented four kinds of heat pump systems for sludge drying and compared the features of different systems. Next, based on the numerical model in Dymola, we calculated the working data of the four systems. With the contrast of the calculation results, it is obvious to find that cascade structure can improve the efficiency of heat pump system because the circulation makes full use of the heating capacity of CO₂ heat pump. Moreover, we concluded the most appropriate utilizing occasion of the four systems and the advantages of CO₂ and R134a cascade system. Also, the reasons of these phenomena were analyzed from two aspects: enthalpy- moisture factors and thermal-dynamic factors. Finally, it can be seen that cascade structure of CO₂ circulation and R134a circulation has excellent efficiency when working condition requires lower moisture

content of sludge at outlet, which results from not only the balance between temperature and moisture content of drying air but also the appropriate working conditions provided by cascade structure. The analysis and results in this paper can be regarded as a good application guide for trans-critical CO₂ heat pump circulation, which contributes to the promotion of trans-critical CO₂ heat pump in this research and technical region.

Keywords: Sludge Drying, Carbon Dioxide, Heat Pump, Thermal-dynamic factors.

Performance Analysis of a Semi-Open Heat Pump Drying System in South African Climatic Conditions

Solomzi M. NGALONKULU^(a), Zhongjie HUAN^(b)

^(a) Tshwane University of Technology 1
Pretoria, 0002, South Africa, ngalonkulus@tut.ac.za

^(b) Tshwane University of Technology 2
Pretoria, 0002, South Africa, HuanZ@tut.ac.za

ABSTRACT

In this study, the operational conditions and the thermal performance of a semi-closed heat pump drying (HPD) system using R134a refrigerant were experimentally investigated in the laboratory at varied ambient temperatures to assess its applicability in the South African climate. The ambient temperatures were controlled and examined from 20 °C to -10 °C at increments of 10 °C.

The results show that the ambient temperatures play a significant role in the operating conditions and the thermal performance of the semi-closed heat pump drying system as the ambient temperature decrease resulted in the decrease of the suction pressure, the discharge pressure, and the compression ratio by 57.1%, 64.6%, and 17.3%, respectively. Furthermore, due to the refrigerant density significantly dropping with the decrease in ambient temperature, the refrigerant mass flow rate decreased by 54.9% from 0.0175 to 0.079 kg/s, consequently reducing the coefficient of performance (COP) of the heat pump drying system by 29.7% from 3.7 to 2.6.

The significant degradation of the COP of the semi-closed HPD in cold ambient conditions emphasises the impact of air-loop configuration on the thermal performance of the HPD system, suggesting the applications of semi-closed configurations for warmer regions of the country or warmer seasons.

Keywords: Heat pump drying, ambient temperature, thermal performance, mass flow rate, COP

Experiments on off-design performance of PV driven refrigerated warehouse based on vapor compression refrigeration with ice thermal storage

Hanwen Rao^(a), Ming Li^{(a)(b)}, Yiting Yang^(a), Yan Yang^(a), Ying Zhang^{(a)(b)}

^(a) School of Energy and Environment Science, Yunnan Normal University
Kunming, 650500, China, zhangying@ynnu.edu.cn

^(b) Key Laboratory of Solar Heating and Cooling Technology of Yunnan Provincial Universities, Yunnan Normal University, Kunming 650500, China, zhangying@ynnu.edu.cn

ABSTRACT

Nowadays, almost 22% of fruits and vegetables are wasted in the process of post-harvest to distribution in the world. As the first kilometer construction in cold chain logistics, photovoltaic driven refrigerated warehouses with ice thermal storage play a vital role to preserve the agri-fresh fruits and vegetables in rural areas. However, due to the variable ambient temperature, solar irradiance, adjustable compressor speed and expansion valve opening, such system inherently operates under off-design operation conditions, resulting in system performance deterioration. In this regard, this paper designed and built a 2 kW platform of vapor compression refrigeration cycle with ice thermal storage of which the refrigerate was R410A with a charging amount of 2 kg. The effects of compressor speed and expansion valve opening on the system temperature, pressure, flow rate, supercooling and superheating were tested, and thereby the off-design performance with functionality limitations were revealed. For the test on the effects of compressor speed, the ambient temperature and expansion valve opening was constant at 26 °C and 80%, respectively. As the decrease of the compressor speed from 1800 rpm to 1000 rpm, the system cooling capacity decreased from 4.7 kW to 2.8 kW, while the COP increased from 2.4 to 3.05. The optimum operating condition of the system was at 1400 rpm, with the cooling capacity of 3.9 kW and COP of 2.7. For the test on the effects of expansion valve opening, the compressor speed and the ambient temperature was constant at 1400 rpm and 11 °C, respectively. As the decrease of the expansion valve opening from 100% to 70%, the system cooling capacity decreased from 4.25kW to 1.78kW, and the COP decreased from 3.1 to 1.3. The optimum expansion valve opening was 100%. The research enables to give a guidance for the control strategy of system under off-design operation conditions.

Keywords: functionality limitations, ice thermal storage, Off-design performance, refrigerated warehouses

Study on the Optimal Working Conditions of Closed Trans-critical CO₂ Heat Pump Drying System

WangTAO^(a), ZhanDENGYI^(a),
HeZHILONG^(b), DongBENZHAO^(a), FuSHAOCHUN^(a)

^(a) Zhengzhou University of Light Industry Zhengzhou,
460000, China, wangtao@zzuli.edu.cn

^(b) Xi'an Jiaotong University
Xi'an, 710049, China, zlhe@mail.xjtu.edu.cn

ABSTRACT

The work aims to develop a thermodynamics model of a drying system powered by trans-critical CO₂ heat pump and obtain the optimal working condition. The thermodynamic model couples the CO₂ cycle and the air cycle. And the program data was compared with experimental data, with errors within an acceptable range, verifying the correctness of the model. Based on the model, The temperature, enthalpy, relative humidity and moisture content of air in the drying cycle are calculated, as well as the temperature, pressure and enthalpy of CO₂ in heat pump system. The coupling mechanism between air cycle and CO₂ heat pump cycle is explored by varying the air temperature after condensation and drying. The optimal CO₂ discharge pressure in the closed drying system under different working conditions is obtained. The results shows that the system has an optimal operating condition. Furthermore, the thermodynamic parameters of the closed drying system under typical process are obtained. The thermodynamic model developed provides a theoretical basis for construction of the

closed drying system (the lectotype of fans, heat exchangers, compressors, etc.) and development of system control methods.

Keywords: Heat Pump Drying, Closed Drying Cycle, Trans-critical CO₂ System, Energy Efficiency Analysis.

Simulation and optimization of solar phase change heat storage heat pump integrated system

Rui XU^(a), Fang LIU^(a,b,c)

^(a) College of Energy and Mechanical Engineering, Shanghai University of Electric Power
2103 Pingliang Road, Yangpu District, Shanghai, 200090, PR China,

*e-mail: fangliu@shiep.edu.cn

^(b) Beijing Key Laboratory of Demand Side Multi-Energy Carriers Optimization and Interaction Technique
(China Electric Power Research Institute), Beijing 100192, China

^(c) Shanghai Non-carbon energy conversion and utilization institute, Shanghai 200240, China

ABSTRACT

In order to improve the penetration rate of renewable energy in the integrated energy system, this paper establishes a solar non-direct expansion heat pump system, and adopts a multi-objective non-simultaneous dynamic optimization strategy to improve the comprehensive performance of solar transcritical CO₂ heat pump with phase change heat storage system in the energy charging process. At the same time, photovoltaic and photothermal are used to increase the temperature on the evaporator side of the heat pump, thereby improving the energy efficiency of the heat pump and providing some of the electric energy required for the operation of the heat pump. The dynamic model of the integrated system was established using Dymola, and the performance of the heat pump was studied by selecting suitable phase change materials. In addition, a single-objective optimization strategy based on the model is established to optimize the geometric parameters of the system and the multi-objective non-direct dynamic optimization strategy is used to obtain the optimal operating parameters. Compared with the pre-optimization period, the COP of the system after coupling optimization is increased by 12.5%, and the average heat storage of the system is increased by 13.65%.

Keywords: Solar heat pump, PCM thermal storage, Nonlinear dynamic system model, Structure and control co-optimization.

Design and Application of a Multi-Objective Optimization Framework for Identifying Optimal Operating Conditions in Hybrid Heat Pump Systems

Junzhuo Wei^(a), Di Wu^(a,b), R.Z. Wang^(a*)

^(a) Institute of Refrigeration and Cryogenics, Shanghai Jiao Tong University, 800 Dongchuan Road, Shanghai, 200240, China

^(b) Shanghai Nuotong New Energy Technology Co., LTD, 1391 Humin Road, Shanghai, 200241, China

ABSTRACT

In recent years, an increasing number of complex hybrid absorption compression heat pump (HACHP) have been developed. Assessing the potential of these systems, particularly in terms of their optimal operating conditions, has become a critical metric. However, due to the unique structural characteristics of HACHP systems, multi-objective optimization algorithms face numerous challenges in practical applications. This research has designed and

implemented a multi-objective optimization framework specifically for HACHP systems to establish a universal optimization method. This framework is capable of handling more than three optimization objectives and addresses several common issues encountered during the optimization of heat pump systems, such as identifying implicit constraints between variables, thoroughly exploring the solution space, and managing sudden changes in objective values. Through this framework, decision-makers can effectively balance conflicts between various objectives and select solutions that best meet their needs and priorities.

Keywords: HACHP, Multi-objective optimization, NSGA-III, Algorithm

1. INTRODUCTION

To achieve greater temperature rises while obtaining better system performance, hybrid absorption-compression heat pump (HACHP) presents a highly promising configuration. Currently, the combination methods of vapor compression heat pump (VCHP) and absorption heat transformer (AHT) sub-cycles in HACHPs mainly include direct coupling and thermal coupling. In direct coupling, the compressor is directly integrated into the absorption cycle. Kim et al.^[1] directly connected the compressor between the generator and absorber, significantly expanding the temperature range of the heat pump for industrial waste heat recovery, achieving the goal of replacing a 90°C hot water boiler with a waste heat recovery heat pump. In terms of thermal coupling, Zhang et al.^[2] achieved a three-stage absorption-compression heat pump by coupling the condenser of the VCHP with the evaporator and absorber of the AHT, resulting in a temperature rise of up to 150°C when the input heat source temperature was 30°C.

Although combining VCHP and AHT is an effective method for achieving higher temperature rises and ensuring overall performance in heat pump systems, this combination also significantly increases the complexity of the entire system. This presents several challenges in the optimization practice of hybrid heat pump systems: managing the complex interdependencies between decision variables, identifying non-dominant solutions near the boundaries, and addressing the impact of abrupt changes on optimization accuracy.

Therefore, this paper designs a multi-objective optimization framework suitable for identifying optimal operating conditions in hybrid heat pump systems. Through differential evolution optimized symbolic regression (DEOSR), inequality expressions are generated to describe the interdependencies of system variables. Secondly, the designed diverse population initialization (DPI) method ensures that the initial population is broadly and uniformly distributed throughout the entire constrained feasible space, avoiding concentration in certain local areas during the search process. To address the abrupt changes, gradual convergence mutation (GCM) method is designed. In the early iterations, the mutation rate is high, allowing for extensive exploration of the solution space. As the evolutionary process progresses, the algorithm gradually reduces the mutation rate, enabling finer search precision in the later stages of optimization, thus mitigating the impact of the mutation phenomenon on the algorithm's results.

The multi-objective optimization framework designed in this paper can serve as a decision-support tool to evaluate the technical, economic, and environmental potential of newly designed HACHP systems. This method not only helps to understand the interrelationships between decision variables and optimization objectives but also reveals the potential correlations between optimization objectives. This framework provides strong support for the design and optimization of hybrid HACHP systems, ensuring optimal performance in all aspects.

2. METHODOLOGY

In the field of multi-objective optimization, the Genetic Algorithm (GA) has been enhanced into the Non-dominated Sorting Genetic Algorithm (NSGA)^[3] by implementing non-dominated sorting and crowding distance calculations for offspring selection. The improved version, NSGA-II^[4], introduces an elite preservation mechanism, significantly enhancing the algorithm's performance and efficiency, making it a standard in multi-objective optimization. When considering more than three objective functions, NSGA-III^[5] is a better choice due to its use of reference points, which improves exploration in high-dimensional objective spaces, offering higher efficiency and accuracy for more

complex multi-objective optimization problems. However, applying the NSGA-III method to practical hybrid heat pump systems still presents numerous challenges.

To address this, the DEOSR method is designed for the data preprocessing step, quantifying the constraints between variables in the form of inequalities. Additionally, DPI and GCM are used in the NSGA-III algorithm for initial population generation and mutation operations, respectively. This multi-objective optimization framework can be applied to optimize operating conditions of various hybrid heat pump systems.

2.1 DEOSR

Symbolic regression^[6] is a method used to find the optimal function form to describe data within a predefined space of mathematical expressions, variables, and constants. However, due to the random generation of constants in symbolic regression, it is often challenging to find the optimal constant values. Therefore, DEOSR method was designed to assist symbolic regression in searching for the optimal coefficient values within the expressions. After testing the performance of different differential mutation operators, an improved mutation operator based on DE/rand/2 was selected.

$$\mathbf{v}_i = \mathbf{x}_{r3} + F(\mathbf{x}_{r1} + \mathbf{x}_{r2} + \mathbf{x}_{r3} + \mathbf{x}_{r4}) \quad (1)$$

where $x_{r1}, x_{r2}, x_{r3}, x_{r4}$ are distinct individuals randomly selected from the population, and F is the scaling factor. In the practical application of hybrid heat pump systems, decision variables can be categorized into free independent variables (FIV) and constrained independent variables (CIV). The value space for FIVs constitutes a continuous rectangular domain referred to as the independent feasible space (IFS) for each variable. Conversely, the values of CIVs are restricted by the values of FIVs. Utilizing the DEOSR methodology, these constraint relationships can be articulated as inequalities, as demonstrated in Eq.2.

$$f_1(x_{FIV1}, x_{FIV2}, \dots, x_{FIVn}) \leq x_{CIV} \leq f_2(x_{FIV1}, x_{FIV2}, \dots, x_{FIVn}) \quad (2)$$

Compared to 'black-box' machine learning methods, DEOSR can explicitly derive specific inequality formulas between variables. This data preprocessing step ensures that subsequent optimization algorithms search within defined boundaries, which is crucial for the convergence and accuracy of the algorithm's results.

2.2 DPI

In the NSGA-III algorithm, obtaining a uniformly distributed initial population can significantly enhance population diversity, expand the coverage of the search space, and reduce the likelihood of converging to local optima. This approach aids the optimization algorithm in efficiently exploring the entire space during the early stages, quickly identifying potential solutions to the optimization problem, and improving global search efficiency.

To address this issue, the DPI algorithm was designed to reduce the number of sample points required to generate a uniform initial population under the inequality constraints calculated by the DEOSR method. When the number of generated sample points is set to m , the n FIVs in the HACHP will construct an $m \times n$ matrix A , where each column of A is a random permutation of the numbers from 1 to m . Subsequently, a matrix B of the same dimensions is constructed, where each element is an independently distributed random number from the interval (0,1). The elements of the sampling matrix S are determined by the following equation:

$$S_{ij} = F^{-1}\left(\frac{A_{ij} - B_{ij}}{m}\right)$$

F^{-1} denotes the inverse function of the cumulative distribution function, where for a uniform distribution, $F^{-1}(x)=x$. Subsequently, the elements of each row in matrix S are used to calculate the corresponding k -dimensional CIVs under given conditions. For the CIVs, the following independent procedure is carried out: Arrange matrix S in ascending order based on the range of values. Then, starting from the first row, randomly sample within the corresponding range. After each sampling, calculate the new value's grid index. If the new value is in the same grid as any existing value, repeat the sampling process.

This method ensures that the selected sample points satisfy the unique constraint relationships of each hybrid heat pump system. Moreover, it guarantees that the initial population generated is uniformly distributed across the entire value space, even with a limited number of sample points.

2.3 GCM

In HACHP, due to the presence of abrupt changes phenomena, the population requires smaller mutation rates in the later stages of iterations to achieve fine-tuned exploration by the algorithm. Therefore, the proposed GCM method in this paper allows for a relatively high mutation rate in the early stages of iterations, facilitating

thorough exploration of the solution space. As iterations progress, the mutation rate gradually decreases, enabling more detailed searches within the optimal solution space. The mutation rate pm is adjusted to control the number of individuals undergoing mutation, and the mutation strength b is modulated to control the extent of mutation. The ratio of the current iteration count t to the total number of iterations T is used to vary the mutation rate over time. The control formula is as follows:

$$\delta = \begin{cases} (x^{\max}(p) - x(p)) \cdot (1 - \text{rand}^{(1-t/T)^b}) & \text{rand} < 0.5 \\ (x(p) - x^{\min}(p)) \cdot (1 - \text{rand}^{(1-t/T)^b}) & \text{rand} \geq 0.5 \end{cases} \quad (3)$$

2.4 MULTI-OBJECTIVE OPTIMIZATION FRAMEWORK

In order to identifying optimal operating conditions of the HACHP system, this paper employs a mathematical modeling approach to transform the designed HACHP into a functional model. This model is capable of producing corresponding target outcomes based on varying input conditions. The inputs to this functional model are divided into two parts: control variables and decision variables. Control variables are declared prior to modeling to initialize components and typically remain constant throughout the modeling and optimization process. These usually include compressor efficiency, solution physical properties, and heat exchange temperature differences. Decision variables are key inputs during the optimization process, directly influencing the model's outputs and acting as independent variables. The output variables of the model typically include system performance indicators (such as coefficient of performance, exergy efficiency, second law efficiency, etc.), system output power, and mass flow rates.

Fig.1 illustrates the workflow of the multi-objective optimization framework. Starting with the construction of the HACHP system, it is then transformed into a corresponding functional model through mathematical modeling. In the preprocessing stage, the DEOSR method is used to establish inequality constraints among decision variables. Utilizing these constraints and predefined variable ranges, the DPI algorithm generates a uniformly distributed initial population, totaling N individuals. Subsequently, an offspring population Q_t is generated through crossover and GCM operations. This offspring population Q_t is then merged with the parent population P_t to form population R_t . Through non-dominated sorting and the reference point mechanism applied to R_t , the best N individuals are selected to form the next generation parent population P_{t+1} . After the iteration process concludes, the individuals in the final population P will constitute the Pareto optimal set for the system across all objectives. To find a single solution that simultaneously optimizes all objectives, this paper employs a weighted approach. By assigning weights to each objective variable, multidimensional objectives are transformed into a composite objective function. Thus, through the method of weighted summation, a unique optimal point can be identified on the Pareto frontier.

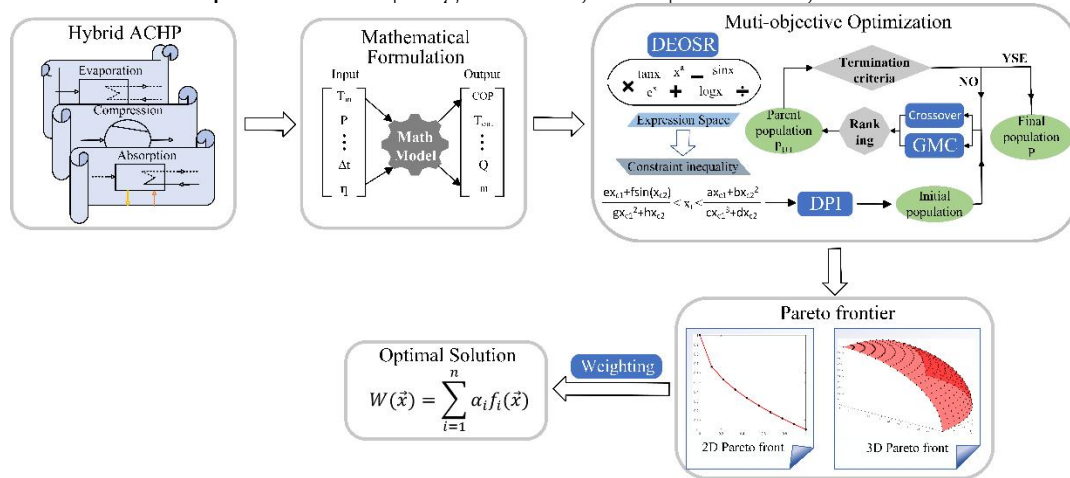


Figure 1: Flowchart of the multi-objective optimization framework

3. CASE STUDY AND RESULT

To validate the applicability of the proposed method in HACHP, this paper applies the designed multi-objective optimization framework to a typical thermally coupled HACHP system, as shown in Fig.2. Considering the system's design objectives and application scenarios, this case study selects temperature as the decision variable, including ambient temperature T_{env} , waste heat temperature T_{was} , coupling temperature T_{cou} , and output temperature T_{out} . The choice of target variables focuses on two crucial performance indicators in the heat pump system: system efficiency and thermal load. However, as there is no unified method for calculating system efficiency in hybrid heat pump systems, this paper employs three different methods of efficiency calculation: COP based on virtual work, second law efficiency based on thermodynamics, and exergy efficiency. For thermal load, the output thermal load Q is chosen as the target variable for investigation.

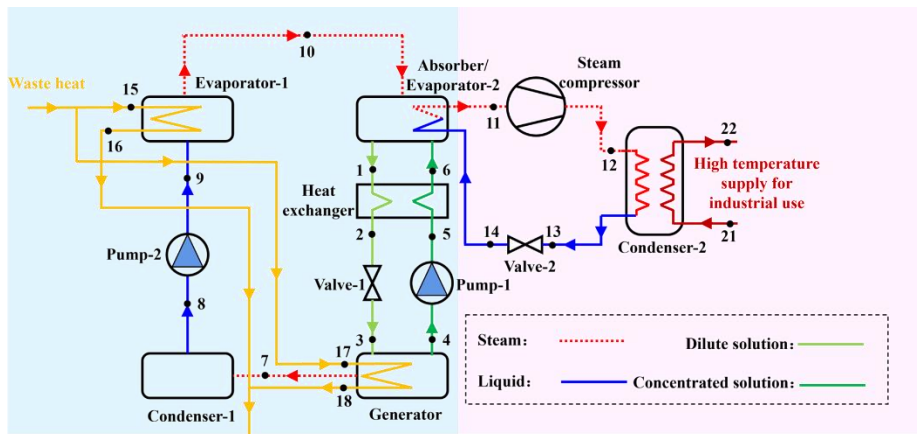


Figure 2: The schematic diagram of the thermally coupled HACHP system

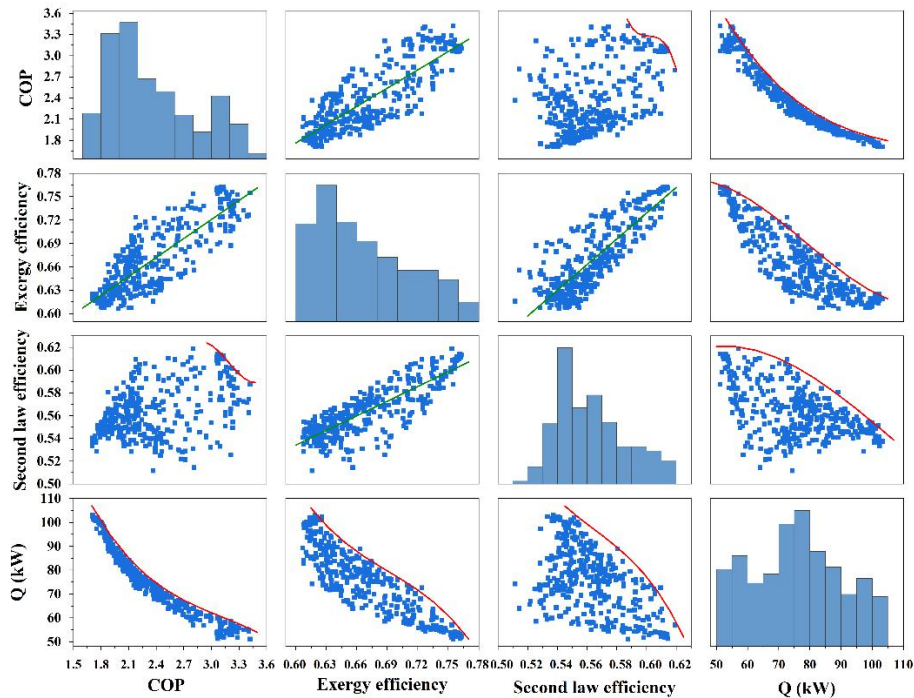


Figure 3: Non-Dominated Solution Set Scatter Matrix for Four-Dimensional Objective Variables of the System

The results of the multi-objective optimization for the system are shown in Fig.3. In this figure, the red lines represent the Pareto frontiers between two objectives, the green line represents the regression line for two positively correlated data sets. The histograms along the diagonal indicate the distribution density of the solution set for each objective variable. This comprehensive visualization helps in understanding the system's performance across multiple criteria. Due to the simultaneous consideration of multiple objective functions, the non-dominated solution scatter plot does not form a single curve (when variables are negatively correlated) or a single point (when variables are positively correlated), but rather spans an area. This area reflects the complex interactions and diverse optimal solutions among the various objective variables.

When two objective variables exhibit negative correlation, improvement in one lead to deterioration in the other. The Pareto frontier (represented by the red line) obtained through multi-objective optimization delineates the optimal solution set between these variables, where any point on this curve represents a solution set that cannot be simultaneously improved upon for both objectives. For instance, in the non-dominated scatter plot of COP versus Q, a COP of 3 corresponds to a Q value of 55 kW, indicating that at a COP of 3, the system can achieve a maximum output heat power of 55 kW. Conversely, when Q is 55 kW, the maximum achievable COP is 3. Through the Pareto frontier, decision-makers can select the optimal solution that best fits their needs. When two variables are positively correlated, improvement in one will simultaneously enhance the other, thus reducing the Pareto frontier to a single point. This point represents the optimal solution that simultaneously achieves both objectives. For example, in the scatter plot of COP versus exergy efficiency, the Pareto frontier point shows a COP of 3.45 and an exergy efficiency of 0.73, indicating this is the unique optimal solution, eliminating the need for decision-makers to choose among multiple optimal solutions. When equal weighting is applied to simultaneously optimize four variables, the results yield a COP of 3.3, exergy efficiency of 0.76, Second Law efficiency of 0.6, and thermal load Q of 51 kW. When only a subset of variables, such as COP and Q, the results indicate a COP of 2.58 and a thermal load Q of 68 kW. At this combination of COP and Q, the values of 0.66 for exergy efficiency and 0.55 for Second Law efficiency, as identified on the Pareto front, represent the optimal values achievable under the specific condition.

Additionally, Fig.3 can be utilized to verify the correctness of the designed system's performance calculation method. The graph displays that the output heat load Q exhibits a negative correlation with three different performance parameters, which substantiates the rationality of the COP calculation method based on virtual

work to a significant extent. Interestingly, in the non-dominated scatter plot of COP versus second law efficiency, there exists a very short Pareto frontier curve, yet over the majority of the value range, COP and second law efficiency show a positive correlation. However, as COP approaches its maximum value, it begins to show a negative correlation with second law efficiency, forming a very short segment of the Pareto frontier. This phenomenon may arise because second law efficiency represents the irreversible losses in the system. For a specific HACHP, there is an upper limit to the degree of irreversibility. Therefore, as the second law efficiency approaches its maximum within the optimization algorithm, any further increases in COP lead to significant declines in second law efficiency.

4. CONCLUSION

This paper successfully develops a multi-objective optimization framework by integrating the specially designed DEOSR, DPI, and GMC algorithms with the conventional multi-objective optimization algorithm NSGA-III, and applies it to the optimization of a typical thermally coupled HACHP system. The DEOSR algorithm can explicitly express the restrictive relationships between variables in the system using clear inequalities, while the DPI algorithm is capable of generating an initial population that uniformly covers the entire irregular value space of the variables and significantly reducing the number of required sampling points. The GMC algorithm refines the search process as the number of iterations increases. The constructed multi-objective optimization framework addresses several common challenges encountered when applying multi-objective optimization algorithms in complex HACHP systems, such as how to clearly articulate implicit constraints between variables; how to thoroughly explore the solution space to prevent missing extreme values near the boundaries common in heat pump systems; and how to handle sudden changes in objective values. Additionally, this framework adopts the reference point mechanism from the NSGA-III algorithm, thus removing the limitations on the number of objectives, unlike NSGA-II (which is typically limited to three or fewer objectives).

The non-dominated solution set obtained through this framework consists of solutions where no single solution outperforms others across all objectives, and each solution is optimal in at least one objective without showing complete inferiority in others. This type of solution set provides decision-makers with an effective means to balance conflicts between different objectives and choose the solution that best meets their specific needs and priorities. For example, in the case study presented in this paper, when prioritizing COP and Q, the optimal operating conditions for the system were found to be a COP of 2.58 and Q of 68 kW, with an exergy efficiency of 0.66 and a second law efficiency of 0.55. At this point, the corresponding decision variables for the system were T_{env} at 28.3°C, T_{was} at 69.7°C, T_{cou} at 87.1°C, and T_{out} at 163.2°C.

ACKNOWLEDGEMENT

This research was supported by the National Natural Science Foundation of China (52306019, 52036004), China Postdoctoral Science Foundation (BX2021175, 2022M712040).

REFERENCES

- [1] KIM J, PARK S-R, BAIK Y-J, et al. Experimental study of operating characteristics of compression/absorption high-temperature hybrid heat pump using waste heat [J]. *Renewable Energy*, 2013, 54: 13-9.
- [2] ZHANG X, HU B, WANG R, et al. Performance enhancement of hybrid absorption-compression heat pump via internal heat recovery [J]. *Energy*, 2024, 286.
- [3] SRINIVAS N, DEB K. Multiobjective optimization using nondominated sorting in genetic algorithms [J]. *Evolutionary computation*, 1994, 2(3): 221-48.
- [4] DEB K, AGRAWAL S, PRATAP A, et al. A fast elitist non-dominated sorting genetic algorithm for multi-objective optimization: NSGA-II; proceedings of the Parallel Problem Solving from Nature PPSN VI: 6th International Conference Paris, France, September 18–20, 2000 Proceedings 6, F, 2000 [C]. Springer.
- [5] DEB K, JAIN H. An Evolutionary Many-Objective Optimization Algorithm Using Reference-Point-Based Nondominated Sorting Approach, Part I: Solving Problems With Box Constraints [J]. *IEEE Transactions on Evolutionary Computation*, 2014, 18(4): 577-601.

绿色驱动，高效供热

EK“火凤凰”系列120°C工业高温热泵

高温性能压缩机

领先高温专用螺杆压缩机，配置闪蒸罐，稳定控制油温，提升性能。

高效换热技术

全新设计的分布式换热管与高效冷凝管，实现最佳换热效果，防结垢，提升系统性能。

高效油路控制技术

配置卧式高效油分离器和油泵，分油效率达到99.99%以上，确保恶劣工况下压缩机稳定供油。

低品位能源利用

利用35~75°C低品位能源，制取80~120°C高温热水，替代传统燃气、纯电、燃油锅炉。

环保冷媒

R245fa高温环保制冷剂设计，无臭氧层破坏，低维护成本，绿色健康。

智能数字控制

强弱电分离控制柜，大屏幕液晶显示，提供全面监控与安全保护。

宽热量范围覆盖



适用场所



锂电新能源



汽车制造



工业制药



石油化工



金属制品



食品行业



屠宰场



纺织印染

广东欧科空调制冷有限公司(南方基地)
地址:广东省东莞市黄江镇清龙路69号
网站:www.euroklimat.com.cn
电话:0769-83660888
传真:0769-83622528

天津欧科环境设备有限公司(北方基地)
地址:天津市武清区京津科技谷产业园
秀园道北侧10号
电话:022-58180659
传真:022-24383808



EK官方微信公众号

更高效 赢未来

霍尼韦尔热泵全系列解决方案, 让您领先一步布局未来

- | | |
|-----------------------|---|
| ● <60°C 低温热泵场景 | Solstice® 454B(HFO-454B)制冷剂 |
| ● 60°C~80°C 中温热泵场景 | Solstice® 513A(HFO-513A)制冷剂 |
| ● 80°C~100°C 高温热泵场景 | Solstice® N15(HFO-515B)制冷剂
Solstice® ze(HFO-1234ze)制冷剂 |
| ● 100°C~150°C 超高温热泵场景 | Solstice® zd(HFO-1233zd)制冷剂 |



扫描二维码下载资料



Honeywell

- [6] AUGUSTO D A, BARBOSA H J. Symbolic regression via genetic programming; proceedings of the Proceedings Vol 1 Sixth Brazilian symposium on neural networks, F, 2000 [C]. IEEE.

Research on Building Resistance-Capacity Model Identification and Indoor Temperature Prediction Based on Genetic Algorithm

Minglu QU^(a), Shanghe DU^(a), Zhen YU^(b), Huai LI^(b)

^(a) University of Shanghai for Science & Technology
Shanghai, 200093, China, quminglu@126.com

^(b) China academy of building research
Beijing, 100029, China, yuzhen@chinaibee.com

ABSTRACT

In order to accurately predict the indoor temperature of buildings, this study adopted the lumped parameter method to establish a building thermal resistance-capacity (RC) model. Corresponding differential equations were derived, and then the model was identified using genetic algorithms, resulting in accurate modeling of the RC indoor thermal response. The average absolute error and R^2 of the temperature in the RC model test set were 0.14°C and 0.99, respectively. Effective short-term prediction can be achieved using the adjusted RC model, with an R^2 of 0.71, providing a basis for optimizing control of the building energy system. Comparing with neural network MLP based black box model and XGBoost based black box model, less data samples are required for the indoor temperature prediction based on the RC gray box model. This paper also discussed the applicability conditions of black box and gray box models. It is necessary to choose appropriate modeling methods based on practical applications and considering factors such as model complexity, prediction accuracy, and interpretability.

Keywords: Indoor temperature prediction, Thermal resistance-capacity (RC) model, Genetic algorithm, Modeling.

A novel power output prediction framework based on an early labelling approach for open absorption heat pump

Yongbao Chen^(a*), Jun Ye^(b)

^(a) University of Shanghai for Science and Technology, Shanghai 200093, China, chenyongbao@usst.edu.cn

^(b) Jun Ye, Jiangsu Blue Sky Heat Transfer Technology Co., Ltd., Wuxi, 214203, China

ABSTRACT

An accurate prediction of power output is critically important for energy planning, optimization, and system performance evaluation in open absorption heat pumps and heating networks. With the development of data-driven modeling technology, extracting information from historical data has become widespread in the field of data-driven modeling. Feature engineering is a key factor in improving the performance of prediction models. Adding input features for different day patterns resulting from varying working situations and weather conditions can help enhance prediction accuracy. Traditionally, pattern labeling primarily focuses on finding a day similar to the prediction day based on the calendar or other information, such as weather conditions. The most intuitive approach for dividing historical time-series power output into patterns is clustering; however, the pattern cannot be determined before the output is known. To address this problem, this study proposes a novel

power output prediction framework integrating an early classification algorithm that uses a stochastic algorithm to create an early input feature representing the scale of future power output for the prediction days.

Additionally, a flexible feature selection strategy is introduced to tailor the proposed prediction framework to different practical scenarios of open absorption heat pumps. The proposed framework was validated using metered data from a practical open absorption heat pump case in Jilin province, China. The results demonstrate that the early labeling approach produces satisfactory prediction accuracy and significantly improves the prediction performance of the LightGBM model.

Keywords: Open absorption heat pump, Power output prediction, Data-driven modelling, LightGBM

Data-driven models when data is missing for heat pumps **Yang Song, Davide Rolando, Hatef Madani**

KTH Royal Institute of Technology
Stockholm, 10044, Sweden, yson@kth.se

ABSTRACT

The proliferation of smart sensors and cost-effective computational technologies has significantly advanced modern heat pump units, which are now equipped with numerous sensors generating extensive data daily. Despite the abundance of data, its utilization remains largely limited to real-time visualization and error alerting, with billions of entries each month underutilized by manufacturers. This study introduces data-driven models designed to harness this underexploited data along the data-information-knowledge-services pathway. Data resources are classified into two categories: high-quantity but low-quality measured data, and high-quality but low-quantity data, alongside non-measured catalog data. Data preprocessing techniques prepare this data for AI application, following which, tailored models are developed for different data types. Machine learning models such as ANNs, XGBoost, and Polynomial regression are employed for abundant, low-quality data, all models with RRMSE under 10%. These models can serve as soft-sensors, reducing costs and enhancing smart control, fault detection, and network planning. Conversely, for high-quality but scarce data like laboratory results, transfer learning models are developed with RRMSE under 7%, especially useful for evaluating heat pumps with new refrigerants or components. In scenarios devoid of measurements, catalog data supports the modeling process through an iterative cycle combining polynomial regression models from various sub-components, providing preliminary estimates of heat pump performance. Because these models are primarily black-box, obscuring underlying physical processes and complicating system fault diagnosis, the study addresses this limitation by developing semi-empirical models (with RRMSE between 20% to 35%) that offer deeper insights and improved diagnostic capabilities.

Keywords: heat pump, data driven, machine learning, semi-empirical model

Investigation on Multiple Degrees of Freedom Hybrid Modeling Method for High Temperature Heat Pump

Wenhui ZHUANG^(a), Shengming DONG^(a), Mingsen JIN^(a), Pengli HU^(a)

^(a) School of Mechanical Engineering, Tianjin University of Commerce, Tianjin, 300072, PR China,
dongshengming@tjcu.edu.cn

ABSTRACT

A reliable multiple degrees of freedom model is the foundation for optimizing the design of high-temperature heat pump (HTHP) under variable operating conditions, accurately evaluating specific architectures and formulating rapid response control strategies. However, for mechanism models, namely white box models, they are mostly

based on specific parameter assumptions under specific operating condition, resulting in low accuracy. The data-driven models, also known as the black box models, require large-scale data for training and give poor extensibility in most cases. Therefore, hybrid model (HM) of the HTHP endowed with both accuracy and extensibility is established by coupling the black box models and the white box models. Additionally, white box models mainly include evaporator and condenser models established by the lumped parameter method, adiabatic compression and isenthalpy expansion processes. The black box model is used to predict the isentropic efficiency of compressor by GA-BPNN, which is trained by experimental data. By introducing the Geysler Algorithm (GEA) as a solver, the efficient convergence issue of multiple degrees of freedom for inlet and outlet temperatures and flow rates on the heat source and heat sink has been solved. The results showed that among the 11979 HTHP configurations involved, 93.5% could converge within 50 iterations under the convergence condition of absolute error of total heat transfer area less than 0.1 m^2 .

Keywords: High-temperature Heat Pump, Hybrid Modeling, Multiple Degrees of Freedom, Variable Working Conditions

1. Introduction

High temperature heat pump (HTHP) has been widely accepted as an effective approach for decarbonizing energy-intensive industries, thus, becoming the main subject of many researchers. Indispensably, a reliable model of the HTHP system should be established, which is an important foundation of system design, optimization and operation. Therefore, great efforts have been made to investigate the HTHP modeling methods.

So far, the HTHP modeling method can be generally categorized into two types, that is, the white box model(WBM) based on thermodynamic mechanism and the black box model(BBM) based on the data-driven algorithm.

The WBM is the most common and productive method for HTHP model. Dai et al. analyzed the sensitivity of the newly configured heat pump system by establishing a dual evaporation temperature with an injector model, indicating that there was an optimum emission pressure to maximize the coefficient of performance^[1]. Wang et al. have analyzed the thermodynamic performance of an innovative jet rotary compressor air source heat pump by utilizing an empirical numerical model. The results indicated that compared with the air source heat pump using a conventional single-stage rotary compressor, the proposed injection structure could increase the heating capacity and COP by 23.1-28.2% and 4.5-8.1%, respectively^[2]. Verdnik et al. have established a thermodynamic model to investigate the influence of operating parameters on a high temperature heat pump, which was capable of raising the waste heat in the 40 to 60 °C range to temperature between subcritical 110 °C and transcritical operation 160 °C^[3].

For data-driven models based on machine learning algorithms, namely the BBM, Kong et al. established an artificial neural network model for predicting the mass flow rate of R290 in a direct expansion solar-assisted heat pump system using R290, suggesting that over 97% of the predicting results were consistent with the experimental data, with a maximum deviation of 10%^[4]. Esen et al. delved into the potential of artificial neural networks in forecasting the performance of horizontal ground coupled heat pump systems. The results showed that the most suitable number of neurons in the hidden layer was 7 and that the root mean square error (RMSE) value was 1%^[5]. Park et al. utilized both multiple linear regression (MLR) and artificial neural networks (ANN) to establish a model for predicting the hourly performance of ground source heat pump systems. They found that the prediction errors of MLR and ANN were 3.56% and 1.75%, respectively^[6].

Generally speaking, BBM gives significant advantages in accuracy and simplicity in handling complex and highly nonlinear relationships over the WBM. Instead, WBM is obviously superior in model extensibility and interpretability. Therefore, the exploration of the hybrid modeling method balancing the strengths of BBM and WBM tends to be essential and meaningful, while there are few studies about that, especially rare in HTHP modeling. Herein, by adopting BP-ANN, which is used to predict the isentropic efficiency, and mechanism models of the main HTHP components, a hybrid model(HM) with multi-degree of freedom is established. Additionally, a new meta-heuristic algorithm-GEA is adopted to solve the hybrid model. Specifically, it endows the HM with

impressive convergence efficiency and reliability, especially for the working conditions with their freedom degrees to be more than 1.

2. METHOD

The basic principle of the multi-degree of freedom hybrid model (MDFHM) is shown in Fig.1. It can be figured out that the model mainly consists of two parts, which are the hybrid model of HTHP and GEA. In addition, the characteristics of the above mentioned MFD are reflected in that two arbitrary parameters out of the heat sink and heat source's mass flow rate (m_{hs} , m_{hsi}), inlet temperature ($T_{in, hs}$, $T_{in, hsi}$) and outlet temperature ($T_{out, hs}$, $T_{out, hsi}$) are only required.

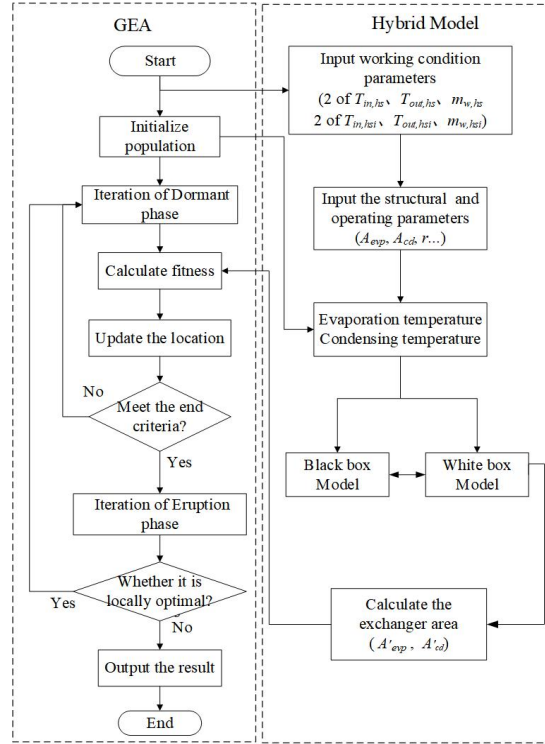


Fig. 1 Flowchart of the MDFHM

2.1 White box model of compressor

The WBM of the compressor, which allows for the calculation of the working fluid mass flow rate (m_r) by inputting the compressor displacement (V_h), volumetric efficiency (η_v) and rotation speed (r), is shown as Eq.1. In Eq.1, v stands for the specific volume corresponding to the working fluid state at the compressor inlet. In addition, the working fluid adopted in this study is R245fa.

$$m_r = \frac{\eta_v V_h r}{60v} \quad (1)$$

Eq.2 is used to calculate the isentropic efficiency (η_s) of the compressor, which is a key parameter to evaluate the compressor performance. Moreover, η_s is also adopted as the connected parameter between the BBM and WBM by determining the compressor outlet state of the working fluid.

$$\eta_s = \frac{e_{out,s} - e_{in}}{e_{out} - e_{in}} \quad (2)$$

where e_{in} and e_{out} represent the enthalpy values at the compressor inlet and outlet. The $e_{out,s}$ stands for the enthalpy value at the compressor outlet after the isentropic compression process.

2.2 White box model of the heat exchanger

The heat exchangers involved in HTHP are evaporator and condenser, where the heat exchange processes are phase-change transfer and non-phase-change transfer processes. As for the phase-change transfer process, the lumped parameter method is utilized by segmenting process into 50 microelements with equal heat transfer capabilities. For clarity and simplicity, the equations involved and the detailed explanations are listed in Table 1. Notably, the type of the evaporator and condenser is the plate heat exchanger and the heat dissipation is neglected.

Table 1 Equations involved in the heat exchanger WBM

No.	Parameter	Equation	Specification
(3) ^[7]	Heat transfer area	$A' = \frac{Q}{U \Delta t_m}$	Q - Heat rate U - Overall transfer coefficient Δt_m - Log mean temperature difference
(4) ^[7]	Overall transfer coefficient	$U = \frac{1}{\frac{1}{h_h} + \frac{\delta}{\lambda} + \frac{1}{h_c}}$	h_h, h_c - Convection heat transfer coefficients for the hot side and cold side δ - Thickness of plate λ - Thermal conductivity of plate
(5) ^[7]	Hydraulic diameter of flow channel	$D_h = \frac{4Wb}{2(W+b)}$	W - Channel width b - Channel spacing
(6) ^[7]	Mass velocity through the plate channels	$G = \frac{m_r}{N_{ch} \cdot b \cdot W}$	N_{ch} - Number of the plate channels
(7) ^[9]	Reynolds number	$Re = \frac{GD_h}{\eta}$	η - Viscosity of fluid
(8) ^[9]	Prandtl number	$Pr = \frac{c_p \eta}{\lambda}$	c_p - Specific heat of fluid
(9) ^[8]	Nusselt number of the single-phase flow	$Nu = 0.724 \left(\frac{6\beta}{\pi} \right)^{0.646} \times Re^{0.583} Pr^{1/3}$	β - Baffle angle of plate heat exchanger ($\beta=30^\circ$)
(10) ^[7]	Convection heat transfer coefficient	$h = \frac{\lambda \cdot Nu}{D_h}$	
(11)	Vapor quality	$x = \frac{e_{out,cd} - e_{liq}}{e_{vap} - e_{liq}}$	e_{vap} / e_{liq} - Enthalpy of saturated steam / liquid $e_{out,cd}$ - Enthalpy of the working fluid at the condenser outlet
(12) ^[10]	Nu of working fluid in condenser	$Nu_{cd} = 4.118 Re_{eq}^{0.4} Pr_1^{1/3}$	Re_{eq} - Equivalent Reynolds number Pr_1 - Prandtl number of saturated liquid
(13) ^[7]	Equivalent mass velocity through the plate channels	$G_{eq} = G \left[1 - x + x \left(\frac{\rho_l}{\rho_v} \right)^{0.5} \right]$	ρ_l / ρ_v - Liquid / Vapor phase density of working fluid
(14) ^[7]	Boiling number	$Bo_{eq} = \frac{q}{G_{eq} \cdot r_{fg}}$	q - Average heat flux of the region r_{fg} - Enthalpy of evaporation of working fluid
(15) ^[11]	Nu of working fluid in evaporator	$Nu_{exp} = 1.926 Pr^{1/3} Bo_{eq}^{0.3} Re^{0.5} \times \left[1 - x + x \left(\frac{\rho_l}{\rho_v} \right)^{0.5} \right]$	

2.3 Black box model of isentropic efficiency

In most of the HTHP WBMs, the η_s is mostly empirically determined as a constant, which deteriorates the accuracy, especially when it comes to the variable operating conditions. It mainly results from the complex and highly nonlinear relationships between the isentropic efficiency and many operating parameters, which challenges the mechanism modeling based on thermodynamic relationships. Therefore, BBM based on the BP artificial neural network model optimized by genetic algorithm (GA-BPANN) is adopted to explore the feasibility for η_s prediction.

By employing the evaporation pressure(P_{evp}), condensation pressure(P_{cd}), overheat degree(Δt) and the mass flow rate(m_r) as the input parameters and η_s as the output parameter, the number of neurons(N_{neu}) in the hidden layer is determined by Eq. 16^[12]. To evaluate the prediction performance, RMSE is employed(Eq.17).

$$N_{neu} = \sqrt{m + n + a} \quad (16)$$

$$RMSE = \sqrt{\frac{1}{n} \sum_{i=1}^n (y_i - y_i')^2} \quad (17)$$

In Eq.16, m and n stand for the number of input and output variables, which is set to be 4 and 1, respectively. Parameter a is a random integer ranging from 1 to 10, and it is commonly determined by test.

2.4 Geysier Inspired Algorithm (GEA)

Geysier Inspired Algorithm (GEA), which was first proposed by Mojtaba Ghasemi et.al in 2023, is an new innovative metaheuristic optimization algorithm^[13]. Inspired by the periodic bursts of geysers, it is dedicated to uncovering the most effective solution in complicated search spaces.

As shown in Fig.1, the algorithm involves the following steps :

- 1) Generate the initial population randomly and specify initialization parameters such as population size and maximum number of iterations.
- 2) Calculate the individual fitness degrees within the initial population.
- 3) Iteration of dormant phase: conduct a local search on the neighborhood of the current best solution to improve the quality of the solution.
- 4) Update location by Levy flight.
- 5) Iteration of Eruption phase: the decision to erupt is made by assessing the likelihood of an eruption, where one or more individuals will be chosen at random to make substantial jumps in the solution space, preventing them from getting stuck in a locally optimal state.
- 6) Examine the quality of the newly devised solution, select outstanding individuals from the current population, and build the following generation populace.
- 7) Check if the convergence condition is satisfied or if the iteration time is equal to the preset maximum value.

Eq.18 shows the convergence condition, where A'_{evp} , A_{evp} and A'_{cd} , A_{cd} are the calculated, input heat transfer areas of the evaporator and condenser, respectively.

$$E = |A'_{evp} - A_{evp}| + |A'_{cd} - A_{cd}| \quad (18)$$

3. RESULT AND DISCUSSION

3.1 Performance analysis of the BBM

In total, 364 groups of experiment data have been adopted as the training and testing set of the BBM. Fig.2 shows the relationships between η_s and P_{evp} , P_{cd} , Δt , m_r . It can be figured out that the variation range of η_s is from 0.641 to 0.900. Additionally, the relationship between η_s and single operating parameter is rather obscure, which reveals the complexity of η_s prediction by WBM and the unreasonability of considering it as a constant in the modelling process.

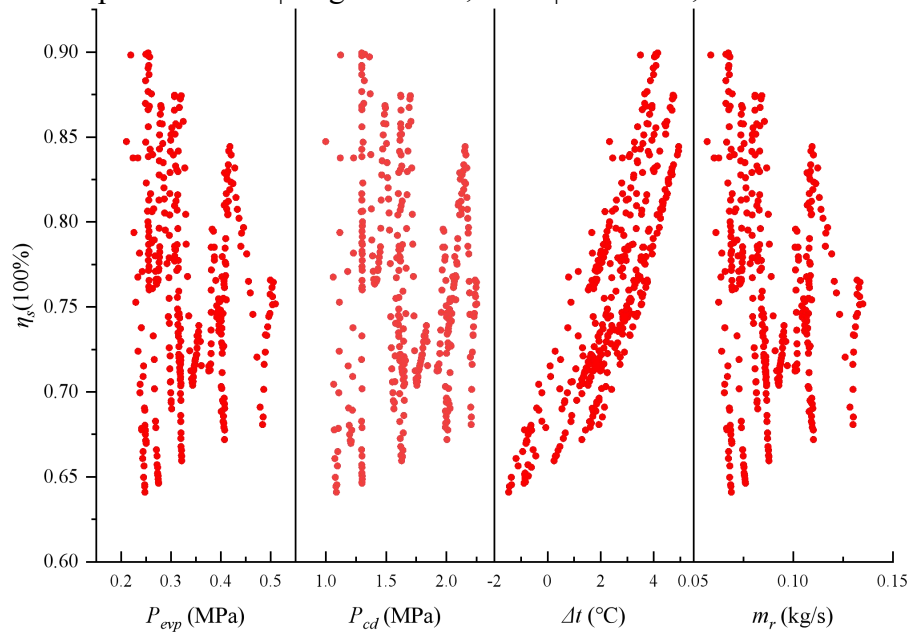


Fig. 2: The relationships between η_s and P_{evp} , P_{cd} , Δt , m_r

To guarantee the BBM prediction accuracy, the performance of GA-BPANN with different N_{neu} and different ratios of training set to testing set ($R_{tr:te}$) is investigated and analyzed, which is shown in Fig.3. Firstly, when $R_{tr:te}=9:1$ and $8:2$, it can be seen that the performance is rarely affected by N_{neu} with the maximum and minimum values of RMSE to be 0.0328 ($N_{neu}=11$) and 0.009 ($N_{neu}=9$), 0.0324 ($N_{neu}=9$) and 0.0113 ($N_{neu}=11$), respectively. For $R_{tr:te}=7:3$ and $6:4$, it is evident that the prediction performance tends to be more sensitive to N_{neu} with the maximum RMSE to be 0.2679 ($N_{neu}=12$, $R_{tr:te}=6:4$). Therefore, a conclusion that the size of the training set in this study, which is 364, is sufficient can be drawn. Moreover, it is noticeable that when $N_{neu}=7$, all the RMSE values are below 0.02 and are kept stable.

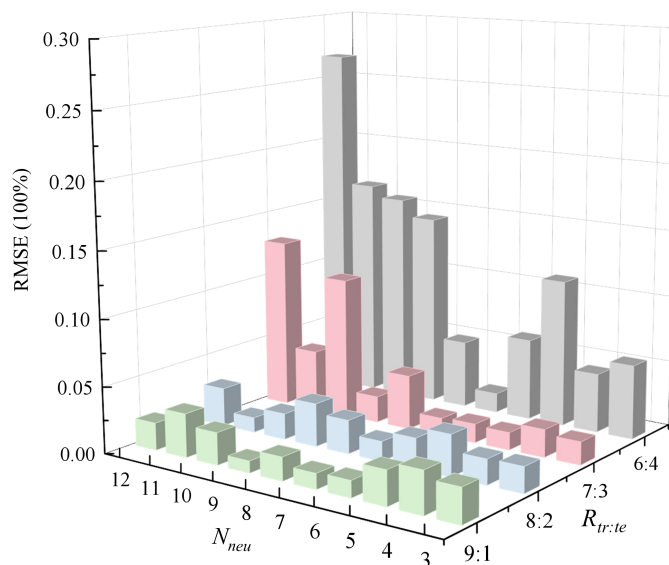


Fig. 3: Comparative results of GA-BPANN under different N_{neu} and $R_{tr:te}$

The prediction results corresponding to the cases that $R_{tr:te}=9:1$ are shown in Fig.4. It can be figured out that the varying trend and predicting values are well-matched with the experimental results. Consequently, it is proved that reliable prediction accuracy can be expected from BBM.

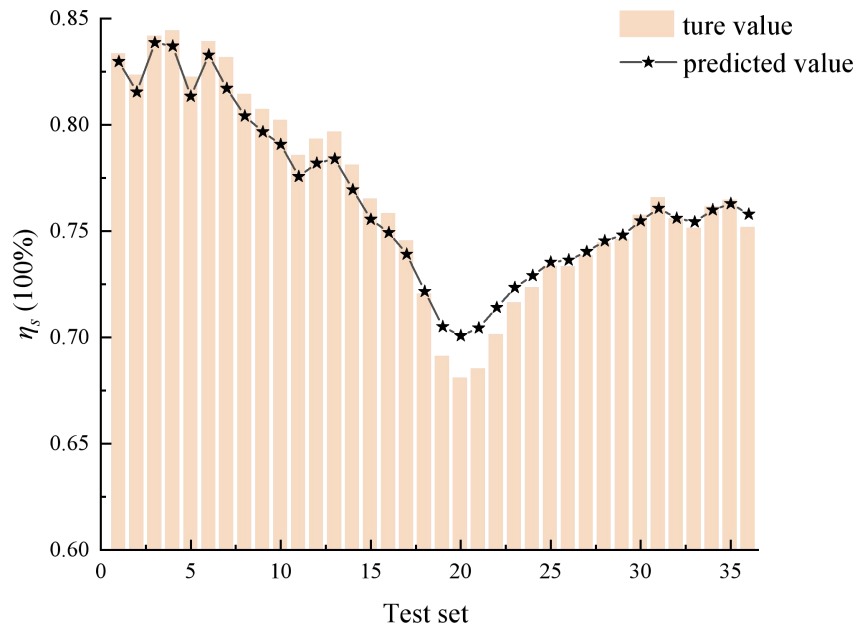


Fig. 4: Predicted outcomes for the $R_{tr:te}=9:1$ circumstance

3.2 Performance analysis of the MDFHM

To evaluate the robustness and convergence accuracy of the MDFHM, conditions with variable heat source inlet temperatures ($T_{in,hs}=50,55,60^{\circ}\text{C}$) and mass flow rates ($m_w=25,30,35,40,45,50\text{m}^3/\text{h}$) are taken into consideration. For each condition, the performances corresponding to different HTHP configurations that the heat exchanger areas (A_{evp} , A_{cd}) are from 10 m^2 to 210 m^2 with their step size to be 20 m^2 and compressor rotation speed is from 1000 r/min to 3000 r/min with the step size to be 200 r/min are calculated. In other word, 1331 HTHP configurations are included in each working condition, that is, 11979 HTHP configurations in total. The preset parameters involved in the MDFHM are listed in Table 2.

Table 2 Preset parameters involved in the MDFHM

Component	Parameter	Value	Algorithm	Parameter	Value
Compressor	Volumetric efficiency	0.9	GEA	Population size	80
	Displacement	$1452\text{m}^3/\text{h}$		Max iterations	50
	Rotation speed	$1000\text{-}3000\text{ r/min}$		Convergence condition	$E \leq 0.1\text{m}^2$
	Channel angle	30°		Training Frequency	100
	Plate Spacing	$2.3 \times 10^{-3}\text{m}$		Learning rate	0.1
Heat exchanger	Plate Width	0.61m	BPANN	Training Target	0.00001
	Plate thickness	$0.8 \times 10^{-3}\text{m}$		Transfer function	Trainlm
	Material	316 stainless Steel		Number of hidden layer neurons	7
Heat source	Evaporator outlet over heat degree	3°C	GA	Evolutional generation number	100
	Inlet temperature	$50\text{-}60^{\circ}\text{C}$		Population size	10
	Mass flow rate	$25\text{-}50\text{ t/h}$		Cross probability	0.4
Heat sink	Inlet temperature	95°C	GA	Mutation probability	0.2
	Target temperature	100°C			

Fig.5 demonstrates the convergence results corresponding to different heat source mass flow rates and the translucent plate represents the critical value of convergence condition ($E \leq 0.1\text{m}^2$). Statistically, there are 11, 21,79,87,194 and 144 calculation cases failing in convergence for $m_w=25,30,35,40,45$ and $50\text{m}^3/\text{h}$ within 50 iterations, respectively. That is to say, a convergence proportion of 93.29% can be achieved for 7986 calculation cases under different heat source mass flow rates. Additionally, the mean E 's value of the convergence cases is 0.062 m^2 .

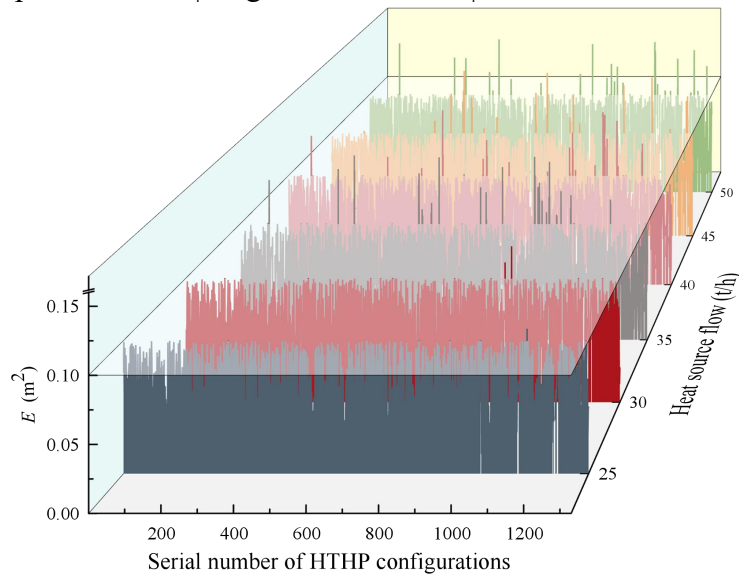


Fig. 5: The convergence results corresponding to different heat source mass flow rates

Fig.6 shows the convergence results of 3993 HTHP configuration calculation processes under different heat source inlet temperatures. Generally, it can be seen that vast major of the cases involved can converge within 50 iterations. To be specific, there are 74,80 and 87 cases failing in convergence for $T_{in,hs}=50, 55$ and 60°C , respectively. It denotes that 93.96% of the 3993 HTHP calculation processes can converge. Moreover, the mean E value corresponding to the convergence cases is 0.062m^2 .

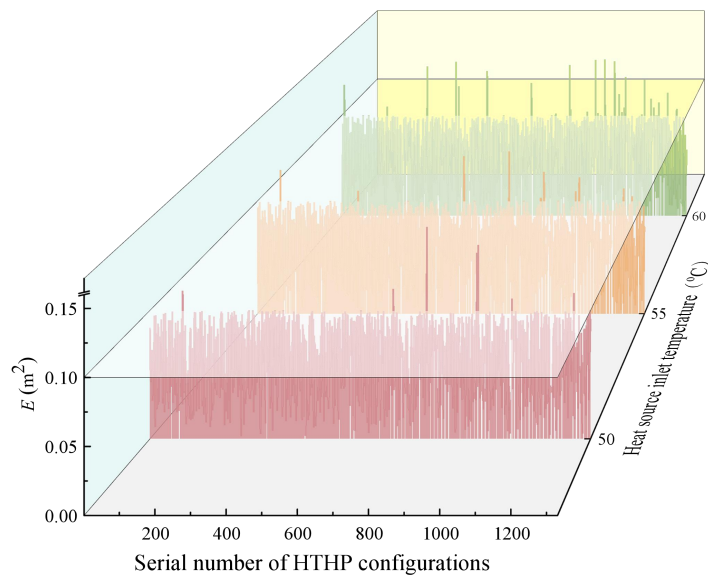


Fig. 6: The convergence results corresponding to different heat source temperatures

Objectively, the convergence condition ($E \leq 0.1\text{m}^2$) is somehow stringent, especially for the HTHP configurations with relatively large A_{evp} and A_{cd} (the maximum value of the heat exchanger area is 210m^2). Consequently, the convergence proportion of all the configurations involved can be as high as 93.50%. So, considerable robustness and convergence accuracy can be expected from the MDFHM, regarding the 11979 calculation samples and demanding convergence condition.

4. CONCLUSION

Through the analysis of the MDFHM performance, conclusions can be drawn as follows:

(1) GA-BPANN is qualified for the exergy efficiency prediction with P_{evp} , P_{cd} , Δt and m_r as the input variables. Additionally, when $N_{neu}=7$, it shows a relatively impressive and stable prediction performance with the RMSE values below 0.02.

(2) The MDFHM can realize a convergence proportion of 93.50% in the 11979 HTHP configuration calculation processes with $E \leq 0.1m^2$ as the convergence condition and the maximum number of iterations to be 50. So, considerable robustness and convergence accuracy can be expected from the MDFHM.

ACKNOWLEDGEMENT

This work was supported by the Special Funding Project for Transformation of Major Scientific and Technological Achievements in Chengde City [202306B002].

REFERENCES

- [1] Dai, B., et al., Life cycle techno-enviro-economic assessment of dual-temperature evaporation transcritical CO₂ high-temperature heat pump systems for industrial waste heat recovery. *Applied Thermal Engineering*, 2023. 219: p. 119570.
- [2] Wang, B., X. Liu and W. Shi, Performance improvement of air source heat pump using gas-injected rotary compressor through port on blade. *International Journal of Refrigeration*, 2017. 73: p. 91-98.
- [3] Verdnik, M. and R. Rieberer, Influence of operating parameters on the COP of an R600 high-temperature heat pump. *International Journal of Refrigeration*, 2022. 140: p. 103-111.
- [4] Kong, X., et al., Mass flow rate prediction of direct-expansion solar-assisted heat pump using R290 based on ANN model. *Solar Energy*, 2021. 215: p. 375-387.
- [5] Esen, H., et al., Performance prediction of a ground-coupled heat pump system using artificial neural networks. *Expert Systems with Applications*, 2008. 35(4): p. 1940-1948.
- [6] Park, S.K., et al., Application of a multiple linear regression and an artificial neural network model for the heating performance analysis and hourly prediction of a large-scale ground source heat pump system. *Energy and Buildings*, 2018. 165: p. 206-215.
- [7] Wang J, Yan Z, Wang M, et al. Multi-objective optimization of an organic Rankine cycle (ORC) for low grade waste heat recovery using evolutionary algorithm[J]. *Energy Conversion and Management*, 2013, 71: 146-158.
- [8] Chisholm D, Wanniarachchi AS. Layout of plate heat exchangers. *ASME/JSME Therm Eng Proc* 1991;4:433-8.
- [9] García-Cascales JR, Vera-García F, Corberán-Salvador JM, González-Maciá J. Assessment of boiling and condensation heat transfer correlations in the modelling of plate heat exchangers. *Int J Refrig* 2007;30:1029-41.
- [10] Yan YY, Lio HC, Lin TF. Condensation heat transfer and pressure drop of refrigerant R-134a in a plate heat exchanger. *Int J Heat Mass Trans* 1999;42:993-1006.
- [11] Yan YY, Lin TF. Evaporation heat transfer and pressure drop of refrigerant R-134a in a plate heat exchanger. *J Heat Trans-Trans ASME* 1999;121:118-27.
- [12] Yu S, Zhu K, Diao F. A dynamic all parameters adaptive BP neural networks model and its application on oil reservoir prediction[J]. *Applied mathematics and computation*, 2008, 195(1): 66-75.
- [13] Ghasemi, M., et al., Geyser Inspired Algorithm: A New Geological-inspired Meta-heuristic for Real-parameter and Constrained Engineering Optimization. *Journal of Bionic Engineering*, 2024. 21(1): p. 374-408.

Physics-Guided Neural Network for Multi-Step Prediction of Heat Pump Heating Capacity

Siyi GUO^(a), Ziqing WEI^(a), Xiaoqiang ZHAI^{(a),*}

^(a) Institute of Refrigeration and Cryogenics, Shanghai Jiao Tong University, Shanghai, 200240, China

*Corresponding author. Tel./fax: +86 21 34206296. E-mail address: xqzhai@sjtu.edu.cn (X.Q. Zhai).

ABSTRACT

Heat pump has attracted plenty of attention as a highly efficient new energy technology, which has been proven to be an energy-saving strategy for building heating. To better align the heating capacity of heat pumps with the thermal needs of buildings, predicting the heat output has become a pivotal challenge. Compared to physics-based models, the black-box models offer advantages such as simplicity in modeling, readily available parameter data, and broad extension. However, the intricate interplay among internal components often leads to diminished prediction

accuracy when relying solely on partial known external inputs. Moreover, to enable more precise control of heat pump operation, multi-step forecasting is deemed essential as a foundation for smart control. This study presents a novel approach: a component-level neural network model guided by physical principles. By leveraging historical operational data, this model aims to forecast the real-time heating capacity of air-source heat pumps over multiple steps. Specifically, the proposed model dissects the heat pump system into distinct subsystems, including the compressor, condenser, and evaporator. Each subsystem is individually modeled, with inputs and outputs determined by theoretical knowledge. Based on the model, the accuracy of multi-step predictions using the recursive approach is investigated. Validation against actual operational data reveals promising results: under a 24-hour prediction horizon, the Mean Absolute Percentage Error (MAPE) using our approach is 0.13, demonstrating robust consistency. These findings underscore the potential of proposed model to facilitate further advancements in energy-saving control strategies and beyond.

Keywords: Physics-Guided Neural Network; Heat Pump; Multi-Step Prediction; Recursive Approach

1. INTRODUCTION

Considering the significant role buildings play in global energy consumption, optimizing heat pump performance is paramount for enhancing overall energy efficiency and reducing environmental impact. Heat pumps, as a leading solution in energy-efficient technologies for building heating systems, necessitate precise alignment of their capacity with buildings' thermal demands. Therefore, the ability to forecast heat output with precision becomes imperative. Implementing multi-step forecasting not only enhances operational efficiency but also lays the groundwork for sophisticated smart control mechanisms. By integrating advanced predictive techniques, building operations can be optimized in real-time, contributing significantly to energy conservation and sustainability goals.

2. PHYSICS-GUIDED HEAT PUMP NEURAL NETWORK

In order to reduce the complexity of the modeling process, enhance the interpretability of the model, and expand the generality of the model, this paper proposes a component-level heat pump model based on Back-propagation neural network, including three subsystems: compressor, condenser, and evaporator[1].

The modeling process, as shown in Figure 1(a), is divided into two steps:

- (1) establishing the inputs and outputs of the three subsystems based on physical knowledge and training them separately with historical operational data;
- (2) determining the initial inputs of the heat pump system. Except for ambient parameters (outdoor temperature and indoor temperature) and control parameters (compressor operating frequency and electronic expansion valve opening), the inputs of the subsequent subsystem are determined by the outputs of the previous subsystem.

The description of each step of the system is shown in Figure 1(b), where the expansion valve is considered an adiabatic process, and the connections between components are considered ideal, without considering energy losses. The initial input of the system is set to the condenser inlet refrigerant enthalpy value, and the output of the system is the heat pump heating capacity, i.e., the difference in refrigerant enthalpy between the condenser inlet and outlet.

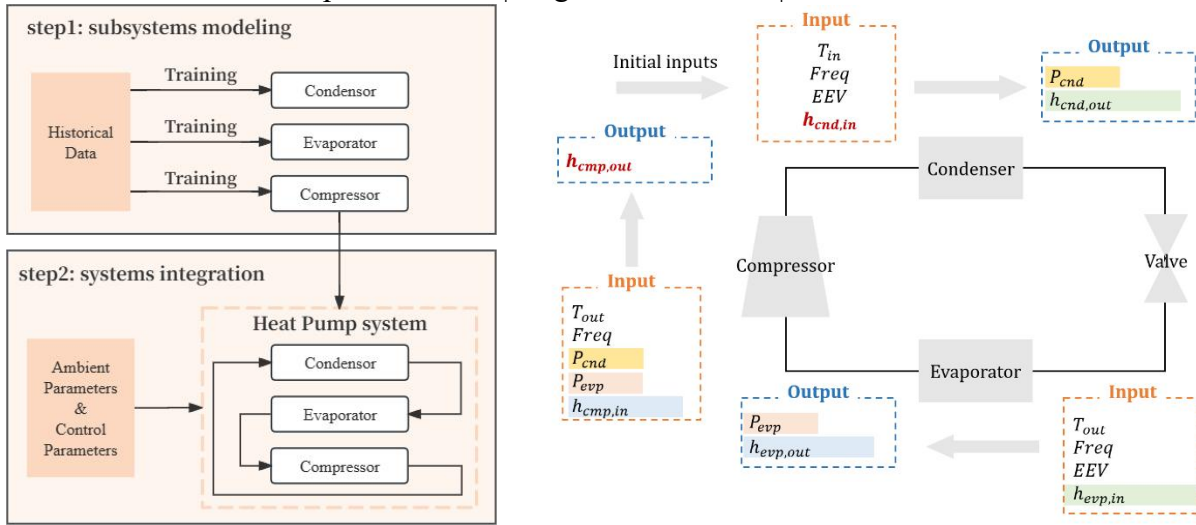


Figure 1(a). The proposed method flowchart.
(b). The schematic of proposed heat pump system.

The advantages of the proposed method mainly include:

- (1) simplifying complex theoretical models into black-box models with inputs and outputs determined by physical knowledge, thereby enhancing model generalization while preserving the rationality and accuracy of the physical model.
- (2) Owing to the fewer inputs and outputs of individual subsystems and the ability to train multiple subsystems in parallel for each sampling data, significant training time is saved, which enables real-time updates of the model while ensuring higher control accuracy.
- (3) The heat pump system only requires inputting the initial condenser inlet refrigerant enthalpy value to achieve multi-step open-loop prediction, offering a promising starting point for integrating modern control methods, such as model prediction control.

3. CONCLUSIONS

The proposed method achieves a Mean Absolute Percentage Error (MAPE) of 0.13 for a 24-hour prediction horizon, demonstrating high reliability. These outcomes highlight the potential of the proposed model to enhance energy-saving control strategies and extend its benefits to other areas.

REFERENCES

[1] Z. Chen, F. Xiao, J. Shi, and A. Li, “Dynamic model development for vehicle air conditioners based on physics-guided deep learning,” *International Journal of Refrigeration*, vol. 134, pp. 126–138, Feb. 2022.

Performance investigations on a nonflammable eco-friendly mixture for an air-source heat pump water heater during wintertime

Kaiyin Yang (a, c), Zhen Zhao (b, c), Yilun Liu (c, d), Qin Wang (c), Long Jiang (c), Ziqian Xue (a), Jieli Luo (a, c,*)

(a)School of advanced energy, Sun Yat-Sen University, Shenzhen, China
 (b)Qingdao Hisense Hitachi Air-conditioning Systems Co., Ltd., Qingdao, China
 (c)Institute of refrigeration and cryogenics, Zhejiang University, Hangzhou, China
 (d)Institute of advanced science facilities, Shenzhen, China (*) Corresponding author. Email: luojielin@mail.sysu.edu.cn

ABSTRACT

As an efficient and clean heating technology, air-source heat pump (ASHP) offers a compelling alternative to fossil fuel combustion, and using mixed refrigerants in ASHP has been confirmed as an effective approach to improve heating efficiency at low ambient temperature. However, existing mixtures used in ASHP do not fully satisfy all aspects of safety, environmental friendliness and efficiency. In this study, with a global warming potential (GWP) below 7 and non-flammability, the binary mixture of CO₂ and trans-1,1,1,4,4,4-hexafluoro-2-butene (R1336mzz(E)) was simulated in a compound ASHP water heater to investigate its seasonal performance during wintertime. Based on genetic algorithm, the performance of heating water from 50°C to 75°C was parametrically optimized, with multiple operating variables being globally regulated. This ASHP using CO₂/R1336mzz(E) achieved a higher coefficient of performance (COP) than that using traditional refrigerants at the ambient temperature ranging from -30°C to 10°C, with an improvement in Heating Seasonal Performance Factor (HSPF) exceeding 10%. Exergy analysis showed that the low irreversible loss of throttling was believed as a main reason for such energy performance improvement. Furthermore, by a sensitivity analysis, the influence of CO₂ concentration on heating performance was found to be the greatest among operating parameters, indicating that concentration regulation was crucial for achieving high efficiency in a thermodynamic system using mixture. The results in this study were compared and discussed with existing studies as well. This study contributes to: 1) providing a safe, eco-friendly and efficient option for the exploration of heat pump working substance; 2) delivering a design and analysis guidance for ASHP evaluation during the whole wintertime.

Keywords: heat pump, mixture, optimization, regulation, eco-friendly, heating performance.

Thermodynamic analysis of a large temperature lift heat pump strategy: combining water vapor compressor and exploring performance boundaries

Hongzhi Yan^(a), Ruzhu Wang^(b)

^(a)School of Energy and Environmental Engineering, Hebei University of Technology, Tianjin, 300401, China, hongzhiyan@hebut.edu.cn

^(b)Institution of Refrigeration and Cryogenics, Shanghai Jiao Tong University, Shanghai 200240, China, rzwang@sjtu.edu.cn

ABSTRACT

As the proportion of renewable power continues to increase and the pursuit of carbon neutrality, heat pump technology has drawn significant attention. This is due to its ability to recover low-grade heat energy and efficiently convert electricity directly into heat energy, thus achieving heat multiplication. Presently, traditional heat pumps are widely utilized in medium and low-temperature applications, such as space heating and hot water generation. However, their application in high-temperature fields remains relatively limited. Specifically, when it comes to supplying high-temperature heat, two primary challenges emerge: firstly, the difficulty in obtaining waste heat resources of sufficient temperature, and secondly, the significant decrease in efficiency when using low-temperature heat sources under conditions of large temperature rises. This decrease in efficiency is particularly evident in scenarios involving high-temperature steam supply based on air heat sources. Practical experience demonstrates that by integrating heat pumps with water vapor compression, efficient steam supply can be realized even under conditions of large temperature lifts over 100. Nevertheless, in practical operations, the comprehensive influence mechanism of the thermodynamic performance of the water vapor compression process and the performance of the heat pump remains unclear within the current system configuration. In particular, there is still theoretical ambiguity when it comes to determining the intermediate temperature and optimizing the performance coupling between the water vapor compressor and the heat pump system. This necessitates a deeper exploration of the optimization potential and boundaries of its thermodynamic efficiency. Therefore, the focus of this paper is to analyze how to strike a balance between the thermodynamic energy efficiency of different stages and determine the optimal thermodynamic performance of

the heat pump coupled with water vapor compression under variable operating conditions. The ultimate goal is to enhance overall energy efficiency. Furthermore, this paper aims to comprehensively evaluate the economic viability of this approach, with the objective of providing theoretical backing and practical guidance for the steam supply technology utilized in large temperature lift heat pumps.

Keywords: Heat pump, Large temperature lift, Thermodynamic optimization, Steam generation.

Application and analysis of two-stage heat recovery and flash vaporization process in high-temperature heat pump systems for steam production.

Zheng HUANG^{(a) (b)}, Yanting ZHANG^(a), Lin WANG^{(b)*}, Yunlong ZHENG^(a)

^(a) School of Mechanical and Electrical Engineering, China University of Petroleum (East China), Qingdao 266580, China, b21040017@s.upc.edu.cn

^(b) Institute of Building Energy and Thermal Science, Henan University of Science and Technology, Luoyang 471023, China, wlhaust@163.com

ABSTRACT

Conventional high-temperature heat pump systems for steam production utilize multi-stage compression systems to reuse low-grade thermal energy. However, the significant temperature and pressure differences between the heat source and heat production lead to considerable energy losses in the compression and expansion processes. This study proposes the use of a two-stage heat recovery and flash vaporization process in a two-stage compression heat pump system. By using a flash vaporization heat exchanger, part of the refrigerant is used to reheat another part of the refrigerant after flash vaporization before entering the compressor, improving the system's COP and reducing energy consumption. This paper employs a multi-variable simulated annealing algorithm to calculate the optimal COP of the system and verifies it through experiments. The performance of different high-temperature heat pump systems at various steam production temperatures is compared and analyzed. The results show that under the same production conditions, the new system has a COP that is 14.28%~17.92% higher and a exergy efficiency that is 16.82%~22.54% higher than that of the traditional two-stage compression heat pump system.

Keywords: High-temperature heat pump, Two-stage compression, Heat recovery, Flash vaporization process, COP, Exergy Efficiency.

Performance study of a quasi-saturated compression high-temperature heat pump system with water vapour

Di Wu^(a,b,*), Jiatong Jiang^(a), Bin Hu^(a,b,*), R.Z. Wang^(a)

^(a) Institute of Refrigeration and Cryogenics, Shanghai Jiao Tong University
Shanghai, 200240, China, rzwang@sjtu.edu.cn

^(b) Shanghai Nuotong New Energy Technology Co., LTD
Shanghai, 200241, China, wd1101@shnuotong.com

ABSTRACT

Water vapour high-temperature heat pump combines the environmental friendliness of natural water and the energy-saving of heat pump, which fully exerts the performance advantages of water work in the field of high-temperature heat pumps. The water spray cooling is more effective to ensure the long-term safety and

stability of the unit and efficient operation. The article analyzes the possibility of building a reverse Carnot cycle in the heat pump system, as well as the main problems faced, and theoretically confirms that in the process of water vapour compression into the working chamber continuously sprayed low enthalpy liquid water to achieve quasi-saturated compression of water vapour, which is not only able to effectively reduce the exhaust superheat at the end of the compression but also conducive to the improvement of the overall performance of the system. The theoretical analysis and experimental investigation of the effects of suction superheat and the number of liquid injection cooling on the system performance was carried out. It was concluded that the existence of suction superheats is not conducive to the improvement of the system performance, and the increase in the number of liquid injections is favourable to the system performance. However, when the water-injection times are more than 5, the improvement of the system performance will be very slow. When the suction superheat was 20°C, the COP decreased by 1.45%-1.54% compared with no suction superheat, and when the water-injection times reached 30, the COP increased by 3.10%-3.73% compared with one-time water-injection. The experimental results also indicate that more water injection times are better for the system performance. Besides, when the injected water is greater than the required maximum, the system performance will no longer vary with the injected volume.

Keywords: High Temperature Heat Pump, Quasi-saturated Compression, Performance Study, Experimental Investigation.

Thermodynamic performance analysis of a novel energy storage power plant based on high-temperature heat pump and molten salt heat storage systems

Mingrui Yang, Yongliang Zhao*, Li Yang, Ming Liu, Junjie Yan

State Key Laboratory of Multiphase Flow in Power Engineering, Xi'an Jiaotong University, Xi'an, 710049, China, * Corresponding Author E-mail: yl.zhao@mail.xjtu.edu.cn

ABSTRACT

High penetration of renewable power leads to a reduction in the installed capacity of thermal power plants in China. Due to the intermittency and randomness of these energy, thermal power plants are needed to meet higher flexibility and deeper peaking requirements frequently. This work proposed a novel energy storage power plant based on a high-temperature heat pump system integrated with a thermal power plant, and focused on the impact of high temperature heat pump system on an energy storage plant. Simulation models validated by comparing the simulation results with the design data of the thermal power plant are developed to evaluate the thermodynamic performance of the energy storage power plant. In the charging process, the condensed water is chosen as low temperature heat source for the heat pump system, and the molten salt is chosen as the heat storage medium to absorb the heat from the high-temperature heat pump system. During the discharging process, the heat stored in molten salt is released to heat feedwater and then produce live steam. The peaking depth and design parameters of the high-temperature heat pump system are obtained by using the optimization algorithm. The equivalent round-trip efficiency, peaking depth and the thermal energy storage capacity are obtained under different heat storage parameters, and the thermodynamic performance of the energy storage power plant can be enhanced by matching the temperature of the heat source with the high-temperature heat pump system. This study provides guidance for flexibility enhancement of energy storage power plant and thermal power plant retrofit.

Keywords: Energy storage power plant, Heat pump, Operation flexibility, Thermal energy storage.

DIGITAL
NEXT



拥抱未来万象 唯格智引领境



欲了解详细信息，请咨询我们的热泵销售工程师

责任
远见
创新

be
think
innovate

格兰富
GRUNDFOS



Application Analysis of Complex High-Temperature Heat Pump in Petroleum Process

Qizixia^(a), Renfulei^(a), Fannana^(b)

^(a) Qingdao Haier Air Conditioning Electronics Co., Ltd.
Qingdao, 266101, China, qizixia@haier.com

ABSTRACT

This paper conducts in-depth research on the use of air source high-temperature heat pumps in petroleum oil-water separation processes, aiming to explore the advantages of this system in energy conservation, environmental protection, and low-carbon energy utilization. The article mainly discusses overview of the complex high-temperature heat pump, the advantages and disadvantages of using the heat pumps in petroleum processes, the design of the heat pump system, and the actual operating effects. Through Haier's analysis and calculation of the oil-water separation process and heat pump unit in an oilfield in Shaanxi, theoretical support is provided for the optimization of the system, then process transformation has been carried out in this oilfield , the original electric boiler turn to high-temperature heat pump, the energy-saving performance of the system in this process was verified through the actual operating effects. On this basis , we make further exploration of the feasibility of using complex high-temperature heat pump in other processes in petroleum process.

Keywords: high-temperature heat pump, oil-water separation processes, COP,

Performance analysis of an air source high temperature heat pump steam system with large temperature rise

Xudong Ma, Yanjun Du^{*}, Yuting Wu, Biao Lei

MOE Key Laboratory of Enhanced Heat Transfer and Energy Conservation, Beijing Key Laboratory of Heat Transfer and Energy Conversion, Beijing University of Technology, Beijing, 100124, China,
duyanjunx@hotmail.com

ABSTRACT

High-temperature heat pump steam systems offer a promising alternative to coal-fired boilers. For obtaining larger temperature rise, a high-temperature autocascade heat pump steam system (AHTHP) with steam injection technology is proposed by utilizing low-temperature air for high-temperature steam production. The paper comprehensively evaluates the interactions between system components and the potential for performance enhancement by using advanced exergy analysis methods, based on conventional approaches for evaluating the performance of heat pumps. The results indicate that the AHTHP is capable of efficiently harnessing low-temperature air ranging from 0-20°C for the production of high-temperature steam, while also demonstrating a substantial reduction in compressor discharge temperature. These results can provide theoretical guidance for the design and optimization of high-temperature heat pump steam systems.

Keywords: High-temperature heat pump, Autocascade heat pump, Advanced exergy analysis, Large temperature rise.

Innovative internal Cooling Thermodynamic Cycles for High-temperature heat pump Thermal Management

Jiatong JIANG^a, Fan JI^a, Bin HU^a, Ruzhu WANG^{a,*}, Hua LIU^b, Yu ZHOU^b

^(a) Institute of Refrigeration and Cryogenics, Engineering Research Center of Solar Power & Refrigeration, Shanghai Jiao Tong University, Shanghai 200240, China

^(b) SKL of Air-Conditioning Equipment and System Energy Conservation, GREE Electric Appliances, INC. Zhuhai 519070, China

ABSTRACT

High-temperature heat pumps (HTHPs) represent a highly effective means of achieving low-carbon industrial heating, emerging as a significant area of research under the dual carbon goals. However, a major challenge impeding the widespread adoption of HTHPs is the degradation of electronic components and lubricants during sustained high-temperature operation, which compromises the safety and stability of the units. Consequently, ensuring reliable thermal management of HTHPs is critical for their broader application and promotion. The traditional method of post-condensation throttling cooling, effective for medium- and low-temperature heat pumps, becomes inadequate as the heat source temperature of HTHPs rises, proving applicable only for conditions where evaporation temperatures remain below 70°C. The alternative approach of using external cooling units demands additional space and results in energy losses within the system. To address these limitations, this paper proposes an innovative internal cooling cycle. This cycle employs throttling cooling of the evaporator refrigerant followed by vapor injection with enthalpy increase, achieved through high-pressure fluid ejection from the condenser. This method accommodates high heat source conditions with evaporation temperatures exceeding 70°C and utilizes the higher-pressure refrigerant from the ejector for enthalpy-increasing vapor injection, thereby enhancing system efficiency by 1.2% to 4.2%.

Keywords: High-temperature heat pump, Thermal management, Coefficient of performance

1. INTRODUCTION

Thermal management is a crucial factor that restricts the long-term safe and stable operation of current HTHP units. While external cooling systems offer a wider range of adjustment, they not only add to the system configuration but also result in energy waste. Built-in cooling systems typically rely on the heat source temperature. As the heat source temperature of the HTHP increases, the internal throttling cools the refrigerant to a temperature below the evaporation pressure, preventing it from returning to the evaporator via pressure difference. This necessitates the use of an additional refrigerant pump, which consumes extra power. To address this issue, this paper proposes a new internal cooling scheme based on the principle of the ejector for conditions with higher heat source temperatures. This scheme utilizes the pressure difference to drive refrigerant flow, significantly enhancing the long-term safe operation of HTHPs under elevated temperature conditions.

2. INNOVATIVE INTERNAL COOLING THERMODYNAMIC CYCLE

To meet the thermal management requirements of HTHPs with higher heat sources, an internal cooling thermodynamic cycle combining throttling and ejection was proposed, as shown in Fig. 1. A portion of the refrigerant liquid is driven by gravity from the bottom of the evaporator through the EV1 throttle, achieving a cooling temperature lower than the evaporation temperature. This cooled refrigerant is used for cooling motors, lubricating oils, etc., and undergoes evaporation in the process. Simultaneously, another stream of fluid is driven by gravity from the bottom of the condenser into the ejector, serving as the ejector fluid to entrain the cooled refrigerant vapor. These fluids mix in the mixing chamber and enter the diffuser chamber, where the pressure increases. The gas-liquid two-phase refrigerant at the outlet enters the gas-liquid separator, with the gas pressure

being higher than the compressor's suction pressure, which can be used to increase the enthalpy of the gas. The saturated liquid is throttled by EV2 and then flows back to the evaporator.

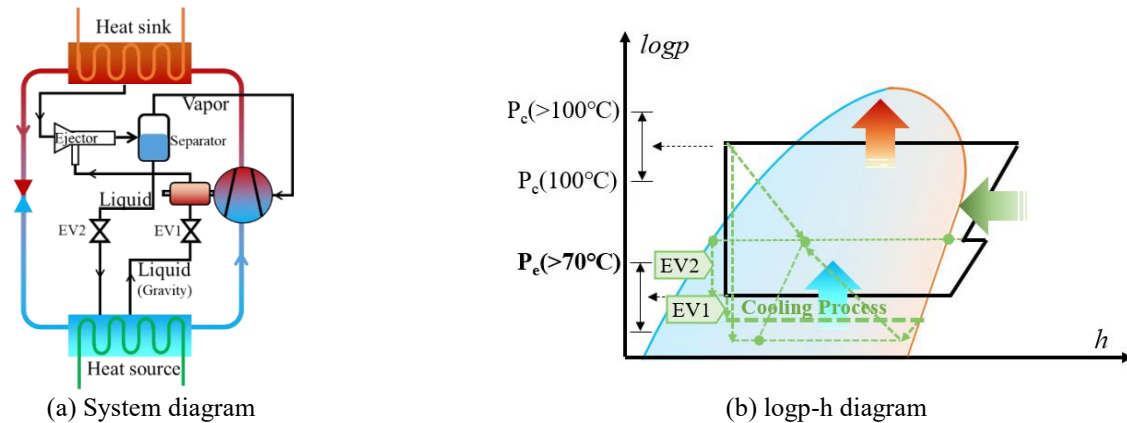
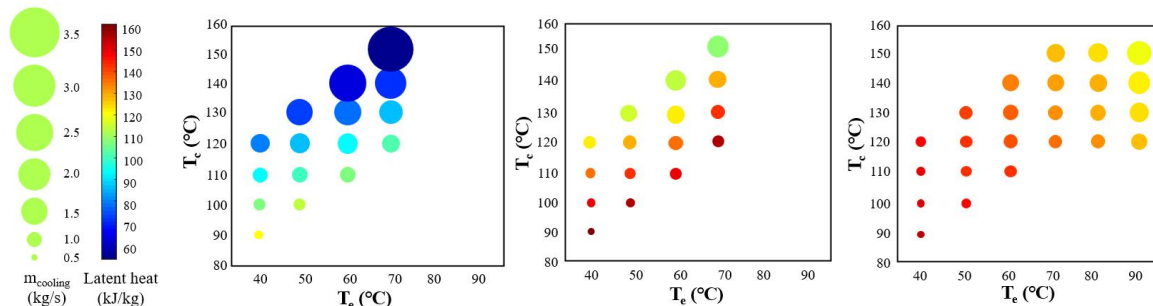


Figure 1: Throttling and ejection cooling system

Maintaining the throttled refrigerant below 70°C is critical for effective cooling. Direct throttling leads to higher gas content and lower refrigerant latent heat, necessitating greater flow rates (3.48 kg/s at 70°C source and 150°C condensation). Subcooling after the condenser increases refrigerant latent heat, reducing flow rates by 45% compared to direct methods. Throttling-ejection cooling, operational above 70°C, achieves temperatures as low as 35°C, suitable for variable frequency drives. This scheme optimizes refrigerant latent heat and minimizes flow rates, as shown in Fig. 2(c), highlighting tailored cooling solutions for efficiency in high-temperature heat pumps.



(a) Internal throttling cooling system (b) Large subcooling cooling (c) Throttling and ejection cooling system

Figure 2: Heating latent heat comparison

3. CONCLUSIONS

Effective thermal management is vital for high-temperature heat pumps. Three internal cooling methods—direct throttling, subcooling after condensation, and throttling-ejection—were compared. Direct throttling requires high refrigerant flow rates but is limited above 70°C. Subcooling reduces flow rates by 45%. Throttling-ejection accommodates temperatures over 70°C and achieves cooling to 35°C, ideal for variable frequency drives. Continuous vapor injection enhances COP by 7% at 90°C to 2.8% at 150°C. These findings emphasize tailored cooling strategies for efficiency and operational reliability in industrial applications.

ACKNOWLEDGEMENT

This research was supported by the Key Project of the National Natural Science Foundation of China (52036004) and (52306019).

SHIMGE
新界泵业

暖通行业 解决方案



供热系统 | 空调循环冷却 | 热水增压 | 热水循环 | 家用增压

新界泵业拥有“国家级制造业单项冠军示范企业”、“国家科学技术进步奖二等奖”、“国家工业产品绿色设计示范企业”等荣誉，拥有国家级博士后科研工作站、国家企业技术中心、国家级绿色工厂，综合实力位居泵行业第一方阵。致力于提供全球顶尖的流体产业全生命周期解决方案。

愿景&使命 引领流体产业 共创品质生活

网址: www.shimge.com 服务热线: 400-888-3868

新界泵业(浙江)有限公司
SHIMGE PUMP INDUSTRY (ZHEJIANG) CO., LTD.

Experimental investigation of a multi-energy complementary absorption heat pump applied for combined cooling and heating in distributed regions

Ding LU^{(a,b,*),} Maoqiong GONG^(a,b)

^(a) Technical Institute of Physics and Chemistry, Chinese Academy of Sciences

Beijing 100190, China, luding@mail.ipc.ac.cn

^(b) University of Chinese Academy of Sciences

Beijing 100049, China, luding@mail.ipc.ac.cn

ABSTRACT

In the process of carbon neutrality, the comprehensive utilization of clean and renewable energy, including solar, geothermal and biomass, is a potential solution to the low-carbon cooling and heating in distributed areas with weak power grids, such as countryside and suburban. In this paper, an absorption heat pump system with multi-energy complementary was built to provide cooling and heating with large temperature range of -20 to 100°C. Solar energy was collected through an evacuated tube collector, where heat conduction oil was used as the heating medium, and a gas boiler was adopted to further heat the oil through natural gas or biogas combustion. Heat collected in the oil circulation was used to drive an ammonia-water absorption heat pump, to meet the cooling and heating demand in distributed areas. Environmental test of the system was performed in Jinan, and during the whole testing period the solar thermal ratio could reach 35%. Through gas proportional regulation, all-weather stable energy supply was achieved. Moreover, a wide range of concentration adjusting was realized by level control of solution tank, so that the system can operate efficiently in a wider temperature zone. It was found that the COP of cooling reached 0.30-0.43 at -20°C, and 0.70-0.78 at 7°C, with cooling water temperatures varies from 30 to 20°C; and the COP of heating reached 1.40-1.90 at 45°C, and 1.35-1.56 at 80°C, with evaporation temperature varies from -15 to 20°C. It was showed that by introducing solar thermal driving and ambient energy recovery, the proportion of renewable energy of the system was over 50%, demonstrating significant carbon reduction potential in distributed areas away from the centralized cooling or heating network.

Keywords: Absorption Heat Pump, Multi-energy Complement, Combined Cooling and Heating, Renewable Energy, Carbon Emission Reduction

Potential of applying a novel trans-critical CO₂ cycle with multi-heat recovery for combined cooling and heating in the ice rank

Yanhua GUO^{(a),} Ningbo WANG^{(a),} Shuangquan SHAO^{*(a),} Congqi HUANG^{(a),} Zhentao ZHANG^{(b),} Xiaoqiong LI^{(b),} Qiu TU^{(c),} Lina ZHANG^(c)

^(a) Huazhong University of Science and Technology

Wuhan, 430074, China, shaoshq@hust.edu.cn

^(b) Technical Institute of Physics and Chemistry

Beijing 100864, China

^(c) Ningbo University of Technology

Ningbo 315211, China

ABSTRACT

Heat pump systems have made a critical aspect for the waste heat recovery, but the remarkable cyclicity and diversity of heat recovery in various industrial fields such as ice rinks weaken the superiority of the system in the design and regulation stages. Therefore, in this paper, a novel trans-critical carbon dioxide cycle with

multi-heat recovery is proposed, integrating parallel compression and ejector to enhance the system performance in the wide temperature range. Firstly, the experimental platform and simulation model of the system are established, and the operation and design scheme of the system are optimized based on heat exchanger network, cycle performance, and economy. Subsequently, an efficient and innovative strategy is developed based on the data-driven model, which can switch the heat exchange network combination and regulate operation parameters in terms of timeliness according to operation environment result in flexibility in responding to changes. Finally, the effectiveness of the system and strategy are further validated through practical testing in the ice rink. The results indicate that the system has improved the coefficient of performance (COP) by 11.8%~28.2% in different application scenarios compared with the basic carbon dioxide cycle. Besides, the evaluation of annual performance proves that the modified strategy is an energy-efficient choice and can gain 15.3%~17.3% annual energy saving for different cities and weather conditions. The proposed system and strategy present a promising solution to meet heating/cooling supply that is worthy of popularization and application in multi-heat recovery.

Keywords: Heat pump; Heat recovery; Carbon dioxide; Data-driven; Ice rink.

Design and Operational Optimization Low Carbon Integrated Energy System between Data Centers and Buildings based on Heating Pump **Songjie Wang^(a), Xiaojie Lin^{(a)(b)}, Long Jiang^(a), Wei Zhong^{(a)(b)}**

^(a)College of Energy Engineering, Zhejiang University
Hangzhou, 310027, China, xiaojie.lin@zju.edu.cn

^(b)Shanghai Institute for Advanced Study, Zhejiang University
Shanghai, 201203, China

ABSTRACT

Developing green Data Centers Integrated Energy system (DC-IES) plays a crucial role in achieving energy conservation and carbon reduction goals in China. However, existing research mainly focuses on renewable energy generation and electrochemical energy storage, with limited attention to the coupled design of Electric-Hydrogen-Cooling-Heating for DC-IES under green energy utilization. Therefore, this paper proposes a DC-IES that integrates photovoltaic-wind power generation with hydrogen systems, which can provide the necessary energy for the servers, chillers and other equipment, serving as energy conversion device to meet different energy demand of data centers. Additionally, to enhance system flexibility and energy efficiency, the proposed system employs heat pumps to recover waste heat from the data centers, and utilizes a vaporizer to recover the cold energy from liquid hydrogen. It also utilizes batteries for energy storage and emergency devices under special conditions. To optimize the operation of DC-IES, this study uses Carbon Emissions, Economic Viability, Power Use Effectiveness (PUE), and Exergy efficiency as indicators to compare and analyse the effects under different schemes, and analyses the characteristics of energy flow distribution under different operating conditions. The results indicate that DC-IES has significant advantages in reducing PUE, decreasing carbon emissions, and enhancing economic benefits. This study primarily provides insights for the design and operational optimization of DC-IES, promoting the sustainable transformation of data centers.

Keywords: Data Centers, Heat Pump, Waste Heat Recovery, Cold Energy Recovery, Integrated Energy System.

1. INTRODUCTION

As the traditional industries integrate with cutting-edge technologies such as cloud computing, big data, and artificial intelligence, a new era of the digital economy has commenced globally. Data centers, as key components of the global information infrastructure, play a critical role in driving various digital industries^[1]. Research indicates that the global data center rack market is expected to grow from USD 4.4 billion in 2022 to USD 6.6 billion in 2027, with a compound annual growth rate of 8.7%. By 2025, the energy consumption of data centers is projected to

account for 3.2% of the global total carbon emissions. However, the energy consumption and environmental issues arising during the full lifecycle of data centers are becoming increasingly prominent^[2]. Consequently, optimizing the energy efficiency of data centers and reducing carbon emissions^[3] have gradually attracted the attention of scholars and governments.

Heat pumps play an important role in the recovery and utilization of waste heat in data centers, significantly enhancing energy efficiency and environmental sustainability. Data centers generate substantial amounts of waste heat through their operations, traditionally released into the environment as a byproduct of cooling processes. By integrating heat pumps, this waste heat can be recovery, either to heat the facilities during colder months or to provide hot water for nearby buildings and industrial parks^[4]. For ^[5]

Therefore, this paper proposes a DC-IES that integrates photovoltaic-wind power generation with hydrogen systems, which can provide the necessary energy for the servers, chillers and other equipment, serving as energy conversion device to the meet different energy demand of data centers and building.

2. THE PLANNING OF WASTE HEAT RECOVERY SYSTEM BETWEEN DATA CENTERS AND BUILDINGS

To address the high energy consumption issue between data centers and buildings, this paper proposed a bi-level planning method for low carbon integrated energy system, the framework of this study is depicted in Figure 1. And the main innovations of this research are in the following three aspects.:

1. Coupling Heat Pump Technology: Recovery waste heat from data centers, enhancing DC-IES efficiency.
2. Leveraging of Liquid Hydrogen Cold Energy: Heat pumps recovery the waste heat from hydrogen fuel cells.
3. Bi-Level Planning Method: The upper level allocation model for heat pumps, and the lower level optimizes scheduling for DC-IES.

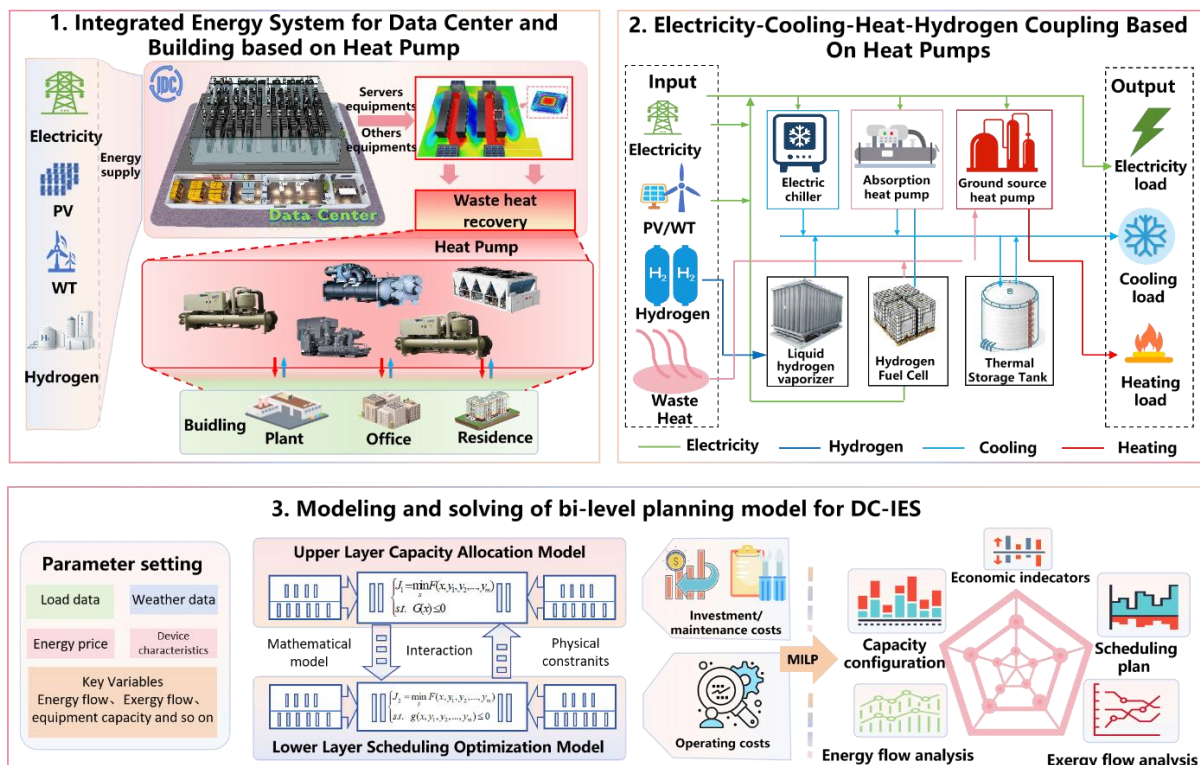


Figure 1: Framework of the waste heat recovery system planning between data centers and buildings

3. CONCLUSIONS

This paper proposed a bi-level planning method a low carbon integrated energy system that facilitates waste heat recovery between data centers and buildings based on heat pumps. The results indicate that DC-IES has significant advantages in decreasing carbon emissions, enhancing economic benefits and flexibility. This study primarily provides insights for the design and operational optimization of DC-IES, promoting the sustainable transformation of data centers.

ACKNOWLEDGEMENT

This work was supported by Zhejiang Province 2024 ‘Leading Wild Goose’ Research and Development Project (No. 2024C03117).

REFERENCES

- [1] Zhou Z., Shojafar M., Alazab M., et al. AFED-EF: An Energy-Efficient VM Allocation Algorithm for IoT Applications in a Cloud Data Center [J]. IEEE Transactions on Green Communications and Networking, 2021, 5(2): 658-669. <http://doi.org/10.1109/TGCN.2021.3067309>.
- [2] Scao T. L., Fan A., Akiki C., et al. BLOOM: A 176B-Parameter Open-Access Multilingual Language Model [J]. ArXiv, 2022, abs/2211.05100.
- [3] Wang Y., Han Y., Shen J., et al. Data center integrated energy system for sustainability: Generalization, approaches, methods, techniques, and future perspectives [J]. The Innovation Energy, 2024, 1(1): 100014. <http://doi.org/10.59717/j.xinn-energy.2024.100014>.
- [4] Niaz H., Shams M. H., Zarei M., et al. Leveraging renewable oversupply using a chance-constrained optimization approach for a sustainable datacenter and hydrogen refueling station: Case study of California [J]. Journal of Power Sources, 2022, 540: 231558. <http://doi.org/10.1016/j.jpowsour.2022.231558>.
- [5] Fan W., Tan Q., Zhang A., et al. A Bi-level optimization model of integrated energy system considering wind power uncertainty [J]. Renewable Energy, 2023, 202: 973-991. <http://doi.org/https://doi.org/10.1016/j.renene.2022.12.007>.

Study and economic analysis of the form of multi-energy complementary system for airport rooms in severe cold regions

Sihang Guan^{(a)(b)}, Wenke Zheng^{(a)(b)}, Yiqiang Jiang^{(a)(b)}, Lian Liu^{(a)(b)}

(a) School of Architecture and Design, Harbin Institute of Technology
Harbin, 150006, China

(b) Key Laboratory of Cold Region Urban and Rural Human Settlement Environment Science and Technology, Ministry of Industry and Information Technology
Harbin, 150001, China.jyq7245@sina.com

ABSTRACT

In typical airport facilities such as bird repellent rooms, which are situated away from the energy station, traditional heating and cooling methods like gas boilers are predominantly used. These systems are characterized by low energy efficiency and high carbon emissions and operational costs. This paper introduces a renewable energy multi-energy complementary system, comprising air-source heat pumps, soil-source heat pumps, and phase-change energy storage underfloor heating technology, tailored for airports in severe cold regions. This system aims to fulfil the indoor environmental needs of personnel and the demand for domestic hot water. A simulation model is established using TRNSYS, and experimental validation is performed to assess the system modules and critical parameters. The findings reveal that the phase-change thermal storage floor significantly influences indoor temperature control during heating and substantially reduces temperature fluctuation amplitudes. Regarding the air-ground source heat pump coupling system, it is observed that the average Coefficient of Performance (COP) increases with the heat pump's start/stop temperature increment,

while the soil temperature decreases as the start/stop switching temperature rises. Specifically, when the start-stop switching temperature reaches -21°C , the soil temperature decreases by approximately 0.11°C after one year of operation. Economically, the most efficient system configuration during the lifecycle involves operating one ground source heat pump and three air source heat pumps simultaneously with a load-bearing ratio of 3.15, whereas the lowest carbon emissions are achieved with one ground source heat pump and two air source heat pumps in operation. Annually, this system conserves around 19,600 kg of standard coal, marking a 25.3% reduction compared to traditional gas boilers and electric cooling systems. Additionally, it reduces CO_2 emissions by 48.41 tonnes, SO_2 emissions by 0.39 tonnes, and soot by 0.2 tonnes annually, highlighting its superior economic performance and environmental benefits.

Keywords: Multi-energy Complementary System, Airport annex, Heat Pumps, TRNSYS.

Study on the operation mode and control strategy of a multi-heat source heat pump coupled energy storage system for plant factory heating and grid peaking

Youdong Wang^{(a)(b)}, Jitian Song^(a), Xiaoqiong Li^{(b)*}, Qing Xu^(a), Zhentao Zhang^(b)

^(a) Tianjin University of Science & Technology, College of Mechanical Engineering
Tianjin, 300222, China, 983736738@qq.com

^(b) Technical Institute of Physics and Chemistry, Chinese Academy of Sciences
Beijing 100190, China, lixiaoqiong@mail.ipc.ac.cn

ABSTRACT

To improve the comprehensive performance of the heating system in a plant factory, reduce operational costs, and address short-term overload issues in the local power grid, an integrated energy system has been designed. This system integrates the operation of a CO_2 air source heat pump and a ground-source heat pump, coupled with energy storage. The system has been designed with four operational modes: CO_2 air source heat pump mode, ground source heat pump mode, combined operation mode of CO_2 air source and ground source heat pumps, and energy storage heating mode. Firstly, based on the equivalent thermal parameter model, the heat demand of the plant factory is analyzed. On this basis, an optimal control strategy for the coupled operation of CO_2 heat pump and ground source heat pump is proposed by adopting the regional energy balance control method, taking into account the influence of key parameters such as peak and valley hours of electricity consumption, return water temperature, and ambient temperature on the system performance. Then, the operational and economic performance of the system under multi-mode is predicted and optimized. At the same time, an operation strategy is proposed in which the system releases energy during the peak hours of electricity consumption and stores energy during the trough hours, which balances the fluctuation of the grid load. The results indicate that the optimised system improves the integrated heating efficiency by 11.2% and reduces the operating cost by 9.6% when compared to the CO_2 air source heat pump system operating alone. Additionally, the peak-to-valley ratio of the system's load-use hours decreased by 36.5%, mitigating short-term overloading of the local power grid and enhancing the stability and reliability of the power system.

Keywords: CO_2 air source heat pump, Ground source heat pump, Thermal energy storage, Peak-to-Valley Ratio;

2024

助力高效热泵采暖

三花发布板式换热器S65A



专为R290冷媒优化打造
兼顾采暖和制冷

采用全新非对称板型和
冷媒分配设计

换热性能提升

20%⁺

换热器内
冷媒充注量减少

37%

较上一代产品



Energy consumption, Exergy and techno-economic analysis of an industrial building temperature and humidity control system based on low-grade waste heat recovery

Fan Wu^(a,b), Jinshuang Gao^(a,b), Xuejun Zhang^(a,b,*)

^(a) Institute of Refrigeration and Cryogenics, College of Energy Engineering, Zhejiang University, Hangzhou-310027, CN

^(b) Key Laboratory of Refrigeration and Cryogenic Technology of Zhejiang Province, Hangzhou 310027, CN.

*Corresponding email: xuejzhang@zju.edu.cn

ABSTRACT

Industry production process generally consumes a large amount of steam, and a huge amount of low-grade waste heat generated is directly released to the environment, in order to effectively utilize this waste heat and improve the energy efficiency of production process. This paper proposes a waste heat recovery system based on a water-source heat pump for temperature and humidity control of the production environment. The validated process model of the system was developed in TRNSYS and parameter evaluation was carried out to analyse the energy performance. The simulation results of the parametric study show that the combined system is capable of recovering waste heat with an 81.5% efficiency and replacing the original steam heat and humidity control system to meet the production requirements of the production space of 26 °C and 60% relative humidity. The findings of this paper provide a scientific basis for the use of low-grade waste heat recovery for heat and humidity control in the built environment, and offer theoretical and technical guidance for engineering practice.

Keywords: Heat Pump, Waste heat recovery, Exergy, Energy consumption analysis, Economic analysis

1. INTRODUCTION

With the rapid development of the economy, the depletion of fossil energy and the deterioration of the ecological environment have become a common crisis faced by the whole world, which is difficult to effectively resolve. Improving the efficiency of traditional energy utilization and increasing the proportion of clean energy utilization has become a consensus for the energy development of various countries. According to data published by the International Energy Agency[1], the industrial sector accounts for over 30% of global energy consumption. In industries such as pharmaceuticals and tobacco, over 50% of energy consumption is used for environmental temperature control and water heating, and a considerable amount of low-grade waste heat is discharged dissipated into the atmosphere by condensing heat[2-4]. Thus, this inefficiency highlights the urgent demand for waste heat and clean energy utilization methods to reduce system energy consumption while ensuring energy demand of the facilities[5, 6].

A significant amount of research has been done on low-grade waste heat recovery from industrial sector for energy system efficiency gains. The methods developed in previous research have mainly focused on waste heat recovery and reuse through direct or indirect heat exchange[7-10]. Zan et al.[11] proposed is a new adsorption ventilation system that combines air thermal conditioning with indoor air cleaning. The system utilizes the adsorption potential of desiccant materials for moisture and gaseous pollution to achieve dehumidification and cleaning of indoor air, aiming to improve indoor air quality and reduce energy consumption for building ventilation. Liu et al.[12] analyzed two condensation heat regeneration desiccant systems and conducted experimental studies on heat pump-assisted conditions, which showed that the use of high-temperature chilled water above 14 degrees Celsius to control the indoor thermal environment was more stable and energy consumption was reduced by 58 % . Seo et al.[13] proposed a compact heat pipe heat exchanger to study its potential for waste heat recovery under low-grade heat sources, and experimental results show that the thermal performance of the new heat pipe structure has been improved by at least 1.8 times. Tang et al.[14] for condensing heat recovery type precision air conditioning performance research, respectively tested and analyzed the compressor frequency, air volume and cooling water

flow four key parameters on the performance of the system, the results show that by the condensing heat recovery, the performance of this type of precision air conditioning system performance changes are relatively complex.

Traditional industrial air conditioning systems typically use electric heating or heat generated from the consumption of fossil fuels, resulting in high energy consumption and significant pollution[15-17]. Zhang et al.[18] proposed a split-range control strategy for temperature and humidity independent control system, temperature is kept constant by chilled water flow rate control and humidity is kept constant by dynamically adjusting the chilled water temperature, minimizing energy consumption. Jia et al.[19] proposed a condensation heat waste heat recovery for solid desiccant regeneration of the system, which uses a heat pump evaporator to control the temperature of the supply air, and the desiccant regeneration is provided by the condenser, and the performance and characteristics of the heat pump-assisted drying system have been investigated through experiments and simulations. Yu et al.[20] proposed a ground source heat pump driven constant temperature and humidity air-conditioning system, which uses part of the condensation heat for system reheating and the other part is discharged to the soil for storage and reuse, experimental and simulation results show that the system reduces the operating cost by 55.8 % and 48.4 % compared with the traditional air source system and chiller with boiler system. Wang et al.[21] proposes a system in which groundwater is led into an air handling unit(AHU) for fresh air treatment, with lower-temperature groundwater pre-treating the air, followed by temperature and humidity regulation, which greatly reduces the energy consumption of the system.

As low-grade waste heat is usually rejected to the ambient, if it could be reused, it can significantly reduce the energy consumption of the system. Xu et al.[22] proposed a two-stage absorption heat pump system to recover low-grade waste heat, which was experimentally investigated by reducing the wastewater temperature from 45.0°C to 15.9°C, thus achieving waste heat recovery, while the experimental prototype heated water to 52.5°C for domestic heating application. Yu et al.[23] studied the waste heat recovery air source heat pump system and proposed a new evaluation model for this type of system, results show that the novel waste heat recovery heat pump system yield 18.9% higher in COP and only 2.1% increase in total cost. Tan et al.[24] for the low-grade waste heat recovery system, the heat pump, steam turbine, and organic Rankine cycle are modeled by Aspen Plus, under the condition of warming up 10-30°C, performed a comparison of energy efficiency and economic benefits, results showed that the heat pump for the best choice of waste heat recovery.

A summary of existing research shows that the study of low-grade waste heat recovery systems for condensing heat is still in primary stage, this type of low-grade waste heat is widely distributed and in large quantities, with great potential for recovery and reuse. Therefore, this study focuses on a novel type of condensing heat recovery coupled solar system to reduce the AHU system thermal supply for increasing the integral energy efficiency, Analyzed and discussed in terms of energy consumption, exergy and technical economics.

2. METHODS

This paper explores a new solution to improve the overall energy efficiency of a building by using chiller condensation waste heat as a heat pump heat source and coupling solar energy to achieve the replacement of the heating end of a conventional AHU. The research focused on a factory building in Hangzhou, which generates a large amount of low-grade condensing heat daily due to production demands. The research aims to reduce the building's space heating requirements by utilizing waste heat and solar energy. Through parametric analysis, the research identified an optimized design based on key performance indicators such as economy, energy and environmental impact. Specifically, the condensing heat from the chiller unit was lifted to a higher temperature level by the heat pump, mixed with solar heat, and reused to raise the ventilation system reheat, thus eliminating/reducing the need for a post-heater to raise the supply air temperature of the building. Therefore, this research uses TRNSYS software to perform transient simulations to determinate the optimal design between the AHU and the components. Figure 1 illustrates the simulated system in TRNSYS and the interaction between the components.

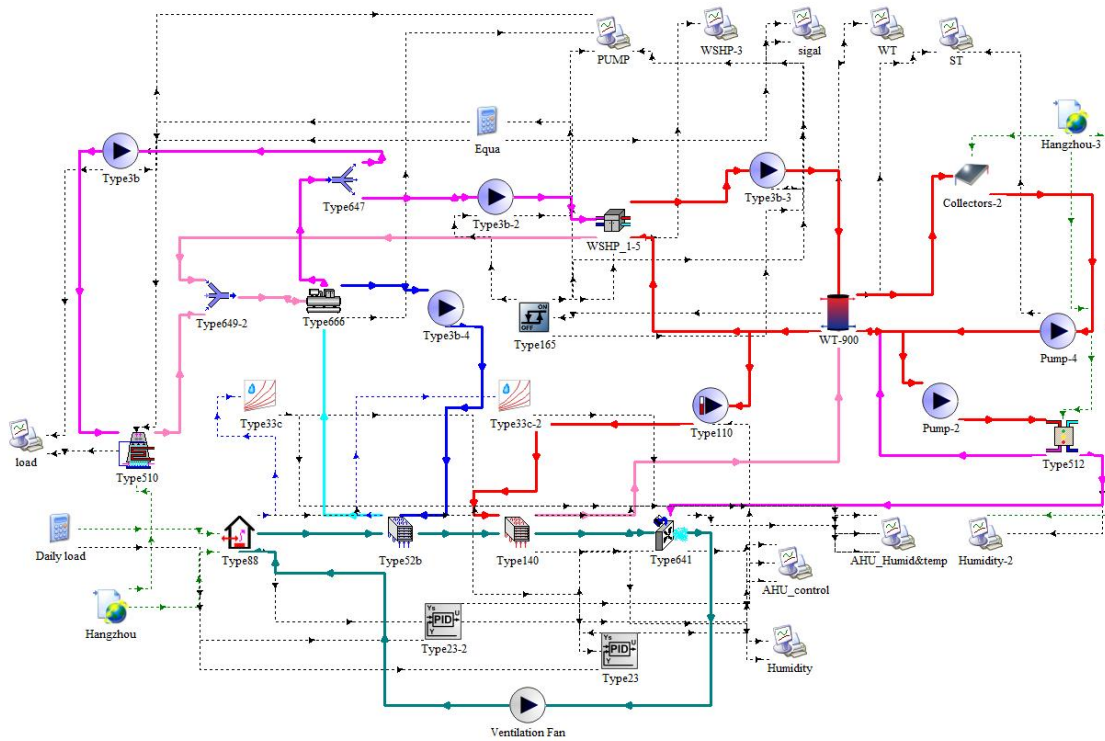


Figure 1: Developed TRNSYS model of the waste heat recovery

2.1 Combined system description

This work investigated the potential of reducing energy consumption by replacing the air reheat unit in the AHU via a waste heat recovery system. Figure 2 provides a brief view of the integrated system consisting of the building, the AHU and the waste heat recovery system. The heat collected by the solar thermal system is gathered in the thermal storage tank which supplies the air reheat in the AHU in case of sufficient illumination. Once the outlet water temperature fails to meet the requirement of the air reheat temperature, the water source heat pump unit is turned on, and the condensation heat from the chiller unit is lifted up to the temperature level and then gathered in the water tank.

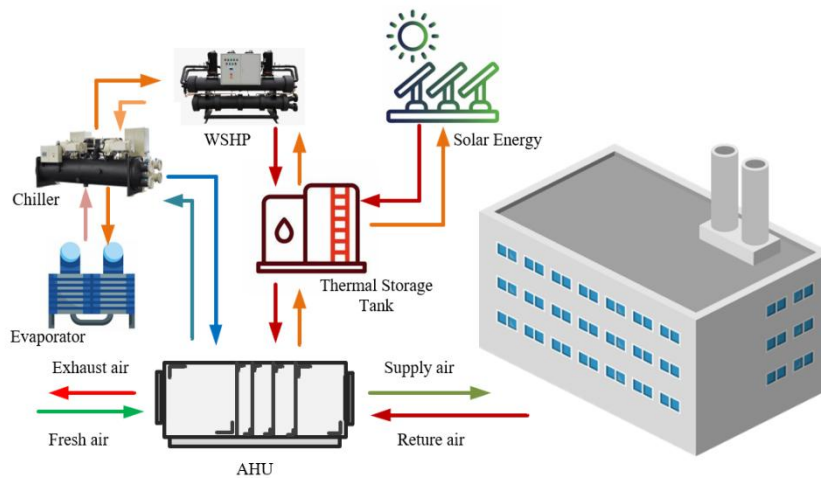


Figure 2: Schematic illustration of the waste heat recovery

2.2 Transient system simulator

Transient simulations were conducted to evaluate the performance of the entire system and its components. The simulation time span is more than one year and the simulation data is derived from the climate data of Hangzhou, China. For this purpose, TRNSYS (Transient System Simulation Tool), a well-known software for transient simulation of energy systems, was used, which calculates the energy and mass balance equations for each component of the simulation in order to evaluate the overall performance metrics defined. The building heating demand is investigated for two scenarios with waste heat recovery system and gas heating, and the total cost and environmental impact are studied. Table 1 details the main components of the system and their corresponding TRNSYS models.

Table 1: System components of the corresponding TRNSYS type.

Component	Type	Description
Chiller	666	This component simulates a vapor compression water-cooled chiller and relies on external data to determine the performance of the chiller.
Water source heat pump	927	This component simulates a single-stage heat pump. The heat pump regulates one stream of liquid by either absorbing energy from another stream (heating mode).
Solar collector	1b	This component simulates the transient performance of liquid solar collectors (or collector arrays)
Heating coil	140	This component simulates air heating coil with internally controlled bypass damper to maintain outlet air temperature above the inlet air temperature and below the user-specified set point temperature.
Humidifier	641	This component simulates an adiabatic humidifier whose outlet air state is determined by the energy balance.
Building	88	This component simulates a certain area that may be affected by infiltration, ventilation, skin loss, internal heat/mass gain and interaction with adjacent areas.

3 EVALUATION METHODS

3.1 Energy consumption evaluation

A package

3.2 Exergy analysis

A package

3.3 Economic evaluation

For waste heat recovery systems, the unit heating cost C_s consists of unit energy cost C_{ec} and unit non-energy cost C_{nc} [25].

4. ANALYSIS AND DISCUSSION

The proposed WSHE can independently handle sensible and latent loads at the same time, which opens up the possibility of achieving ultrahigh efficiency for a broad range of temperature- and humidity-control applications.

4.1 Design parameters

4.2 Thermodynamic perfection analysis

4.3 Energy consumption analysis

4.4 Economic analysis

5. CONCLUSION

ACKNOWLEDGEMENT

This research was supported by Zhejiang Province 2024 ‘Leading Wild Goose’ Research and Development Project (No. 2024C03117), the Basic Research Funds for the Central University ‘Innovative Team of Zhejiang University’ under contract number (2022FZZX01-09), We declare that we do not have any commercial or associative interest that represents a conflict of interest in connection with the work submitted.

REFERENCES

- [1] Agency IE. <https://www.iea.org/fuels-and-technologies/data>.
- [2] Wei J, Hua Q, Wang J, Jiang Z, Wang J, Yuan L. Overview of the Development and Application of the Twin Screw Expander. *Energies*. 2020;13.
- [3] Zhang L, Li Y, Zhang H, Xu X, Yang Z, Xu W. A review of the potential of district heating system in Northern China. *Applied Thermal Engineering*. 2021;188.
- [4] Zhang XJ, Yu CY, Li S, Zheng YM, Xiao F. A museum storeroom air-conditioning system employing the temperature and humidity independent control device in the cooling coil. *Applied Thermal Engineering*. 2011;31:3653-7.
- [5] Ni H-P, Chong WO, Chou J-S. Optimizing HVAC systems for semiconductor fabrication: A data-intensive framework for energy efficiency and sustainability. *Journal of Building Engineering*. 2024;89.
- [6] Shafiee Roudbari E, Kantor I, Menon RP, Eicker U. Optimization-based decision support for designing industrial symbiosis district energy systems under uncertainty. *Applied Energy*. 2024;367.
- [7] Duan Y, Zhang X, Han Z, Liu Q, Li X, Li L. Numerical investigation of coupled heat transfer and flow characteristics in helical coil heat exchanger for mine water waste heat recovery. *International Journal of Thermal Sciences*. 2024;202.
- [8] Xu Y, Xue Y, Cai W, Qi H, Li Q. Experimental study on performances of flat-plate pulsating heat pipes without and with thermoelectric generators for low-grade waste heat recovery. *Applied Thermal Engineering*. 2023;225.
- [9] Tian X, Yang J, Wang T, Tian Y, Zhou Z, Wang Q. Effective waste heat recovery from industrial cohesive granular materials: A moving bed indirect heat exchanger with special flow control. *Journal of Cleaner Production*. 2024;437.
- [10] Zhao W, Li H, Wang S. A generic design optimization framework for semiconductor cleanroom air-conditioning systems integrating heat recovery and free cooling for enhanced energy performance. *Energy*. 2024;286.
- [11] Zan Li DL. Study on the Dehumidification and Indoor Air Cleaning Performance of Rotary Desiccant Rotor ScienceDirect. 2017;205:497-502.
- [12] Liu S, Jang H, Yeo M-S. Experimental study on the operating characteristic of the desiccant cooling systems with the potential of condensing heat recovery. *Energy*. 2023;283.
- [13] Seo J, Kang S, Kim K, Lee J. Compact heat pipe heat exchanger for waste heat recovery within a low-temperature range. *International Communications in Heat and Mass Transfer*. 2024;155.
- [14] Tang F, Gao J, Wu X, Hu G, Yao H, Zhu X. Performance investigation on a precision air conditioning system with a condensation heat recovery unit under varying operating conditions. *Applied Thermal Engineering*. 2024;236.
- [15] Rebelo FWD, Ismail KAR, Lino FAM, Sousa GA. Experimental investigation of a photovoltaic solar air conditioning system and comparison with conventional unit in the context of the state of Piauí, Brazil. *Solar Energy*. 2024;272.
- [16] Desideri U, Proietti S, Sdringola P. Solar-powered cooling systems: Technical and economic analysis on industrial refrigeration and air-conditioning applications. *Applied Energy*. 2009;86:1376-86.
- [17] Men Y, Liu X, Zhang T. Frost prevention research of the enthalpy wheel in air conditioning systems and industrial heat recovery systems. *Building and Environment*. 2022;222.
- [18] Zhang XJ, Xiao F, Li S. Performance study of a constant temperature and humidity air-conditioning system with temperature and humidity independent control device. *Energy and Buildings*. 2012;49:640-6.
- [19] Jia CX, Dai YJ, Wu JY, Wang RZ. Analysis on a hybrid desiccant air-conditioning system. *Applied Thermal Engineering*. 2006;26:2393-400.
- [20] Yu X, Wang RZ, Zhai XQ. Year round experimental study on a constant temperature and humidity air-conditioning system driven by ground source heat pump. *Energy*. 2011;36:1309-18.
- [21] Wang Z, Wang L, Ma A, Liang K, Song Z, Feng L. Performance evaluation of ground water-source heat pump system with a fresh air pre-conditioner using ground water. *Energy Conversion and Management*. 2019;188:250-61.
- [22] Xu ZY, Gao JT, Mao HC, Liu DS, Wang RZ. Double-section absorption heat pump for the deep recovery of low-grade waste heat. *Energy Conversion and Management*. 2020;220.
- [23] Yu X, Jiang R, Lu G, Liu H, Tong Y, Qian G, et al. A novel energy-economic-environmental evaluation model for heat pump air conditioners integrated with waste heat recovery in electric vehicles. *Case Studies in Thermal Engineering*. 2023;41.

[24] Tan Z, Feng X, Yang M, Wang Y. Energy and economic performance comparison of heat pump and power cycle in low grade waste heat recovery. *Energy*. 2022;260.

[25] Khaljani M, Khoshbakhti Saray R, Bahlouli K. Comprehensive analysis of energy, exergy and exergo-economic of cogeneration of heat and power in a combined gas turbine and organic Rankine cycle. *Energy Conversion and Management*. 2015;97:154-65.

Optimising steam generating heat pump integration in industries: performance analysis across different heat sources and heating demands

BoYANG^(a), AzadehJAFARI^(a), MaziarARJOMANDI^(a)

^(a) School of Electrical and Mechanical Engineering, the University of Adelaide
Adelaide, 5005, Australia, bo.yang01@adelaide.edu.au

ABSTRACT

Steam has been widely used as an energy carrier in industrial processes. As the world aims for decarbonisation, steam generating heat pumps serve as potentially sustainable alternatives to conventional boilers for producing steam at low to medium temperatures (below 300°C). Despite the commercial availability of steam generation heat pumps for temperatures up to about 250°C, an understanding of these technologies is essential for optimising their integration into industrial processes. This study investigates the performance of various steam generating heat pumps, including open- and closed-cycle, as well as cascaded systems, for producing steam ranging from 160°C to 300°C, utilising heat sources from ambient to 120°C. The findings reveal how the type of working fluids and boundary conditions such as waste heat temperature and heating demand, affect the performance of different steam generating heat pump technologies. Consequently, guidelines are provided to assist industries in selecting the most suitable heat pump technology, tailored to meet their specific demands.

Keywords: Steam generating heat pump, mechanical vapor recompression, thermal vapor compression, COP.

Experimental Research of CO₂ Two-stage Compression Refrigeration System with Vapor-injection

Xiaoqiong Li^(a), Qing He^(a,b), Youdong Wang^(a,c), Zhentao Zhang^(a), Junling Yang^(a), Jian Dai^(a).

^(a) Technical Institute of Physics and Chemistry, Chinese Academy of Sciences, Beijing 100190, China

^(b) China University of Petroleum (East China), Qingdao 266555, China

^(c) Tianjin University of Science & Technology, College of Mechanical Engineering, Tianjin, 300222, China

ABSTRACT

CO₂ refrigeration is considered the optimal approach for the development of refrigeration technology in the context of carbon peaking and carbon neutrality. This paper presents the design and construction of a CO₂ two-stage compression refrigeration system with vapor-injection. The effects of the evaporating temperature, discharge pressure of the high-pressure stage compressor, outlet temperature of intercooler and frequency of high-pressure stage compressor on the two-stage compression refrigeration system were investigated. The experimental results showed that the performance of this system was more influenced by the evaporation temperature than the outlet temperature of the intercooler. And when the evaporation temperature increased from -28°C to -20°C, the system COP increased by 23.9%. The system COP reached a maximum value of 1.78 at a high pressure of 8.4 MPa. As the frequency of the high-pressure stage compressor increased, the COP of the system showed a trend of increasing and then decreasing, and the COP reached its maximum value of 1.73 at a

compressor frequency of about 52Hz. This study guides the application of CO₂ two-stage compression refrigeration system for actual use in the cryogenic cold chain.

Keywords: CO₂ two-stage compression refrigeration; vapor-injection; COP; discharge temperature

Research and analysis on the usage patterns and typical scenarios of people in public spaces based on machine vision

**HuanWANG^(a), QuanJIANG^(b), TianhangLI^(b), GuoLI^(b), ChenjiyuLIANG^(a),
YuanJIU^(a), XiantingLI^(a#)**

^(a) Department of Building Science, Beijing Key Laboratory of Indoor Air Quality Evaluation and Control, Tsinghua University, Beijing, 10084, China, xtingli@tsinghua.edu.cn

^(b) Zhuhai Huafa Industrial Co., LTD
Zhuhai, 519030, China

ABSTRACT

The differences in the distribution of people and their dwell times within architectural environments give rise to various practical usage scenarios for buildings and result in significant variations in the energy consumption of lighting, air conditioning, and other building service systems. Understanding the distribution of people can also enhance the efficiency of work and living spaces, enabling the optimization of workflows, improvements in spatial layouts, or adjustments to heat pump and other equipment configurations to boost efficiency. In the current architectural environment, obtaining data for typical scenarios typically relies on manual on-site surveys, which limit the scope and temporal dimension of the research, can easily influence activities and scenarios within rooms, and make it difficult to determine the precise locations of people in actual usage scenarios.

Our research team previously proposed a non-contact personnel positioning system utilizing binocular vision cameras, which enables accurate, real-time, and continuous acquisition of indoor personnel positioning information. This system combines binocular cameras with personnel recognition algorithms to obtain indoor personnel distribution information over long periods, typically measured in weeks. Utilizing big data analysis methods on this basis, we can derive typical personnel usage patterns and locations of personnel stays within measured spaces. Through clustering, typical indoor usage scenarios and their distribution proportions can be identified. Leveraging this technology, our team conducted continuous real-time indoor personnel positioning data collection for over 10 days in six typical buildings. Through cluster analysis of over a hundred million lines of personnel positioning data, we identified five typical scenarios and proportions of personnel distribution in small to medium-sized public spaces. Our findings revealed that the average occupancy rate of public spaces surveyed was less than 50%, and the proportion of actual design scenarios occurring within these spaces was less than 30%. This research method and its results can provide fundamental data for indoor heat pump design, intelligent construction, and energy-efficient operation of indoor environmental service systems.

Keywords: Machine Vision, Actual Usage Patterns, Typical Scenarios, Energy Efficiency, Personnel Positioning System.

Advanced control strategy of ground-source heat pump

Yiming Li^(a), Suxin Qian^(a)

^(a)Department of Refrigeration and Cryogenic Engineering, Xi'an Jiaotong University
Xi'an, 710049, China, qiansuxin@xjtu.edu.cn

ABSTRACT

Ground source heat pump (GSHP) systems have gained significant attention in recent years for space heating applications. In traditional GSHP control strategy, the supply water temperature and flow rate are typically maintained constant, which is inefficient and may decrease user thermal comfort under part load operation. In order to optimize GSHP power consumption, this study aimed to minimize unnecessary power consumption in circulating pumps under variable load operation by employing an advanced load-predictive control strategy. The load-side return water temperature was fixed in this advanced control strategy, and the load-side optimal supply water temperature and flow rate were determined through a performance map, while the source-side optimal flow rate was computed iteratively because the soil heat transfer rate was not possible to explicitly predict. Using a typical office building located in Xi'an as a case study, a transient GSHP simulation model was developed in TRNSYS and WAS validated by the experimental data. Based on the simulation model, the load-predictive control strategy was numerically studied to investigate the energy-saving potential. Through the modulation of supply water temperature and flow rate, the advanced control strategy demonstrated a noteworthy energy-saving of 11% compared to the traditional control strategy.

Keywords: Ground source heat pump, Control strategy, Water flow rate, TRNSYS.

Finite time thermodynamics optimization of indirect sewage source heat pump system

Qian Jian-feng^(a), Huang Cheng-chao^(b), Li-Tao^(c), Kong Fan-peng^(d)

^(a)School of Energy&Construction Engineering, Harbin University of Commerce, Harbin 150028,China,13054261117@163.com

^(b)School of Energy&Construction Engineering, Harbin University of Commerce, Harbin 150028,China.851346474@qq.com

^(c)School of Energy&Construction Engineering, Harbin University of Commerce, Harbin 150028,China,1713611138@qq.com

^(d)School of Energy&Construction Engineering, Harbin University of Commerce, Harbin 150028,China,1317055378@qq.com

ABSTRACT

This article studies the finite-time thermodynamic optimization of indirect sewage source heat pump systems. Taking a hotel in Beijing as an example, the operation of the system in winter was investigated, and relevant data were collected, including sewage temperature, hot water preparation temperature, heat supply, energy consumption, and COP performance coefficient. Then, the indirect sewage source heat pump system was optimized using finite-time thermodynamics, considering heat leakage, thermal resistance, and irreversibility of the cycle. Based on this, a sewage source heat pump cycle model was constructed, and the objective function was optimized using the Lagrangian multiplier method to study the proportional relationship between various heat transfer areas under optimal conditions for the heat pump's heating performance coefficient. The relationship between various parameters was also studied under the condition of minimizing the total heat transfer area of the heat exchanger. Finally, the optimization results were verified through specific examples.

This article uses TRNSYS software to build a simulation model of the indirect sewage source heat pump system, simulating the original system and the optimized system separately, and analyzing the changes in hot water temperature, heat supply, energy consumption, and COP produced by the two systems. The results show that the optimized system has improved hot water temperature, heat supply, and COP by 11.78%, 28.33%, and 18.42% respectively, with a total heat supply 26.50% higher than the original system and energy savings of 14.41%. It can be seen that the comprehensive performance of the optimized system has been improved, and the optimization effect is significant.

Keywords: Sewage source heat pump system, Finite time thermodynamics, TRNSYS simulation

1. INTRODUCTION

With the increase in the total number of buildings in China, the energy consumption of their operation has also intensified, resulting in a large number of environmental pollution problems that persist. The sewage source heat pump system can effectively save energy, and urban sewage has the potential to be used as a heat pump cold and heat source due to its stable temperature. Therefore, recycling low-grade energy such as sewage can effectively solve the energy supply and demand problems in various regions. In northern China, most rural and urban areas use fossil fuels such as coal, oil, and natural gas to obtain heat for winter heating, but the extensive use of fossil fuels can cause serious environmental problems, so the contradiction between heating and environmental protection is difficult to resolve at this stage. In northern China, the climate is cold and there is a lack of suitable heat pump cold and heat sources. The emergence of sewage heat energy makes up for this gap. The temperature of urban sewage remains basically stable throughout the year, and the operating efficiency of sewage source heat pump systems in both winter and summer is higher than traditional air conditioning, with less energy consumption and significant comprehensive benefits.

2. Research content

Based on the research progress of sewage source heat pump system optimization at home and abroad, this article focuses on the following aspects:

(1) Simulation and building experimental platforms are currently the most common methods for heat pump research, but these methods neglect the monitoring of specific engineering operating conditions and lack realistic support. The conclusions drawn are not rigorous, so this study conducted field tests on existing demonstration projects of heat pump systems to understand the changes in relevant parameters during the operation of indirect sewage source heat pump systems, and analyzed the experimental data to draw some conclusions, providing a basis for further research on indirect sewage source heat pump systems.

(2) Utilizing the theory of finite-time thermodynamics, establish a steady-state irreversible cycle model for indirect sewage source heat pump systems, paying attention to the effects of thermal resistance, heat leakage losses between heat sources, and internal irreversible losses in the cycle. Under given thermal loads and other fixed parameters, optimize the model to study the optimal relationship between the main design parameters and performance parameters of the system when the objective function (coefficient of performance and minimum total heat transfer area) is optimized.

(3) Utilize TRNSYS software to conduct simulation studies on unoptimized and optimized systems. Compare and analyze the changes in hot water temperature, system heat supply, system energy consumption, and system COP for both systems to determine the optimization effect.

3. CONCLUSIONS

Compared with the original system, the optimized system has improved hot water temperature, heating capacity, and COP, and the total heating capacity is 26.50% higher than the original system, resulting in a 14.41% energy saving. Therefore, it can be seen that the comprehensive performance of the optimized system has been improved, and the optimization effect is significant.

ACKNOWLEDGEMENT

This work was supported by the Natural Science Foundation of Heilongjiang Province Joint Guidance Project (No.LH2023E028).

REFERENCES

- [1] Medjo Nouadje Brigitte Astrid et al. Exergetic optimisation of a four-temperature-level absorption heat pump based on finite-time thermodynamics[J]. International Journal of Sustainable Energy, 2022, 41(3):257-288.
- [2] Guo P, Zhou J, Ma R, et al. Dynamic Heating System of Multiphase Flow Digester by Solar-Untreated Sewage Source Heat Pump[J]. International Journal of Photoenergy, 2020, 20:1-15.

Study on the characteristics and influence of cold and wet island effect from air source heat pump array

XueFengGAO^(a), ShiMinLIANG^(a), HanWANG^(a)

^(a) School of Environmental and Municipal Engineering, Qingdao University of Technology, Qingdao, 266520, China, liangshimin@qut.edu.cn

ABSTRACT

With the expansion of air source heat pump (ASHP) space heating scale from household to million square meters level, ASHP array had become the main form of site layout. However, the cold and wet island effect (C-WIE) was easily formed in the center of the ASHP array, and current research mostly focused on the single cold island effect (CIE), ignoring the wet island effect (WIE). This paper relied on three ASHP array space heating projects and used field test method to explore the characteristics and influence of C-WIE from ASHP array. The results indicated that the C-WIE was widely present and coupled with each other, and was affected by many factors such as ambient temperature and humidity, power on ratio, array scale, and surrounding barrier. The long-term test results showed that the average C-WIE intensities of the center unit in array were $0.8^{\circ}\text{C} \sim 5.5^{\circ}\text{C}$ and $3.2\% \sim 17\%$, respectively. The heating performance loss coefficient of C-WIE for the center unit was $0.06 \sim 0.32$, and *COP* was decreased by $7\% \sim 33\%$. This study has important guiding significance for improving the operating energy efficiency of ASHP array.

Keywords: Air source heat pump array; Cold island effect; Wet island effect; Field test.

Research on energy-saving optimization control of air-cooled heat pump combined with floor heating system

Xiaoxi Hong^(a), Ye Yao^(a,*)

^(a) Institute of Refrigeration and Cryogenics, School of Mechanical Engineering, Shanghai Jiao Tong University
Shanghai, 200240, China, yeyao10000@sjtu.edu.cn

ABSTRACT

The floor heating system using air-cooled heat pumps as the heat source is a new and effective economic strategy to replace coal-fired heating. With the widespread application of this system, the overall energy-saving optimization control of the system has become an important research content to achieve carbon peak and carbon neutrality goals. This study establishes a neural network model based on actual data, taking into account the goals of energy conservation and human thermal comfort. Under certain environmental temperature and humidity, solar radiation intensity, and building orientation, the optimal pump frequency and chilled water supply temperature are obtained through an optimization algorithm. Compared with the unoptimized working conditions, the system using the optimization strategy can maintain indoor temperature between $19.5\text{-}20.5^{\circ}\text{C}$ and achieve an energy-saving rate of 15.3%. This study can achieve energy-saving optimization while ensuring

human thermal comfort, providing an effective solution for the low-carbon development of air-cooled heat pump with floor heating system.

Keywords: Air-cooled heat pump, Floor heating system, Energy saving optimization control

Investigation of a novel dual-temperature district heating substation for radiant combined with convection systems

Tiancheng LI^(a,b), Mengdi CUI^(a,b), Wenxing SHI^{(a,b)*}, Xianting LI^(a,b), Baolong WANG^(a,b)

^(a) Department of Building Science, Tsinghua University, Beijing, 100084, China, hvac@tsinghua.edu.cn

^(b) Beijing Key Laboratory of Indoor Air Quality Evaluation and Control, School of Architecture, Tsinghua University Beijing, 100084, China, hvac@tsinghua.edu.cn

*Corresponding author: wxshi@tsinghua.edu.cn

ABSTRACT

Radiant combined with convection systems are favored for providing a heating environment with good air quality and comfort, coupled with high heating efficiency. However, one kind of temperature of hot water is sent to different heating terminals, leading to inefficient utilization of thermal energy and exergy loss. Due to the significant differences between the radiant and convective terminals, a novel dual-temperature district heating substation system employing one absorption heat pump and two heat exchangers is proposed to meet the different heating demands and reduce the water temperature of the primary network as much as possible. Results showed that at the designed primary supply water temperature of 90°C, the return water temperature of the primary network could be reduced to 19.9°C over the whole heating season, and the coefficient of performance of the system can reach 8.26. Compared to schemes of single-temperature district heating systems with a heat exchanger or with an absorption heat exchanger, the proposed system can reduce the return water temperature of the primary network by 12.8°C to 9.1°C. Additionally, the primary network water flow rate can be reduced by 9.03% and 29.42%, respectively, while the coefficient of performance (COP) can be increased by 38.6% and 41.9%, respectively.

Keywords: Dual-temperature, District heating substation, Absorption heat pump, Return water temperature

1. INTRODUCTION

Creating an energy-efficient, comfortable, and healthy heating environment is an important aspect of ensuring the quality of people's lives and promoting energy-saving and carbon reduction in buildings. Radiant combined with convection systems are favored for providing a heating environment with good air quality and comfort, coupled with high heating efficiency[1]. However, due to the significant differences between the radiant and convective terminals, one kind of temperature of hot water is sent to different heating terminals, leading to inefficient utilization of thermal energy and exergy loss[2]. Therefore, the development of a dual-temperature district heating substation is essential to study to meet the different heating requirements of different terminals, reduce heat transfer losses, improve the system efficiency, and increase the heating capacity of the primary network[3-5].

In this study, a dual-temperature district heating substation with an absorption heat pump(AHP) and two exchangers(1AHP+2HX), which utilizes primary network water as the heat source to produce two different temperatures of water to separately supply heat to the radiant floor heating(RFH) and fresh air handling unit(FAHU).

2. SCHEME OF THE DUAL-TEMPERATURE DISTRICT HEATING SUBSTATION

2.1 The system principle

A novel dual-temperature district heating substation system has been proposed recently as shown in Fig.1 (a). The primary network hot water sequentially passes through the generator, high-temperature hot water heat exchanger, low-temperature

hot water heat exchanger and evaporator, and then returns to the power plants. On the secondary side, the return water of RFH is divided into two parts. One part is heated by the absorber of AHP, while another part is heated by the low-temperature heat exchanger. Similar to the radiant floor heating, the return water of FAHU is also divided into two parts. One part is heated by the condenser of AHP, while another part is heated by the high-temperature heat exchanger.

When the outdoor temperature is relatively low, the system adjusts the circulation flow rate of the solution and changes the proportion of the return water entering the heat exchangers and absorption heat pumps to meet the changes in heating loads. However, when the outdoor temperature is high the absorption heat pump is switched off, and only two heat exchangers are activated for heating, as shown in Fig.1(b).

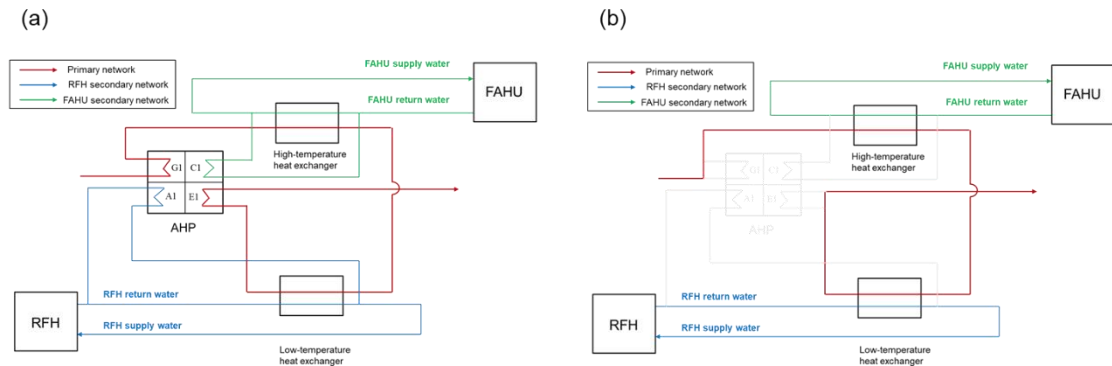


Figure 1: Schematics of dual-temperature district heating substation system with one absorption heat pump and two heat exchangers: Mode 1 (a), Mode 2 (b).

2.2 Performance of the dual-temperature district heating substation

Taking an office building in Beijing as an example of system design. The heating load of FAHU and RFH is 2224.73 kW and 5225.71 kW, respectively. With a primary network water supply temperature of 90°C, the return water temperature of the primary network can be reduced to 19.1°C. The designed primary network water flow rate is 25.1 kg/s. The primary network and secondary network water flow rates and temperatures of the system under design conditions are shown in Fig.2.

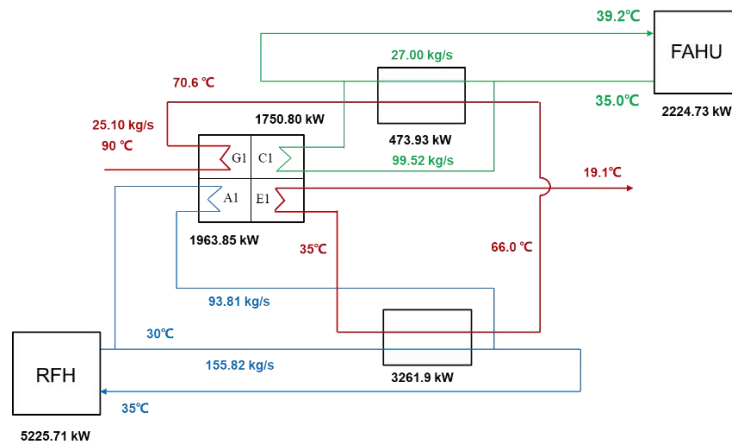


Figure 2: Schematics and specific design parameters of 1AHP+2HX system.

Fig.3 (a) and (b) respectively illustrate the variation of supply and return water temperatures for RFH and FAHU in the primary and secondary networks when quality regulation is adopted. According to Fig.2(a), in Mode 1 operation of the system, the supply water temperature of the primary network decreases linearly, while the return water temperature remains almost constant. When the system switches to Mode 2 above the outdoor temperature of 7°C, the return water temperature of the system increases because it cannot decrease below the return water temperature of RFH due to the limitations of the heat exchanger. As the primary network's supply water flow rate remains constant, the supply water temperature of the primary network increases accordingly. Fig.3 (b) reflects the variation of supply and return water temperatures for RFH and FAHU in the secondary network when the quality regulation is adopted. The proportion of mass flow rate of secondary network water entering the absorption heat pump and heat exchanger changes to adapt to the variation of building load according to the different ambient temperatures. Meanwhile, both the supply and the return water temperatures of the secondary network decrease.

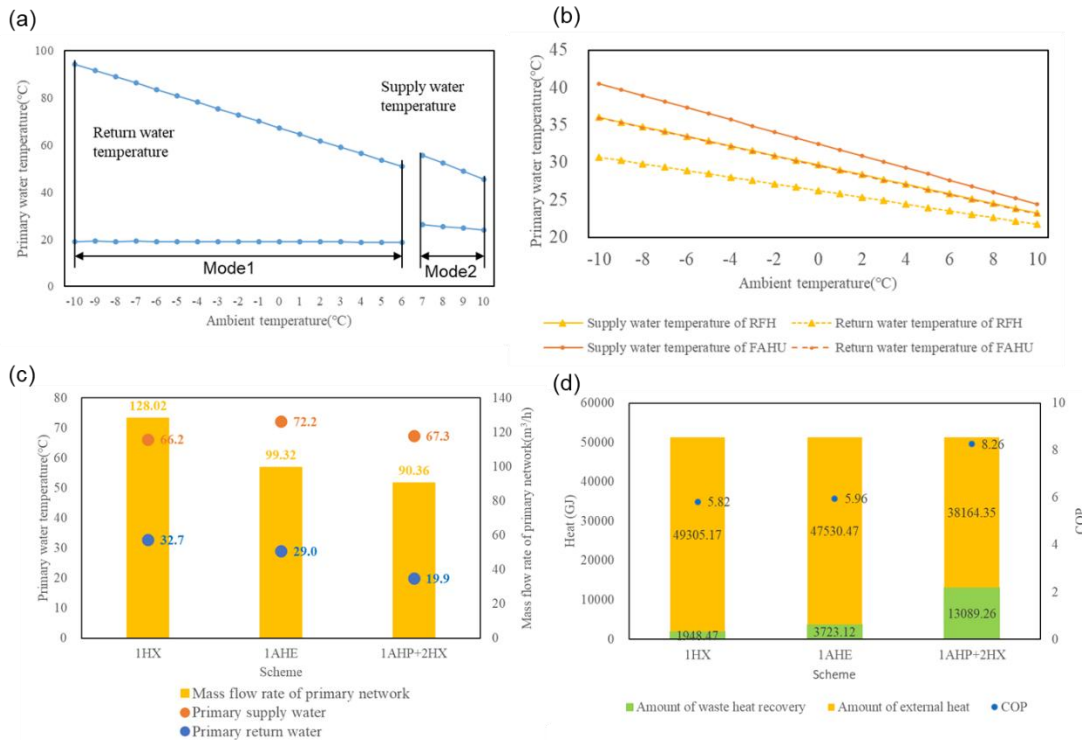


Figure 3: The operational performance of the 1AHP+2HX system and its comparison with other systems: Temperature of the primary network (a), Temperature of the secondary network (b), Thermodynamic comparison of different schemes over the entire heating season (c), Waste heat recovery and COP of three schemes (d).

Fig.3(c) and (d) respectively present a comparison between this system and two single-temperature heating systems using heat exchangers and absorption heat exchangers, respectively. Compared to schemes of single-temperature district heating systems with a heat exchanger or with an absorption heat exchanger, the proposed system can reduce the return water temperature of the primary network by 12.8°C to 9.1°C. Additionally, the primary network water flow rate can be reduced by 9.03% and 29.42%, respectively, while the coefficient of performance (COP) can be increased by 38.6% and 41.9%, respectively. Due to the 1AHP+2HX system's primary network return water having the lowest temperature and minimum flow rate, it recovers more waste heat from the exhausted steam in the power plant. Therefore, it achieves the highest equivalent COP.

3. CONCLUSIONS

To address the inefficient utilization of thermal energy and exergy loss caused by using a single-temperature heat source to heat FAHU and RFH in the radiant combined with convection systems, a dual-temperature district heating substation, namely 1AHP+2HX system, is proposed. This system uses the primary hot water as the heat source and provides higher temperature water for FAHU and low-temperature water for floor heating. Under design conditions, it can reduce the return water temperature of the primary network to 19.1°C. Compared to two single-temperature hot water schemes using heat exchangers and absorption heat exchangers, the proposed system can respectively reduce the return water temperature of the primary network by 12.8°C to 9.1°C, decrease the primary network water flow rate by 9.03% and 29.42%, and increase the COP by 38.6% and 41.9%. This scheme provides a reference for designing district heating systems with different heating demands.

ACKNOWLEDGEMENT

This work was supported by the Huaneng Group Science and Technology Research Project (HNKJ20-H50) and the China National Key R&D Program “Integrated convection/ radiation coupling terminals for local environment” (Grant No.2022YFC3801502).

REFERENCES

[1] F. Causone, F. Baldin, B. W. Olesen and S. P. Corgnati. 2010, Floor heating and cooling combined with displacement ventilation: Possibilities and limitations. *Energy and Buildings*. **42**, 2338-2352.

- [2] S. Huang, F. Zhou, J. Liu and X. Zhang. 2024, Comparison of various dual-temperature zones space heating systems based on energy cascade utilization principle. *Applied Thermal Engineering*. **236**, 121606.
- [3] J. Liu and Z. Lin. 2021, A novel dual-temperature ejector-compression heat pump cycle-exergetic and economic analyses. *International Journal of Refrigeration*. **126**, 155-167.
- [4] H. Averfalk and S. Werner. 2017, Essential improvements in future district heating systems. *Energy Procedia*. **116**, 217-225.
- [5] T. Li, W. Chen, X. Li, B. Wang and W. Shi. 2024, Investigation of control strategies for dual-temperature district heating substations with two absorption heat pumps and two heat exchangers. *Energy Conversion and Management*. **309**, 118431.

High-Performance Hydrogen-Powered Heat Pumps

Bruno CARDENAS^(a), Seamus GARVEY^(a), Zahra BANIAMERIAN^(a), Ramin MEHDIPOUR^(a)

(A) University of Nottingham, Department of Mechanical, Materials and Manufacturing Engineering
Nottingham, NG7 2RD, United Kingdom, bruno.cardenas@nottingham.ac.uk

ABSTRACT

Hydrogen is being considered as one of the main options to decarbonise space heating. One of the key advantages is the possibility of seasonal energy storage using underground caverns. However, a disadvantage of using hydrogen is that when combusted in boilers, only ~60% of the energy that went into making it reaches a house in the form of low-temperature heat for space-heating.

Electrical heat pumps are the other low-carbon solution being considered. Heat pumps can deliver up 4x the amount of energy they consume. However, the current electricity grid (in the UK) does not have the capacity to support their widespread use. The upgrades and reinforcements required to ‘*electrify domestic space-heating*’ and enable the electricity grid to take on the gas network’s duty are not feasible due to the extremely high costs.

This paper presents a novel concept called *High-Performance Hydrogen-Powered Heat-Pump (HP3)*, which combines the best attributes of heating by hydrogen combustion and electrically driven heat-pumping. HP3 systems are thermo-mechanical systems that blend a heat-engine and a heat-pump to deliver a large quantity of low-grade heat using a small amount of high-grade (high temperature) heat from the combustion of H₂ or another clean fuel.

Initial calculations show that the system can achieve attractive performance levels with realistic operating parameters. Considering an ambient temperature of -9°C and flow/return temperatures of 55/35 °C, respectively, the system could see a *CoP* of ~2.4.

One of the main design challenges is to achieve a high isentropic efficiency in the expander(s) of the heat engine section, which is key to achieve a high overall *CoP*. The work carried out thus far has revealed that the design of these turbomachines simplifies as the output of the system increases. This indicates that HP3 systems are better suited for district heating systems (>200 kW).

Keywords: Space Heating, Low-Carbon Heating, Hydrogen Boilers, Heat-Driven Heat Pumps, Hybrid Heat Pumps, COP

LET THE BUILDING BREATHE FREELY / 让建筑自由呼吸



麦克维尔官方微信 麦克维尔官方网站



开启“双碳”环保新局面

谁说高温热水、节能减排不可兼得？麦克维尔致力于环保低碳的理念，推出复叠式高温热泵热水机MHAS，代替燃煤锅炉，减少对环境的污染；最高可提供90℃高温出水及蒸汽超高温前处理、预热处理等，满足各类工业、商业用水要求，提供安全、环保、减碳的服务！



°C



复叠式高温热水机MHAS
制热量：16-56kW
产水量：200~1200L/h



90℃高温出水

55-90℃宽出水温度可调，不受室外气温影响；



节能超效

采用高效全变频系统，无燃烧，安全又环保；



-26℃制热运行

EVI系统-26℃超低环境温度运行，环境适应能力强；



智能控制

触摸按键式控制屏，简单易操作，控制更便捷；

空调热泵维修利器

德图 testo 数字冷媒表系列

保压、真空、充注、检漏、运行测试...



更多产品 更多选择

德图仪器国际贸易（上海）有限公司

热线：400 882 7833

邮箱：info@testo.com.cn



www.testo.com.cn

An Advanced Cascade Method for Optimal Industrial Heating Performance in Air Source Hybrid Heat Pump

Qiang Ji^(a, b), Yonggao Yin^(a), Gongsheng Huang^(b), Yikai Wang^(a)

^(a) School of Energy and Environment, Southeast University
Nanjing, 211189, China, y.yin@seu.edu.cn

^(b) Department of Architecture and Civil Engineering, City University of Hong Kong
Hong Kong, 518057, China, gongsheng.huang@cityu.edu.hk

ABSTRACT

Air is a readily available and renewable source, but its efficient utilization for industrial heating is hindered by the significant temperature mismatch between the low-grade air source and the high-temperature industrial demand. Heat pumps can elevate the source temperature from low to high levels. However, there is still a significant knowledge gap in achieving output temperature exceeding 90°C when the input source is below 30°C. While there are some preliminary studies on air-source heat pumps operating in the mentioned temperature range, they have yet to distinguish the respective coupling temperatures required for different cascaded components. Therefore, the optimal cascade configuration between various sub-cycles has not been established, and the full efficiency potential remains untapped. To address the identified limitations, in this work, an advanced cascade mode is proposed and applied to the air source compression-absorption heat pump (CAHP). The novel cascade method allows independent control of the coupling temperature in different branches as needed, facilitating an optimal cascade configuration between various subloops. Consequently, the operating efficiency of CAHP is optimized. Simulation results show that the proposed cascade mode reduces the exergy destruction of CAHP by 6.3% compared to the existing mode. Moreover, it always achieves higher efficiencies in the studied conditions, with a maximum increase in the coefficient of performance and exergy coefficient of performance by 16.2% and 19.2%, respectively. Under ambient temperature of 10°C to 30°C and an output temperature of 100°C, the improved cascade CAHP exhibits an increase in heating capacity, ranging from 51.8% to 336.4% higher than the existing mode. These advantageous features contribute to achieving cleaner industrial heating with air source heat pumps.

Keywords: Absorption heat pump; Ionic liquid; Compression-absorption cascade; Efficiency optimization; Industrial heating

Multi-Objective Optimization of a Direct Air Capture System Integrated with Air-Source Heat Pumps

Weikai Shi^(a), Renyu Xie^(a), Xuejun Zhang^(a), Long Jiang^(a)

^(a) Institute of Refrigeration and Cryogenics, Zhejiang University
Hangzhou, 310027, China, jianglong@zju.edu.cn

ABSTRACT

Direct air capture (DAC) processes meet challenges in considerable heat demand. The method of integrating heat pumps shows excellent potential for low-grade heat utilization. This study aims to introduce and design a flexible DAC system with the superiority of enhancing adsorption capacity and reducing heat consumption. It utilizes the concept of synergetic cooling and heating achieved by the air-source heat pump. To investigate the performance of the integrated system, different refrigerants are screened to be compatible with working cycles of DAC using LEWATIT VP OC 1065, and the combination of numerical modelling and multi-objective algorithm is proposed to optimize productivity, purity, and energy efficiency of the DAC outputs. The results indicate that the concept can maximize cycle capacity up to 1.3 mmol·g⁻¹ and eliminate 36.2 % of the required sensible heat demand. The heat transfer rate significantly affects productivity, and the purities are sensitive to

levels of operating pressures. The interaction of operating parameters, including purge velocities, temperature differences and step durations, are also investigated to demonstrate the applicability of the synergistic strategy. The Pareto fronts provide suggestive design parameters of DAC configured in various regional meteorology. It is proved that the productivity is enhanced to $452.1 \text{ kg}\cdot\text{day}^{-1}$ in a year and achieves an average heat consumption of $2.1 \text{ MJ}\cdot\text{kg}^{-1}$ when applied in Hangzhou. Furthermore, the adsorption step requires an additional 30-75 min to reach the equilibrium status, showing the trade-off between kinetics and energy consumption should be carefully balanced in the proposed system.

Keywords: Direct Air Capture, Heat Pump, Process intensification, Adsorption, low-grade heat

Preliminary characterization of a three-source passive condenser air conditioning integrating sky radiative cooling and evaporative cooling

**Wenjie Wang^(a,b), Jingyu Cao^(*,a,b), Jingqing Peng^(b), Yixing Chen^(b), Mingke Hu^(c),
Qiliang Wang^(d), Jie Ji^(e), Gang Pei^(e)**

^(a) Research institute of HNU in Chongqing
Chongqing, 401120, China

^(b) College of Civil Engineering, Hunan University
Changsha, 410082, China

^(c) School of Mechanical Engineering, Southwest Jiaotong University
Chengdu, 610031, China

^(d) Department of Architecture and Built Environment, University of Nottingham
University Park, Nottingham NG7 2RD, UK

^(e) Department of Thermal Science and Energy Engineering, University of Science and Technology of China
Hefei 230027, PR China

*Corresponding Author. Email: jycao@hnu.edu.cn

ABSTRACT

Split air conditioning at high temperatures is not conducive to condensation heat dissipation, resulting in reduced cooling efficiency. Sky radiative cooling and evaporative cooling, as low-carbon emission passive sustainable cooling techniques, are integrated with air conditioning condensers by many scholars in direct or indirect ways to optimize condensation heat dissipations. However, the uncertainty of climatic conditions and the limitations of cooling power hinder their practical application. To address this issue, a novel three-source passive condenser cooling scheme integrating sky radiative cooling and evaporative cooling has been proposed for split air conditioning. A distribution parameter mode has been established and verified using MATLAB. The impact of outdoor and indoor temperatures, irradiation, relative humidity, and wind speed on the thermodynamic parameter change and steady performance of the system are discussed in detail. The simulation results indicate that the energy consumption of the system has been effectively reduced, and the refrigeration capacity exhibits higher stability in response to outdoor environment variations. The coefficient of performance under various outdoor boundary conditions has increased by 7.45% to 25.10% compared to traditional split air conditioning. The study confirms that the novel three-source passive condenser is adaptable to various outdoor environments, further expanding the application of passive cooling in the field of air conditioning.

Keywords: Sky radiative cooling, Evaporative cooling, Split air conditioning, Energy efficiency

A novel hybrid-energy heat pump using refrigerant/ionic liquids for solar cooling

Yunren Sui^(a,b), Wei Wu*^(a,b)

^(a) School of Energy and Environment, City University of Hong Kong, Hong Kong, China

^(b) Shenzhen Research Institute, City University of Hong Kong, Shenzhen, China

FABSTRACT

Heat pump technologies play a significant role in building energy saving and emission reduction. Combining the opposite characteristics of the electrical and absorption heat pumps, a hybrid-energy heat pump can be applied for flexible solar cooling. In this work, refrigerant/ionic liquids are proposed as novel working fluids for efficient hybrid-energy heat pump and overcoming its crystallization problem. A time-dependent model of hybrid-energy heat pumps has been established based on the mass/energy conservation and verified with high accuracies. The optimum working fluid is screened among the several ionic-liquid-based alternatives: $\text{NH}_3/[\text{MMIM}][\text{DMP}]$ achieves the highest electrical COP of 20.4 at an inlet driving source temperature of 90 °C. For different types of refrigerants, the cycle performance is in the order of: $\text{NH}_3 > \text{HFC} > \text{HFO}$. Compared with NH_3 , fluorine refrigerants have higher technical maturity in the electrical sub-cycle, and there will be no toxicity and explosivity problems. The dynamic simulation results show that a higher absorption-side refrigerant ratio is preferred in hotter conditions owing to the higher efficiency and less electricity consumption of the absorption sub-cycle. The electrical COP with an absorption-side refrigerant ratio of 0.8 is 33.1% higher than that with an absorption-side refrigerant ratio of 0.6. This study focuses on the performance improvement and stable operation of the novel hybrid-energy heat pump for solar building cooling.

Keywords: Heat pump, Hybrid cycle, Ionic liquid, Solar cooling, Energy efficiency.

Experimental investigation on heat transfer characteristics of a reversible reaction-based heat exchanger-reactor for chemical heat pump

SuzhouDAI^(a), YonggaoYIN^(a)

^(a) Southeast University

Nanjing, 210096, China, daisuzhou@foxmail.com

ABSTRACT

Compared with the physical phase change process, some chemical reactions have more potential in low-grade heat thermal management, storage, and utilization due to the relatively more significant physico-chemical thermal effects. The reversible decomposition of ammonium carbamate (AC) into NH_3 and CO_2 is such a reaction suitable for low-grade heat utilization. A novel chemical heat pump based on the reversible reaction of AC (AC-CHP) was established. It has advantages in efficiency and environmental friendliness over conventional compression heat pump. Heat exchanger-reactor is one of the most important components, which significantly impacts the performance and even the feasibility of AC-CHP. The coupled chemical reaction of AC, heat and mass transfer complicate the process in the reactors. The research on AC-based heat exchanger-reactor is still insufficient. The heat transfer characteristics of the reactor under the working condition of the heat pump is in lack. In this study, a coil-type heat exchanger-reactor is designed, and its performance is experimentally investigated based on a prototype of AC-CHP. AC is used in the form of a solution by dissolving the solid AC in solvent ethylene glycol to realize continuous cycle operation and promote

the reaction process. The reversible reaction takes place outside the coil pipe. This study focuses on the heat transfer characteristics of the heat exchanger-reactor of the decomposition reaction. The temperature distribution of the reactor was investigated. The average temperature at the upside, middle and downside of the reactor is determined as the characteristic temperature. It is found that the decomposition reaction of AC can enhance the heat transfer of the heat exchanger-reactor because of the endothermic thermal effect and disturbance of bubbles generated during the decomposition of AC. The results can provide guidance for the reactor design and operation optimization of the chemical heat pump or other technologies based on AC.

Keywords: Heat exchanger-reactor, Heat transfer, Chemical heat pump, Reversible reaction, Ammonium carbamate, Experimental investigation.

Cooling load analysis and energy-saving strategies for VAC system in subway station: A case study

Jiewei Wang^(a), Yusheng Yin^(b), Ziqing Wei^(a), Xiaoqiang Zhai^(a)

(a) Institute of Refrigeration and Cryogenics, Shanghai Jiao Tong University
Shanghai, 200240, China

(b) China-UK Low Carbon College, Shanghai Jiao Tong University
Shanghai, 201306, China

ABSTRACT

Subway stations play a crucial role in urban transportation. Their enormous energy use offers significant energy-saving potential. However, there is a lack of detailed energy models for calculating the overall cooling load of subway stations and evaluating their energy conservation potential. This study mainly established a cooling load evaluation model for ventilation and air-conditioning system based on actual operational data and field test data from a subway station in Shanghai, China. This model takes into account passengers, infiltration wind, mechanical fresh air and equipment, etc. The model allows for the calculation of the station's hourly overall cooling load by inputting parameters such as hourly passenger flow, temperature and humidity of outdoor air and average train departure density, etc. Furthermore, several energy-saving methods were applied to evaluate the energy conservation potential of the subway stations. The model serves as an effective way to evaluate energy consumption and provide guidance for actual energy-saving retrofit projects for subway stations.

Keywords: Subway station, Cooling load, Energy conservation potential.

A Comparative View on Challenges and Opportunities of District Heating's Zero-Carbon Transition in China and Sweden

Tianhao XU^(a), Shan HU^(b), Hatf Madani^(a)

(a) Energy Technology Department, KTH Royal Institute of Technology
Stockholm, 114 28, Sweden, txu@kth.se

(b) Building Energy Research Center, Tsinghua University, Beijing, China
Beijing, 100086, China, hushan@tsinghua.edu.cn

ABSTRACT

Heating decarbonisation is one of the most important areas of low-carbon energy system transition to mitigate global climate change. Both China and Sweden predominantly use district heating systems for covering heating

demands in urban built environment. Although both countries share the same transition goals to reach carbon neutrality in the district heating sectors, variations in energy supply, business models, network configurations, heating terminal systems, and other technical or economic factors between the two countries create varied challenges and opportunities for the district heating transition under different contexts. An in-depth study and comparison of China and Sweden's heating decarbonisation pathways can reveal key issues of heating system transition and may provide useful lessons for similar regions. For instance, low-grade waste heat is expected to become the dominant heat source for district heating systems in China due to widespread industries producing waste heat in Northern China, while the abundance of nuclear and hydro power as well as woody resources in Sweden tends to shape its decarbonized district heating sector based on electrification and biomass. District heating in Sweden has transformed into a free market since 1996, while district heating is provided as public welfare in China still much supported by governmental subsidies. Therefore, a comparative view to present and discuss how socio-techno-economic factors have influenced the design and implementation of transitional pathways in the two countries is helpful to promote mutual understanding and provide lessons learnt for district heating practitioners in both countries. In this paper, we will firstly compare the overall technical and market conditions of district heating in China and Sweden. Similarity and difference in technical modes of combined heat and power production and generic policy framework between China and Sweden will be discussed. Notably, the roles of heat pumps in district heating transition will be discussed, especially considering the more significant use of large-scale centralized heat pumps in Sweden. This paper aims to show challenges and opportunities of district heating's zero-carbon transition in China and Sweden with an international and holistic perspective and provide insights for transition pathway design.

Keywords: District heating, heat pump, comparative view, China, Sweden.

Analysis of energy consumption and energy efficiency of the central air conditioning system of water source heat pump: taking an energy station in Nanjing as an example

Xuejing Yang^(a), Yu Wang^(a), Bei Zhou^(b)

^(a) Nanjing Tech University

Nanjing Jiangsu 21000 China 2541816311@qq.com

^(b) Nanjing Jiangbei Public New Energy Co., LTD

Nanjing Jiangsu 211100 China 112228265@qq.com

ABSTRACT

Water source heat pump has a broad application prospect in the field of renewable energy. In this paper in Nanjing the data variations in a water source heat pump central air conditioning energy system near Yangtze river was researched. Based on the annual operation data of one energy station in 2023, the energy consumption, power, comprehensive energy efficiency ratio and the change of the host pressure change data in the heating and cooling season was analyzed. The results show that the cooling season system energy consumption is higher than the heating season, it is found that the comprehensive energy efficiency ratio in cooling season presents a steady rising trend, while in heating season the volatility of comprehensive energy efficiency ratio is strong. By analyzing the pressure data of the heat pump host evaporator and condenser, it is found that the pressure of mainframe one fluctuates too much during the operation, which may affect the stable operation of the system and cause the increase of energy consumption. By optimizing the system control strategy, improving equipment configuration and strengthening maintenance measures, the comprehensive energy efficiency ratio of the system will be improved and can be stabilized between 4.2 and 4.5. The research results in this paper provides strong support for its efficient operation, energy saving and emission reduction of the water source heat pump.

Keywords: Water source heat pump; Energy station; Energy consumption data; Performance improvement; heating and cooling season

Study on a micro-cogeneration system coupled with PV/T solar energy and air source heat pump

Haoran Ning, Fu Liang *, Zexuan Wang, Zeyu Zhang, Ying Xu, Shuai Zheng

School of Energy and Civil Engineering, Harbin University of Commerce, Harbin, 150028,China,

Y2311700001@163.com

ABSTRACT

In order to achieve the goal of "carbon neutrality" and promote the development of clean energy technologies, it is necessary to improve the utilization rate of renewable energy. Currently, the main solar energy utilization is photovoltaic power generation. However, the photoelectric conversion efficiency is only 16% to 20%, and the power generation efficiency will decline as the temperature increases. In this paper, the micro-cogeneration system of solar photovoltaic/thermal PV/T module coupled with air source heat pump is studied. Basis on improving the efficiency of solar photovoltaic power generation, solar thermal resources are effectively used combined with air source heat pump to supply hot water to buildings. The micro-cogeneration system was established in winter in Fuzhou city and the experiment was conducted. The preliminary results show that: When the air source heat pump is operated alone, the average COP of the system can reach about 3.5. When the PV/T component is combined with the air source, the COP of the system can reach 5.37. The operation efficiency of the PV/T system is higher than that of the air source heat pump system alone, and the average thermal power of 16 PV/T plates is 12 kW. The average power generation is 5.12kW, the hot water generated does not need secondary heating, and the average water temperature of the thermal storage tank can reach 46.8°C, which can directly meet the needs of domestic hot water users. TRNSYS was used to build a model to simulate the thermal power, generation power, compressor power and COP of the coupled system in winter. The simulation results are close to the measured values, which proves the accuracy of the model. The coupled system can realize the cogeneration and economic low carbon operation in the building. Generally, this system has a good application and promotion value for energy efficient buildings.

Keywords: Solar energy; PV/T; Air source heat pump; COP; System simulation

1. INTRODUCTION

The main utilization of solar energy includes photovoltaic power generation. Crystalline silicon solar cells are an important mode of solar energy utilization, and their photoelectric conversion efficiency is usually 16%-20%^[1]. In terms of energy consumption nationwide, the energy consumption of building operation is about 800 to 1 million tons of standard coal, accounting for about 25% of the total social energy consumption. The emissions of pollutants from coal burning in China's construction field account for more than 20% of the total emissions of pollutants^[2]. In order to reduce the temperature of the photovoltaic module, and at the same time, the excess heat can be extracted and used, the heat generated by the module is collected, and the overall performance is improved, and the cooling channel is integrated on the back of the photovoltaic module, that is, the solar photovoltaic/thermal integrated module system^[3]. PV/T systems are currently mainly divided into three forms, which are air cooled, liquid cooled and refrigerant^[4], PV/T system using liquid as working medium has the advantages of stable thermodynamic performance and high average efficiency, and has been widely studied and applied at present.

2. PV/T SYSTEM COUPLED SOLAR HEAT PUMP

The micro-cogeneration system is mainly composed of four parts, including an air source heat pump, a heating water tank, a heat storage water tank and a PV/T photovoltaic photothermal module. The combined heat and

power system generates photoelectric effect by absorbing solar radiation through photovoltaic photovoltaic panels, so that electricity and heat can be produced simultaneously. The electricity produced by the system is stored through the connected battery, the heat is carried away through the medium circulation in the plate, compressed into high temperature and high pressure liquid by the compressor, and the heat is transferred to the heat exchanger.

The PV/T module and air source heat pump are combined to convert the generated low-grade heat energy into high-grade heat energy and achieve efficient cogeneration.

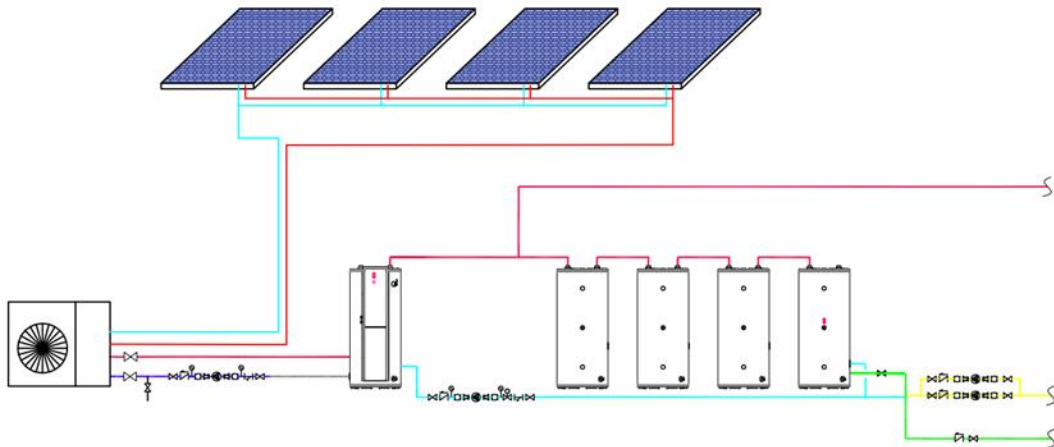


Figure 1 Schematic diagram of cogeneration system

During the day, when the PV/T heat pump system runs the heating mode, the evaporation plate of the lower layer absorbs the heat generated by the upper solar photovoltaic module, which can improve the thermal efficiency of the heat pump system. At the same time, the lower evaporation plate can also play a role in cooling the panel, so as to improve the comprehensive utilization efficiency of solar energy. To achieve both thermal energy output and electrical energy output, combine a variety of energy sources together to form a multi-energy composite system to achieve more efficient energy utilization.



Figure 2 Actual PV/T components



Figure 3 Actual picture on site

3. CONCLUSIONS

The PVT system is coupled with the air source heat pump. During the test, the maximum COP of the unit is 5.32, the minimum COP is 4.55, and the average COP is 5.22 in good weather. The average COP of the system was 4.76 under cloudy and rainy conditions. The average COP of the air source heat pump running alone is 3.68.

The average water temperature of the heating water tank is 46.24°C, and the average water temperature of the storage water tank is 47.56°C, 48.15°C and 49.45°C respectively, which can meet the heat demand of users throughout the day.

This is equivalent to a reduction in CO₂ emissions of 11.38 tons per year.

ACKNOWLEDGEMENT

This work was supported by the Joint Guidance Project of Natural Science Foundation of Heilongjiang Province (LH2021E089) and 2021 Harbin University of Commerce Teacher Innovation Support Plan Project.

REFERENCES

- [1] Wang Runze, Research on Optimization of Solar photovoltaic comprehensive utilization system [D]. Beijing: Beijing Electric Power University, 2021.
- [2] Zhang Jili, Application prospect analysis of PV/T heat pump technology in carbon neutral urban and rural construction in northern China [R]. Dalian: Institute of Building Energy, Dalian University of Technology, 2022.
- [3] Hydrogel [J]. *Adv Mater*, 2020, 32(17): e1907307. PU S, FU J, LIAO Y, et al. Promoting Energy Efficiency via a Self-Adaptive Evaporative Cooling.
- [4] Cao Meng, Zhang Chenyu, Zhang Jianfei, et al. Experimental study on performance of solar PV/T-PCM system under different thermal control strategies [J], 2021, 36(2):107-114.

Performance Analysis of a DC inverter Heat Pump System for PV integrated Building in Hot-summer and Cold-winter Region Tianhang Wang¹, Yilin Li^{1*}, SHiji Zong¹, Yang Lu¹, Tongyu Zhou²

⁽¹⁾ University of Shanghai for Science and Technology

⁽²⁾ University of Nottingham Ningbo China

ABSTRACT

As the application of solar PV systems has been increasing, it is of great significance to develop and investigate direct current (DC) powered equipment in buildings with flexible operational strategies. The aim of this study is to analyse the performance of a DC inverter heat pump system for applying in PV integrated building. Firstly, the PV power fluctuation and demand-side load characteristic were analysed based on a case study building. Then, numerical models were developed for a reference building. A control strategy of a DC inverter heat pump was proposed considering both the PV power generation and demand-side heating load. MATLAB/Simulink software was used for simulation. The results indicate that the proposed control strategy can achieve stable operation of the DC inverter heat pump, while maintaining satisfactory thermal comfort level of the indoor environment under fluctuated DC bus voltage. By expanding the setting range of the room temperature, it can significantly affect the allowable standby time of heat pumps. The duration of standby time of heat pumps can extend to about 20~30% by reducing the room temperature from Class I ~ II comfort criteria.

Keywords: BIPV; DC inverter heat pump; PV power; Demand side

1. INTRODUCTION

With the continuous growth of energy demand and severe environmental problems, China established the 'dual-carbon' goal. Among different sectors, power industry and building sector are the key areas of energy consumption and carbon emission ^[1], and play crucial roles in achieving the 'dual carbon' goal. Solar photovoltaic (PV) has developed rapidly as the most widely used form of renewable energy source (RES) ^[2]. Building integrated photovoltaic (BIPV) technology has attracted attention for its ability to reduce energy consumption in buildings and to reduce CO₂ emissions ^[3]. However, the randomness and volatility of PV system, and the varied of electrical load of buildings ^[4], brought uncertainty for application of building equipment ^[5]. Among different types of HVAC equipment, heat pumps are energy efficient devices which can be readily to be used in PV integrated buildings. The traditional heat pump only considers the load-side effects, and neglect the influence of source-side bus voltage. Currently, there are few theoretical studies and practical applications of heat pump systems suitable for PV integrated buildings. This paper investigates the performance of a DC heat pump system for application in PV integrated buildings. The power supply and electrical load characteristics of an actual case building in hot-summer and cold-winter region were analysed. Experimental study on a DC heat pump was conducted under various working conditions. Simulations by using MATLAB/Simulink software was carried out to evaluate the performance of the DC inverter heat pump system under a novel operational strategy.

2. HEAT PUMP SYSTEM WITH NOVEL OPERATIONAL STRATEGY

Fig. 1a shows the schematic diagram of the DC inverter heat pump system, which consists of the energy supply side, the DC heat pump unit, and the load side. The DC heat pump unit is comprised of a compressor, condenser, expansion valve, and evaporator. Fig. 1b presents the control logic of the DC inverter heat pump which depends on both DC bus voltage and the indoor temperature setup. When the DC bus voltage exceeds the setpoint, the compressor operates at a higher frequency and stores the excess energy in the envelope. When the voltage falls below the setpoint, the compressor operates at a lower frequency and discharges the insufficient energy from the envelope to meet the user demand.

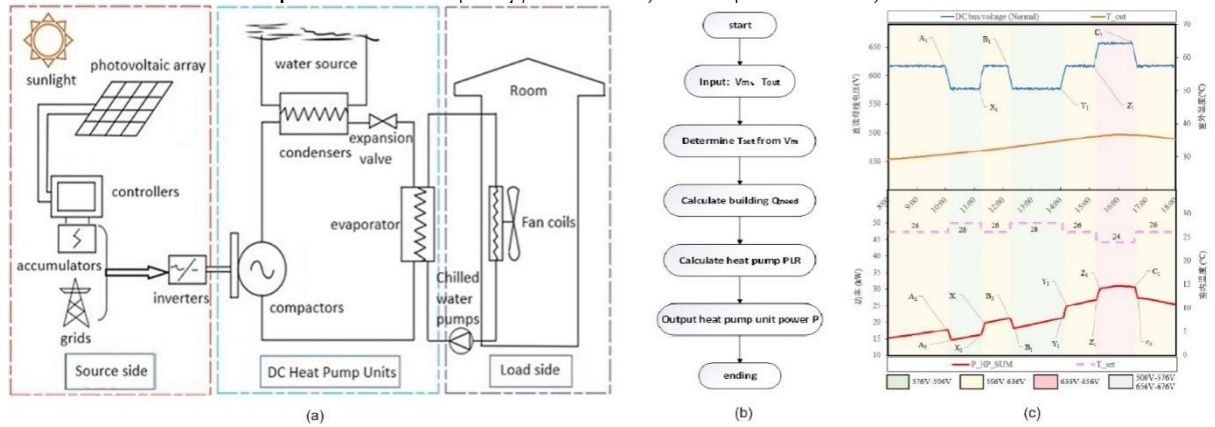


Figure 1: Schematic diagram of DC inverter heat pump system composition (a); DC inverter heat pump unit control logic (b); Power profile of heat pump, DC bus voltage profile, and ambient temperature (c)

When the bus voltage is in normal mode (DC596 V~DC636 V), the PV system generates electricity normally, and the indoor temperature is set to be within the temperature range of Class I ~ II comfort criteria. When the bus voltage is in energy-saving mode (DC576 V~DC596 V), the PV power generation is declined, and the indoor temperature is set to be the lower limit of Class II comfort criteria to provide flexible load for achieving smoothness of DC bus voltage; when the bus voltage is in over-limit mode (DC636 V~DC656 V), the PV resource is abundant, and the indoor temperature is set to be the upper limit of Class I comfort level. When the bus voltage is in overrun mode (DC636 V~DC656 V), the PV resource is extremely rich, and the indoor temperature is set as the upper limit of the comfort level I criteria. When the bus voltage is in derating mode (DC500 V~DC576 V or DC656 V~DC676 V), the maximum safe working power for the DC heat pump unit is combined with the load prediction model to supply enough power for the building.

3. CONCLUSIONS

This paper investigates the operational strategy of DC inverter heat pump system considering the source-side power supply and load-side electrical load characteristics of PV integrated buildings. A PV integrated buildings were selected and analysed as case study to obtain the fluctuation characteristics of the bus voltage. Experimental study was conducted on a DC inverter heat pump unit under variable voltage condition. The effectiveness of the proposed strategy is simulated by using MATLAB/Simulink software and validated by the experimental data. The results indicate that the proposed operational strategy for the DC inverter heat pump system can reach a balance between fluctuated PV power supply and the varied load-side demand in the reference building.

REFERENCES

- [1] Zhu J, Dong H, Zheng W, et al. Review and prospect of data-driven techniques for load forecasting in integrated energy systems. *Applied Energy*, 2022, 321: 119269.
- [2] IRENA. Trading into a bright energy future (The case for open, high-quality solar photovoltaic markets). Organization, WT, Ed. <https://www.irena.org/publications/2021/Jul/Trading-into-a-bright-energy-future-Solar-photovoltaic;2021>.
- [3] L Ding, Y Zhu, L Zheng, et al. What is the path of photovoltaic building (BIPV or BAPV) promotion? The perspective of evolutionary games[J]. *Applied Energy*, 2023, 340: 121033.
- [4] X Wang, E Virguez, W Xiao, et al. Clustering and dispatching hydro, wind, and photovoltaic power resources with multi-objective optimization of power generation fluctuations: A case study in southwestern China[J]. *Energy*, 2019, 189: 116250.
- [5] J Zhu, M Li, L Luo, et al. Short-term PV power forecast methodology based on multi-scale fluctuation characteristics extraction[J]. *Renewable Energy*, 2023, 208: 141-151.

Design and Operating Experiences of a High Temperature Heat Pump for Steam Generation

Drew SCHMIDT^(a), Ke TANG^(a), Stefan ELBEL^(a,b)

^(a)Creative Thermal Solutions, Inc.
Urbana, IL 61802, USA, info@creativethermalsolutions.com

^(b)Technische Universität Berlin
10587 Berlin, Germany, elbel@tu-berlin.de

ABSTRACT

High Temperature Heat Pumps (HTHP) are seen as promising alternative to technologies relying on fossil fuels to meet demanding decarbonization targets. HTHPs make most sense in applications that are connected to a stream of low-grade energy. This paper presents the development and operation of a high-temperature heat pump (HTHP) system with a target heating capacity of 30kW. The engineering design and test procedure are introduced. Initial performance data was obtained with a HTHP breadboard system. Based on the results the design was refined and implemented in a HTHP prototype unit that has been evaluated at different conditions. One of the aims of the study was to obtain experimental data obtained from an operation period 6 months in length resembling actual field operation experience. This was done to obtain important conclusions with respect to reliability of the technology and possible performance degradation effects. The prototype HTHP recovers waste heat from an 80°C heat source to produce low-pressure steam at 120°C and higher, thus providing at least a 40°C temperature lift. It uses a single-stage design approach featuring brazed plate heat exchangers and a scroll compressor. Three different refrigerant options have been evaluated, including R245fa, R1233zd(E), and R1336mzz(Z). While it was possible to meet the target COP of 3.6 at the design condition with all fluids included in the study, the two low-GWP refrigerant options performed substantially better. R1233zd(E) resulted in a peak COP of more than 4.5. Due to the shape of the two-phase dome R1336mzz(Z) required control of compressor discharge superheat instead of suction superheat.

Keywords: High Temperature Heat Pump, Steam Generation, Low-GWP Refrigerant, Energy Efficiency, Long-term Operation

Thermal- structural coupling characteristic analysis of shield energy tunnel under typical condition

Shouheng Shin^(a), Yongming Ji^(a), Xinru Wang^(a), Hui Zhang^(a), Songtao Hu^(a)

^(a) School of Environmental and Municipal Engineering, Qingdao University of Technology
Qingdao, Shandong, China, shinshouheng@163.com

ABSTRACT

As society grows and the population expands, the demand for energy is on the rise. A promising solution to this challenge lies in utilizing subway source heat pump technology to harness shallow geothermal energy for cooling or heating. This innovation transforms shield tunnels into energy-efficient conduits, addressing the pressing issue of energy demand. However, the thermal effects of heat exchanger operation on tunnel structures require further investigation.

In this study, using the COMSOL Multiphysics software, we explore the heat exchange performance of the Capillary Heat Exchanger (CHE) in energy tunnels and the resulting structural responses of shield tunnel segments under typical cooling and heating season conditions.

Our findings reveal the outstanding performance of precast CHE in energy tunnels. A single-ring energy tunnel can achieve cooling capacities of 601.62W and heating capacities of 466.28W during the cooling and heating seasons, respectively. The corresponding heat transfer efficiencies are 63.46W/m² and 49.19W/m². During the cooling season, the operation of the CHE results in tunnel segment elongation, while during the heating season, compression is observed. The maximum tensile and compressive stresses generated during these seasons are within safe limits, being 0.60 MPa and 0.73 MPa for heating and 0.56 MPa and 0.87 MPa for cooling. Importantly, these stresses remain well below the compressive limit of C50 concrete, with tensile stresses accounting for 33% and 23% of the axial tensile strength, during cooling and heating seasons, respectively.

Overall, under the design conditions of the heat pump unit and once the heat exchange between the CHE and the tunnel stabilizes, the impact on the structural integrity of the shield tunnel appears to be minimal.

Keywords: Energy tunnel, SSHPS, Thermal-structural coupling characteristic, CHE

1. INTRODUCTION

According to the data released in the "Annual Development Research Report on Building Energy Conservation in China 2022" [1], in 2020, the energy consumption during the operational phase of buildings in China was 1.06 billion tec, accounting for 21.3% of the total national energy consumption. The carbon emissions were 2.16 billion tons of CO₂, approximately 21.7% of the total national carbon emissions [2].

Against this backdrop, the importance of promoting clean energy heating becomes increasingly prominent. Shallow geothermal energy, as a type of clean energy, mainly utilizes the heat energy from the Earth's interior through technologies like heat pumps to achieve centralized heating. Shallow geothermal energy has advantages such as renewability, high efficiency, energy conservation, and environmental friendliness. It not only reduces energy consumption and environmental pollution but also improves heating efficiency and comfort.

The waste heat within subway tunnels, as a form of shallow geothermal energy, has also received widespread attention. Academician Qihu QIAN [3], a member of the Chinese Academy of Sciences, recipient of the highest international science and technology award, and professor at the Army Engineering University, clearly stated at the "Geothermal Energy Development and Utilization with Earth Energy Storage Systems" seminar: "We should strengthen research and utilization efforts on 'tunnel energy' to turn waste heat in tunnels into sources for heating and cooling".

Laying the heat exchange pipeline in underground continuous walls, building foundation piles, and tunnel linings, and utilizing geothermal heat pump technology to extract shallow geothermal energy, allows the building's foundation components to become part of an underground energy structure. Among these, the underground energy structure based on tunnels as foundation components is referred to as an energy tunnel.

Brandl [4] conducted on-site experiments in the Lainz Tunnel in Austria, testing its heat exchange capacity. Through geothermal heat pump technology, they used energy piles buried in the tunnel as front-end heat exchangers to provide heating or cooling for a nearby school, further exploring the economic feasibility and viability of installing heat exchangers in tunnels. Adam and Markiewicz [5] proposed an innovative construction method where they placed the ground heat exchanger pipes in geotextile fabric, referred to as "energy geotextile." This technique enables the prefabricated construction of tunnel linings and ground heat exchangers. By employing this construction method, not only can the waterproofing performance of tunnel linings be ensured, but also protection for the heat exchange pipeline can be provided, thus enhancing construction efficiency. To further reduce the difficulty of laying heat exchange pipes and their impact on tunnel structures, the team led by Songtao HU at Qingdao University of Science and Technology proposed laying capillary heat exchangers (CHE) in the lining of subway tunnels, as front-end heat exchangers for ground heat pump systems [6]. The capillary front-end heat exchanger extracts waste heat generated by various equipment in the subway tunnel to provide heating for users, thus this ground heat pump system is referred to as a subway source heat pump system (SSHPS). These capillary heat exchangers have advantages such as simple construction method, small footprint, large heat exchange area, uniform heat exchange, high overall heat transfer coefficient, flexible layout, and easy integration with subway tunnel structures. The applicability, heat exchange performance, and design parameters of capillary heat exchangers in mining method tunnels have been validated through scaling experiments, numerical simulations, and demonstration projects.

Currently, shield tunnel, due to its relatively high technical and economic feasibility, is increasingly serving urban construction in China. Combining capillary heat exchangers (CHE) with shield tunnel segments as front-end heat exchangers for subway source heat pumps is referred to as shield tunnel energy segments. This can make a

significant contribution to urban energy conservation, emissions reduction, and sustainable development. However, the service life of urban tunnels is typically around 100 years, and the thermal stresses generated by the operation of heat exchangers should not be ignored. Xia et al. [7][8] established a thermal-structural coupling finite element model for energy tunnels and studied the mutual influence between heat exchangers installed in tunnels and tunnel structures in cold regions. Zhu [9] analyzed the maintenance process, construction process, as well as stress and strain changes in tunnel segments during the heat exchange process based on the energy tunnel experimental section of the Qinghua Garden on the Beijing-Zhangjiakou Railway. Donna et al. [10], based on the energy tunnel section of Line 1 of the Turin Metro in Italy, studied the stress and strain performance of shield tunnel segments during heat exchange through on-site experiments. The experimental results showed that the stress and strain generated in the lining during heat exchange are within an adjustable range.

The research results mentioned above demonstrate that the impact of heat exchangers on tunnel structures during heat exchange in energy tunnels is relatively small. However, different types of heat exchangers, due to their different installation forms, may have varying mechanical impacts on tunnel structures during heat exchange.

There are significant differences in structure, physical performance, and construction methods between capillary heat exchangers and traditional ground heat exchangers. Therefore, one cannot simply infer the heat transfer characteristics and the structural-mechanical impact on tunnel structures of one type of heat exchanger based on the other. This study analyzed the thermal-structural coupling characteristics of prefabricated capillary heat exchangers in energy shield tunnel segments during heat exchange based on a specific engineering project in Qingdao city..

2. MODEL ESTABLISHMENTS

The principle of the SSHPS based on shield tunnel, as shown in Figure 1. The system utilizes capillary tubes laid inside the shield tunnel segments as front-end heat exchangers, with each shield tunnel segment serving as a heat exchange unit. Utilizing the reverse Carnot cycle of the heat pump unit, in cooling season, heat is extracted from buildings and transferred and released into the subway tunnel to achieve cooling. In heating season, waste heat or residual heat is extracted from the subway tunnel and used for heating buildings to maintain comfortable temperatures.

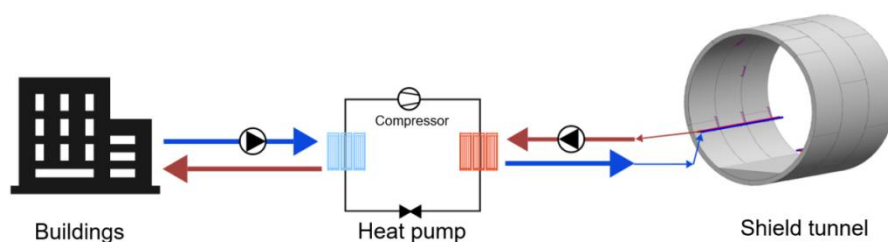


Figure 1: Principle of the SSHPS

2.1 Geometric model

The shield tunnel segments are arranged in a 1+2+3 combination, comprising the crown segment (F), adjacent segment (L1, L2), and standard segment (B1, B2, B3). CHE are prefabricated only in the two adjacent segments (L1, L2) and the two standard segments (B1, B3) adjacent to the adjacent segments. Therefore, each ring of the shield tunnel contains two capillary loops on the left and right sides. The main capillary pipes inside the segments are arranged along the circumferential direction of the tunnel, while the branch pipes are arranged using a non-uniform distribution method.

In this study, the spacing between individual capillary branch pipes inside the tunnel segment is 5mm, and the spacing between each group of capillary branch pipes is 44mm. The diameter of the CHE branch pipes is 4.3mm with a wall thickness of 0.85mm. The diameter of the main branch pipe is 18mm with a wall thickness of 2mm. The way of laying CHE in segments is shown in Figure 2.

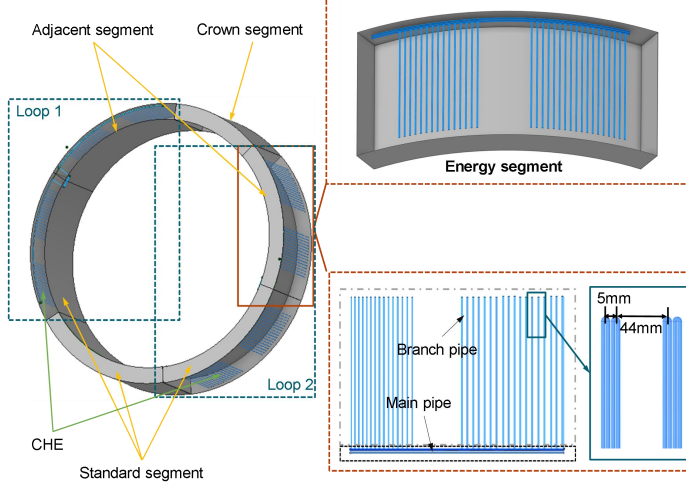


Figure 2: CHE layout

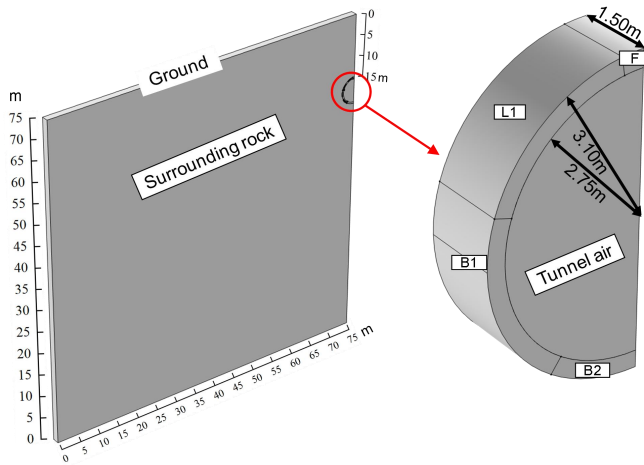


Figure 3: Geometric model of energy tunnel

Referring to the demonstration project, the inner diameter of the shield tunnel segment is 5.5 meters, the outer diameter is 6.2 meters, and the height is 1.5 meters. The depth of the tunnel top is approximately 15 meters. The shield tunnel segments in the actual engineering project are assembled in a staggered manner. To reduce computational complexity, this simulation only considers the case where the top block is located directly above the tunnel. Following the principle of symmetry, only half of the tunnel segment is considered for calculation, comprising half of the crown segment (F), half of the standard segment (B2), as well as the adjacent segment (L1) and the standard segment (B1). To minimize the influence of boundary conditions on the model calculation results, the length and width of the surrounding rock are both set to 75 meters. The geometric model is established as shown in Figure 3.

2.2 Numerical model

This study utilized the COMSOL Multiphysics finite element software to simulate the heat exchange performance of the CHE and the structural-mechanical response of the shield tunnel segments under typical cooling season and heating season design conditions in energy tunnels. The simulations were conducted using the Turbulent Flow Module, Heat Transfer in Solids and Fluids Module, Non-Isothermal Pipe Flow Module, Solid Mechanics Module, and Beam Module, respectively, to model the airflow in the tunnel, heat transfer between tunnel air, tunnel segments, and surrounding rock, heat transfer between CHE and tunnel segments, and tunnel stress.

The research focus of this study is the analysis of the thermal-structural coupling characteristics of tunnel segments in energy shield tunnels. It explores the heat transfer characteristics of the prefabricated CHE and the structural-mechanical response of shield tunnel segments during CHE operation, involving several complex coupled physical field problems. To simplify calculations, the following assumptions are made:

- (1) Surrounding rock, lining, and CHE have constant material properties and are isotropic.
- (2) Contact thermal resistance is neglected.
- (3) The influence of groundwater flow on the heat transfer process is disregarded.
- (4) During system operation, the fluid inside the CHE and the airflow in the tunnel remain constant.
- (5) The surrounding rock is simplified as a linear elastic model.
- (6) Gravity is ignored.

Based on the aforementioned simplifications, the numerical model obtained in this study is as follows:

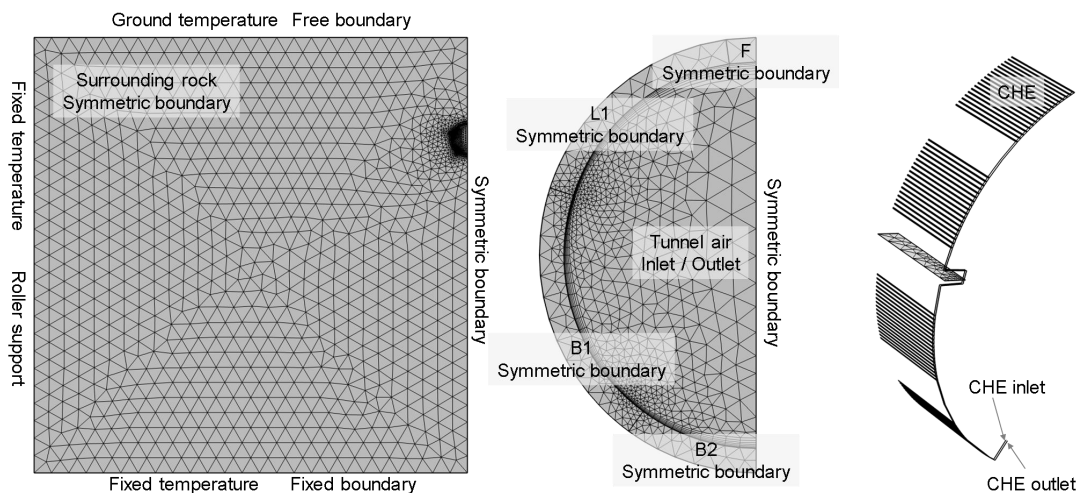


Figure 4: Geometric model of energy tunnel

As shown in figure 4, the numerical model is configured as follows:

- The left boundary is set as roller support, allowing only vertical displacement and restricting horizontal displacement.
- The top boundary is set as the ground (free boundary).
- The bottom boundary is set as a fixed boundary, allowing for settlement of the surrounding rock.
- For shield tunnels with more than 4 segments, the "Code for Design of Metro" recommends using a beam-spring model for calculation [11]. This method considers that the bolted joints of circular lining structures can bear certain forces, and the deformation of the joints is linearly related to internal forces, treating the joints as elastic hinges.

3. CONCLUSIONS

This study, based on COMSOL Multiphysics finite element analysis software, utilized steady-state numerical calculation methods to simulate the thermal-structure coupling characteristics of the prefabricated capillary heat exchanger (CHE) in the energy shield tunnel under design conditions, leading to the following conclusions:

(1) Under the design conditions of the heat pump unit, the system exhibits good heat transfer performance. When the inlet temperatures are 35°C in cooling season and 6°C in heating season, the outlet water temperatures of CHE are approximately 32.12°C and 8.22°C, respectively. Each ring of the energy shield tunnel can provide heat transfer rates of 601.62W and 466.28W in heating season and cooling season, respectively, with heat transfer efficiencies reaching 63.46W/m² and 49.19W/m².

(2) In cooling season, CHE operation causes the segments to stretching, while in heating season, it leads to contract of the segments. However, the deformation of the segments is influenced by the surrounding rock of the tunnel, resulting in compression on the outer arc surface and tension on the inner arc surface in cooling season, with the opposite occurring in heating season.

(3) Due to CHE operation, the maximum tensile and compressive stresses generated in cooling season are 0.87MPa and 0.56MPa, respectively, while in heating season, they are 0.60MPa and 0.73MPa, respectively. The compressive stresses are far below the compression limit of C50 concrete, while the tensile stresses account for 33% and 23% of the axial tensile strength, respectively.

(4) The distribution of equivalent stresses reveals that the maximum stress points on the segments are located at the CHE inlet in both cooling season and heating season, reaching 0.88 MPa and 0.74 MPa, respectively.

Therefore, the prefabricated CHE in the energy shield tunnel demonstrates good heat transfer performance, with minimal impact on the tunnel segment. However, caution should be exercised to avoid complete overlap between the inlet and outlet of CHE on the segments and the positions of maximum tensile stress occurring during the tunnel construction process.

ACKNOWLEDGEMENT

This work was supported by the National Natural Science Foundation of China (Grant no. 52108079).

REFERENCES

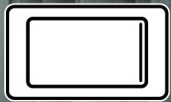
- [1] National Bureau of Statistics, 2022, China Statistical Yearbook, Beijing shu tong dian zi chu ban she. (In Chinese)
- [2] Y. Jiang, S. Hu, Y. Zhang, et al., 2022, China building energy efficiency annual development research report. (In Chinese)
- [3] Geothermal energy information., 2023 Qian, Q.H: establish and improve the mechanism of shallow geothermal energy application. Available at: <https://mp.weixin.qq.com/s/r9odhwxjE340mrIfddnxjA> (Accessed: 15 August 2023).
- [4] H. Brandl, 2006, Energy foundations and other thermo-active ground structures. *Géotechnique*, 56(2), 81-122.
- [5] D. Adam, and R. Markiewicz, 2009, Energy from earth-coupled structures, foundations, tunnels and sewers. *Géotechnique*, 59(3), 229-236.
- [6] H.Y. Wang, S.T. Hu, and Z Chang, et al., 2014 The invention relates to a capillary soil source heat pump system applied to a subway tunnel. (2014-03-05). CN103615841A.
- [7] C.C. Xia, Y. Yang, G.Z. Zhang, and Y.C. Zou., 2014, The internal source heat pump heat exchange tube and tunnel structure interact. *Journal of Tongji University (Natural Science Edition)*, (1), 51-57. (In Chinese)
- [8] Y. Yang, C.C. Xia and J.L. Zhu., 2014, Study on temperature stress induced by heat exchange tube of tunnel ground source heat pump. *Journal of Central South University: Natural Science Edition*, 45(11), 3970-3976. (In Chinese)
- [9] Z.N. Zhu., 2020, Analysis of heat transfer, stress and construction problems of energy shield tunnel. (Master's thesis, Tsinghua University).
- [10] A. Di Donna, and M. Barla, 2016, The role of ground conditions on energy tunnels heat exchange. *Environmental geotechnics*, 3(4), 214-224.
- [11] Ministry of Construction of the People's Republic of China., 2013, GB 50157-2013 Code for design of metro. Beijing: China Building Industry Press.
- [12] Ministry of Construction of the People's Republic of China., 2005, GB 50366-2005 Technical code for ground-source heat pump system. Beijing: China Building Industry Press.
- [13] H.H. Zhu, and L.B. Tao., 1998, A beam-spring system model for stress analysis of shield tunnel lining structures. *Journal of Rock and Soil Mechanics*, 19(2), 26-32. (In Chinese)
- [14] Y. Zhang, Q. Zhang, H.Q. Bi and J.Y. Wang., 2020, Experimental study on wind speed and its variation in metro piston duct. *Refrigeration and air conditioning (Sichuan)*, 34(04), 463-467. (In Chinese)
- [15] Y.M. Ji, W.Z. Wu, and S.T. Hu., 2023, Long-term performance of a front-end capillary heat exchanger for a metro source heat pump system. *Applied Energy*, 335, p.120772.
- [16] H. Gao., 2015, Research on Heat Transfer Characteristics of Capillary Heat exchangers in Subway Tunnel (Doctoral dissertation, Qingdao: Qingdao University of Technology).
- [17] Y.Q. Lu., 2008, Practical heating and air conditioning design manual. second ed. Beijing: China Construction Industry Press. (In Chinese).
- [18] Y.M. Ji, W.Z. Wu, H.Y. Qi, W.Q Wang, and S.T. Hu., 2022, Heat transfer performance analysis of front-end capillary heat exchanger of a subway source heat pump system. *Energy*, 246, 123424.

空气源热泵 高效解决方案

CAREL



c.pCO
可编程控制器



pGDX
触摸屏用户界面



EEV
电子膨胀阀 & 传感器



Power+
BLDC变频器



为满足当今市场对节能和绿色技术的需求，我们提供一套完整的先进的空气源空调机组管理控制器平台。



Transient and steady performance of a microchannel membrane-based absorption refrigeration system

Chong Zhai^(a), Wei Wu^(b)

^(a) School of Energy and Mechanical Engineering, Nanjing Normal University
Nanjing, 210023, China, zhaichong@nnu.edu.cn

^(b) School of Energy and Environment, City University of Hong Kong
Hong Kong, 999077, China, weiwu53@cityu.edu.hk

ABSTRACT

Microchannel membrane-based absorption refrigeration system (MMARS) has been extensively studied through simulation, which has shown its potential for providing efficient spacing cooling in a compact size. However, rigorous experimental verification and cycle performance studies were lacking until this research. In this study, an experimental setup of the MMARS was constructed, and its cycle performance using H₂O-LiBr as working fluids was investigated under various operating conditions, including inlet heat source temperature ranging from 80°C to 95°C, and inlet cooling water temperature ranging from 22°C to 30°C. The transient experimental results of the MMARS demonstrated that the system tended to run smoothly after 15 minutes. Driven by a 0.8 kW heat source, the MMARS was able to provide a cooling capacity of 0.32 kW. Steady-state experimental results revealed that increasing the heat source temperature and reducing the cooling water temperature facilitated the system reaching the steady state faster, resulting in a higher COP. The highest COP achieved was 0.443, observed at an inlet heat source of 95°C and inlet cooling water temperature of 22°C. It is anticipated that with careful membrane selection, optimization of MMARS geometries, and refinement of experimental setups in future studies, even more competitive COP can be achieved. This research has verified the feasibility of the MMARS under various operating conditions, providing a solid foundation for potential practical applications in future compact and efficient spacing cooling systems.

Keywords: Microchannel membrane-based, Absorption refrigeration, Cycle performance, COP, Experimental study

Study on the Drainage Performance of Microchannel Heat Exchangers (Louvered Fins) Combining CFD and Image Recognition Technologies

Yizhe Nie^(a), Liu Yang^(a), Luyao Guo^{(a) (b)}, Long Huang^(a)

^(a) Xi'an Jiaotong-Liverpool University, School of Mathematical and Physics
Suzhou, 215000, China, Yizhe.Nie20@student.xjtlu.edu.cn

^(a) Xi'an Jiaotong-Liverpool University, School of Mathematical and Physics
Suzhou, 215000, China, Liu.Yang@student.xjtlu.edu.cn

^(a) Xi'an Jiaotong-Liverpool University, School of Intelligent Manufacturing Ecosystem,
Suzhou, 215000, China

^(b) University of Liverpool, School of Engineering
Liverpool, L34AF, United Kingdom, lyguo@liverpool.ac.uk

^(a) Xi'an Jiaotong-Liverpool University, School of Intelligent Manufacturing Ecosystem,
Suzhou, 215000, China, long.huang@xjtlu.edu.cn

ABSTRACT

Microchannel heat exchangers are known for their compact construction and efficient heat transfer capacity. It has an advanced design and has shown excellent performance in a variety of cooling and heating applications in recent years. However, due to the small size of the channel, the flow resistance increases, and the surface tension effect increases, which hinders the smooth discharge of fluid. Therefore, it is very important to study the drainage of micro-channel heat exchanger. It can improve heat exchange efficiency, reduce corrosion, improve the durability and reliability of equipment, and meet the requirements of modern miniaturization and energy saving. In this study, the single-fin flat tube structure (excluding the drain in the flat tube) of the single-fin micro-channel heat exchanger was simulated to analyze the force on the droplet and predict the retention of the droplet on the surface of the fin. Computational fluid dynamics (CFD) is used to simulate the drainage scene, and the experimental comparison is verified, and the new image recognition technology is used to try to evaluate the results within a certain error range. By arranging heat exchangers at different angles, the drainage efficiency in different directions is compared. The results show that when the heat exchanger is rotated 60 degrees, the remaining water in the equilibrium state is the most, and when the heat exchanger is rotated 90 degrees, the remaining water is the least. In addition, through the error analysis of the experimental data, CFD simulation data and image recognition data, it is found that the error in each angle can be controlled within 21% and 17.5%, which proves the feasibility of this method for auxiliary verification.

Keywords: Microchannel heat exchanger, Water drainage, Gravity Angle, CFD simulation, Image recognition

1. INTRODUCTION

In the contemporary industrial and technological sectors, microchannel heat exchangers, often defined as heat exchangers with hydraulic equivalent diameters less than 1 mm, have emerged as a focal point of research in the field of heat exchange. These exchangers are characterized by their compact structure, cost-effective material usage, high heat transfer efficiency, broad applicability, and resistance to pressure and corrosion. Demonstrating exceptional performance in various cooling and heating applications, they are gradually replacing traditional tubular heat exchangers, marking the next phase in the evolution of heat exchanger technology.

However, the extremely small channel sizes of microchannel heat exchangers increase flow resistance and amplify surface tension effects, thereby impacting the smooth expulsion of fluids. This is particularly problematic during regular frosting and defrosting conditions, leading to an accelerated rate of frosting and difficulties in removing melted frost. Additionally, the expulsion of condensation water becomes challenging when microchannel heat exchangers operate under humid conditions. These issues are directly related to the equipment's heat exchange efficiency and durability [3]. Therefore, in the current development of microchannel heat exchangers, investigating their drainage capabilities, including hydrophobic efficiency and water retention on fins, is crucial.

2. METHODOLOGY

The Fig.1a and Fig. 1b illustrate the three-dimensional structure and fin configuration of the examined microchannel heat exchanger sample. The fin arrangement within the heat exchanger is characterized by periodic repetition. To simplify the computational process, the modeling focused on the distribution of residual liquid in and between individual fins. This experiment explores the drainage behavior of the micro-channel heat exchanger under standard temperature and pressure conditions, in the absence of wind.

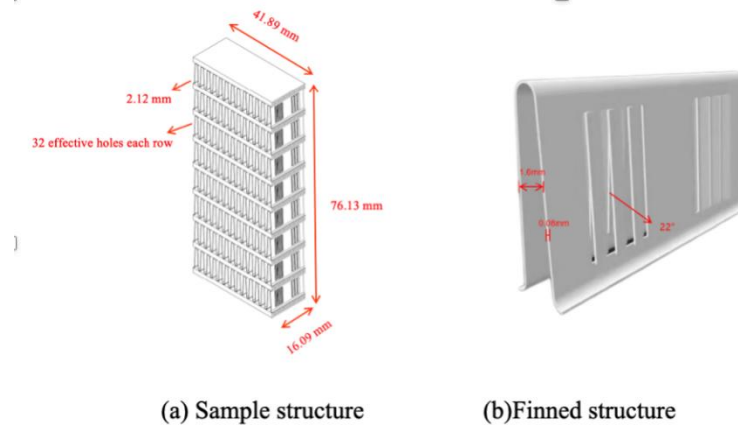


Figure 1 : Sample and fin structure diagram

In the image recognition process, OTSU method is used for automatic threshold processing. First, the image needs to be converted to grayscale to reduce complexity. According to grayscale adjustment, the image can be divided into two parts according to pixels: the air part and the non-air part, where the air part is the part of the pixel below the threshold value and is displayed as 255, and the non-air part is the part of the pixel above the threshold value and is regarded as 0. The method of separating the air portion is to select the threshold by the maximum inter-class variance.

In this study, the drainage experiments of heat exchanger specimens were carried out under the actual conditions (ambient temperature and pressure, no wind). By comparing with the experimental data, we try to verify the applicability of the falsifications in the simulation and image recognition and identify the possible errors in the two processes. The experimental device and the schematic diagram are shown in the Fig.2a and Fig.2b.

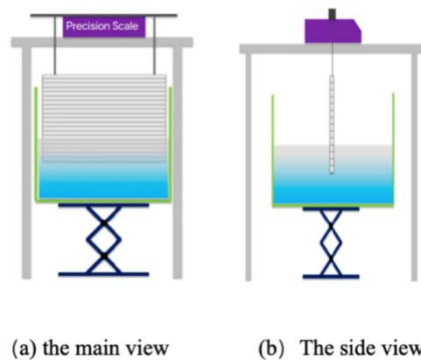


Figure 2: Experimental apparatus

3. CONCLUSIONS

The drainage efficiency of microchannel heat exchanger fins is influenced by the contact angle, surface tension, and gravity. By combining the contact angle between water droplets and the fin surface with the Volume of Fluid (VOF) model, a predictive model for the drainage performance of the fins can be constructed. This study not only employed CFD simulations but also utilized image recognition technology for validation, comparing both simulated and experimental data. The simulation results showed a trend in residual water quantity that was consistent with experimental data, with an error of approximately 21%, whereas the results from image recognition had an error of about 17.5% compared to experimental data, demonstrating the effectiveness of the model in predicting drainage performance.

ACKNOWLEDGEMENT

This work was supported by the National Natural Science Foundation of China (Grant No. 52306026), and State Key Laboratory of Air-conditioning Equipment and System Energy Conservation Open Project (Project No. ACSKL2021KT01).

REFERENCES

- [1] K. El Kadi, F. Alnaimat, and S. Sherif, 'Recent advances in condensation heat transfer in mini and micro channels: A comprehensive review', *Appl. Therm. Eng.*, vol. 197, p. 117412, 2021.
- [2] R. K. Shah and D. P. Sekulić, *Fundamentals of Heat Exchanger Design*, 1st ed. Wiley, 2003. doi: 10.1002/9780470172605.
- [3] T. Xiong, G. Liu, Q. Gao, G. Yan, and J. Yu, 'Thermal-hydraulic and drainage performance of microchannel heat exchangers for refrigeration and heat pump systems under frosting, defrosting, and wet conditions: A comprehensive review', *J. Build. Eng.*, vol. 64, p. 105654, 2023.
- [4] M. G. Khan and A. Fartaj, 'A review on microchannel heat exchangers and potential applications', *Int. J. Energy Res.*, vol. 35, no. 7, pp. 553–582, Jun. 2011, doi: 10.1002/er.1720.
- [5] B. Vestergaard, M. Yanik, and J. Jianlong, 'Increasing cost effectiveness of high efficiency commercial air conditioners with MCHE evaporators', *DVS-Berichte*, no. TN.297, p. 2013, 2013.
- [6] W. Sheng, P. Liu, C. Dang, and G. Liu, 'Review of restraint frost method on cold surface', *Renew. Sustain. Energy Rev.*, vol. 79, pp. 806–813, Nov. 2017, doi: 10.1016/j.rser.2017.05.088.
- [7] X. U. Xiangguo, Z. Sicheng, L. Haobin, W. Xiaofei, and Z. Ziwen, 'Review of Methods to Simulate and Improve the Surface Wettability of Heat Exchanger and Corresponding Influence on Air Conditioning Systems', *J. Mech. Eng.*, vol. 53, no. 4, p. 122, 2017.
- [8] J. Yin and A. M. Jacobi, 'Condensate Retention Effects on the Air-Side Heat Transfer Performance of Plain and Wavy-Louvered Heat Exchangers', *Air Cond. Refrig. Cent. Coll. Eng. Univ. Ill. Urbana-Champaign*, 2000.
- [9] L. Lu, D. Guoliang, Z. Dawei, Y. Yifei, and D. Xinyuan, 'CFD simulation of water drainage performance of louver-typed microchannel heat exchanger', *CIESC J.*, vol. 72, no. S1, p. 91.
- [10] H. Osada, H. Aoki, and T. Ohara, 'Research on Corrugated Multi-Louvered Fins under Dehumidification', *Heat Transfer—asian Res.*, vol. 30, no. 5, pp. 383–393, 2001.

High Differential Pressure Expansion Work Recovery in Trans-Critical CO₂ Heat Pumps using a Rotary Gas Pressure Exchanger

AzamTHATTE

Energy Recovery Inc.

San Leandro, 94577, USA, athatte@energyrecovery.com

ABSTRACT

Trans-Critical CO₂ heat pumps provide significant thermodynamic advantage over natural gas fired boilers in terms of energy consumed per unit heat supplied. Additionally, they facilitate transition away from environmentally harmful HFCs and HFOs towards natural refrigerants with ultra-low global warming potential. However, the saturation pressure and thus the heat rejection pressure for CO₂ is much higher compared to that for HFCs, resulting in higher compression power requirement per unit heat delivered. This reduces the heat pump cycle COP. Further, the COP of trans-critical CO₂ cycle drops at high load return temperatures due to excessive production of flash gas. One of the key reasons for cycle inefficiency is the exergy destroyed during the throttling process over a high differential pressure between heat source and heat sink. To increase the exergetic efficiency of the cycle, this paper presents some novel heat pump architectures utilizing rotary gas pressure exchanger (PXG) for high differential pressure expansion work recovery. PXG achieves up to 95% pressure recovery coefficient using direct fluid-to-fluid contact acoustic pressure exchange between high pressure supercritical CO₂ and low pressure gaseous CO₂. Through these acoustic waves, both the compression

of low pressure gaseous CO₂ and the expansion of high pressure supercritical CO₂ is achieved inside the rotating axial ducts of PXG rotor. The gas dynamics of this trans-critical compression & expansion processes and the species transport taking place inside PXG's rotating duct will be described. PXG can compress up to 30% of the total system mass flow without consuming any external mechanical or electrical energy but only through the expansion work recovery, thus providing "free compression" for significant portion of the system flow through the entire differential pressure of the cycle (as much as 70 bar). The paper presents the cycle analyses for several of the PXG based novel heat pump architectures and compares the energy savings provided by PXG. A case study on 10 MW scale district heating application using PXG based heat pump and the ocean water as the low temperature heat source will also be presented. Exergy analysis highlighting second law efficiency improvement provided by PXG and the experimental data on trans-critical compression-expansion performance achieved by PXG at conditions relevant to district heating will also be presented. Lastly, the de-carbonization potential of PXG integrated heat pump systems in Europe and USA will be discussed.

Keywords: Heat Pump, Carbon Dioxide, Trans-Critical, Rotary Pressure Exchanger, Energy Recovery, Pressure Recovery, Isentropic, Isenthalpic, Compressors, COP, Energy Efficiency.

Research and optimization of cold water phase change heat exchanger

Ying Xu^{(a), (*)}, Linfeng Zhou^(a), Shuang Zhang^(a)

^(a) School of Energy and Architecture Engineering,
Harbin University of Commerce,
No.1 Xuehai Street, Harbin, Heilongjiang, China

Email: joexying@126.com

^(*)Corresponding author. Email: joexying@126.com

ABSTRACT

The core part of the heat pump system is the phase changer heat exchanger, which determines the heat transfer performance of the whole heat pump system. Cold water phase changer heat exchanger stands out for its advantages of stable heat transfer temperature, easy access to heat source and large latent heat of phase change. In order to improve the heat transfer efficiency of the phase changer heat pump system, the factors affecting the heat transfer efficiency of the phase changer heat exchanger were analyzed by combining theoretical analysis, experimental verification and numerical simulation, so as to optimize the heat transfer performance of the phase changer heat exchanger.

Firstly, through theoretical analysis, it is concluded that ice thickness is mainly related to cold water velocity, temperature and ice related parameters. Secondly, the experimental data are analyzed, and it is found that the inlet temperature of cold water has little influence on the total heat transfer coefficient and icing condition within the experimental range, while the inlet flow of cold water has a greater influence on the ice sheet, and the growth rate of the ice sheet accelerates with the increase of the discharge. Finally, the optimal heat transfer efficiency condition within the experimental range is obtained through numerical simulation, and the analysis shows that the influence of cold water inlet flow on the ice sheet is significantly greater than that of the inlet water temperature, and the decrease of both will lead to the increase of the overall thickness of the ice sheet, but the decrease of the flow will increase the growth rate of the ice sheet.

The study of phase changer heat exchanger not only lays a foundation for optimizing the deicing device, but also for improving the heat transfer efficiency of phase changer heat pump system.

Keywords: phase changer heat pump system, phase changer heat exchanger, Ice sheet formation, Numerical analysis.

英华特

专业涡旋压缩机制造商

提供全面完善的涡旋压缩机解决方案



广泛应用于

HEAT
热泵

AIR COOLING
空调冷水机

FREEZING
冷冻冷藏

电驱动车



Effect of fin structure variation on performance of finned-tube heat exchangers in air-source heat pumps

Di MA^(a), Qi CHEN^(a), Gang YAN^(a)

(a) Department of Refrigeration & Cryogenic Engineering, School of Energy and Power Engineering, Xi'an Jiaotong University
Xi'an, 710049, China, qichen@mail.xjtu.edu.cn

ABSTRACT

The finned-tube heat exchanger exhibits advantages such as excellent heat transfer performance and strong environmental adaptability, thus it is widely used in dual-purpose room air conditioners for heating and cooling. Currently, most outdoor heat exchangers for room air conditioners have a tube diameter of 7 mm. To meet the trend of miniaturization in room air conditioner heat exchangers, there is an urgent need to develop fins suitable for 5 mm tube diameter finned-tube heat exchangers. This paper establishes a three-dimensional physical model and mathematical model for the louver fins of 5 mm tube diameter finned tube heat exchangers. Computational Fluid Dynamics (CFD) software is utilized to simulate the effects of different louver opening angles and tube spacing on fin performance. Evaluation criteria for fin performance are based on heat transfer and pressure drop under the same incoming air velocity and pump power. Simulation results indicate that the optimal louver opening angle for the louver fins is 20°, with an optimal tube spacing of 17.1 mm for the best overall fin performance.

Keywords: Finned-tube heat exchanger; Heat transfer enhancement; Numerical simulation; Slit Angle; Tube spacing

Steady-state heat pump performance model including irreversibility in the heat exchangers and the compressor for R290 and R32

Thomas Meyer^(a), Felix Ziegler^(a), Stefan Elbel^(a),

^(a) Technische Universität Berlin
Berlin, D-10587, [Germany, thomas.meyer@tu-berlin.de](mailto:thomas.meyer@tu-berlin.de)

ABSTRACT

Heat pumps will be indispensable for providing useful heating power from renewables, when using non-fossil based electrical energy. It is well-known that the sizing of the heat exchangers plays a crucial role for achieving high energy efficiency. Nevertheless, the (re-)design of heat exchangers and compressors for the large variety of refrigerants which, due to environmental and safety regulations, is constantly changing is an ongoing process. For that reason, a simple steady-state simulation tool has been developed in this study, providing fast insight into dependencies of heat pump performance. It employs the NTU-effectiveness method to the heat exchangers and a clearance volume approach to a piston compressor for a single stage heat pump, working in the present version, with R290 and R32.

For a fixed displacement volume of the compressor, the effects on the power density of different heat exchanger designs for various rotational frequencies and the two refrigerants are presented and discussed. An

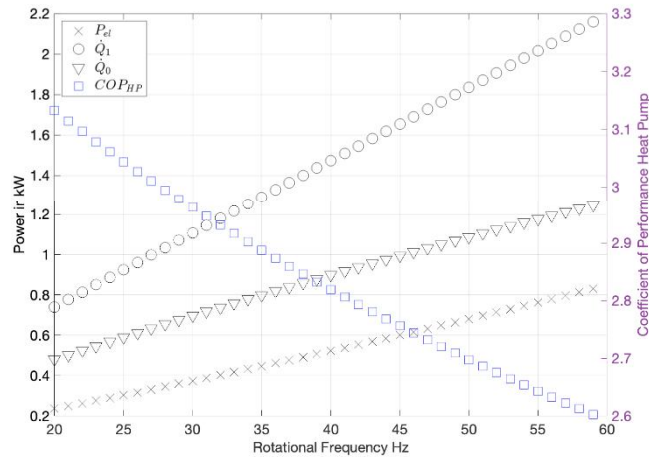


Figure 1 - Evolution of the power and the coefficient of performance of the heat pump using R290 as refrigerant for $t_{0,in}=0^{\circ}\text{C}$ and $t_{1,in}=50^{\circ}\text{C}$.

As can be seen in Fig. 1 for a piston compressor with a nominal volume flow rate of $1.5\text{m}^3/\text{h}$ and an external temperature lift of $t=50\text{K}$ the heating capacity increases from 0.7 kW at 20 Hz to around 2.2kW at 60Hz while the COP drops from 3.1 to 2.6 due to the increased pressure ratio at increased heating capacity.

The simulation allows not only for comparison of different compressors and heat exchanger designs but also for providing more practical insight to the “drop-in” discussion for various refrigerants, namely R32 and R290 in the current study.

Keywords: efficiency, heat pumps, piston compressor, NTU effectiveness, process design.

Theoretical Study on the Mismatch of Thermal Quality and Heat Capacity in the Heating Process of Transcritical CO_2 Heat Pumps

Lingxiao Yang^(a), Xin Wang^(a), Bo Xu^(a), Zhenqian Chen^(a)

(a) School of Energy and Environment, Southeast University
 Nanjing, 210000, China, 230228133@seu.edu.cn, xinx_wang@seu.edu.cn, xubo@seu.edu.cn,
zqchen@seu.edu.cn

ABSTRACT

Transcritical CO_2 heat pumps are attracting more and more attention due to its outstanding environmental performance, higher heating temperature and excellent low-temperature performance. However, affected by the unique properties of CO_2 in the critical region, improperly set operating parameters can lead to a mismatch of thermal quality and heat capacity in the heat transfer process of the gas cooler, and consequently have a serious negative impact on the performance of the system. In this study, we proposed and modified the models of compressor and gas cooler based on the existing transcritical CO_2 water source heat pump water heater. Relying on the models, the inner details of the heat transfer process occurring in the gas cooler were investigated; the cooling pressure of CO_2 in the gas cooler in relation to the thermal quality and the consequent effect on the heating temperature of the system were revealed; the heat capacity matching of the heat transfer media on both sides in the gas cooler and the further effect on the heating performance of the system was studied. This study

can not only provide an important reference for the theoretical analysis and control strategy of the transcritical

CO₂ heat pump, but also guide the related simulation and the design of the gas cooler.

Keywords: Transcritical CO₂ heat pump, COP, Thermal quality, Heat capacity.

Thermodynamics analysis of the transcritical CO₂ heat pump for heating applications

Wenke Zhao^(a), Weitao Cao^(a), Xin Chen^(b), Yaning Zhang^(a), Bingxi Li^(a)

^(a)School of Energy Science and Engineering, Harbin Institute of Technology, Harbin, 150001, China,

zhaoweke@hit.edu.cn.

^(b)School of Energy and Civil Engineering, Harbin University of Commerce, Harbin, 150028, China

ABSTRACT

An experimental transcritical CO₂ heat pump system was implemented in Harbin, China to conduct the system thermodynamic analysis. The effects of regenerator efficiency, high pressure, low pressure, and outlet temperature of the gas cooler on COP and heating load were investigated. Furthermore, the sensitivity analysis was applied to ensure the sensitivity degrees of the parameters on COP and heating load. The results show that when the regenerator efficiency increased from 0 to 0.8, COP increased from 2.7 to 3.3 and the heating load changed from 14.7 kW to 22.6 kW. COP was maximum (4.1) at the high pressure of 10.0 MPa, and the heating load increased from 20.0 kW to 36.6 kW as the high pressure climbed from 8.5 MPa to 11.0 MPa. When the low pressure increased from 4.5 MPa to 7.0 MPa, COP increased from 4.1 to 8.0 and the heating load decreased from 33.6 kW to 22.0 kW. When the outlet

temperature of the gas cooler increased from 30 °C to 55 °C, COP decreased from 5.8 to 2.3 and the heating load decreased from 36.6 kW to 16.9 kW. The improvements of COP and heating load should preferentially increase the high pressure due to its maximum average sensitive degree of 0.192 on the COP and 4.328 on the heating load.

Keywords: Carbon Dioxide, COP, Heating Load, Thermodynamics Analysis, Sensitivity Analysis

1. INTRODUCTION

Energy plays a significant role in global development and progression, however, fossil fuels emit plenty of greenhouse gases and air pollution, such as CO₂, NO_x, SO₂, and PM (Particulate Matter), easily causing humans to sick and extremely harmful to human's health [1]. To reduce the air pollution, the transcritical CO₂ heat pump for building heating is attracting more and more attention. CO₂ is a natural working medium and it has the advantages of low viscosity, high latent heat, high specific heat [2], non-flammability, nontoxicity, competitive price, zero ODP (Ozone Depression Potential), and negligible GWP (Global Warming Potential) [3].

Many researchers have studied the transcritical CO₂ heat pump to improve its operation efficiency, such as that Nguyen et al. [4] theoretically investigated the effective effect of the internal heat exchanger on the CO₂ direct expansion ground source heat pump in Canada with the highest COP (Coefficient Of Performance) of 3.66, Wang et al. [5] experimentally studied the COP of an air source transcritical CO₂ heat pump with a TES (thermal energy storage) for residential heating and the COP were 1.73 and 1.48 with and without TES, respectively, and Velasco et

al. [6] experimentally performed the COP, compressor energy consumption, and available thermal energy of the CO₂ water-to-water heat pump with a water storage tank to produce domestic hot water by 9 samples, and the COP, compressor energy consumption, and available thermal energy were in the ranges of 2.5 ~ 4.0, 1.4 ~ 1.5, and 149 ~ 159 MJ, respectively. Also, some researchers have proposed novel transcritical CO₂ cycles to promote heating performances, for example, Peng et al. [7] experimentally investigated the COP, heating capacity, and refrigerant discharge temperature of the transcritical CO₂ single-stage and vapor injection heat pumps, indicating that the vapor injection heat pump had a better heating performance because its COP (2.5 ~ 4.2) was 4% higher, heating capacity was 7% greater, and refrigerant discharge temperature was 8 ~ 12 °C lower than single-stage heat pump, respectively, Qin et al. [8] proposed a novel compression/ejection transcritical CO₂ heat pump for simultaneously heating and cooling to improve the evaporator efficiency, and the simulations presented that the system COP was 11.7 when the compressor frequency was 30 Hz and the discharge pressure was 80 bar, and Illan-Gomez et al. [9] numerically studied the performance of the water source transcritical CO₂ heat pump by using dedicated mechanical subcooling in ten configurations to generate hot water, and the best configuration had a 26% higher COP and 160% greater heating capacity than the base configuration.

In this study, the thermodynamics analysis of a transcritical CO₂ heat pump for heating applications was conducted. The system performances (COP and heating load) as affected by the regenerator, high pressure, low pressure, and outlet temperature of the gas cooler were compared and analyzed. The sensitivity analysis was implemented to obtain the influence degree of the pressures at high- and low-pressure side, and outlet temperature of the gas cooler.

2. Experimental and models

2.1 Experimental system

Fig. 1 presents the photos of the transcritical CO₂ heat pump and water-loop system. The experimental system has a nominal working condition of 7.86 kW and a maximum heating load of 27.1 kW, mainly including a CO₂ semi-enclosed piston compressor from Bitzer, an evaporator, a gas cooler, an internal heat exchanger, a liquid reservoir, a constant pressure valve, and an expansion valve. The expansion valve is an electrical control valve EX5-U21 produced by Emerson Electric Company. The inlet and outlet diameters are 16 and 22 mm, respectively, the highest working pressure is 45 bar, and the working temperature range is -40 ~ 55 °C [10].



(a) Water-loop systems.



(b) Transcritical CO₂ heat pump.

Fig. 1. Photos of the transcritical CO₂ heat pump system.

K-type thermocouples were used to measure the inlet and outlet temperatures of the compressor, evaporator, gas cooler, internal heat exchanger, and expansion valve. The supplied and returned water flow rates were measured by the turbine flowmeter SDLWGY-40COSSBN, and the power consumption of the compressor was recorded by the three-phase multifunctional power detector JCYJ-96W3YS. The accuracies of the K-type thermocouple, turbine flowmeter, and power detector were ± 0.5 °C, 0.5%, and 0.2%, respectively.

2.2 Thermodynamic analysis

Fig. 2 illustrates the system schematic diagram of the transcritical CO₂ heat pump system. The ground source exchanger and residential building were replaced by the cold and hot water tanks, respectively, and the cold water tank was sustained at 8 °C nearly to the ground temperature. The experimental transcritical CO₂ heat pump absorbed the heat from the cold water tank by the evaporator and then heated the hot water tank with the gas cooler.

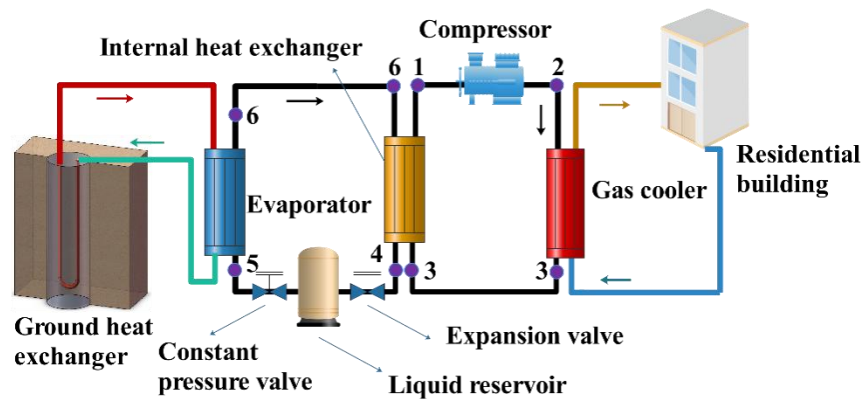


Fig. 2. Schematic diagram of the transcritical CO₂ heat pump system.

Fig. 3 presents the P - h diagrams of the transcritical CO_2 heat pump. The working fluid CO_2 was compressed from state points 1 to 2 in the compressor, cooled from state points 2 to 3 in the gas cooler, throttled from state points 4 to 5 in the expansion valve, and evaporated from state points 5 to 6 in the evaporator. Processes 3-4 and 6-1 were the heat exchanges in the internal heat exchanger. The high pressure, low pressure, superheat degree, regenerator efficiency, outlet temperature of the gas cooler, and compressor efficiency were set at first, and other parameters (temperature, pressure, and enthalpy) were obtained by the software REFPROP according to Fig. 3.

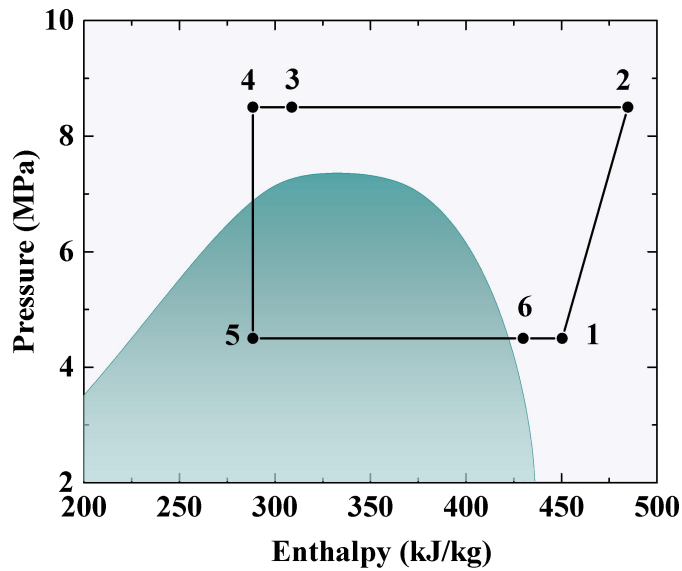


Fig. 3. p - h diagram of the transcritical CO_2 heat pump system.

2.3 Model validation

The heat pump parameters and COP at the supplied temperatures of 40, 50, and 60 °C are shown in Table 1. The high pressure, low pressure, compressor outlet temperature, and gas cooler outlet temperature were obtained from the experimental measurements. For the experiments, system COP for the supplied water temperatures of 40, 50, and 60 °C were 2.2, 2.3, and 2.4, respectively, whereas, the calculated COP were 3.1, 3.3, and 3.5, respectively. The differences were because (a) the power consumptions of two water pumps (rated power 740 W), control unit, turbine flowmeter, and power detector were not reckoned in the thermodynamic calculation, (b) the temperature measure points were at the outside of the refrigerant pipes, causing that the temperature errors were high, and (c) the thermodynamic state points were ideal without the operation variations of the compressor efficiency and regenerator efficiency.

Table 1 Heat pump parameters and COP at different supplied temperatures.

Sup. temp. (°C)	High P (MPa)	Low P (MPa)	Compressor outlet temp. (°C)	Gas cooler outlet temp. (°C)	Cal. COP	Exp. COP
40	7.0	4.0	72	38	3.1	2.2
50	8.0	4.3	89	46	3.3	2.3
60	9.0	4.6	100	56	3.5	2.4

3. Results and discussion

The regenerator efficiency, high pressure, low pressure, and the outlet temperature of the gas cooler were selected to compare the system performance variation and analyze the parameter effects. The parameter values are listed in the Table 2. The regenerator efficiency, high pressure, low pressure, and the outlet temperature of the gas cooler ranges were 0 ~ 0.8, 8.5 ~ 11.0 MPa, 4.5 ~ 7.0 MPa, and 30 ~ 55 °C, respectively. The sensitivity analysis of COP and heating load as affected by the high pressure, low pressure, and outlet temperature of the gas cooler were conducted.

Table 2 Parameter variations list.

Parameter	Value
Regenerator efficiency	0, 0.2, 0.4, 0.6, 0.8
High pressure (MPa)	8.5, 9.0, 9.5, 10.0, 10.5, 11.0
Low pressure (MPa)	4.5, 5.0, 5.5, 6.0, 6.5, 7.0
Outlet temperature of the gas cooler (°C)	30, 35, 40, 45, 50, 55

3.1 Effect of regenerator efficiency

Fig. 4 presents the heating loads and COPs at different regenerator efficiencies. The low pressure, high pressure, outlet temperature of the gas cooler, compressor isentropic efficiency, and superheat degree were set as 4.5 MPa, 8.5 MPa, 40 °C, 0.8, and 3 °C, respectively. When the regenerator efficiencies were 0, 0.2, 0.4, 0.6, and 0.8, COP were 2.7, 2.9, 3.1, 3.2, and 3.3, and heating loads were 14.7, 17.0, 19.0, 20.9, and 22.6 kW, respectively. When the regenerator efficiency increased from 0 to 0.8, COP increased from 2.7 to 3.3 and heating load changed from 14.7 kW to 22.6 kW. Compared with no regenerator, the heating load increased by 16.0%, 29.9%, 42.5%, and 54.3%, COP increased by 7.7%, 14.0%, 18.8%, and 22.9% as the regenerator efficiencies were 0.2, 0.4, 0.6, and 0.8, respectively.

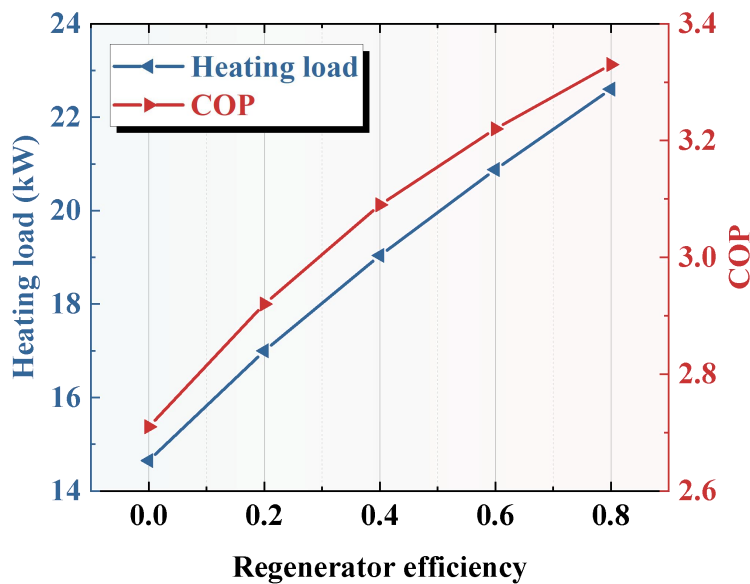


Fig. 4. Heating loads and COPs at different regenerator efficiencies.

The improvement of the regenerator efficiency can increase the heat obtained before CO₂ entered the compressor and improved the superheat, leading to the increase of COP. The increase in heating load is because when the gas cooler outlet state point 3 is unchanged, the compressor curve shifted to the right, resulting in an increase in the enthalpy difference of heating load, and thus more heat was supplied.

3.2 Effect of high pressure

The heating loads and COPs at different high pressures are shown in Fig. 5. The low pressure, outlet temperature of the gas cooler, compressor isentropic efficiency, regenerator efficiency, and superheat degree were set as 4.5 MPa, 40 °C, 0.8, 0.5, and 3 °C, respectively. When the high pressures were 8.5, 9.0, 9.5, 10.0, 10.5, and 11.0 MPa, COP were 3.2, 3.9, 4.1, 4.1, 4.1, and 4.0, and heating loads were 20.0, 26.9, 31.2, 33.6, 35.2, and 36.6, respectively. When the high pressure climbed from 8.5 MPa to 11.0 MPa, COP had a maximum value of 4.1 and heating load changed from 20.0 kW to 36.6 kW.

The increase in the heating load was because (a) the higher pressure caused the greater the enthalpy value of point 2, and (b) at the same supplied temperature, the higher pressure led to the lower the enthalpy value of point 3, finally resulting in a larger enthalpy difference between points 2 and 3. COP had the best value because the increase rate of heating load was greater than the increase rate of compressor power consumption, indicating that there is an optimal high pressure that can make the COP reach the maximum value of the current working condition.

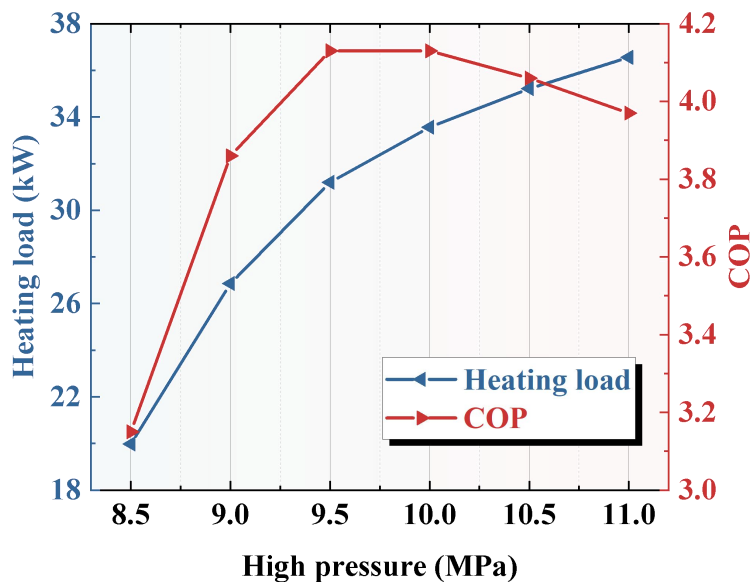


Fig. 5. Heating loads and COPs at different high pressures.

3.3 Effect of low pressure

Fig. 6 presents the heating loads and COPs at different low pressures. The high pressure, outlet temperature of the gas cooler, compressor isentropic efficiency, regenerator efficiency, and superheat degree were set as 10 MPa, 40 °C, 0.8, 0.5, and 3 °C, respectively. When the low pressures were 4.5, 5.0, 5.5, 6.0, 6.5, and 7.0 MPa, COP were 4.1, 4.6, 5.2, 6.0, 6.9, and 8.0, and heating loads were 33.6, 31.2, 29.0, 26.7, 24.4, and 22.0 kW, respectively. When the low pressure increased from 4.5 MPa to 7.0 MPa, COP increased from 4.1 to 8.0 and heating load decreased from 33.6 kW to 22.0 kW.

The heating load decreased and COP increased as the low pressure was increased because the enthalpy of point 2 decreased whereas the point 3 was not changed, causing that enthalpy difference declined and the heating load decreased. COP cannot increase indefinitely because (a) the low pressure value needed to be lower than the critical pressure of carbon dioxide 7.38 MPa, and (b) the decreased heating load was unable to meet the needs of users.

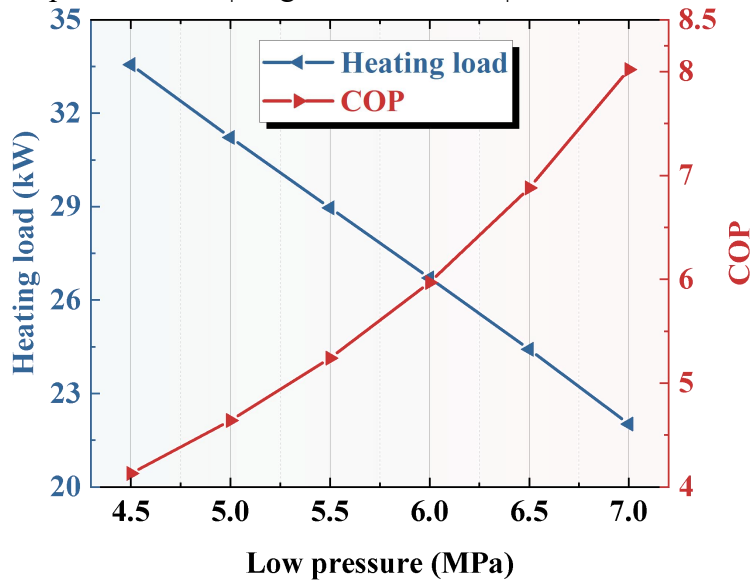


Fig. 6. Heating loads and COPs at different low pressures.

3.4 Effect of outlet temperature of the gas cooler

The heating loads and COPs at different outlet temperatures of the gas cooler are shown in Fig. 7. The high pressure, low pressure, compressor isentropic efficiency, regenerator efficiency, and superheat degree were set as 10 MPa, 5 MPa, 0.8, 0.5, and 3 °C, respectively. When the outlet temperatures of the gas cooler were 30, 35, 40, 45, 50, and 55 °C, COP were 5.8, 5.3, 4.6, 3.7, 2.9, and 2.3, and heating loads were 36.6, 34.5, 31.2, 25.8, 20.3, and 16.9 kW, respectively. When the outlet temperature of the gas cooler increased from 30 °C to 55 °C, COP decreased from 5.8 to 2.3 and heating load decreased from 36.6 kW to 16.9 kW.

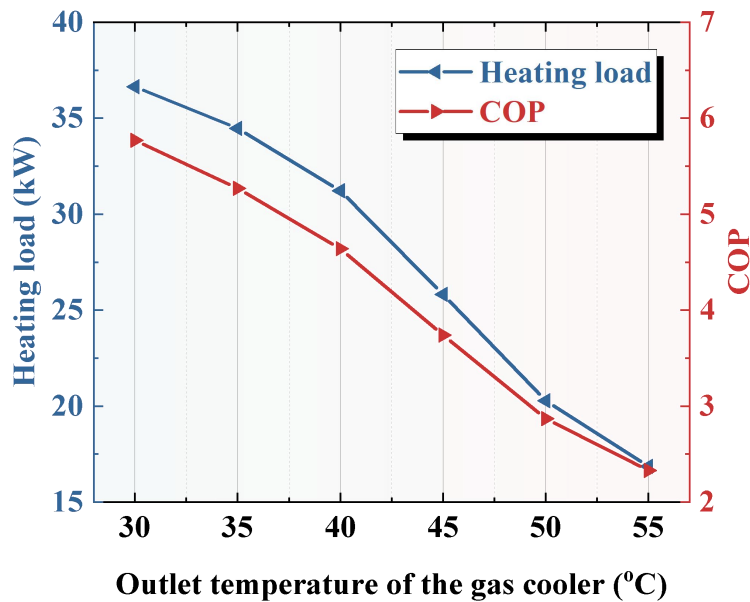
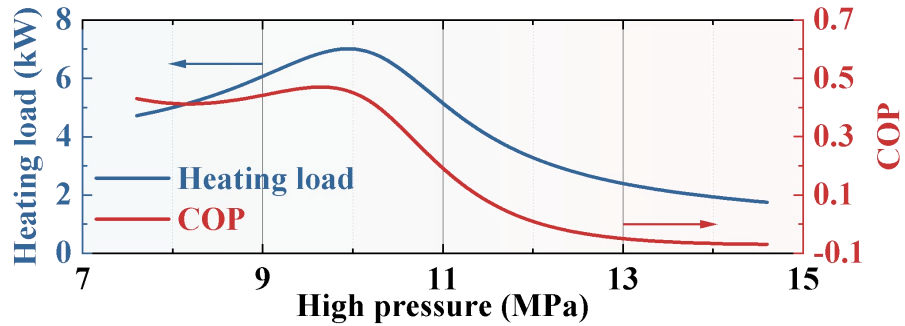


Fig. 7. Heating loads and COPs at different outlet temperatures of the gas cooler.

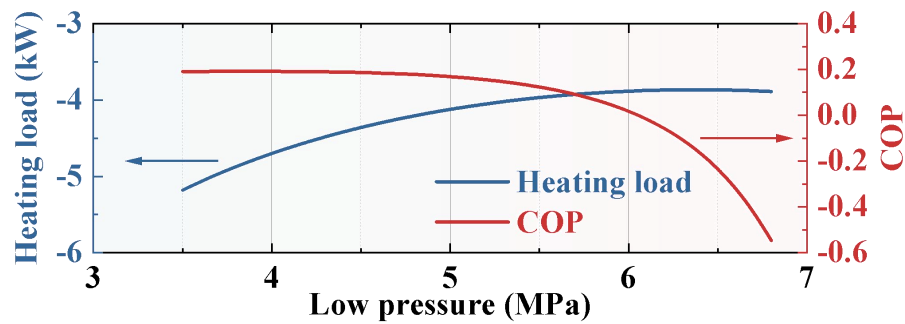
The decrease of the heating load was because the enthalpy of point 2 was not changed whereas the point 3 increased, causing that enthalpy difference declined and the heating load decreased. COP decreased was due to the fact that the heating load decreased higher than the compressor power consumption increased.

3.5 Sensitivity analysis

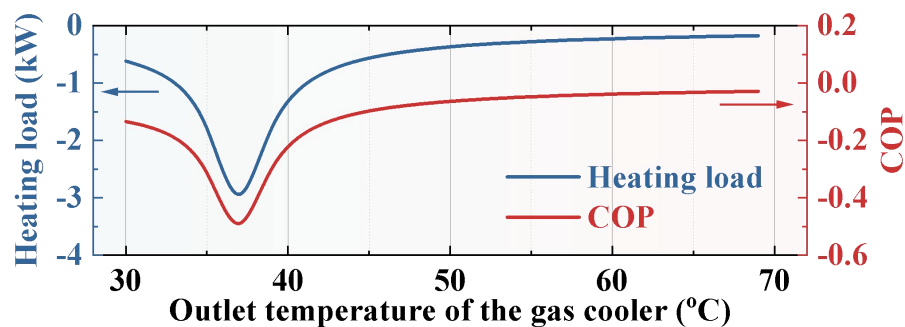
The sensitivity analysis of COP and heating load as affected by the high pressure, low pressure, and outlet temperature of the gas cooler were conducted, as shown in Fig. 8.



(a) High pressure.



(b) Low pressure.



(c) Outlet temperature of the gas cooler.

Fig. 8. Heating load and COP variations at different parameters.

The improvements of COP and heating load should preferentially to increase the high pressure due to its maximum average sensitive degree of 0.192 on the COP and 4.328 on the heating load, as shown in Table 3.

Table 3 Sensitivity analysis of COP and heating load.

Parameter	COP		Heating load	
	Range	Average	Range	Average
High pressure	-0.069~0.431	0.192	1.749~7.035	4.328
Low pressure	-0.547~0.191	0.064	-5.180~-3.890	-4.227
Gas cooler outlet temperature	-0.521~-0.029	-0.121	-3.133~-0.176	-0.696

4. Conclusions

The thermodynamics analysis of a transcritical CO₂ heat pump for heating applications was conducted. Some conclusions were obtained.

When the regenerator efficiency increased from 0 to 0.8, COP increased from 2.7 to 3.3 and the heating load changed from 14.7 kW to 22.6 kW.

COP was maximum (4.1) at the high pressure of 10.0 MPa, and the heating load increased from 20.0 kW to 36.6 kW as the high pressure climbed from 8.5 MPa to 11.0 MPa.

When the low pressure increased from 4.5 MPa to 7.0 MPa, COP increased from 4.1 to 8.0 and the heating load decreased from 33.6 kW to 22.0 kW.

When the outlet temperature of the gas cooler increased from 30 °C to 55 °C, COP decreased from 5.8 to 2.3 and the heating load decreased from 36.6 kW to 16.9 kW.

The improvements of COP and heating load should preferentially increase the high pressure due to its maximum average sensitive degree of 0.192 on the COP and 4.328 on the heating load.

5. Acknowledgments

The authors are grateful for the financial support from the National Natural Science Foundation of China (52276056) and the Special Foundation for Major Program of Civil Aviation Administration of China (MB20140066).

6. References

- [1] Xu J, Akhtar M, Haris M, Muhammad S, Abban OJ, Taghizadeh-Hesary F. Energy crisis, firm profitability, and productivity: An emerging economy perspective. *Energy Strateg Rev* 2022; 41: 100849.
- [2] Ge YT, Tassou SA. Thermodynamic analysis of transcritical CO₂ booster refrigeration systems in supermarket. *Energy Convers Manage* 2011; 52: 1868-1875.
- [3] Gullo P, Elmegaard B, Cortella G. Energy and environmental performance assessment of R744 booster supermarket refrigeration systems operating in warm climates. *Int J Refrigeration* 2016; 64: 61-79.
- [4] Nguyen A, Eslami-Nejad P, Badache M, Bastani A. Influence of an internal heat exchanger on the operation of a CO₂ direct expansion ground source heat pump. *Energy Build* 2019; 202: 109343.
- [5] Wang Z, Wang F, Li G, Song M, Ma Z, Ren H, Li K. Experimental investigation on thermal characteristics of transcritical CO₂ heat pump unit combined with thermal energy storage for residential heating. *Appl Therm Eng* 2020; 165: 114505.

- [6] Velasco FJS, Haddouche MR, Illán-Gómez F, García-Cascales JR. Experimental characterization of the coupling and heating performance of a CO₂ water-to-water heat pump and a water storage tank for domestic hot water production system. *Energy Build* 2022; 265: 112085.
- [7] Peng X, Xie J, Liu X, Wang G, Wang D, Yang Y. Experimental investigation and comparison on heating performance characteristics of two transcritical CO₂ heat pump systems. *Energy Build* 2021; 250: 111296.
- [8] Qin W, Zhang Y, Wang D, Chen J. System development and simulation investigation on a novel compression/ejection transcritical CO₂ heat pump system for simultaneous cooling and heating. *Energy Convers Manage* 2022; 259: 115579.
- [9] Illan-Gomez F, García-Cascales JR, Velasco FJS, Oton-Martínez RA. Numerical performance of a water source transcritical CO₂ heat pump with mechanical subcooling. *Appl Therm Eng* 2023; 219: 119639.
- [10] Zhao W, Zhang Y, Li H, Cao X, Li L, Li B. Decarbonization performances of a transcritical CO₂ heat pump for building heating: A case study. *Energy Build* 2023; 289: 113052.

Enhancing carbon dioxide (CO₂) refrigeration efficiency in different climates: experimental analysis of four configurations and annual performance prediction in different Cities

**Ana PAEZ^(a), Bénédicte BALLOT-MIGUET^(a), Pascal TOBALY^(b,c),
Benoit MICHEL^(d), Rémi REVELLIN^(d)**

^(a) EDF R&D

Écuelles, 77250, France, ana.paez@edf.fr, benedicte.ballot-miguet@edf.fr

^(b) LaFSET, Laboratoire du Froid, des Systèmes Energétiques et Thermiques Paris, 75003, France, pascal.tobaly@lecnam.net

^(c) Université Sorbonne Paris Nord Villetaneuse, 93430, France

^(d) Univ Lyon, INSA Lyon, CNRS, CETHIL, UMR5008 69621 Villeurbanne, France, benoit.michel@insa-lyon.fr, remi.revellin@insa-lyon.fr

ABSTRACT

Carbon dioxide (CO₂) is an excellent alternative to conventional refrigerants due to its non-toxic and non-flammable nature, zero ozone layer impact, and minimal contribution to global warming compared to other refrigerants. However, its efficiency in warm climates remains a challenge. This article addresses this issue by experimentally comparing the energy efficiencies of four configurations: a first configuration works with a parallel compressor, a second configuration works with two internal heat exchangers, a third one with an economizer and a last one with a flash gas valve.

All configurations were tested in the same conditions. The cooling capacity was varied between 20 and 40 kW, and the ambient temperature was varied between 15 to 38 °C. Coefficients of performance (COP) were measured under steady-state conditions and compared. Subsequently, the results were used to develop polynomial regressions predicting the annual COP for each system operating in different cities.

Steady-state experimental results in transcritical conditions showed a great COP improvement using a parallel compressor, by more than 15%, compared to the flash gas system. The other configurations showed a COP improvement by less than 11% compared to the flash gas system at the same conditions. However, the annual COP (subcritical and transcritical conditions) showed that the parallel compressor configuration does not always provide the highest efficiencies. This depends on the city's annual temperature profile.

The article will provide numerous schemes of configurations, cycles, cities temperature and COP profiles as well as summarised conclusions.

Keywords: Carbon Dioxide, Parallel compressor, Energy Efficiency, Internal heat exchangers, Refrigeration.

Study on Performance of Trans-critical CO₂ Air Source Heat Pump System in Cold Region

Shuai Zheng^(a), Haoran Ning^(b), Guofeng Xu^(c), Ying Xu^(d), Yi Liu^(e)

(School of Energy and Civil Engineering, Harbin University of Commerce, Harbin 150028, China)

(a) (School of Energy and Civil Engineering, Harbin University of Commerce, Harbin 150028, China, 985682156@qq.com)

(b) (School of Energy and Civil Engineering, Harbin University of Commerce, Harbin 150028, China, 102989@hrbcu.edu.cn)

(c) (School of Energy and Civil Engineering, Harbin University of Commerce, Harbin 150028, China, xgf_6@163.com)

(d) (School of Energy and Civil Engineering, Harbin University of Commerce, Harbin 150028, China, joexying@126.com)

(e) (School of Energy and Civil Engineering, Harbin University of Commerce, Harbin 150028, China, 985682156@qq.com)

Abstract

The winter temperature in the northern regions of China is relatively low, and the heating efficiency of traditional air source systems is low, and it cannot operate normally in severe cold weather. So it is proposed to use trans-critical CO₂ air source heat pumps for winter heating and summer cooling in severe cold areas. The change of ambient temperature has a great impact on the performance of the trans-critical CO₂ air source heat pump system. In order to study the operating characteristics of the trans-critical CO₂ air source heat pump system in cold regions, TRNSYS simulation software is used to test and analyze key parameters such as indoor and outdoor temperature, water supply and return temperature, COP and so on. The results show that there is a large difference between the average supply and return water temperature in the early and middle heating period, but the temperature of supply and return water in the heating period and the cooling period does not fluctuate much, which indicates that the heating and cooling effect of the trans-critical CO₂ air source heat pump system is better when applied in cold areas.

Keywords: Cold Region; Air source heat pump; COP

1. INTRODUCTION

At present, with the rapid development of China's economy, the aggravation of environmental pollution and the large consumption of energy have become typical problems in our country. China has been the world's largest energy consumer since 2010, and coal consumption is the largest part of China's energy consumption. In recent years, CO₂ refrigeration refrigerant has gradually entered people's vision with its good use economy and good environmental protection. CO₂ air source heat pumps first began to develop in Japan, and then were widely used in European countries. Compared to other heat pump systems, CO₂ air source heat pumps have many advantages.

In this paper, TRNSYS simulation software is used to establish the simulation model of the trans-critical CO₂ air source heat pump system. The performance of an air source heat pump system operating in a cold area is simulated, and the changes of ambient temperature, system heat production and cooling capacity, system and unit input power, system and unit performance coefficient and water supply and return temperature are analyzed

in a typical day.

2. STUDY ON PERFORMANCE OF TRANS-CRITICAL CO₂ AIR SOURCE HEAT PUMP SYSTEM

Through the parameter setting of each part of the simulation software model, the annual hourly load of the building is simulated, as shown in Figure 1.

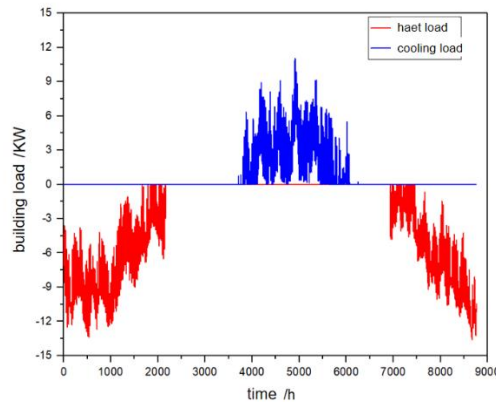


Figure 1: Hourly load of buildings throughout the year

Taking January 1st as the starting point, the hourly load result of the office building for the whole year is obtained. The simulation results show that the maximum annual thermal load of the office building is 13.6kW, the maximum annual thermal load index is 57W/m², the maximum annual cooling load of the office building is 11.8kW, the maximum annual cooling load index is 49W/m².

Through simulation software, the environmental temperature in Harbin and the building temperature of an office building in a year are statistically analyzed, and the simulation results are shown in Figure 2.

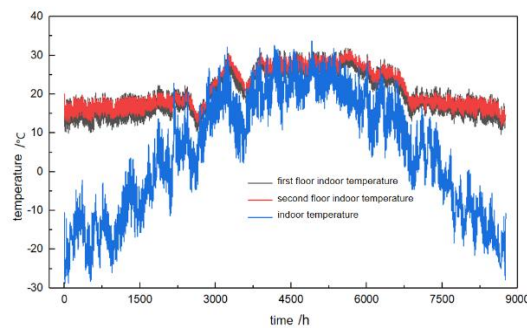


Figure 2: Building temperature and ambient temperature

As shown in the figure, according to the statistical results of annual ambient temperature, Harbin is in winter for a long time and the ambient temperature is low. Harbin is in the summer time is short, the duration of high temperature weather is short. It can be seen from the curves and values in the figure that the temperature of the office building can be maintained at about 20 ° C in the heating season and 26 ° C in the cooling season, which meets the requirements of heating and cooling in cold areas.

3. CONCLUSIONS

Through the simulation results, it can be found that the use of the air source heat pump in summer can make the temperature in the building meet the office requirements and meet the comfort of the human body; In winter, when the air source heat pump is used to heat an office building in a cold area, the building temperature can reach the set temperature, indicating that the air source heat pump heating system is feasible in the cold area.

ACKNOWLEDGEMENT

This work was supported by the Joint Guidance Project of Natural Science Foundation of Heilongjiang Province (LH2021E089) and 2021 Harbin University of Commerce Teacher Innovation Support Plan Project.

REFERENCES

- [1]LOWE R J, DRUMMOND P. Solar , wind and logistic substitution in global energy supply to 2050 Barriers and implications [J]. Renewable & sustainable energy reviews,2022,153:111720.
- [1]Liu S, Zheng L, Dai B, et al. Energetic, economic and environmental analysis of air source trans-critical CO₂ heat pump system for residential heating in China[J]. Applied Thermal Engineering, 2018, 148(2): 1425-1439.

Performance analysis and research on optimization of CO₂ heat pump system for hybrid electric vehicles based on Dymola

Pengtao Ju ^(a), Fang Liu ^(a,b)

^(a)College of Energy and Mechanical Engineering, Shanghai University of Electric Power
2103 Pingliang Road, Yangpu District, Shanghai, 200090, China

^(b)Shanghai Non-carbon energy conversion and utilization institute
Shanghai, 200240, China

ABSTRACT

New energy vehicles can truly achieve zero pollution and zero emissions, which has become an important direction for the development of new energy vehicles in the future. At present, the traditional refrigerant Freon, which is mainly used in the air conditioning system of new energy vehicles, has serious environmental pollution. PTC auxiliary heating is required for insufficient heat production when running in low-temperature conditions in winter. Too much energy consumption of the air conditioning system leads to a serious reduction in mileage. Studies have shown that the maximum range of new energy vehicles running air conditioning, heating, and cooling devices can be reduced by 40%. Therefore, an efficient vehicle-mounted heat pump air conditioning system can improve the energy utilization rate of new energy vehicles, ensure the safety and reliability of batteries, and reduce the impact of heat pump air conditioning energy consumption on vehicle mileage. To solve the above problems, the natural refrigerant CO₂ is used in this paper. The double evaporator heat pump system is used to realize the cascade utilization of energy. The injector recovers the expansion power to improve the system efficiency. An CO₂ compression/injection dual evaporator heat pump system for hybrid electric vehicles was proposed. The heat pump system model was established in the dymola platform using Modelica language, and the performance and energy conversion efficiency of the heat pump system were predicted and analyzed by simulating the COP and operating conditions of the system under different vehicle driving conditions and environmental conditions. Through the mathematical model, the system is optimized to improve the efficiency of the system further and obtain the best operating conditions. The economic feasibility of the system is analyzed, which provides a reference for the development of the onboard heat pump system for hybrid electric vehicles.

Keywords: Vehicle-mounted Heat Pump, CO₂, Ejector, COP

author.

E-mail addresses: 724528897@qq.com (PT. Ju) .

E-mail addresses: fangliu@shiep.edu.cn , fangliu_shiep@163.com (F. Liu) .

Performance Analysis of an Integrated Thermal Management System for Electric Buses

Wencong Shao ^{a,b}, Yunchun Yang ^{a,b}, Huiming Zou ^{a,b,*}, Tianyang Yang ^{a,b}, Changqing Tian ^{a,b}

^a Technical Institute of Physics and Chemistry, Key Laboratory of Cryogenic Science and Technology, Chinese Academy of Sciences, Beijing 100190, China

^b University of Chinese Academy of Sciences, Beijing 100049, China

* Corresponding author. E-mail address: zouhuiming@mail.ipc.ac.cn

Abstract

High-efficiency integrated thermal management systems are crucial for ensuring the safety, comfort, and driving range of new energy vehicles. In this study, an integrated thermal management system for electric buses was purposed, the system performances were experimentally investigated in different modes under both heating and cooling conditions, and the characteristics and regulations were analyzed considering the changes in compressor speed and electronic expansion valve opening. The results show that the purposed system with the vapor-injection technology can operate in an ambient temperature range from $-25\text{ }^{\circ}\text{C}$ to $45\text{ }^{\circ}\text{C}$. It provides a heating capacity of 11.48 kW with a coefficient of performance (COP) of 1.50 at $-25\text{ }^{\circ}\text{C}/20\text{ }^{\circ}\text{C}$ (ambient/in-cabin temperatures), and provide 19.40 kW with a COP of 1.73 at $-10\text{ }^{\circ}\text{C}/20\text{ }^{\circ}\text{C}$. The optimal COP of 2.17 (at a compressor speed of 50 Hz) and 1.87 (at 60Hz) correspond the relative pressure ratios of 1.75 and 1.64 at $7\text{ }^{\circ}\text{C}/20\text{ }^{\circ}\text{C}$, respectively. Considering the cooling demand of the cabin and battery, the system can provide 25.04 kW with a COP of 2.53 at an ambient temperature of $35\text{ }^{\circ}\text{C}$. This study would provide a data support for developing automotive thermal management technology.

Keywords: vapor injection; heat pump; integrated thermal management system; electric bus

Research on efficient heating method of solar composite heat pump based on evaporative thermal accumulator

Jinshuang Gao ^(a,b), Sheng Li ^(a,b), Fan Wu ^(a,b), Gaoshou Wu ^(a,b),

Yazhou Zhao ^(a,b) *, Xuejun Zhang ^(a,b) **

^(a) Institute of Refrigeration and Cryogenics, College of Energy Engineering, Zhejiang University
Hangzhou 310027, CN, xuejzhang@zju.edu.cn

^(b) Key Laboratory of Refrigeration and Cryogenic Technology of Zhejiang Province
Hangzhou 310027, CN, xuejzhang@zju.edu.cn

ABSTRACT

The combined heating of solar energy and heat pump systems holds profound significance for reducing carbon emissions. However, issues persist with the discontinuity, instability of solar energy, and the limited application of

heat pumps in low-temperature environments. By integrating the two and employing phase change heat storage technology, on the one hand, the use of phase change slurry can reduce the operating temperature of photovoltaic panels to enhance photovoltaic performance. On the other hand, the heat in the phase change slurry can be directly utilized to heat the evaporator, raising the evaporation temperature to improve the heat pump's performance. In light of this research prospect, a solar composite heat pump system based on an evaporative thermal accumulator is proposed in this paper, with the effects of two heat transfer fluids on the composite system's performance analyzed and discussed. Experimental results indicate that when water is used as the heat transfer fluid, there is a significant decrease in temperature during the heat release process, whereas when phase change slurry is employed as the heat transfer fluid, the temperature drop during the heat release process is smaller. Compared with water, the average COP of the heat pump using phase change emulsion as the heat carrier is as high as 4.74, and the average power generation efficiency reaches 20.41%, which is 2.79% higher than the average power generation efficiency of water.

KEYWORDS: Heat pump, Solar energy, Evaporative thermal accumulator, Composite system.

1. INTRODUCTION

As China's economy enters a stage of high-quality development, the demand for heating in industrial and civil sectors becomes more prominent [1]. Hindered by the uneven distribution of fossil resources, some regions require long-distance transportation of coal or gas for centralized heating, leading not only to the consumption of large amounts of fossil energy but also causing serious environmental pollution issues [2, 3]. Heat pumps as a mature technology that can extract heat from the environment or waste heat with a bit electricity consumption for heating, have the advantages of high efficiency and environmental friendliness, making them one of effective technical means to address heating issues [4]. However, heat pumps are susceptible to factors such as fluctuations in heat source temperature, leading to issues of heating instability and insufficient heating capacity [5]. The integration of heat pumps with solar energy to form solar composite heat pump systems not only addresses the aforementioned issues but also enhances the heating performance of the system, offering significant potential for energy saving and consumption reduction [6].

Therefore, in recent years, research on composite systems has aroused great interest among scholars both domestically and internationally. Studies have found that despite being compact in structure and having excellent performance, direct expansion solar heat pumps are still affected by solar radiation intensity, leading to unstable thermal performance [7]. While series, parallel, and hybrid solar heat pumps have improved system operational stability, they require large land areas and have complex piping systems [8]. Zhao et al. [9] conducted experimental research on the relationship between solar radiation and heating temperature, showing that reducing the heating temperature can significantly improve the heating and energy-saving effects of solar composite heat pumps. Ni et al. [10, 11] conducted experimental studies on a solar-air source heat pump combined heating and cooling system based on a triple-tube energy storage heat exchanger under annual working conditions. They found that under heating conditions, increasing the solar hot water temperature and flow rate can significantly improve the system's heating energy efficiency. Ji et al. [12] proposed a photovoltaic solar-assisted heat pump system and experimentally studied its performance. The results showed that the maximum COP of the photovoltaic solar-assisted heat pump for heating reached 10.4, with an average COP of 5.4. Based on this work, a photovoltaic solar-assisted heat pump

system with a heat pipe photovoltaic/thermal (PV/T) demonstrated significant performance advantages in terms of energy and exergy [13].

It can be seen that the photovoltaic-thermal hybrid utilization technology can improve the utilization efficiency of solar energy and is expected to be widely applied in solar energy conversion and utilization [14, 15]. However, in previous studies, heat pumps combined with PV/T typically used water or air as the heat transfer fluid [16, 17]. Compared to phase change materials, there are issues such as low heat storage density and poor system compactness, necessitating the improvement of solar energy utilization and composite heat pump performance through efficient heat storage/transfer/release technologies. Phase change slurry (PCS), as a latent heat type functional fluid formed by dispersing phase change materials in water in the form of micro-scale particles, not only exhibits excellent heat storage/transfer/release performance but also integrates heat storage/transfer/release functions [18, 19]. Applying PCS as the heat transfer fluid instead of water and air in solar composite heat pump systems increases heat storage capacity compared to non-phase change fluids. Through effective storage, transportation, and release of solar thermal energy via slurry flow, it can enhance heat pump heating performance. Additionally, leveraging the characteristic of constant temperature during the absorption/release process of phase change particles in the slurry allows PV/T to operate in a suitable temperature range, thereby improving photovoltaic performance [20]. Therefore, this paper proposes a solar composite heat pump system based on an evaporative thermal accumulator. A testing platform is constructed, and experiments are conducted to explore and reveal the performance advantages of PCS in increasing solar thermal storage, raising evaporation temperature, and lowering photovoltaic operating temperature.

2. DESCRIPTION OF THE PROPOSED SYSTEM

The schematic diagram of the proposed combined heating system is shown in Figure 1a, mainly consisting of a PV/T system, heat pump system, evaporative thermal accumulator, and circulating water pump. The physical diagram of the experimental test platform is shown in Figure 1b, which is primarily divided into the refrigerant loop and the circulating water loop. Before turning on the heat pump unit, circulating water or PCS is heated through the solar collector and transported to the evaporative thermal accumulator for heat storage. When the temperature of the water or PCS in the evaporative thermal accumulator reaches a certain value, the heat pump unit is activated. The refrigerant, throttled after passing through the expansion valve, enters the evaporative thermal accumulator, absorbing heat from the water or PCS, thereby evaporating into a gaseous state. Subsequently, after being compressed into superheated air in the compressor, it releases heat to the water tank (simulating the heating terminal) when passing through the condenser. Meanwhile, the electricity generated by the solar photovoltaic panels powers components such as the compressor and water pump in the system, with excess electricity being fed into the grid for additional revenue.

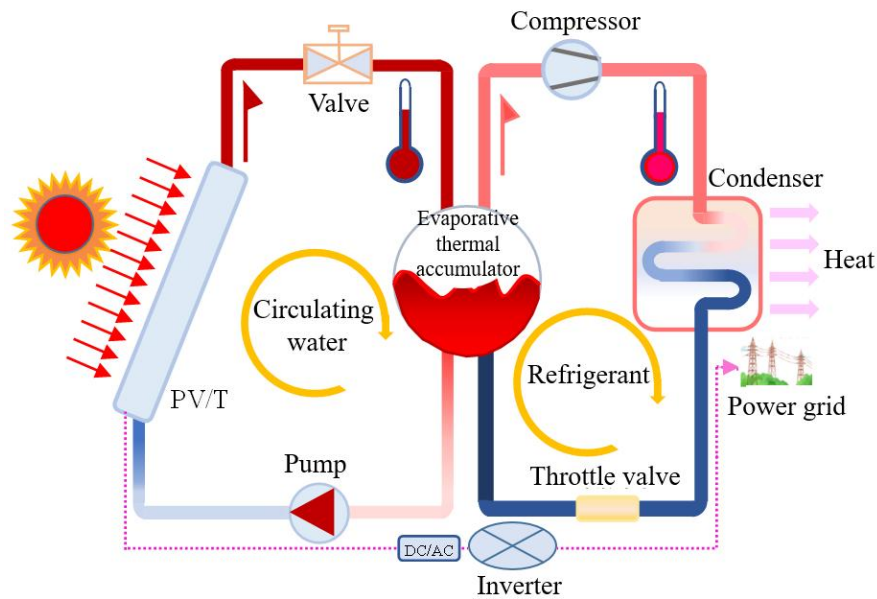


Figure 1a: Schematic diagram of a solar composite heat pump system based on evaporative heat storage.

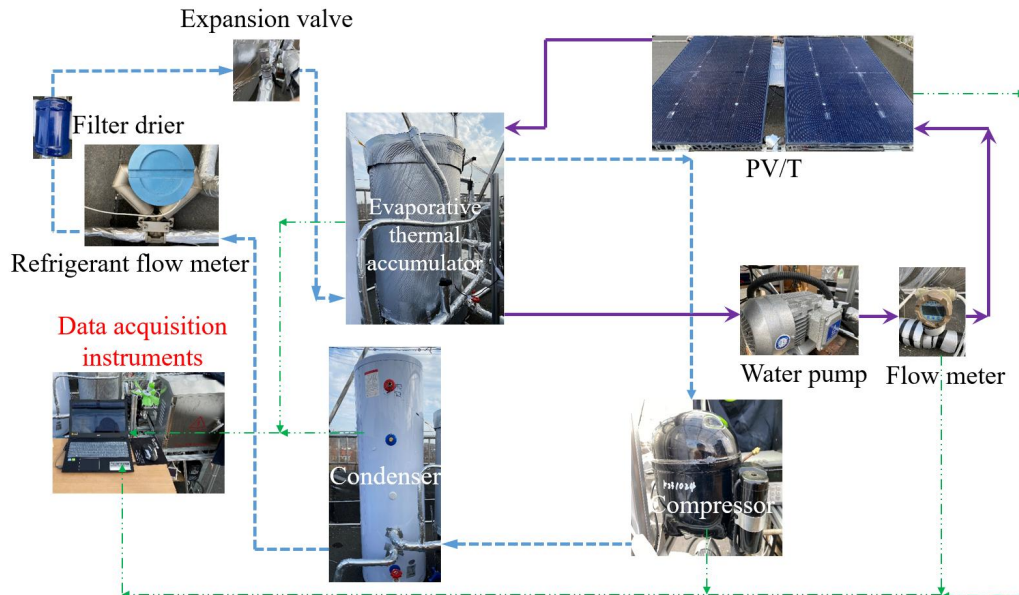


Figure 1b: Physical diagram of the solar composite heat pump system based on evaporative heat storage.

As shown in Figure 1c, the evaporative thermal accumulator, composed of an evaporator and a heat storage tank, is the core component of the system. It consists of continuous bent pipes and cylindrical chambers. Foam plastic is filled in the chamber interlayers, and the outer shell is wrapped with insulation cotton. Water or PCS is poured into the evaporative thermal accumulator. Considering that the nominal operating temperature of photovoltaic cells in the PV/T panels is 25°C [21], the phase change temperature range of PCS should include the nominal operating temperature of the PV/T panels, i.e., the nominal temperature should fall within the phase change temperature range. The peak phase transition temperature of octadecane is approximately 28.50°C , and the phase transition temperature range is approximately $24.30\sim 32.50^{\circ}\text{C}$. Therefore, this paper selects octadecane as the phase change materials. Phase change microcapsules are synthesized using the water phase separation method, and then, using a composite emulsifier, PCS suitable for PV/T heat pumps is synthesized under laboratory conditions using a "two-step method."



Figure 1c: Physical diagram of evaporative heat accumulator.

3. PERFORMANCE EVALUATION

As the power component of the system, the compressor's actual power consumption, W (kW), is obtained from the theoretical power consumption and the electrical efficiency of the compressor:

$$W = \frac{m_r(h_2 - h_1)}{\eta_{\text{comp}}} \quad (1)$$

in the formula, h_1 and h_2 are the enthalpy values of the compressor inlet and outlet, $\text{kJ}\cdot\text{kg}^{-1}$; the compressor electrical efficiency η_{comp} is the product of the indicated efficiency η_i , mechanical efficiency η_m and motor efficiency η_{mt} , which is taken as 0.48 for calculation [22], m_r is refrigerant flow rate of the compressor, $\text{g}\cdot\text{s}^{-1}$, is given by:

$$m_r = \eta_V \frac{V_{\text{th}}}{v_{\text{in}}} \quad (2)$$

in the formula, v_{in} is the specific volume of the refrigerant at the compressor inlet, $\text{m}^3\cdot\text{kg}^{-1}$, η_V is the volumetric efficiency, and V_{th} is the theoretical gas transmission volume, $\text{m}^3\cdot\text{kg}^{-1}$, which is given by the following formula:

$$\eta_V = 1.058 - 0.06764 \frac{P_2}{P_1} \quad (3)$$

$$V_{\text{th}} = \frac{n \cdot V_p}{60} \quad (4)$$

here P_2 and P_1 are the discharge and suction pressures of the compressor, Mpa, n is the actual speed of the compressor, $\text{r}\cdot\text{min}^{-1}$, and V_p is the cylinder volume of the compressor, m^3 .

In this system, while ignoring a small amount of losses in the heat transfer process, all the heat released by the condensation of the refrigerant in the condenser is given to the water in the water tank. Therefore, the heating power of the heat pump can be calculated based on the heat gain on the water side. As shown in Equation 5:

$$Q = c_p m_w (T_1 - T_0) \quad (5)$$

here T_0 and T_1 are the initial water temperature and final water temperature of the water tank, °C, m_w is the water flow rate, $\text{g}\cdot\text{s}^{-1}$, c_p is the specific heat capacity of water, $\text{J}\cdot\text{kg}^{-1}\cdot\text{°C}^{-1}$.

The thermal efficiency η_{th} of a solar photovoltaic panel is equal to the ratio of the heat absorption of water G_{th} (kW) to the total amount of radiation G (kW), as shown in Equation 6. The electrical efficiency η_{el} is equal to the ratio of the solar energy G_{el} (kW) converted into electrical energy to the total radiation G (kW), as shown in Equation 7.

$$\eta_{\text{th}} = \frac{\int_{t_1}^{t_2} G_{\text{th}} \cdot dt}{\int_{t_1}^{t_2} G_{\text{sun}} \cdot dt} = \frac{m \cdot c_{\text{pw}} \cdot (T_{\text{wout}} - T_{\text{win}})}{A_{\text{PVT}} \cdot G \cdot (t_2 - t_1)} \quad (6)$$

$$\eta_{\text{el}} = \frac{\int_{t_1}^{t_2} G_{\text{el}} \cdot dt}{\int_{t_1}^{t_2} G_{\text{sun}} \cdot dt} = \frac{\int_{t_1}^{t_2} G_{\text{el}} \cdot dt}{A_{\text{PVT}} \cdot G \cdot (t_2 - t_1)} \quad (7)$$

here m is the mass flow rate of water, $\text{g}\cdot\text{s}^{-1}$, c_{pw} is the specific heat capacity of water, $\text{kJ}\cdot\text{kg}^{-1}\cdot\text{°C}^{-1}$, T_{wout} and T_{win} are the inlet and outlet temperatures of water, °C. A_{PVT} is the area of the solar collector, m^2 . G is solar irradiance, $\text{W}\cdot\text{m}^{-2}$; t_1 and t_2 are the start and end times, s.

In the original setting of the system, the power generated by the PV/T panel will be provided to the compressor and other components. However, due to cost reasons, the voltage stabilizing effect of the inverter currently used in this project is average, so this article only discusses the heat pump COP_h of this system, that is, the ratio of the heat pump heating power, Q , and the compressor power consumption, W , as shown in the equation 8 shown.

$$\text{COP}_h = \frac{Q}{W} \quad (8)$$

4. RESULTS AND DISCUSSION

4.1. Circulating Medium: Water

Firstly, verification experiments were conducted using water as the circulating medium between the PV/T and the evaporative thermal accumulator. Preliminary tests obtained the system's performance during the solar energy supply phase and the heat pump circulation phase.

Figure 2 illustrates the variation of PV/T panel temperature over time. During the heat storage phase, the temperature of the PV/T rises significantly. However, as solar radiation intensity decreases substantially, the temperature of the PV/T panel gradually decreases. Since water enters from PV/T-1, absorbs heat, and exits from PV/T-2, the temperature of PV/T-1 is always slightly lower than that of PV/T-2. Additionally, the low-temperature medium starts absorbing heat from the bottom of the PV/T panel and exits from the outlet at the top of the panel. Therefore, the temperature at the bottom of the same PV/T panel is lower than that at the top. Sudden changes in solar radiation intensity in the figure are caused by cloud cover blocking the sun. The average solar irradiance during the testing period was $416.38 \text{ W}\cdot\text{m}^{-2}$.

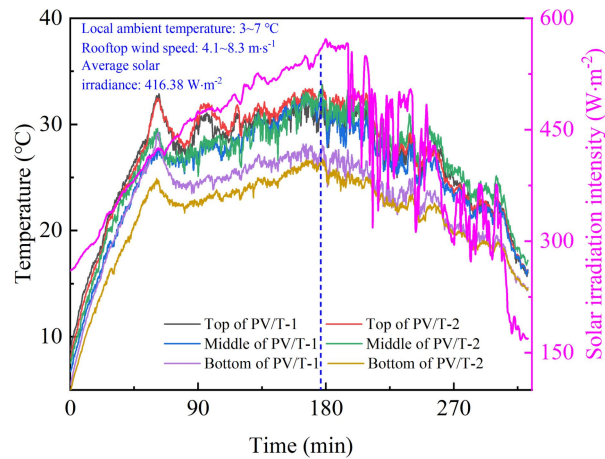


Figure 2: Changes of PV/T panel temperature and solar radiance over time.

Figure 3 illustrates the temperature distribution in the evaporative thermal accumulator when water is used as the heat transfer fluid in the experiment. During the heat storage process, the temperature gradually decreases from top to bottom in the evaporative thermal accumulator. The temperature at the highest point ($y=85\text{ cm}$) is the first to respond, while the temperature at the lowest point ($y=6\text{ cm}$) reacts the slowest. During the heat storage phase, the water temperature in the evaporative thermal accumulator continues to rise until the temperature difference between each measuring point is small, indicating the completion of initial heat storage. Subsequently, the heat pump is activated to initiate synchronous heat storage/release experiments. At this point, while the evaporative thermal accumulator is storing heat, it also provides heating for the heat pump system. As the solar radiation intensity decreases significantly, the water temperature continues to decrease until the end of the experimental test.

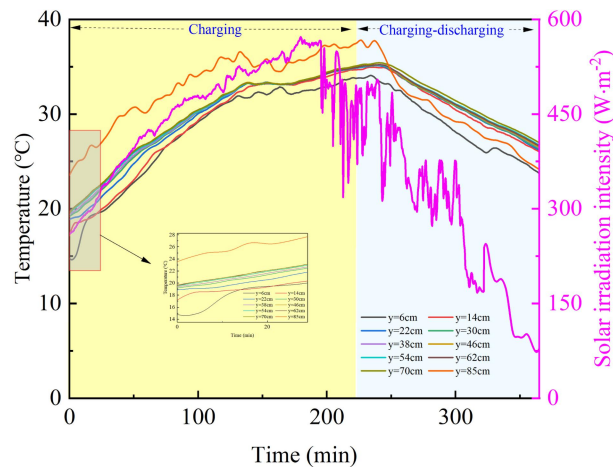


Figure 3: Temperature distribution of working fluid in evaporative regenerator.

Figure 4 depicts the trends of temperature in the condensate water tank, exhaust pressure, and compressor power. The initial temperature of the cold water in the tank is 16°C, eventually heated to 60°C, resulting in a temperature rise of 43°C. During the heat storage phase, the temperature of the water tank remains constant. As the heat pump is activated, solar energy passes through the PV/T, evaporative thermal accumulator, and condenser before entering the water tank, causing the water tank temperature to continuously rise. Throughout this process, both the exhaust temperature and compressor power consumption increase gradually with the progress of the experiment, with the exhaust temperature reaching a maximum of 100.9°C.

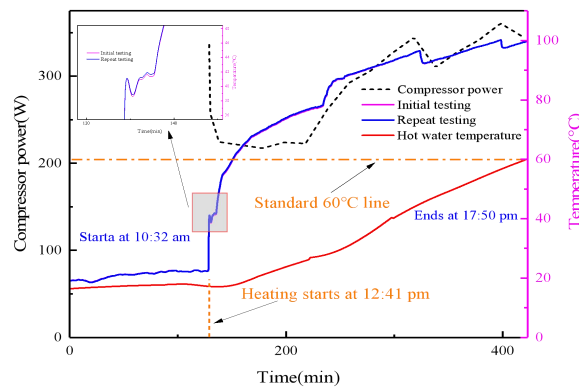


Figure 4: Changes of water tank temperature, exhaust temperature and compressor power over time.

Figure 5 illustrates the trends of compressor power and COP over time. As the temperature of the water tank continues to rise, the compressor power consumption increases accordingly, with an average power consumption of 278.89 W throughout the entire process. The COP of the heat pump decreases continuously, decreasing from a peak of 4.17 to 2.54, with an average COP of 3.30 for the entire duration.

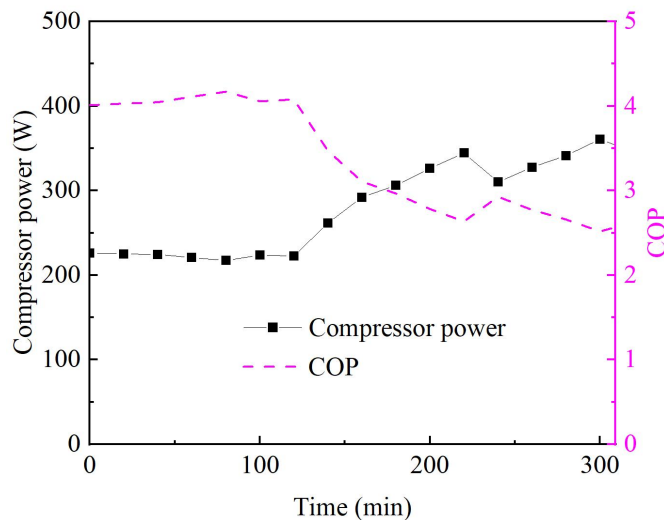


Figure 5: Compressor power and COP changes over time.

4.2. Circulating Medium: Slurry

After obtaining the preliminary performance of the system using water as the circulating medium, a further experiment was conducted using PCS on a day with similar weather conditions (solar radiation, temperature, wind speed) as the day when water was used. Considering factors such as the flowability of PCS, heat storage performance, and the operating temperature of PV/T, phase change microcapsule content of the slurry selected for this experiment ranged from 15 vol% to 25 vol%, with a phase change temperature range of 22-29°C.

Figure 6 illustrates the variation in PV/T panel temperature. Similar to Figure 2, when solar radiation intensity is high, the temperature of the PV/T panel gradually rises, and when solar radiation intensity is low, the temperature of the PV/T panel gradually decreases. Comparing the results of the two figures, it is evident that under conditions of high radiation intensity, whether water or PCS is used as the circulating medium, the corresponding surface temperature of the PV/T panel increases rapidly. However, when there is a phase change in PCS, the temperature fluctuation range of the PV/T panel is smaller and shows good temperature stability.

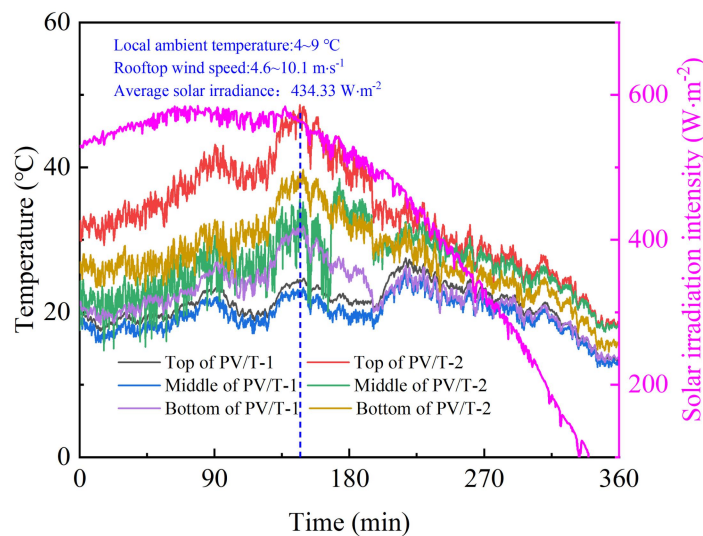


Figure 6: PV/T plate temperature changes with time.

Figure 7 shows the temperature distribution in the evaporative thermal accumulator when PCS is used as the heat transfer fluid. At the beginning of the heat storage process, the average temperature of the slurry is 21.4°C, and there is a noticeable temperature stratification phenomenon during heat storage. The low-temperature slurry flows into the PV/T, absorbs heat, and its temperature increases, causing the phase change microcapsules within it to undergo phase change. It can be observed from the figure that some phase change microcapsules begin to undergo phase change at the beginning of the heat storage process, and after the completion of phase change in the later stage of heat storage, the temperature rises rapidly. Since PCS enters the evaporative thermal accumulator through the top inlet, the temperature of the slurry at the upper part of the evaporative thermal accumulator will be significantly higher than that at the lower part. Additionally, due to the large amount of slurry in the evaporative thermal accumulator and the existence of the phase change process, temperature stratification occurs within the slurry. As the heat storage progresses, the temperature difference between different parts of the slurry gradually decreases. After a period of time of heat pump operation, the heat storage reaches saturation, and the temperatures of different parts tend to be consistent. During the subsequent

synchronous heat storage/release process, due to supplying heat to the heat pump and the decrease in solar radiation intensity, the slurry temperature decreases, but this decrease is relatively slow. This is because PCS has a significant latent heat within the phase change temperature range.

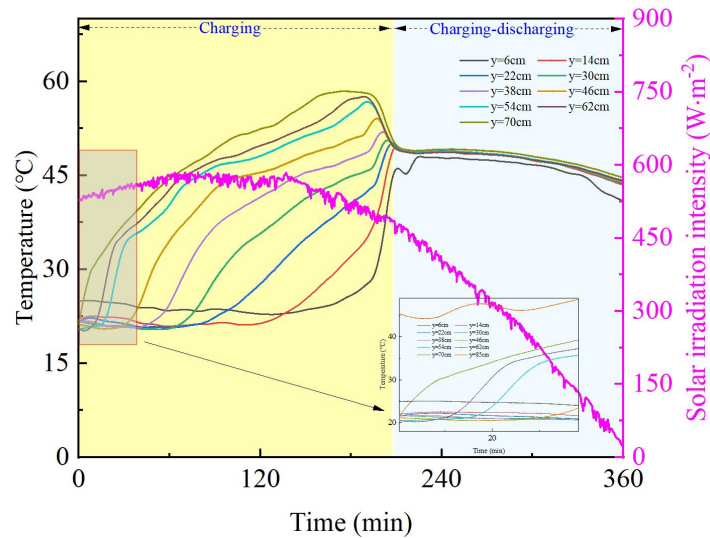


Figure 7: Temperature distribution of working fluid in evaporative regenerator.

Figure 8 illustrates the variations in compressor power, exhaust temperature, and water tank temperature of the solar-assisted heat pump system using PCS as the heat transfer fluid. Similar to the changes observed in the water system, as the heat pump operates, the exhaust temperature continuously increases, reaching a maximum of 118.9°C. The cold water in the water tank is still heated to 60°C, and as the temperature of the cold water in the tank continues to rise, the compressor power also increases.

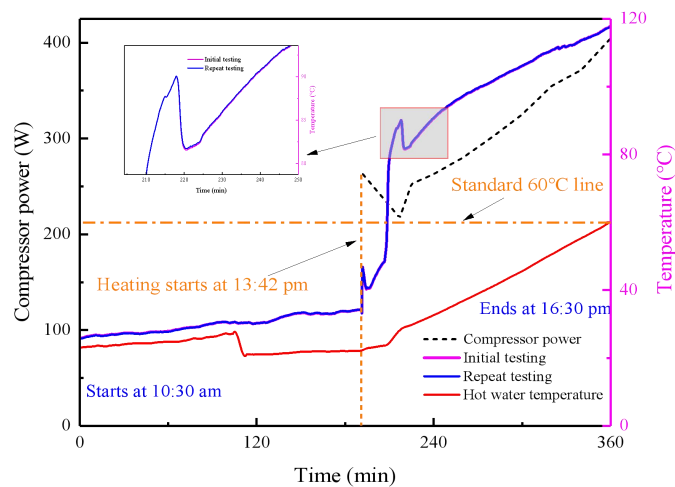


Figure 8: Changes of water tank temperature, exhaust temperature and compressor power over time.

Figure 9 presents the trends of compressor power and COP. During the heating process, as the temperature of the hot water in the water tank gradually increases, the compressor power also increases continuously, with an average power consumption of 313.43 W throughout the process. The COP of the heat pump decreases continuously, with an average COP of 4.74 throughout the process.

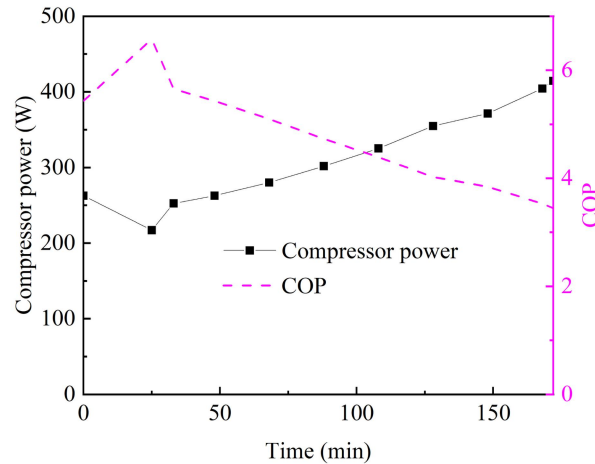


Figure 9: Compressor power and COP changes over time.

In addition, the experimental results using PCS as the circulating working fluid show that due to the phase change temperature range of PCS, the temperature of the PV cells remains relatively stable, so the electrical output performance remains stable, and the power generation efficiency remains above 14%. The average power generation efficiency reaches 20.41%, which is higher than the average power generation efficiency of water of 17.62%.

Comparison between Figure 3 and Figure 7 reveals that regardless of whether water or PCS is used as the heat transfer fluid, the temperature of the working fluid in the evaporative heat storage during the heat storage phase continues to rise. However, during the simultaneous heat storage and release when the heat pump is activated, the temperature of the working fluid in the evaporative heat storage starts to decrease. In the case of water, the temperature drops significantly to 14.6°C, whereas for the slurry system, the temperature only slightly decreases to 6.4°C. This difference is primarily attributed to the fact that in the water system, supplying heat to the heat pump consumes sensible heat of water, leading to a significant decrease in water temperature. Conversely, in the slurry system, during heat supply to the heat pump, the phase change microcapsules in the slurry undergo phase change, resulting in the consumption of not only sensible heat but also the latent heat of the phase change process. Therefore, the overall average temperature of the slurry does not decrease significantly.

In addition, After the PCS was left to stand for 17 hours, the temperature dropped by only 5.1°C compared to the temperature at the end of the previous day's test. Therefore, the heat storage process was completed in only 70 minutes in this test due to the high initial temperature of the PCS.

5. CONCLUSIONS

This paper proposes a solar-assisted heat pump system based on evaporative thermal accumulator. After constructing the experimental platform, key parameters of the composite system were explored using water and PCS as the heat transfer fluids, and the performance of the system with these two fluids was analyzed and compared preliminarily. The conclusions are as follows:

(1) When water is used as the heat transfer fluid, the temperature distribution in the evaporative heat storage device is relatively uniform. During the heat release process, there is a significant temperature drop, with an average temperature decrease of 14.6°C. In contrast, when PCS is used as the heat transfer fluid, there is a noticeable temperature stratification phenomenon during the heat storage process in the evaporative heat storage device, and the temperature drop during the heat release process is smaller, only 6.4°C.

(2) When PCS is used as a heat carrier, the average COP of the heat pump is as high as 4.74, and the average power generation efficiency of PCS reaches 20.41%, which is 2.79% higher than the average power generation efficiency of water. It can be seen that using PCS instead of water as a heat carrier in a solar composite heat pump system can, on the one hand, increase the heat storage capacity compared to water, and effectively store, transport and release light and heat through the flow of emulsion, which can improve the heating performance of the heat pump; on the other hand, the temperature of the phase change particles in the emulsion remains unchanged during the absorption/release process, which can make PV/T operate in a suitable temperature range, thereby improving photovoltaic performance.

ACKNOWLEDGEMENT

This research was supported by the Key Research and Development Program of Zhejiang Province (No.2024C03117) and National Natural Science Foundation of China (No. 52376017).

REFERENCES

- [1] Tang L, Qu J, Mi Z, et al. Substantial emission reductions from Chinese power plants after the introduction of ultra-low emissions standards[J]. *Nature Energy*. 2019, 4(11): 929-938.
- [2] Shen X, Liu P, Qiu Y, et al. Estimation of change in house sales prices in the United States after heat pump adoption[J]. *Nature Energy*. 2021, 6(1): 30-37.
- [3] Zhang F, Cai J, Ji J, et al. Experimental investigation on the heating and cooling performance of a solar air composite heat source heat pump[J]. *Renewable energy*. 2020, 161: 221-229.
- [4] Zhao X L, Fu L, Zhang S G, et al. Study of the performance of an urban original source heat pump system[J]. *Energy Conversion and Management*. 2010, 51(4): 765-770.
- [5] Wang Y, Quan Z, Zhao Y, et al. Performance and optimization of a novel solar-air source heat pump building energy supply system with energy storage[J]. *Applied Energy*. 2022, 324: 119706.
- [6] Fu H D, Pei G, Ji J, et al. Experimental study of a photovoltaic solar-assisted heat-pump/heat-pipe system[J]. *Applied Thermal Engineering*. 2012, 40: 343-350.
- [7] Cai J, Ji J, Wang Y, et al. Numerical simulation and experimental validation of indirect expansion solar-assisted multi-functional heat pump[J]. *Renewable Energy*. 2016, 93: 280-290.
- [8] Shao N, Ma L, Zhang J. Experimental investigation on the performance of direct-expansion roof-PV/T heat pump system[J]. *Energy*. 2020, 195: 116959.
- [9] Zhao M, Gu Z L, Kang W B, et al. Experimental investigation and feasibility analysis on a capillary radiant heating system based on solar and air source heat pump dual heat source[J]. *Applied energy*. 2017, 185: 2094-2105.
- [10] Ni L, Qv D, Shang R, et al. Experimental study on performance of a solar-air source heat pump system in severe external conditions and switchover of different functions[J]. *Sustainable Energy Technologies and Assessments*. 2016, 16: 162-173.
- [11] Ni L, Qv D, Yao Y, et al. An experimental study on performance enhancement of a PCM based solar-assisted air source heat pump system under cooling modes[J]. *Applied Thermal Engineering*. 2016, 100: 434-452.
- [12] Ji J, Pei G, Chow T, et al. Experimental study of photovoltaic solar assisted heat pump system[J]. *Solar energy*. 2008, 82(1): 43-52.

- [13] Huide F, Xuxin Z, Lei M, et al. A comparative study on three types of solar utilization technologies for buildings: Photovoltaic, solar thermal and hybrid photovoltaic/thermal systems[J]. *Energy Conversion and Management*. 2017, 140: 1-13.
- [14] Tyagi V V, Kaushik S C, Tyagi S K. Advancement in solar photovoltaic/thermal (PV/T) hybrid collector technology[J]. *Renewable and Sustainable Energy Reviews*. 2012, 16(3): 1383-1398.
- [15] Yuan W, Ji J, Modjinou M, et al. Numerical simulation and experimental validation of the solar photovoltaic/thermal system with phase change material[J]. *Applied energy*. 2018, 232: 715-727.
- [16] Qu M, Chen J, Nie L, et al. Experimental study on the operating characteristics of a novel photovoltaic/thermal integrated dual-source heat pump water heating system[J]. *Applied Thermal Engineering*. 2016, 94: 819-826.
- [17] 邱国栋, 许振飞, 位兴华, 等. 太阳能与空气源热泵集成供热系统研究进展[J]. *化工进展*. 2018, 37(7): 2597-2604. Qiu Guodong, X. U. Zhenfei, Wei Xinghua, et al. Research progress on integrated heating system of solar energy and air source heat pump[J]. *Chemical Industry and Engineering Progress*. 2018, 37(7): 2597-2604.
- [18] Diaconu B M, Varga S, Oliveira A C. Experimental assessment of heat storage properties and heat transfer characteristics of a phase change material slurry for air conditioning applications[J]. *Applied Energy*. 2010, 87(2): 620-628.
- [19] Chananipoor A, Azizi Z, Raei B, et al. Optimization of the thermal performance of nano-encapsulated phase change material slurry in double pipe heat exchanger: Design of experiments using response surface methodology (RSM)[J]. *Journal of Building Engineering*. 2021, 34: 101929.
- [20] Liu L, Niu J, Wu J. Improving energy efficiency of photovoltaic/thermal systems by cooling with PCM nano-emulsions: An indoor experimental study[J]. *Renewable Energy*. 2023, 203: 568-582.
- [21] Poulek V, Matuška T, Libra M, et al. Influence of increased temperature on energy production of roof integrated PV panels[J]. *Energy and Buildings*. 2018, 166: 418-425.
- [22] Na S, Shin M, Choi G, et al. Effect of pressure ratio and oil viscosity on rotary compressor efficiency[J]. *Journal of Mechanical Science and Technology*. 2018, 32: 4971-4981.

